eman ta zabal zazu

Universidad del País Vasco
Euskal Herriko Unibertsitatea

In vivo strategies for the study of ubiquitination and ubiquitin-related diseases: application to Angelman syndrome

Juan Manuel Ramírez Sánchez

2016

eman ta zabal zazu

Universidad del País Vasco
Euskal Herriko Unibertsitatea

Zientzia eta Teknologia Fakultatea

Genetika, Antropologia Fisikoa eta Animalia Fisiologia Saila

Urria 2016

In vivo strategies for the study of ubiquitination and ubiquitin-related diseases: application to Angelman syndrome

Memoriaren aurkezlea

Juan Manuel Ramirez Sanchez

Lan hau Biozientzerako Ikerkuntza Kooperatiboko Zentroaren (CIC bioGUNE) Genomika Funtzional Sailan burutu egin da, Ugo Mayor Doktorearen zuzendaritzapean.

CIC bioGUNE
Biozientzietako Ikerkuntza Kooperatiboko Zentroa
Centro de Investigación Cooperativa en Biociencias

"Accidental observations might

be the most important ones"

Avram Hershko

Nobel Laureate in Chemistry in 2004 for discovering the ubiquitin system

Acknowledgments

Thanks to a very good advice I got a few years ago, I had the chance to meet my supervisor, Ugo Mayor. Ugo encouraged me to join his lab and get the PhD, and this is something I will always be grateful for. It has been a long way and sometimes tough, but overall it has been a learning experience that has allowed me to grow, not only as a scientist, but also at the personal level. Of course, I would not have got that far without all the support received throughout this period. For this reason, I would like to thank all the people that in one way or another have helped me over those years.

First, I would like to express my sincere gratitude to you Ugo. You have been a wonderful mentor. Thanks to you I feel now confident enough to face whatever challenge I might encounter during my research career, as well as during my personal life. Thank you very much for giving me this opportunity, and thank you very much for believing in me.

I will also like to thank my labmates, past and present, for all their help and friendship. Special thanks go to So Young, who has been a great teacher with a lot of patience. Aitor, we mostly coincided in the lab last year, but this has been more than enough time for me to realize that you are a wonderful person and a brilliant scientist. Thank you for all the coffees and discussions we have had. Maribel and Benoit thank you for all the advices you have given to me. Nere, eskerrik asko emandako laguntza guztiagatik, momentu txarretan ere ni laguntzeko denbora atera egin baituzu. *Eres una crack!!* Eider, Nagore eta Javi, mila esker emandako animo guztiengatik eta beti laguntzeko prest egoteagatik.

Acknowledgments

Eskerrak eman nahiko nizkioke ere Miren Josuri, Jabiri, Kermani, Jesus Mariri eta Irantzuri, Unibertsitatean leku bat egiteagatik, kafetxoengatik eta laborategian hain gustura sentiarazteagatik. Gracias a mis antiguos vecinos de laboratorio, Rosa, Jim, Cora, Laura, Leire, Lucia, Monika, por todo el apoyo, consejos y ayuda que me habéis dado. Ha sido un placer teneros al lado durante todo este tiempo. Isabel, Mertxe, Iratxe y Maitane gracias por vuestros ánimos. Thank you very much too to all the people in Memphis, Larry, Nora, Sarita, Colleen, Ben and Brandon. You made my stay in USA amazing.

También me gustaría agradecer a mi familia todo el apoyo que me han dado. Aita y ama, muchísimas gracias por todo el sacrificio que habéis hecho para ayudarme a llegar hasta aquí. Sin lugar a dudas, sin vuestra ayuda esto no hubiese sido posible. *¡Os quiero muchísimo!* Y a vosotros también, amama, Javi, Eva, Neretxu y Eider. Gracias por todas esas risas y por ayudarme a ver las cosas desde otro punto de vista. Itxaso, mila esker bai momentu honetan, bai txarretan ere beti nire alboan egoteagatik. *Maite zaitut laztana!!* Y a mi otra familia también, Itzi, Miguel, Nere, Eneko, Sheila, Gorka, Ane, Leize, Joseba, Maritxu, Begoña y Carmen, muchísimas gracias por todo vuestro apoyo.

Eskerrik asko nire lagun guztioi ere, Arkatiz, Inma, Joana, Peio, Jon Hanni, Amagoia, Olatz, Aitor, Amago, Amaia, Amaiur, Andoni, Saio, Itzi, Itsasne, Maria, Jenni, Dani, Naiara, Natxo, Oihane, Iñi, Oihane, Andrea, Janire, Sergio, Olga, Gorka, Leire, Goros, Galder, Arturo, Jon, Trebor, Gamero, Jose, Luja eta Zigor, animo guztiengatik eta behar izan zaitudanean hor egoteagatik. Iñik abesten duen moduan *Tabernan ikusiko gara!!!*

Finally, I would like thank CIC bioGUNE, the Basque Government, Asociación Síndrome de Angelman and March of Dimes Foundation for economical support.

Eskerrik asko guztioi!! Thank you all!! Gracias a todos!!

Table of contents

I. Abbreviations

15B: Flies carrying a deletion on the *Ube3a* gene

A3: Flies overexpressing the Ube3a E3 ligase protein

AIB1: Amplified in breast cancer 1 protein

ALK: Anaphase lymphoma kinase protein

AMPAR: α-amino-3-hydroxy-5-methyl-isoxazole-4-propionic acid receptor

APC/C: Anaphase-promoting complex/cyclosome E3 ligase

Arc: Activity-regulated cytoskeleton-associated protein

AS: Angelman syndrome

ASD: Autism spectrum disorder

Atpα: Alpha subunit of the Na^+/K^+ ATPase protein

BDSC: Bloomington *Drosophila* Stock Center

BCCP: Biotin carboxyl carrier protein component

^{bio}Ub: Biotinylated ubiquitin/flies expressing the $^{UAS}(^{bio}Ub)_6$-BirA construct

BirA: Biotin holoenzyme synthetase enzyme/flies expressing the BirA enzyme

CP: Proteasome core particle

Cul1: Cullin1 protein

Ddi1: DNA-damage inducible protein 1 protein

Di-gly: Di-glycine signature of ubiquitin left after trypsin digestion

DMEM: Dulbecco's modified Eagle medium

DPSC: Dental pulp stem cell

DRSC: *Drosophila* RNAi Screening Center

DSHB: Developmental Studies of Hybridoma Bank

DTT: Dithiothreitol

DUB: Deubiquitinating enzyme

E1: Ubiquitin-activating enzyme

E2: Ubiquitin-conjugating enzyme

E3: Ubiquitin-ligase enzyme

EIF-1A: Eukaryotic initiation factor 1A protein

elav^{GAL4}: embryonic lethal abnormal vision-GAL4 driver

Eps-15: Epidermal growth factor receptor pathway substrate clone 15

ESI: Electrospray ionization

Fabp: Fatty acid binding protein

Fax: Failed axon connections protein

FBS: Fetal bovine serum

GFP: Green fluorescence protein

GMR^{GAL4}: Glass multimer reporter-GAL4 driver

HECT: Homologous to the E6-AP carboxyl terminus

HHR23A: Human homologue of Rad23

HRP: Horseradish peroxidase

Hs^{GAL4}: Heat shock inducible-GAL4 driver

hTERT: Human telomerase reverse transcriptase

IBR: In-between RING domain

JAMM: JAB1/MPN/MOV3 protease

L1: *Drosophila* first instar larva

L2: *Drosophila* second instar larva

L3: *Drosophila* third instar larva

LFQ: Label free quantification

Lqf: Liquid facets protein

Mcm7: Multicopy maintenance 7 subunit protein

MDC: Max Delbrück Center for Molecular Medicine

MJD: Machado-Joseph disease protease

MS: Mass spectrometry

m/z: Mass-to-charge ratio

NCS: Newborn calf serum

Nedd4: Neural precursor cell expressed, developmentally down-regulated 4 E3

NEM: N-ethylmaleimide

Nrt: Neurotactin protein

nSyb: Neuronal synaptobrevin protein

OK371^{GAL4}: Vesicular glutamate transporter-GAL4 driver

OTU: Ovarian tumour protease

Pbl: Pebble protein

PBS: Phosphate buffered saline

PWS: Prader-Willi syndrome

Rad23: Radiation sensitivity abnormal 23 protein

Ras: Raspberry protein

RBR: RING between RING

Rbx1: RING-box protein 1

RhoGEF: Rho-guanine-nucleotide exchange factor

RING: Really interesting new gene

Rngo: Rings lost protein. *Drosophila* homologue of Ddi1

RP: Proteasome regulatory particle

Rpn10: Regulatory particle non-ATPase 10 protein

Rpn10^{DN}: C-terminal half of the Regulatory particle non-ATPase 10 protein

Rps10b: Ribosomal protein S10b

SCF: Skp1-Cul1-F-box E3 ligase

SDS: Sodium dodecyl sulfate

Skp1: S-phase kinase associate protein

Snap25: Synaptosomal-associated protein 25

SNARE: N-ethylmaleimide-sensitive factor attachment protein receptor

Syx1A: Syntaxin 1A protein

T: Cysteine peptidase Tan protein

TBPH: TAR DNA-binding protein 43

Tub^{GAL4}: Tubulin-GAL4 driver

$Tub^{GAL80ts}$: Tubulin-GAL80 temperature sensitive driver

UAS: Upstream activating sequence

UBA: Ubiquitin-associated domain

UBE3A: E6-associated protein (E6-AP) E3 ligase enzyme

UBC: Ubiquitin-conjugating catalytic domain

UBD: Ubiquitin-binding domain

UCH: Ubiquitin C-terminal hydrolase enzyme

Uch-L5: Ubiquitin carboxy-terminal hydrolase L5 orthologue

UIM: Ubiquitin-interacting motif

UPD: Uniparental disomy

UPS: Ubiquitin-proteasome system

USP: Ubiquitin-specific protease enzyme

UTHSC: University of Tennessee Health Science Center

VWFA: Von Willebrand factor A domain

II. Index of Figures and Tables

III. Summary

The post-translational modification of proteins with ubiquitin, a process known as ubiquitination, regulates a wide range of cellular processes. In the nervous system it is essential for the development of neurons and their correct functioning. Indeed, its failure is associated to a number of neurological disorders. The identification of the proteins that are being ubiquitinated *in vivo* in neurons, or that are differentially ubiquitinated under certain circumstances, can greatly contribute to better understand the roles that this modification plays in the brain. However, the low stoichiometry at which ubiquitin-modified proteins are found within the cells makes the study of this modification quite challenging.

Dr. Mayor's lab developed a strategy, based on the *in vivo* biotinylation of ubiquitin, that allowed the isolation and enrichment of hundreds of ubiquitin conjugates from the embryonic nervous system of the fruit fly. During this Thesis project, we have expanded this strategy to *Drosophila* photoreceptor cells, providing an *in vivo* system for the study of neuronal ubiquitination pathways in the context of a mature neuron. Furthermore, we have confirmed that this strategy can be combined with fly mutants in order to detect changes in the ubiquitin proteome. Using this approach we have identify the first *in vivo* substrate of the *Drosophila* Ube3a, an ubiquitin E3 ligase that in humans is involved in the Angelman syndrome. On the other hand, we have developed a GFP-pulldown assay that favours the isolation of just one specific protein, in order to facilitate the characterization of its ubiquitinated fraction. By the application of this protocol in a neuron-like cell system, four additional substrates of the fly Ube3a have been biochemically validated.

Both methodologies used during this Thesis have proven to be suitable approaches for the *in vivo* analysis of ubiquitinated proteins. In addition, they offer unique advantages that complement other strategies for ubiquitome study. The combination of these two protocols with disease models in which the ubiquitin proteasome system is affected will contribute to provide further insight into the mechanisms underlying these pathologies.

IV. Laburpena

Proteinen aldaketak ubikuitina molekularekin, ubikuitinazioa izenarekin ezagutzen den prozesua, bidezidor ugari kontrolatzen ditu zelulen barnean. Nerbio sisteman, adibidez, neuronen garapenerako eta funtzionamendurako ezinbesteko da. Hori dela eta, ubikuitina eranstean gertatzen diren akatsak zenbait gaixotasunekin erlazionatu dira. Neuronetan ubikuitina itsatsita daukaten proteinen identifikazioak asko lagunduko luke prozesu honek garunean dituen zereginak hobeto ulertzeko. Baina ubikuitinatuak dauden proteinak kopuru oso txikian aurkitu ohi direnez, haien identifikazioa lan zaila da.

Ugo Mayor Doktorearen laborategiak ubikuitinak kontrolatzen dituen proteinak ikertzeko estrategia eraginkor bat garatu du. Hain zuzen ere, estrategia ubikuitina biotinarekin markatzean datza. Horren bidez, ubikuitina lotuta daukaten ehunka proteina identifikatu ziren ozpin euliaren embrio-nerbio sisteman. Tesi honetan zehar, estrategia hori *Drosophila*-ren foto-errezeptoreetara hedatu dugu, ubikuitinazio bidezidorrak neurona heldu baten markoan ikertzeko *in vivo* eredu bat hedatuz. Bestalde, estrategia hori euli mutanteekin elkar daitekeela konfirmatu dugu. Horrela, ubikuitinatutako proteoman gertatzen diren aldaketak ere aurkitu daitezke. Hain zuzen ere, metodologia horren bidez *Drosophila* Ube3aren lehendabiziko *in vivo* substratua aurkitu dugu. E3 ligasa hori gizakietan Angelman sindromearen arduraduna da. Gainera, GFP-erauzketa metodo bat garatu dugu proteina bakarra isolatu eta bere ubikuitinatutako frakzioaren ikerkuntza errazten duena. Protokolo horretaz baliatuz, Ube3aren beste lau substratu biokimikoki balioztatu ditugu neurona-antzeko zelula sistema batean.

Laburpena

Tesi honetan garatutako bi metodologiak *in vivo* ubikuitinatutako proteinak aztertzeko oso baliogarriak dira. Horrez gain, ubikuitinazioa ikertzeko dauden beste estrategiak osatzen dituzten abantaila apartak eskaintzen dituzte. Protokolo bi hauen eta ubikuitinazioan arazoak dituzten gaixotasun animali ereduen konbinazioak, patologia hauen mekanismoak hobeto ulertzen lagunduko du etorkizunean.

V. Introduction

1. Ubiquitin-Proteasome System

At the beginning of the twentieth century it was generally believed that the proteins of an organism were predominantly stable and that only those coming from the diet were subjected to catabolism. In 1939, however, experiments performed with isotopically labelled compounds (Schoenheimer *et al.*, 1939) demonstrated that the proteins of an organism were rather in constant renewal, and so they must also be exposed to degradation. This notion was strengthened by the discovery of the lysosomes in the mid 50's (De Duve *et al.*, 1955), but the presence of a cellular organelle containing various hydrolytic enzymes did not fully explain the energy requirement of protein breakdown (Etlinger and Goldberg, 1977) or the different degradation rates at which certain proteins were removed (Goldberg and St John, 1976). Instead, it suggested the existence of other, non-lysosomal, proteolytic system (Etlinger and Goldberg, 1977). It was not until the description in the late 70's of an ATP-dependent reaction in which proteins were covalently modified with a small heat-stable polypeptide (Hershko *et al.*, 1980), known as ubiquitin (Wilkinson *et al.*, 1980), that all these questions started to be elucidated.

The post-translational modification of proteins with ubiquitin, referred to as ubiquitination, is nowadays known to be the main cellular mechanism by which the majority of intracellular proteins are targeted for degradation (Ciechanover, 2013). This process, conserved among eukaryotes, is brought about by the orchestrated activity of three different enzymes: an ubiquitin-activating E1, an ubiquitin-conjugating E2 and an ubiquitin-ligase E3 (**Figure 1**). Briefly, ubiquitin is initially activated by the E1 in an

ATP-requiring reaction. This step is followed by the transfer of the activated ubiquitin to an E2 enzyme, which next attaches ubiquitin to substrates with the assistance of an E3 ligase (**Figure 1**), typically on a lysine residue of the target protein (Glickman and Ciechanover, 2002). With some types of E3s, known as HECT-type (see **Figure 1** and Introduction section 1.1.4: *Ubiquitin-ligase enzymes*), ubiquitin is instead transferred once again from the E2 to the E3 before it is conjugated to proteins. In this case, the attachment of this small polypeptide relies exclusively on the ligase enzyme (Berndsen and Wolberger, 2014).

Ubiquitin has itself seven lysine residues along its sequence that can also be ubiquitinated. By successive repetitions of the E1-E2-E3 cycle, therefore, more ubiquitins can be attached to the previously conjugated ubiquitin to give rise to a poly-ubiquitin chain on the targeted protein (Komander and Rape, 2012). Classically, ubiquitin chains that are formed through the lysine at position 48 of ubiquitin (known as K48 ubiquitin chains) trigger the transport of the modified proteins to a multicatalytic enzyme complex, known as the proteasome (Finley *et al*., 2016), where they are subjected to degradation (**Figure 1**) (Glickman and Ciechanover, 2002). The fate of these proteins, however, is not completely written yet as its degradation can still be prevented by the counteracting activity of the so called deubiquitinating (DUBs) enzymes (**Figure 1**), which remove the attached ubiquitins from the modified proteins (Komander et al., 2009a). Collectively, the whole pathway is usually designated in the literature as the ubiquitin-proteasome system (UPS), as ubiquitinated proteins are often targeted to the proteasome for degradation. However, the research performed on the field since this system was first described (Hershko *et al*., 1980), has revealed that the

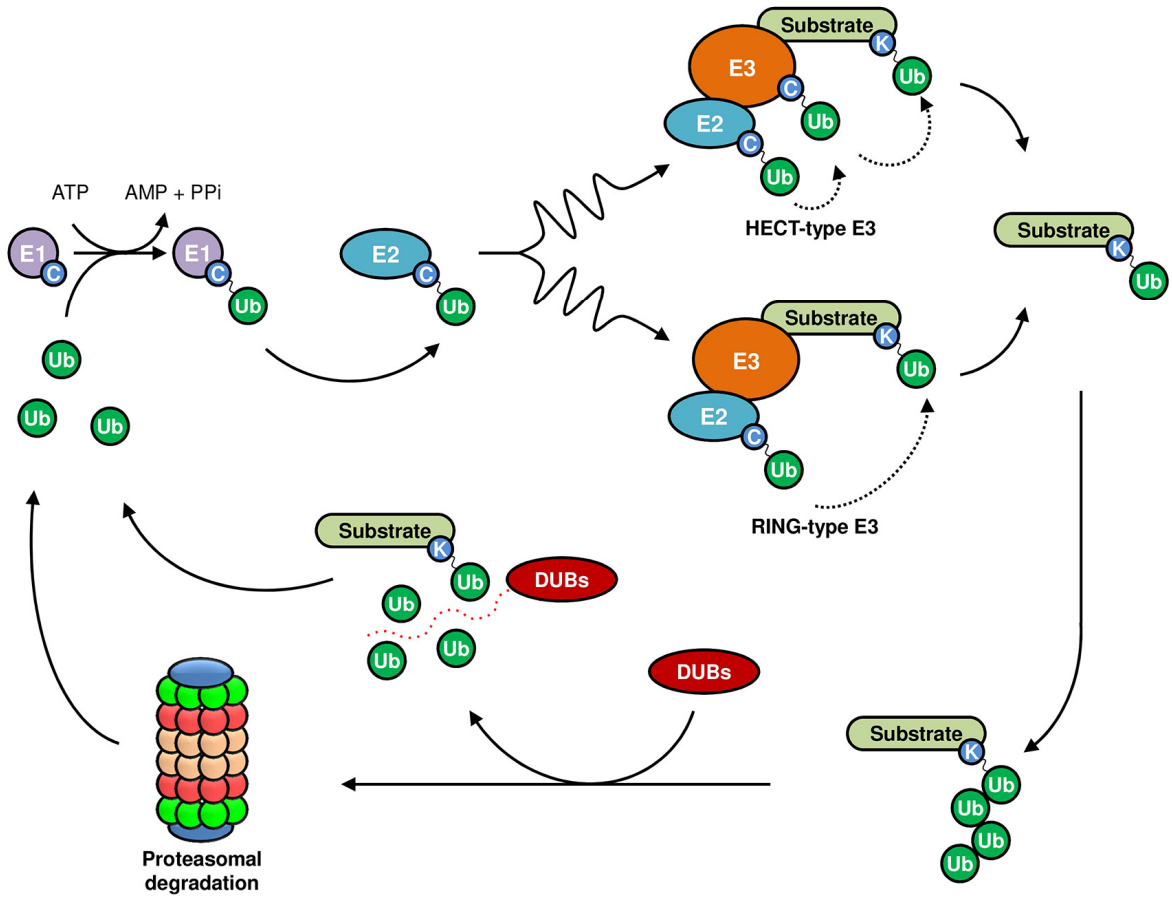

Figure 1. The ubiquitin-proteasome system cycle.

Ubiquitin is activated by the ubiquitin-activating enzyme E1 in an ATP dependent reaction to generate an E1~ubiquitin thioester intermediate. Subsequently, the activated ubiquitin molecule is transferred to the active cysteine residue of an ubiquitin-conjugating enzyme E2, forming a thioester bond. Ubiquitin-charged E2s can then interact with an ubiquitin-ligase E3 enzyme so the ubiquitin is conjugated to a lysine on the target protein via an isopeptide bond. According to the type of E3 that is implicated, ubiquitin can be directly conjugated to the substrate from the E2 (if a RING-type E3 is involved) or transferred once more to a cysteine residue of a HECT-type E3 ligase. The final outcome is the conjugation of one ubiquitin molecule on the target protein, which can be transformed into a poly-ubiquitin chain by the successive repetitions of the E1-E2-E3 cycle. The most common type of ubiquitin chain in the cell is the K48-linked chains, which usually targets tagged proteins to the proteasome where they are degraded and ubiquitin is recycled. Ubiquitinated proteins can also be subjected to the activity of deubiquitinating enzymes (DUBs), in which case their degradation is prevented. Modified from Ciechanover, 2013.

modification of proteins with ubiquitin go far beyond the removal of old or misfolded cellular proteins (Komander and Rape, 2012).

1.1. Components of the Ubiquitin-Proteasome System

1.1.1. Ubiquitin

Ubiquitin is a small polypeptide (8.5 kDa) composed of 76 amino-acids that was first isolated in the search for thymic hormones (Goldstein *et al*., 1975). However, it was not linked with protein degradation until 1980, when it was shown that the ATP-dependent proteolysis factor 1 (APF-1) described by Rose and co-workers (Hershko *et al*., 1980) was indeed ubiquitin (Wilkinson *et al*., 1980). In the genome of eukaryotes ubiquitin is encoded by several genes. In all the cases, it is translated as a precursor, either in the form of a single ubiquitin molecule fused to a ribosomal protein or as a linear poly-ubiquitin chain, which needs to be later digested by DUBs to produce free ubiquitin entities (Kimura and Tanaka, 2010). The attachment of ubiquitin is typically mediated by an isopeptide linkage formed between the carboxyl group of its C-terminal glycine residue and the ε-NH_2-group of an internal lysine of the target protein (Glickman and Ciechanover, 2002). Less commonly, however, ubiquitin can also be attached to the α-NH_2-terminal group of the substrate by a peptide bond (Ciechanover and Ben-Saadon, 2004), as well as to cysteine or serine/threonine residues by thio- or oxy-ester bonds, respectively (Wang *et al*., 2012).

Conjugation of ubiquitin is not restricted to cellular proteins, but it can be additionally bound to ubiquitin molecules that are already associated with a protein. The attachment between distinct ubiquitins can be mediated either through the N-terminus or any of the seven lysines that are found within its sequence (K6, K11, K27, K29, K33, K48 and K63). Consequently, ubiquitin chains of different topology can be built up (Komander and Rape, 2012). This versatility of ubiquitin provides the system with a high complexity capable of regulating not only the degradation of proteins, but also a wide range of biological processes (see Introduction section 1.2: *Roles of protein ubiquitination*).

1.1.2. Ubiquitin-activating enzyme (E1)

Conjugation of ubiquitin requires an initial step in which ubiquitin becomes activated (Glickman and Ciechanover, 2002). This reaction, which entails energy consumption, was discovered to be carried out by an enzyme designated as the ubiquitin-activating enzyme or E1 (Ciechanover *et al*., 1981; Haas *et al*., 1982). The E1 is conserved from yeast to humans, but while in yeast only one gene encodes for it (McGrath et al., 1991), in humans two genes are found to do so (Pelzer *et al*., 2007). Activation of ubiquitin by this enzyme is carried out in a two-step reaction. In the first step, the E1 binds ATP and ubiquitin in order to generate a transient ubiquitin-adenylate intermediate. In the second step, ubiquitin is transferred to a conserved catalytic cysteine of the E1 to which ubiquitin is linked through a thioester bond (Haas *et al*., 1982; Schulman and Wade Harper, 2009). The E1 plays an essential role in the UPS pathway, since in the absence of ubiquitin activation protein ubiquitination is impeded. In fact, deletion of the E1 has

been shown to cause lethality in yeast (McGrath *et al*., 1991), while in humans, missense and synonymous mutations on the E1 gene have been associated with the X-linked Infantile Spinal Muscular Atrophy (Ramser *et al*., 2008).

1.1.3. Ubiquitin-conjugating enzymes (E2s)

The next family of proteins required for the attachment of ubiquitin molecules are the ubiquitin-conjugating enzymes or E2s. This enzymes accept the activated ubiquitin from the E1 and form another thioester bond with ubiquitin (Hershko *et al*., 1983; Glickman and Ciechanover, 2002). There are dozens of genes encoding for E2s throughout the genome of eukaryotes. In humans for instance, 37 genes have been described (Michelle *et al*., 2009). At first, they were considered to be mere transporters of ubiquitin with auxiliary roles. However, it is now known that they have an active role in ubiquitination by determining the length and the topology of the ubiquitin chain that is formed, thereby, determining the fortune of the modified proteins (Ye and Rape, 2009).

Members of this family are characterized by a conserved (~150 amino-acids) ubiquitin-conjugating catalytic (UBC) domain, which embraces a key cysteine that serves as a docking site for ubiquitin (Wijk and Timmers, 2010). Additionally, this domain provides a binding platform for the E1 and E3 enzymes (Burroughs *et al*., 2008). Some E2s present further extensions to the UBC domain, a characteristic that has been historically used to classify them into four categories. Those composed only of the UBC domain, are grouped into the class I enzymes, while those containing extensions either at the N-terminal, C-terminal, or at both sides of the UBC domain, are classified as class

II, III and IV, respectively (WENZEL *et al*., 2010; Wijk and Timmers, 2010). These extensions are involved in functional differences among E2 enzymes, having a role in their subcellular localization, stabilization of the interaction with E1 or in the regulation of the interacting E3 activity (Wijk and Timmers, 2010).

1.1.4. Ubiquitin-ligase enzymes (E3s)

The final step of ubiquitination is carried out by the ubiquitin-ligase enzymes or E3s (Hershko *et al*., 1983; Glickman and Ciechanover, 2002). Among the three types of enzymes involved in ubiquitin conjugation this is by far the largest family, with at least 600 genes encoding for E3 ligases in humans (Li *et al*., 2008). Substrate specificity in ubiquitination is attributed to E3 enzymes, who are able to interact with both the ubiquitin-charged E2s and the substrates to which ubiquitin is going to be transferred (Metzger *et al*., 2014). Typically, one E3 ligase is able to modify several substrates, as well as to bind different E2s. Consequently, the same protein can be ubiquitinated by different E2/E3 combinations, leading to different ubiquitination patterns according to the E2/E3 pair that is involved (Metzger *et al*., 2014). Based on conserved structural domains that participate in E2/E3 interaction and the mechanism by which ubiquitin is transferred from the E2 to the substrates, two main families of E3 ligases are usually distinguished: the Really Interesting New Gene (RING) family and the Homologous to the E6-AP Carboxyl Terminus (HECT) family (Berndsen and Wolberger, 2014).

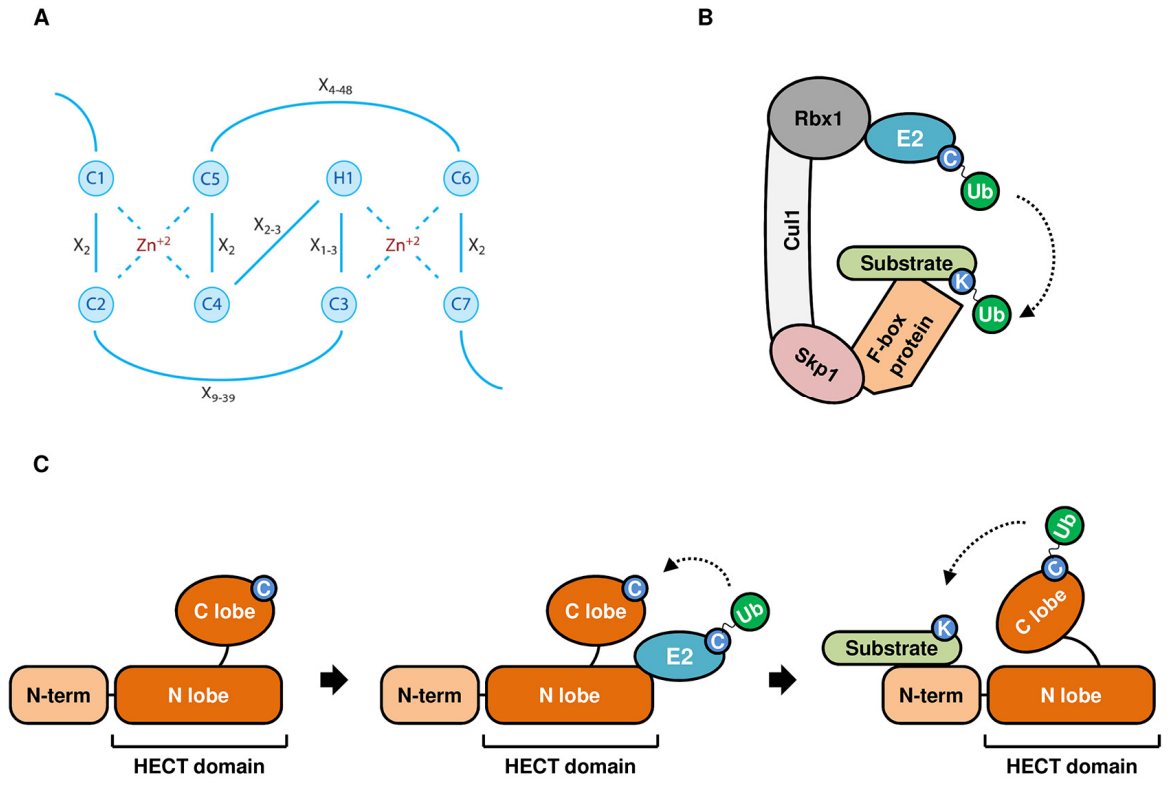

Figure 2. RING and HECT type families of ubiquitin E3 ligases.

A. Sequence of the canonical RING finger domain. It is characterized by several cysteine (C1-C7) and histidine (H1) residues, which are buried within the domain's core and are bound to two molecules of Zn^{2+}. The interaction with Zn^{2+} helps in maintaining the overall structure. X refers to any amino-acid, while the subscript numbers indicate the amount of amino-acids in the region. Taken from Deshaies and Joazeiro, 2009. **B.** Mechanism of RING-type E3 ligase mediated ubiquitin conjugation. RING E3s bind both the E2~ubiquitin and the substrate to be ubiquitinated, and put them close enough to allow the direct conjugation of ubiquitin from the E2. In the representation the SCF E3 complex is shown. Cul1 acts as the main pillar of the complex where the RING Rbx1 protein and an F-box protein, the latter through the adaptor Skp1, are bound. The ubiquitin-loaded E2 interact with Rbx1, while the substrate does with the F-box protein. Modified from Bassermann *et al.*, 2014**. C.** Mechanism of HECT-type E3 ligase mediated ubiquitin conjugation. HECT-domain has an N-lobe and a C-lobe. The E2~ubiquitin binds to the E3 through the N-lobe and transferred the ubiquitin to the catalytic cysteine of the E3, located on the C-lobe. The C-lobe~ubiquitin thioester then rotates to allow the ubiquitin conjugation to the substrates, which is bound to the N-terminal domain of the E3. Modified from Berndsen and Wolberger, 2014**.**

RING-type E3 ligases are characterized by an E2-binding motif, called RING domain, composed of a series of specifically spaced cysteine and histidine residues that adopt a cross-brace structure with two Zn^{2+} ions (**Figure 2A**) (Metzger *et al*., 2014). A related domain is the U-box domain, which adopts a similar structure as the RING motif but does not contain Zn^{2+} ions (Morreale and Walden, 2016). Unlike E1 and E2s, RING-type E3s do not form a catalytic intermediate with ubiquitin. Instead, they function as scaffolding proteins that bring together the E2 and the substrate, so as to facilitate the direct conjugation of ubiquitin from the E2 to the target protein (**Figure 1** and **Figure 2B**) (Deshaies and Joazeiro, 2009; Metzger *et al*., 2014). Members of this family can operate either as monomers, dimers or as part of multi-subunit complexes, such as the Skp1-Cul1-F-box (SCF) or the anaphase-promoting complex/cyclosome (APC/C) E3 ligases (Metzger *et al.*, 2014; Morreale and Walden, 2016). In the case of SCF the RING-box protein 1 (Rbx1) and the S-phase kinase associate protein 1 (Skp1) are organized around the scaffold Cullin 1 (Cul1) protein (**Figure 2B**). Rbx1 provides the E2 binding capacity while Skp1 serves as an adaptor that binds interchangeable F-box proteins, the substrate-binding subunits (Bassermann *et al*., 2014). APC/C, which control cell cycle progression by targeting several proteins for degradation, contains at least 12 subunits (Manchado *et al*., 2010).

HECT-type E3 ligases are characterized by a C-terminal region of about 350 amino-acids, which is homologous to the C-terminal part of its founding member, the human E6-Asociated Protein (E6AP)/UBE3A (Huibregtse *et al*., 1995). This domain adopts a bilobal structure, in which the N-terminal lobe provides the E2-binding area and the C-terminal one a catalytic cysteine residue that associates with ubiquitin via a thioester

linkage (**Figure 2C**) (Scheffner and Kumar, 2014). Alike RING-type E3 ligases, HECT-type enzymes first accept the ubiquitin from the E2 to form a thioester intermediate and then directly perform the conjugation of ubiquitin to the substrate (**Figure 1** and **Figure 2C**) (Huibregtse *et al*., 1995; Scheffner and Kumar, 2014). The binding of the proteins to be ubiquitin-modified is performed through the N-terminal extension of the enzymes, which is additionally used to further classified them into three subfamilies: NEDD4/NEDD4-like E3s, if carrying tryptophan-tryptophan domains, HERC E3s, if Chromosome Condensation 1-like domains are presence, and other HECT type, if neither of this motifs are found (Scheffner and Kumar, 2014).

There are some E3 ligases that combine features with the RING- and HECT-type families. Similar to HECT-type, these enzymes have the ability to generate a thioester intermediate with ubiquitin and like RING-type family members, they contain RING binding domains (Morreale and Walden, 2016). They are known as RING between RING (RBR) E3 ligases, because two RING domains (RING1 and RING2) are separated by a conserved sequence called the in-between RING (IBR) domain (Eisenhaber *et al*., 2007). While the RING1 serves as the E2 binding platform, the RING2 contains a catalytic cysteine that mediates ubiquitination in a HECT E3 ligase fashion (Berndsen and Wolberger, 2014). On the other hand, the IBR is involved in the arrangement of the RING1 and RING2 in order to facilitate the ubiquitination of the target proteins (Beasley *et al*., 2007). Among the E3 ligases comprising this group, Parkin, the enzyme involved in Parkinson's disease is found (Shimura *et al*., 2000; Berndsen and Wolberger, 2014).

1.1.5. Deubiquitinating enzymes (DUBs)

As it happens with other post-translational modification, such as phosphorylation, ubiquitination is also a reversible process. The enzymes counteracting the action of ubiquitin ligases, and hence responsible for removing ubiquitin moieties from target proteins, are called deubiquitinases or deubiquitinating enzymes (DUBs). DUBs are cysteine- and metallo-proteases, encoded in the human genome by about 80 genes, that brake away the isopeptide and peptide bond formed between the ubiquitin and the target proteins (Nijman *et al*., 2005). They are classified into five categories according to sequence and structural similarities of their catalytic domain: ubiquitin C-terminal hydrolases (UCHs), ubiquitin-specific proteases (USPs), ovarian tumour proteases (OTUs), Machado-Joseph disease (MJD) proteases, also known as Josephins, and JAB1/MPN/MOV34 (JAMMs) (Amerik and Hochstrasser, 2004). USP is the largest subfamily of DUBs and together with the other cysteine-proteases (UCHs, OTUs and Josephins) account for more than 80 % of all the DUBs. On the contrary, JAMMs are zinc dependent metallo-proteases (Amerik and Hochstrasser, 2004; Komander et al., 2009a).

At a first glance it might appear that DUBs are exclusively involved in the stabilization of ubiquitinated proteins by preventing their proteasomal degradation. However, the ability of DUB enzymes to discriminate between ubiquitin chains of different topology, together with their capacity to cleave the ubiquitin linkages either from the most proximal part (i.e., from the ubiquitin that is attached to the substrate) or within the ubiquitin chains, have demonstrated that their physiological roles are much wider (Komander et al., 2009a). For instance, it has been shown that DUBs are responsible for

the generation of free ubiquitin (Kimura and Tanaka, 2010), for the maintenance of appropriate ubiquitin levels by recycling the ubiquitin molecules from the proteins that are degraded by the proteasome (Yao and Cohen, 2002), for promoting chromosomal condensation during the metaphase by histone deubiquitination (Mueller *et al*., 1985) and even for controlling the release of neurotransmitters by removing ubiquitin from proteins on the pre-synaptic region (Rinetti and Schweizer, 2010).

1.1.6. Ubiquitin receptors

The coordinated action of E2s, E3s and DUBs can accomplish different type of ubiquitin modifications on the target proteins, ranging from the attachment of a single ubiquitin molecule to the conjugation of mixed and branched poly-ubiquitin chains (see Introduction section 1.2 in: *Roles of protein ubiquitination*). Consequently, the particular signal that each modification triggers needs to be faithfully decoded by the cell. In this process, proteins containing ubiquitin-binding domains (UBDs), known as ubiquitin-receptors, are of special relevance. These proteins interact non-covalently with ubiquitin through their UBDs and translate the ubiquitinated target signal into biochemical cascades in the cells (Dikic *et al*., 2009).

UBDs are structurally diverse and are found in proteins exerting a wide range of biological functions. The first UBDs to be described were the ubiquitin-interacting motifs (UIMs) of the human regulatory particle non-ATPase 10 (PSMD4/RPN10) proteasomal subunit (Young *et al*., 1998). Shortly after, it was shown that the ubiquitin-associated (UBA) domains of the yeast DNA-damage inducible protein 1 (Dd1) and the

radiation sensitivity abnormal 23 (Rad23) protein, also present in many members of the UPS (Hofmann and Bucher, 1996), interact with ubiquitin (Bertolaet *et al*., 2001). Since then, more than twenty families of UBD have been described in the literature, which based on their structure are classified into five subfamilies: α-helices structures (where UIM and UBA are found), zinc fingers, pleckstrin homology fold, ubiquitin conjugating-like structures and others structures (Husnjak and Dikic, 2012).

There are some UBDs that selectively interact with specific poly-ubiquitin chains (Raasi *et al*., 2005; Trempe *et al*., 2005; Sims and Cohen, 2009). An example of those is one of the UBA domains found on Rad23, which shows a stronger preference for K48-linked chains (Raasi *et al*., 2005). In contrast, there are other UBDs that promiscuously bind any type of ubiquitin chain (Raasi *et al*., 2005; Zhang *et al*., 2008). These differences in the specificity of each UBD towards particular ubiquitin modifications is believed to be dictated by the structure of the domain as well as by its localization within the protein (Sims and Cohen, 2009). The exact mechanism by which UBDs recognize various ubiquitin signals and how they are later decoded into specific cellular responses is still not well understood.

1.1.7. Proteasome

Protein degradation is the best characterized role of ubiquitination. This is typically achieved by tagging proteins with a K48-linked poly-ubiquitin chain (Swatek and Komander, 2016). This type of ubiquitin modification triggers the recognition and subsequent transport of the modified proteins to the proteasome, an ATP-dependent

multicatalytic enzyme complex (Matthews *et al*., 1989). Found both in the cytoplasm and the nucleus of eukaryotic cells (Peters *et al*., 1994; Wójcik and DeMartino, 2003), the proteasome is in charge of the degradation of all the ubiquitinated proteins that are brought to it. It is composed of two subunits (**Figure 3A**), the 19S regulatory particle (RP) and the 20S core particle (CP), which are involved in the recognition and degradation of the ubiquitinated substrates, respectively (Finley *et al*., 2016).

The RP flanks both ends of the CP and is subdivided into two sub-complexes (**Figure 3B**), the base and the lid (Lander *et al*., 2012). The lid consists on nine non-ATPase proteins. Of those, the best characterized one is the regulatory particle non-ATPase 11 (Rpn11), a DUB metallo-protease that removes ubiquitin from substrates favouring their translocation to the 20S CP (Verma *et al*., 2002). The remaining subunits are thought to play a scaffolding role to hold Rpn11 on place and regulate its activity (Dambacher *et al*., 2016). Mammalian proteasomes contain two additional associated DUBs, Usp14 and Uch-L5 (Maiti *et al*., 2011).

The base is formed by six ATPase (Rpt1-6) and four non-ATPase proteins: Rpn1, Rpn2, Rpn10 and Rpn13 (**Figure 3B**) (Lander *et al*., 2012). The Rpts form a heterohexameric ring that is predicted to produce a mechanical force on the proteins, at the expense of ATP hydrolysis, so they are unfolded and translocated into the CP of the proteasome (Tomko *et al*., 2010). Rpn10 and Rpn13 are ubiquitin receptors involved in the recognition of poly-ubiquitinated proteins (Deveraux *et al.*, 1994; Husnjak *et al*., 2008), while Rpn1 and Rpn2 perform a similar task by binding ubiquitin-like domains usually found in ubiquitin receptors (Rosenzweig *et al*., 2012).

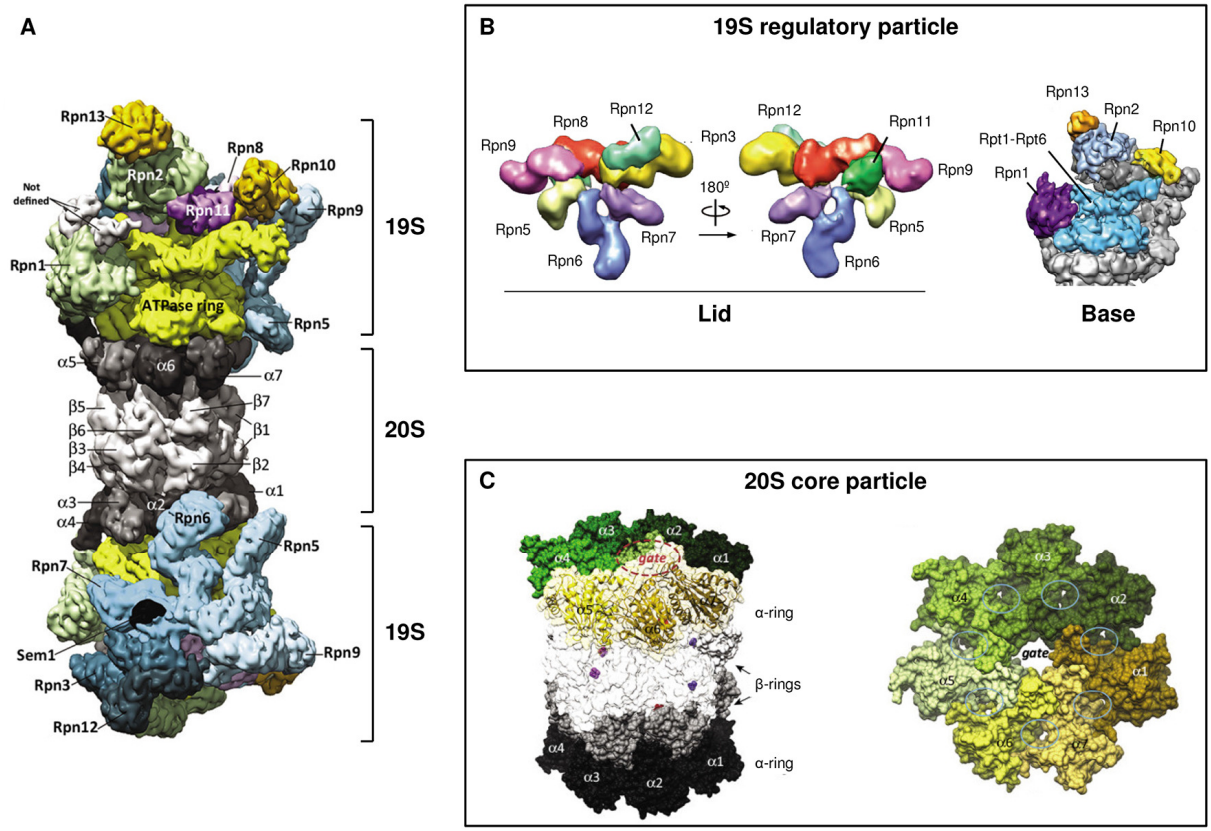

Figure 3. The structure of the 26S proteasome.

A. Cryoelectron microscopy of the yeast proteasome. The 20S core particle (CP) and the two 19S regulatory particles (RP) are indicated. Each 19S RP appears rotated relative to each other by 180º. The name of each subunit is given. Taken from Finley *et al.*, 2016. **B.** The 19S RP of yeast. On the left a 3D reconstruction of the subunits that composed the 19S lid is shown. On the right a cryoelectron microscopy image of the 19S RP, where only the subunits that formed the 19S base are coloured, is provided. Modified from Lander *et al.*, 2012. **C.** The 20S CP of yeast. Lateral (left) and top (right) views of the CP are represented. In both drawings the gate through which proteins are translocated into the CP is indicated. Taken from Finley *et al.*, 2016.

Once proteins are deubiquitinated and unfolded in the RP, they are translocated into the CP (Finley *et al.*, 2016). This barrel-shape structure is composed of 28 subunits that are assembled into four stacked heteroheptameric rings (**Figure 3C**) (Groll *et al.*, 1997).

The two outer rings are composed of α-type subunits, while the two inner rings of β-type subunits (Löwe *et al*., 1995; Finley *et al*., 2016). Three of the β subunits (β1, β2 and β5) are proteolytically active and process hydrophobic, basic and acidic residues, respectively (Finley *et al*., 2016). Their proteolytic sites face toward the interior of the CP (Groll *et al*., 1997). Substrates entering this chamber are rapidly degraded (Finley *et al*., 2016).

1.2. Roles of protein ubiquitination

The extensive research performed during the past 35 years has revealed that, in addition to protein degradation, ubiquitination is involved in a wide range of biological processes (Popovic *et al*., 2014; Swatek and Komander, 2016). This is achieved by the ability of ubiquitin to be further modified, either at its N-terminus or in one of its seven lysine residues (K6, K11, K27, K29, K33, K48, K63) once the first ubiquitin has been conjugated (**Figure 4A**) (Swatek and Komander, 2016). Depending on the lysine of the previously attached ubiquitin that is used for the chain formation, diverse conformations can be generated (**Figure 4B**). Chains built up through the lysine at position 48 (K48-linked chains), for instance, produce a compact conformation (Eddins *et al*., 2007). In contrast, those linked through the lysine at position 63 (K63-linked chains), or through the N-terminus of ubiquitin, present a more open conformation (Komander *et al*., 2009b). Moreover, the lysines used throughout the poly-ubiquitin chain may be the same (homogenous chains), may be alternated (mixed chains) or even multiple lysines of the same ubiquitin may be modified at the same time (branched chains). Consequently, the number of distinct conformations that can be produced are

huge (**Figure 4B**), each of which will have a different readout by the cell (Swatek and Komander, 2016).

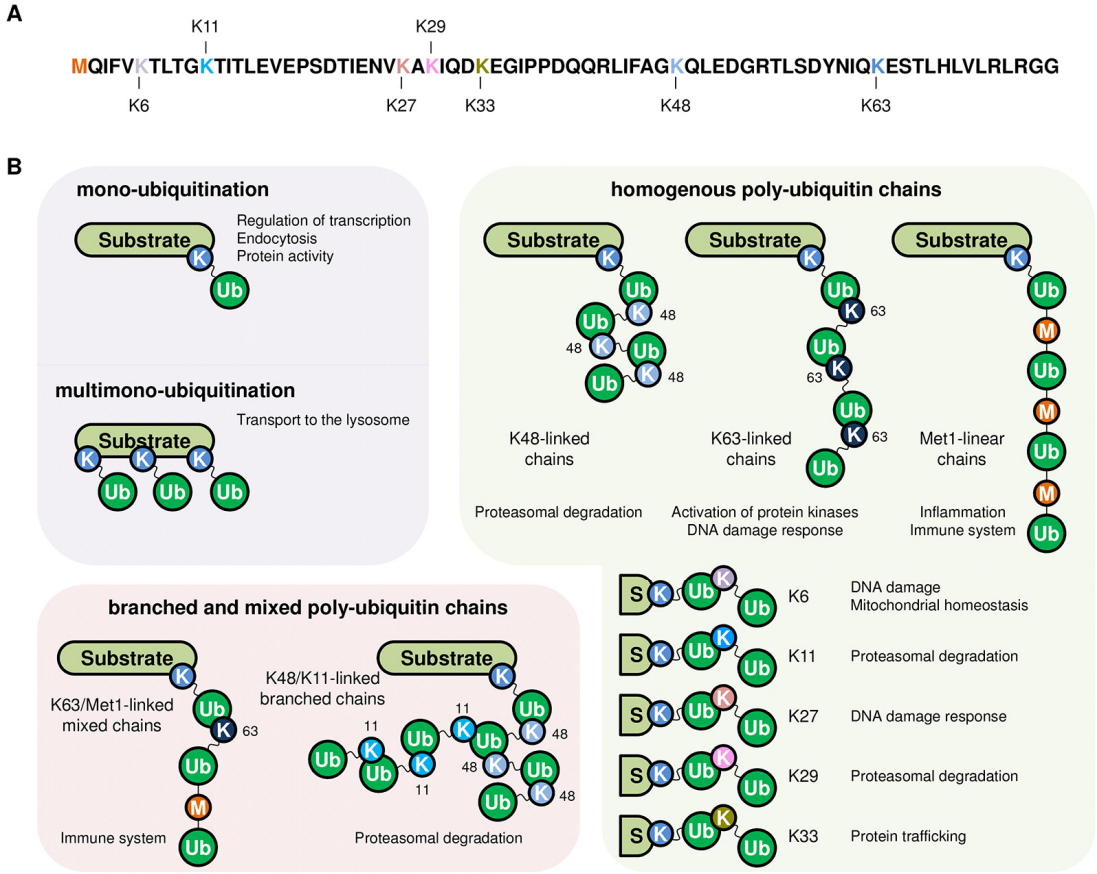

Figure 4. Type of ubiquitin modifications.

A. The protein sequence of ubiquitin. The seven lysine (K) residues found along its sequence, as well as the initial methionine (M), can be used as targets for ubiquitin attachment so poly-ubiquitin chains are built up. M and K are coloured. **B.** Illustration of the different ubiquitin modification that can be performed. Some of the cellular functions in which they are involved are indicated. K48-, K63- and Met1-linked chain are represented with a distinct chain shape (compact, open and linear, respectively) to summarize the diverse ubiquitin chain conformation that can be generated. Modified from Swatek and Komander, 2016.

The simplest conformation consists on the attachment of a single ubiquitin molecule to the substrate (**Figure 4B**), designated as mono-ubiquitination (Hicke, 2001). Protein mono-ubiquitination is an abundant event, accounting for more than 50 % of all the cellular ubiquitin pool (Kaiser *et al*., 2011). This type of modification is known to be involved in many essential cellular roles, such as the regulation of transcriptional activity (Pham and Sauer, 2000), the internalization of plasma membrane proteins (Terrell *et al*., 1998) and the control of protein activity (van Delft *et al*., 1997; Di Fiore *et al*., 2003). Proteins can also be mono-ubiquitinated at multiple lysines (**Figure 4B**), which has been shown to induce the endocytosis and transport of the ubiquitinated proteins to the lysosome (Haglund *et al*., 2003). In this case the term multimono-ubiquitination is used.

Regarding poly-ubiquitin chains (**Figure 4B**) homogenous ones are the best characterized. Among them, the linkage more abundantly found within the cells is that formed through the K48 of ubiquitin, followed by K63-linked chains (Kaiser *et al*., 2011; Swatek and Komander, 2016). K48-linked chains have been classically associated with proteasomal degradation (Thrower *et al*., 2000), but a non-degradative role has also been reported (Flick *et al*., 2006). In contrast, ubiquitin chains form through the K63, have been mainly related to non-degradative roles (Chen and Sun, 2009), such as activation of protein kinases (Deng *et al*., 2000; Newton *et al*., 2008) and recruitment of DNA-damage response elements (Hoege *et al*., 2002; Zhao *et al*., 2007; Bennett and Harper, 2008). However, an involvement on lysosomal degradation of membrane proteins has also been described for K63-linked chains (Huang *et al*., 2013).

The remaining ubiquitin chain types are considered to be atypical due to their lower abundance, but they have also been associated with important biological processes. K6-linked chains have been involved in mitochondrial homeostasis by controlling Parkin activity (Durcan *et al*., 2014). K11-linked chains serves as a proteasomal degradation signal during cell division (Wickliffe *et al*., 2011). K27-linked chains have been proposed to be involved in the recruitment of proteins during the DNA damage response (Swatek and Komander, 2016). K29-linked chains on Rpn13 have been reported under proteasomal stress, suggesting that this chain type may control the proteasomal degradation by preventing the recognition of poly-ubiquitinated proteins (Besche *et al*., 2014). K33-linked chains have been implicated in protein trafficking (Yuan *et al*., 2014) and DNA-damage response (Elia *et al*., 2015). And linear N-terminus ubiquitin chains are implicated in inflammation and immune response (Gerlach *et al*., 2011).

Taking into account the different roles that distinct ubiquitin arrangements can trigger and the complexity that mixed and branched ubiquitin chains (**Figure 4B**) might add to the system (Swatek and Komander, 2016), it is not a surprise to find that failures in this pathway are involved in many human diseases, including cancer (Popovic *et al*., 2014) and neuronal diseases (Kishino *et al*., 1997; Shimura *et al*., 2000; Bertram *et al*., 2005; Ding and Shen, 2008).

1.3. Ubiquitination and nervous system

Evidence of the involvement of the UPS in the nervous system came first from the discovery that ubiquitin was present in the neurofibrillary tangles of various

neurodegenerative diseases (Mori *et al*., 1987; Lennox *et al*., 1988). Henceforth a variety of failures at different levels of the UPS cascade have been linked to several neurodevelopmental disorders: mutations in the E1 are associated with X-linked Infantile Spinal Muscular Atrophy (Ramser *et al*., 2008); the E2-25K E2 enzyme has been implicated in the pathogenesis of Huntington's disease (Wilson *et al*., 2009) and Alzheimer's disease (Song and Jung, 2004); the UBE2H enzyme is associated with autism (Vourc'h *et al*., 2003); loss of the ligase activity of Parkin and UBE3A E3 ligases are linked to autosomal recessive juvenile parkinsonism and Angelman syndrome, respectively (Kishino *et al*., 1997; Shimura *et al*., 2000); down-regulation of the UCHL1 DUB enzyme has also been linked with Parkinson's and Alzheimer's disease (Leroy *et al*., 1998; Choi *et al*., 2004); variants of the Ubiquilin-1 ubiquitin receptor protein are associated with a higher risk of developing Alzheimer's disease (Bertram *et al*., 2005); and disruption of the Rpt2 subunit of the proteasome has been reported to be enough to trigger neurodegeneration (Bedford *et al*., 2008). Such studies have highlighted the relevance of the UPS in neurons.

Nowadays, it is well known that the correct performance of the ubiquitination machinery is essential for the appropriate establishment of neuronal networks, as it regulates the length and the number of axons, dendrites and dendritic spines (Hamilton and Zito, 2013). An accurate balance between the action of E3 ligases and DUBs activities is mandatory for a correct axonal growth. For instance, disruption of Highwire E3 ligase, or overexpression of the Fat facets DUB, leads to a synaptic overgrowth in *Drosophila* neuromuscular junctions (DiAntonio *et al*., 2001). Similarly, mutations in Highwire results in axon guidance defects during the development of the axonal lobes in

Drosophila mushroom body (Shin and DiAntonio, 2011). In addition to orchestrating neuronal connections during development, ubiquitination is also imperative for neurogenesis to successfully take place, as deficiency of the Fbw7 F-box protein, a substrate recognition component of a SCF-type E3 ligase, is sufficient to impair neuronal differentiation in mice (Hoeck *et al*., 2010).

This post-translational modification is not only restricted to development, but is also involved in regulating neuronal function once connections have been established (Yi and Ehlers, 2007). Ca^{2+}-dependent depolarization at the pre-synaptic zone stimulates the exocytic release of neurotransmitters (Pang and Südhof, 2010) and induces a fast decrease of the total levels of the ubiquitinated proteins in rat-brains (Chen *et al*., 2003). Increased neurotransmitter release has also been observed upon proteasome inhibition in cultures hippocampal neurons (Rinetti and Schweizer, 2010). The alterations produced on synaptic transmission by the UPS are typically attributed to an acute control of the synaptic protein turnover, as reported for the vesicle priming-proteins DUNC13 (Speese *et al*., 2003) and Rab3-interacting molecule 1 (RIM1) factor (Yao *et al*., 2007). But the fast deubiquitination of pre-synaptic ubiquitin-modified proteins seems also to contribute to it (Chen *et al*., 2003; Rinetti and Schweizer, 2010).

By contrast, at the post-synaptic side ubiquitination is mainly involved in regulating the composition of the proteins that form the post-synaptic density and the abundance of membrane receptors (Yi and Ehlers, 2007). The stimulation of synaptic activity induces a two-fold increase in protein ubiquitination on post-synaptic density fractions isolated from rat cortical neurons (Ehlers, 2003). On the other hand, neurotransmitter

receptors, such as the α-amino-3-hydroxy-5-methyl-isoxazole-4-propionic acid receptors (AMPARs) have been reported to be ubiquitinated by the neural precursor cell expressed, developmentally down-regulated 4 (Nedd4) E3 ligase, which facilitates their endocytosis from the plasma membrane surface (Lin *et al*., 2011).

2. Angelman syndrome

Angelman syndrome (AS; OMIM #105830) is a rare neurodevelopmental disorder with a prevalence of approximately 1/15.000 individuals (Margolis *et al*., 2015). The first reference to it dates back to 1965, when Dr. Harry Angelman classified three unrelated children with similar physical abnormalities within the same syndrome (Angelman, 1965). AS is characterized by a severe intellectual and developmental delay, movement or balance disorders, speech impairment and a happy demeanour (**Figure 5**) that includes episodes of frequent laughter and easy excitability (Williams *et al*., 2010). Very frequently (>80 % of the cases) these symptoms are accompanied by seizures, sleep disturbances and microcephaly (Williams *et al*., 2010; Bird, 2014).

The syndrome is commonly diagnosed when children are 1-2 years old, as clinical symptoms are usually manifested after the first year of age (Margolis *et al*., 2015).

Figure 5. Pictures of children with Angelman syndrome.

Six patients with a genetically confirmed diagnosis of AS. A happy expression is commonly observed in affected individuals. Taken from Williams *et al*., 2010.

Affected people's lifespan is not reduced and both development and fertility are normal. However, independent living is not possible for adults with AS, so they require the presence of a caregiver along their life (Bird, 2014). Currently there is not specific treatment for AS, but drugs to mitigate seizures and sleeping problems are usually administered in combination with physical therapies to improve the motor deficits (Margolis *et al*., 2015).

2.1. Genetic causes of Angelman syndrome

In 1987 two unrelated females, with clinical feature consistent with AS, were found to carry a deletion on the 15q11-q13 chromosomal region (Magenis *et al*., 1987). This chromosomal deletion had been previously found on patients diagnosed with Prader-Willi syndrome (PWS), a complex genetic disorder characterized by infantile hypotonia, obesity and behavioural issues (Kalsner and Chamberlain, 2015). How the same deletion could result in different syndromes was soon elucidated. The parental origin of the deletion was discovered to have a great influence in the development of each syndrome. Whereas deletions inherited on the paternal chromosome lead to PWS, those inherited on the maternal chromosome result on AS. These findings suggested that genes within the 15q11-q13 locus were subjected to genomic imprinting (Knoll *et al*., 1989; Magenis *et al*., 1990). Currently, it is known that some of the genes within this chromosomal region are either maternally, paternally or biallelically expressed (**Figure 6A**) (Margolis *et al*., 2015).

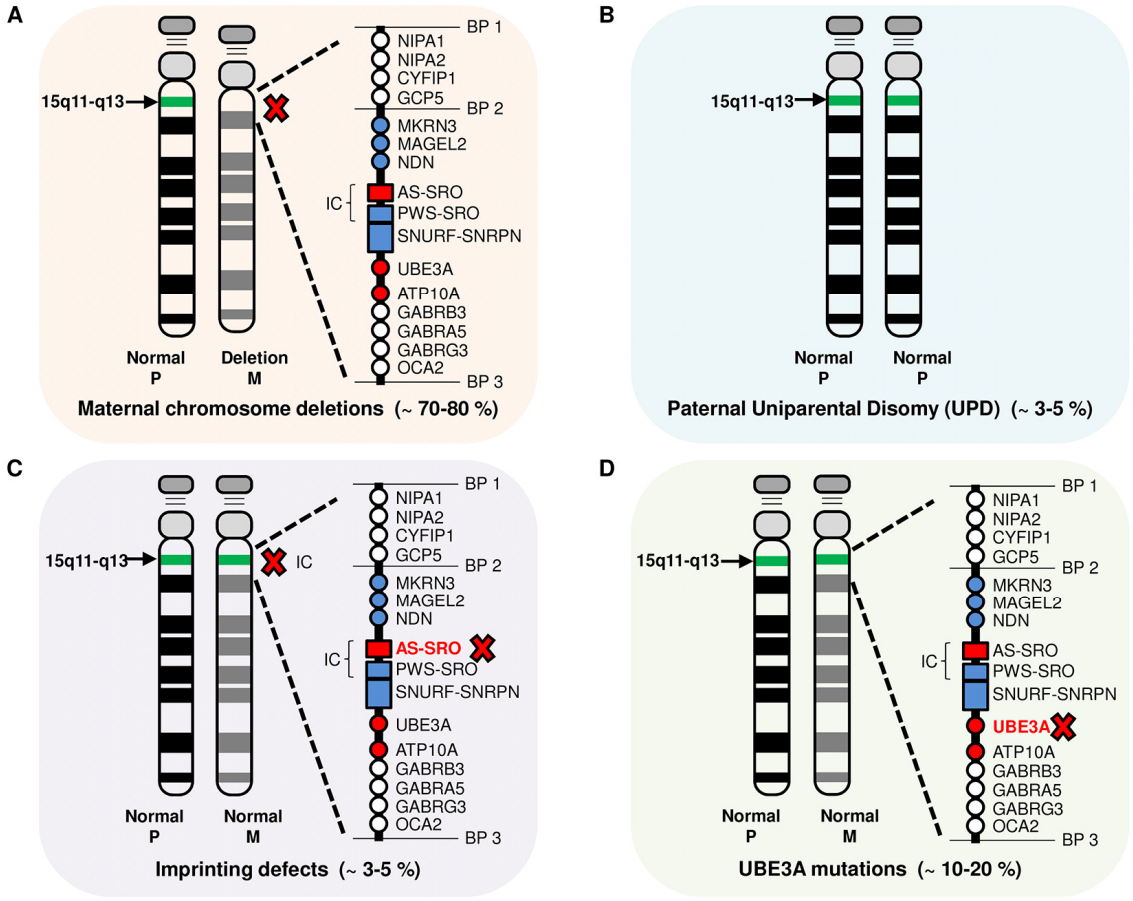

Figure 6. Genetic mechanisms that produce Angelman syndrome.

A. Maternal deletions of the 15q11-q13 chromosomal regions are the most frequent genetic mechanism that lead to AS. Genes on this region are either biallelically expressed (white), paternally expressed (blue) or maternally expressed (red). The most common breakpoints involved in the deletions (BP1, BP2 and BP3), where low copy repeats are found, are indicated. **B.** Inheriting both chromosomes 15 from the father, known as paternal uniparental disomy, results in the loss of maternally expressed genes as both chromosomes present equal imprinting pattern. **C.** Aberrant methylation patterns or microdeletion on a chromosomal region designated as imprinting centre (IC), results in imprinting defects that produce silencing of maternally expressed genes. The deleted region shared by all affected individuals has been shown to be 880 bp long, which is designated as the shortest region of deletion overlap (SRO). **D.** Mutations on the *UBE3A* gene that disrupt the encoded protein have been found in AS patients. Thus the loss of function of this gene is considered the underlying molecular mechanism of AS. Modified from Williams *et al*., 2010.

Deletions on the long arm of the maternal chromosome 15 are typically a result of non-allelic homologous recombination due to the presence of low copy repeats in the 15q11-q13 area (LaSalle *et al*., 2015). They span about 5-7 Mb and are usually produced through three breakpoints (BP1, BP2 and BP3 in **Figure 6A**). According to the breakpoints that are involved two classes of deletions are distinguished. Class I are those produced through BP1 and BP3, while in class II BP2 and BP3 are implicated (Sahoo *et al*., 2007). This type of genetic defect, however, accounts for about ~70-80 % of all the AS cases (Margolis *et al*., 2015). Additionally, ~3-5 % (**Figure 6B**) of the cases have been reported to be arisen from paternal uniparental disomy (UPD), i.e., if both chromosomes 15 are of paternal origin (Nicholls *et al*., 1992; Margolis *et al*., 2015). The presence of two paternal chromosomes 15 results in the loss of function of maternally expressed genes. Another ~3-5 % are due to imprinting defects on the maternal chromosome (**Figure 6C**), which are derived either from microdeletions in a region of the chromosome 15 designated as imprinting centre (Buiting *et al*., 1995) or from epigenetic mutations that lead to abnormal DNA methylation patterns (Buiting *et al*., 2003). Similar to UPD cases, imprinting defects result in silencing of maternally expressed genes. The phenotype produced by UPD or imprinting defects has nevertheless been reported to be less severe than that one brought about by deletions (Williams *et al*., 2010; Bird, 2014). This suggests that biallelically expressed genes within the 15q11-q13 locus can affect the severity of the disease (LaSalle *et al*., 2015)

The underlying molecular cause behind the mentioned chromosomal and epigenetic anomalies was discovered to be the loss of function of the UBE3A protein (**Figure 6D**). Mutations leading to truncated forms of UBE3A were reported to be enough to develop

the syndrome (Kishino *et al*., 1997; Matsuura *et al*., 1997). Additionally, this gene, located on the 15q11-q13 critical region, was confirmed to be paternally imprinted in the brain (Rougeulle *et al*., 1997). Therefore, either deletions, UPD or imprinting defects on the maternal chromosome would also lead to the loss of UBE3A function, further supporting a central role of this gene in the aetiology of AS. During the last years different mutations on UBE3A, most of them nonsense and frameshift mutations, have been found in AS patients, accounting for ~10-20 % of the AS cases (Sadikovic *et al*., 2014; Margolis *et al*., 2015).

2.2. UBE3A E3 ligase protein

UBE3A is an ubiquitin E3 ligase enzyme of approximately 100 kDa (Scheffner *et al*., 1993). According to *in vitro* studies it catalyses the preferential attachment of K48-linked chains, thus presumably targets its substrates for proteasomal degradation (Wang and Pickart, 2005). It was first discovered by its ability to form a complex with the E6 oncoprotein of the human papillomavirus types 16 and 18 and promote p53 ubiquitin-dependent degradation (Huibregtse *et al*., 1991; Scheffner *et al*., 1993). This is why it was first named as E6-Associated Protein (E6-AP) (Huibregtse *et al*., 1991). The discovery that this enzyme could form a thioester intermediate with ubiquitin through a cysteine residue located at its C-terminal part (Scheffner *et al*., 1995), as well as that this region of over 350 amino-acid was conserved among different proteins (Huibregtse *et al*., 1995; Scheffner *et al*., 1995), led to the characterization of the HECT (Homologous to the E6-AP Carboxyl Terminus) domain (**Figure 2C**) and the functionally related HECT-type E3 ligase family (see Introduction section 1.1.4: *Ubiquitin-ligase enzymes*).

In humans, the *UBE3A* gene encodes at least three different isoforms that differ in their amino-terminal part due to alternative splicing of the first 8 exons (Yamamoto *et al*., 1997; LaSalle *et al*., 2015). Three isoforms have also been described in mice, but only the isoform 2 (equivalent to human isoform 3) has been reported to have the capability to rescue the dendritic phenotype found in an AS mouse model (Miao *et al*., 2013). In *Drosophila* only one isoform has been described (Wu et al., 2008). The physiological functional differences of the alternative isoforms are still not well understood. Neither it is their significance toward AS. However, transcripts corresponding to the human isoform 3 have been found in a variety of organism, suggesting that this isoform might be of higher relevance (LaSalle *et al*., 2015).

In neurons, while the paternal UBE3A allele is silenced (Rougeulle *et al*., 1997) the maternal copy is expressed, both in the nucleus and the cytoplasm (Dindot et al., 2008). Interestingly, the paternal imprinting is found restricted to the brain since biallelical expression of UBE3A is detected in other tissues (Rougeulle *et al*., 1997; Vu and Hoffman, 1997). This suggests that the levels of this enzyme have to be tightly controlled in the brain so its function is properly accomplished. In fact, while absence of UBE3A is the base of AS, extra doses of this protein in the brain are associated with autism spectrum disorders (ASDs) (Smith *et al*., 2011; Urraca *et al*., 2013; Noor *et al*., 2015; Yi *et al*., 2015). Despite a secondary function as a coactivator for nuclear hormone receptors has also been described for UBE3A, mutations affecting its ubiquitin-ligase activity, but that leave intact the coactivator function, have been reported on AS patients (Nawaz et al., 1999). Consequently, the ligase activity is thought to be responsible of the AS phenotype. Similarly, the ligase activity has also been associated with ASDs (Yi *et al*.,

2015). Thus, identifying the ubiquitin substrates of UBE3A in neurons is required for the better understanding of the pathophysiology of both AS and ASD.

2.3. UBE3A ubiquitin substrates

Since AS was linked to UBE3A mutations (Kishino *et al*., 1997; Matsuura *et al*., 1997) many attempts have been performed in order to identify the substrates of this enzyme. The first one to be reported as a UBE3A target was p53. An increase in the total levels of p53 in UBE3A deficient mice brains was reported, suggesting it was due to the failure of the ubiquitin dependent degradation of p53 (Jiang *et al*., 1998). Over the following year several proteins were proposed as UBE3A substrates. The multicopy maintenance protein (Mcm) 7 subunit, a protein involved in DNA replication, and the proapoptotic Bak protein were shown to interact with UBE3A in HeLa and HEK293 cells, respectively (Kühne and Banks, 1998; Thomas and Banks, 1998). A reduction of the total protein level in the presence of UBE3A was described for Blk, a membrane-bound non-receptor tyrosine kinase, in COS-7 cells (Oda *et al*., 1999). The yeast Rad23 human homologue (HHR23A) was shown to be ubiquitinated by UBE3A *in vitro* (Kumar *et al*., 1999). And even UBE3A was described to be itself auto-ubiquitinated *in vitro* as a self-regulatory mechanism (Nuber *et al*., 1998).

The arrival of mass spectrometry-based strategies allowed the identification of additional proteins as potential UBE3A ubiquitin substrates. The Rho-guanine-nucleotide exchange factor (RhoGEF) Pebble (Pbl) and the Na^+/K^+ ATPase (Atpα) were proposed as UBE3A targets in *Drosophila melanogaster* heads (Reiter *et al*., 2006; Jensen

et al., 2013). Similarly, the activity-regulated cytoskeleton-associated (Arc) protein and the RhoGEF Ephexin 5 were proposed as UBE3A candidates in mice brain (Greer *et al*., 2010; Margolis *et al*., 2010). And Annexin A1 was suggested as being regulated by UBE3A in human carcinoma cells (Shimoji *et al*., 2009).

Several other proteins have been described as UBE3A substrates in the literature, including the amplified in breast cancer 1 (AIB1) protein (Mani *et al*., 2006), p27 (Mishra *et al*., 2009a) and Ring1B (Zaaroor-Regev *et al*., 2010). The biochemical validation of the *in vivo* ubiquitination of all these UBE3A potential substrates in a neuronal context, however, has still remained a challenge. Evidence of the direct ubiquitination of some UBE3A putative substrates (AIB1, Bak, Blk, Mcm7, p53, Pbl) remains absent, as changes in their total protein levels in the presence/absence of UBE3A or interaction with UBE3A have only been reported (Jiang *et al*., 1998; Kühne and Banks, 1998; Oda *et al*., 1999; Mani *et al*., 2006; Reiter *et al*., 2006; Margolis *et al*., 2010). The direct ubiquitination by UBE3A of other putative substrates (Arc, HHR23A, Na^+/K^+ ATPase, p27, Ring1B, UBE3A) has only been validated *in vitro* (Nuber *et al*., 1998; Kumar *et al*., 1999; Greer *et al*., 2010; Mishra *et al*., 2009a; Zaaroor-Regev *et al*., 2010; Jensen *et al*., 2013). Or in the case of Annexin A1 and Ephexin 5 using non-denaturing immunoprecipitation approaches, which leaves the possibility to the detected signal been due to co-purifying proteins (Shimoji *et al*., 2009; Margolis *et al*., 2010).

The lack of *in vivo* evidence of the direct ubiquitination of the potential substrates by UBE3A has, as a consequence, produced controversial results. Arc ubiquitination, for

instance, was recently shown not be controlled by UBE3A in cells (Kühnle *et al*., 2013) and additionally suggested that it could rather be regulated by a different E3 ligase enzyme (Mabb *et al*., 2014). Similarly, the Na^+/K^+ ATPase was found to be upregulated in AS mouse model, but was reported not to be a substrate of UBE3A since no interaction between Na^+/K^+ ATPase and UBE3A could be detected from mice brain hippocampal homogenates (Kaphzan *et al*., 2011). The fact that proteins that might not be directly ubiquitinated by UBE3A are also affected in AS or ASD patients, suggests an indirect effect produced by the misregulation of upstream proteins (the "true" UBE3A substrates) in the affected pathways (Sell and Margolis, 2015). The relevance that these indirect substrates has in the phenotype of these two syndromes should not be undervalued, but it should be kept in mind that identifying the direct UBE3A ubiquitin substrates is indispensable in order to properly understand the pathophysiology of AS.

3. Methodology to study ubiquitination

Isolation and identification of ubiquitinated proteins under physiological conditions from *in vivo* tissues is a challenging task, as the ubiquitin modified proteins are generally found at very low levels within the cells. Besides, the fast kinetics at which some of the proteins conjugated with ubiquitin are degraded (Choi et al., 2013), the action of the deubiquitinating enzymes (Stegmeier *et al*., 2007) or the fact that proteins might be modified with ubiquitin only in well-defined temporal windows (Clute and Pines, 1999), make even more difficult their analysis. The identification of the proteins that are ubiquitinated in a given tissue is, however, mandatory in order to better understand the role that ubiquitination plays *in vivo*. In recent years, mass spectrometry (MS) based ubiquitin proteomics have proven to be a good strategy for this purpose, and thus, it has become a routinely used technique for the large-scale identification of ubiquitinated proteins.

3.1. Mass spectrometry

In proteomics a mass spectrometer is used to measure the mass-to-charge ratio (m/z) of previously ionized peptides and make a record of their abundance (Steen and Mann, 2004). In a typical MS-based proteomics experiment, proteins extracted from cells or tissues are subjected to trypsin digestion. Afterwards, the resulting peptides are separated by chromatography and loaded into the mass spectrometer, where they are ionized and separated according to their m/z ratio. The molecular weights of the

peptides relative to their charge are then measured and used to identify the proteins they correspond to.

A mass spectrometer is typically composed of four main components: an ion source, a mass analyser, a fragmentation chamber and an ion collection/detection system (Yates *et al*., 2009). The ion source converts the molecules to be analysed, such as the peptides generated by trypsin digestion, into charged ions. The mass analyser is responsible for separating the produced ions according to their m/z ratio. The fragmentation chamber is where ionized peptides (precursor ions) are further chopped into fragment ions, so information of their amino-acid sequence can be obtained. And the ion collection/ detection system records the number of ions at each m/z values (Finehout and Lee, 2004; Steen and Mann, 2004; Yates et al., 2009).

The Electrospray Ionization (ESI) and the Matrix Assisted Laser Desorption/ Ionization (MALDI) are the most used ionization techniques in proteomics (Karas and Hillenkamp, 1988; Fenn *et al*., 1989). In the case of ESI, ions are produced from samples found in solution by applying high voltage, resulting in a spray of highly charged droplets that are then desolvated. By contrast, samples are co-crystalized within an organic matrix and then irradiated with laser pulses in MALDI, resulting in ions in the gas phase (Yates *et al*., 2009).

The peptides that have been transformed into ions are then separated according to their m/z ratio by the application of an electrical or magnetic field in the mass analyser. Four types of mass analysers are commonly used in proteomics: Quadrupole, Ion-Traps,

Time-Of-Flight and Fourier-Transform Ion Cyclotron Resonance, which vary in their physical principles and analytical performance (Yates *et al*., 2009). For instance, the amount of time required for an ion to travel a known distance is measured in Time-Of-Flight analysers, but different voltages are applied in Quadrupole and Ion-Traps, so ions with a particular m/z ratio are only allowed to pass through the analyser. In addition, they have different sensitivities, resolution and scanning rates, thus, according to the researcher requirements the use of some might be more suitable than others (Domon and Aebersold, 2006; Yates *et al*., 2009).

After determining the m/z of the peptides a second stage of MS can be applied. This is known as tandem MS and is abbreviated as MS/MS. At this stage selected ions (precursors) are further broken into pieces in a fragmentation chamber in order to obtain additional information about the composition of the peptide sequence (Steen and Mann, 2004). The precursor and corresponding fragment ions are then loaded into specific software suits that determine the identity of the proteins present in the sample by comparing the experimental MS data with the theoretical mass of the proteins defined in a database. As the sequence of each protein is unique, so are the peptides that can be generated from each protein by proteolytic cleavage. Thus, knowing the mass of each peptide their sequence can be determined and ultimately the proteins they come from identified.

The number of ions of a given m/z ratio are also recorded by the detector/collection system and translated into a measurable electric current. This value, usually designated as intensity, correlates with the peptide abundance and thus can be employed for

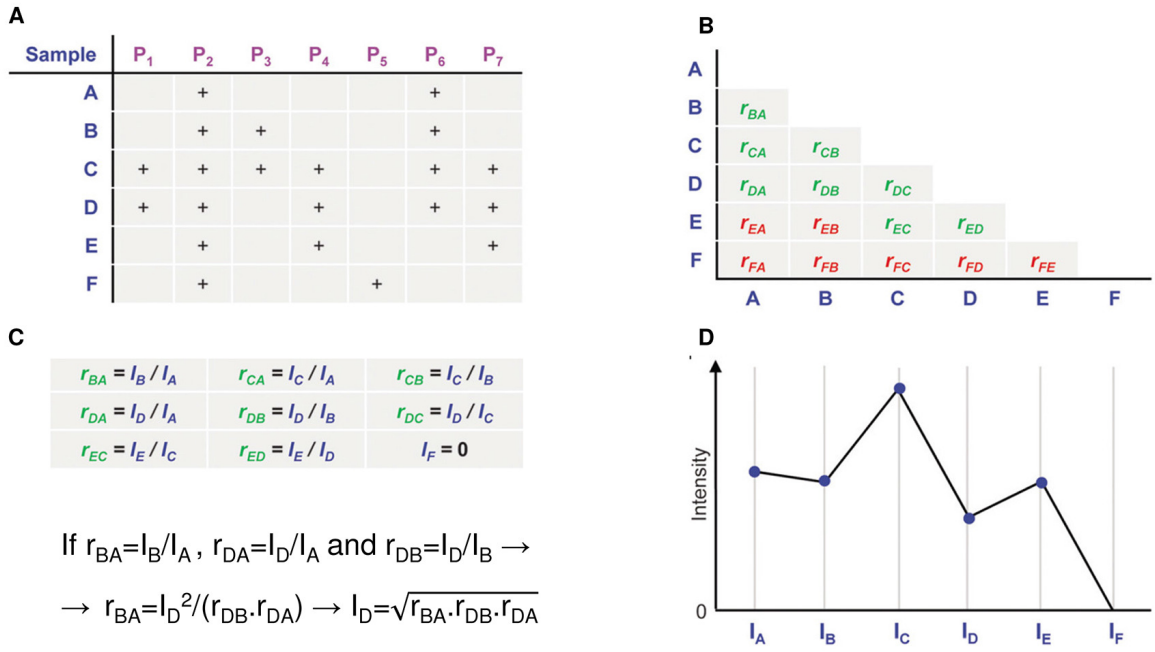

Figure 7. LFQ quantification method used by MaxQuant software.

A. Occurrence matrix of peptide species (P_1-P_7) in six MS samples (A-F). Peptide presence is indicated by a plus symbol. MaxQuant employs the intensities occurring in both samples to calculate peptide ratios. For instance, to calculate the ratio between sample B and C only P2, P3 and P6 will be taken into account. **B.** Matrix of protein ratios between samples. Median of the peptide ratios is calculated in order to provide a protein ratio (r) between samples. Only if a minimum number of two peptide ratio are available the protein ratio is considered valid. Valid and invalid protein ratios are shown in green and red respectively. **C.** System of equations that need to be solved to obtain the protein abundance profiles (I). If a sample has no valid ratio with any other sample, like sample F, the intensity is set to 0. An example of how I_D would be calculated is shown. **D.** The protein abundance profile obtained after solving the equations from C. The absolute profile scale is adapted to match the summed-up raw peptide intensities. Modified from Cox *et al.*, 2014.

quantification purposes. However, distinct peptides have different physico-chemical properties that influence their MS behaviour, and hence their intensity. For this reason, peptides intensities have to be first normalized in order to appropriately estimate the

protein abundance. One of the most commonly used protein quantification strategy at present that employ peptide intensities is the so called Label Free Quantification (LFQ). Among the softwares available, MaxQuant has been used during this Thesis project to process the raw MS files and calculate the LFQ intensity (Luber *et al*., 2010; Cox *et al*., 2014). Using a specific algorithm that normalizes the data across different mass spectrometric runs (**Figure 7**) the LFQ data provides accurate quantification of the protein abundance within the samples (Cox *et al*., 2014).

3.2. Historically used strategies to enrich ubiquitinated material

Despite the great potential of MS analysis, the low stoichiometry at which ubiquitinated proteins are found within the cells makes it necessary to carry out an enrichment of the ubiquitinated material prior the MS analysis (Mayor and Peng, 2012). So far several methods have been developed with that purpose with the help of ubiquitin-specific antibodies (Matsumoto *et al*., 2005; Vasilescu *et al*., 2005; Xu *et al*., 2010), ubiquitin-binding domains (UBDs) (Bennett *et al*., 2007; Lopitz-Otsoa *et al*., 2012) or epitope-tagged versions of ubiquitin (Greer *et al*., 2010; Peng *et al*., 2003). Employment of ubiquitin antibodies, UBDs or certain types of epitope-tags, such as HA, however, requires the purification to be performed under native conditions. Affinity pulldowns that cannot withstand denaturing conditions usually result in the co-purification of proteins that are probably not ubiquitin conjugates, but interacting proteins (Tirard *et al*., 2012). Additionally, non-denaturing conditions are favourable to any protease or DUB activity, so a reduction in the yield of purified material might also occur.

The proteolytic digestion with trypsin that usually precedes the MS analysis produces peptides that contain either an arginine or a lysine residue at their C-terminal (Olsen *et al*., 2004). Modification with ubiquitin, however, prevents tryptic digestion after the modified lysines, and additionally, it leaves the last two glycine residues of ubiquitin still covalently attached to the lysine (**Figure 8**). This signature peptide, commonly known as di-gly signature, produces a mass shift on the peptides of 114.1 Da that is detectable by MS (Peng *et al*., 2003). In recent years, this di-gly signature has been exploited for the development of specific antibodies that allow the isolation and enrichment of di-gly containing peptides (Xu *et al*., 2010). Ubiquitin-remnant di-gly specific antibodies have been used so far for the isolation and identification of thousands of putative ubiquitination sites in a number of systems (Xu *et al*., 2010; Kim *et al*., 2011; Wagner *et al*., 2011; Na *et al*., 2012; Wagner *et al*., 2012; Sarraf *et al*., 2013). It should be noted, however, that a di-gly remnant is also left by other ubiquitin-like proteins, such as Nedd8 or ISG15. Under physiological circumstances Nedd8 and ISG15 modifications are found at lower levels than ubiquitination, but their concentration dramatically increases if the proteasome is blocked, a strategy commonly used in ubiquitome studies (Leidecker *et al*., 2012). Besides, the use of di-gly specific antibodies requires the proteins to be trypsin digested, preventing any immunoblotting on the purified material to validate and further characterize their ubiquitination.

Alternatively, enrichment of ubiquitinated proteins can be carried out under denaturing condition, so interacting proteins are discarded and the material is further protected from the activity of proteases. Classically, poly-histidine tagging has been used for that purpose (Hitchcock et al., 2003; Peng et al., 2003; Mayor et al., 2007; Xu et al.,

2009). However, one concern using this approach would be the presence of too many endogenous histidine-rich proteins in mammals, which would also be trapped in the nickel affinity beads, resulting in excessive background.

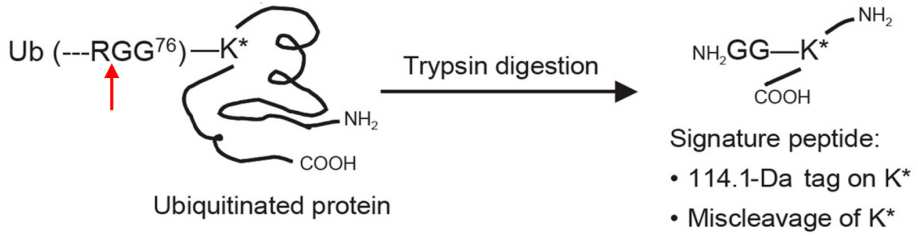

Figure 8. The di-gly signature left on ubiquitinated proteins after trypsin digestion.

Trypsin digests proteins after arginine and lysine residues. When an ubiquitin molecule is attached, however, the modified lysine is protected from the proteolytic activity of the enzyme and the last two glycines of ubiquitin are left covalently attached to it, resulting in a small increase of the peptide's molecular weight (114.1 Da). Red arrow denotes the trypsin cleavage on the last arginine residue of ubiquitin. Taken from Peng *et al*., 2003.

3.3. *In vivo* biotinylation of ubiquitin: the ^{bio}Ub strategy

Biotin-dependent carboxylases are a type of enzymes, widely distributed in nature, that are involved in the metabolism of fatty-acids, amino-acids and carbohydrates. They contain a biotin carboxyl carrier protein (BCCP) component where a covalently linked biotin molecule serves as an acceptor-donor of CO_2 molecules (Tong, 2013). The attachment of biotin to BCCP is mediated through the ε-amino group of a lysine residue and is catalysed by the so called biotin holoenzyme synthetase enzymes (Kwon and Beckett, 2000). This biotinylation reaction is highly specific and only few proteins are

found to be modified with biotin *in vivo* (Chandler and Ballard, 1985). Interestingly, the minimal peptide that can be efficiently biotinylated by the *E.coli* biotin holoenzyme synthetase enzyme (BirA) was described to be 14 amino-acid long (Beckett et al., 1999). This finding provided a powerful tool for the generation of fusion proteins that can be easily purified or detected thanks to their biotin tag.

Based on this, the laboratory of Dr. Ugo Mayor developed a strategy for the *in vivo* isolation of ubiquitin conjugates (Franco et al., 2011). This approach has so far allowed the purification and enrichment of hundreds of ubiquitin conjugates from flies (Franco *et al*., 2011; Ramirez *et al*., 2015), mice (Lectez *et al*., 2014) and human cell lines (Min *et al*., 2014). The system relies on the *in vivo* expression of the *E. coli* BirA enzyme as a fusion protein with multiple copies of ubiquitin, each of which bear a 16 amino-acid long biotinylatable motif at their N-terminal part (**Figure 9A**). Six modified ubiquitins and BirA are produced as a precursor polypeptide. As it happens with the endogenous ubiquitin genes (Kimura and Tanaka, 2010), the precursor is digested by the endogenous DUBs, so individual ubiquitin molecules and BirA are released (**Figure 9B**). BirA then recognizes the biotinylatable motif at the N-terminus of the ubiquitin moieties and conjugates a biotin molecule on them (**Figure 9C**). That way, a pool of biotinylated ubiquitin is generated within the cells, which is employed by the UPS machinery together with the endogenous ubiquitin (**Figure 9D**). Having the cellular proteins conjugated with biotinylated ubiquitin allows the use of avidin-beads for their isolation and enrichment (**Figure 9E**). Thanks to the strong affinity ($K_d \sim 10^{-15}$ M) of the avidin-biotin interaction (Marttila et al., 2000), very stringent washes can be applied to the biotinylated material that is bound to avidin resins (Franco *et al*., 2011). Therefore, all

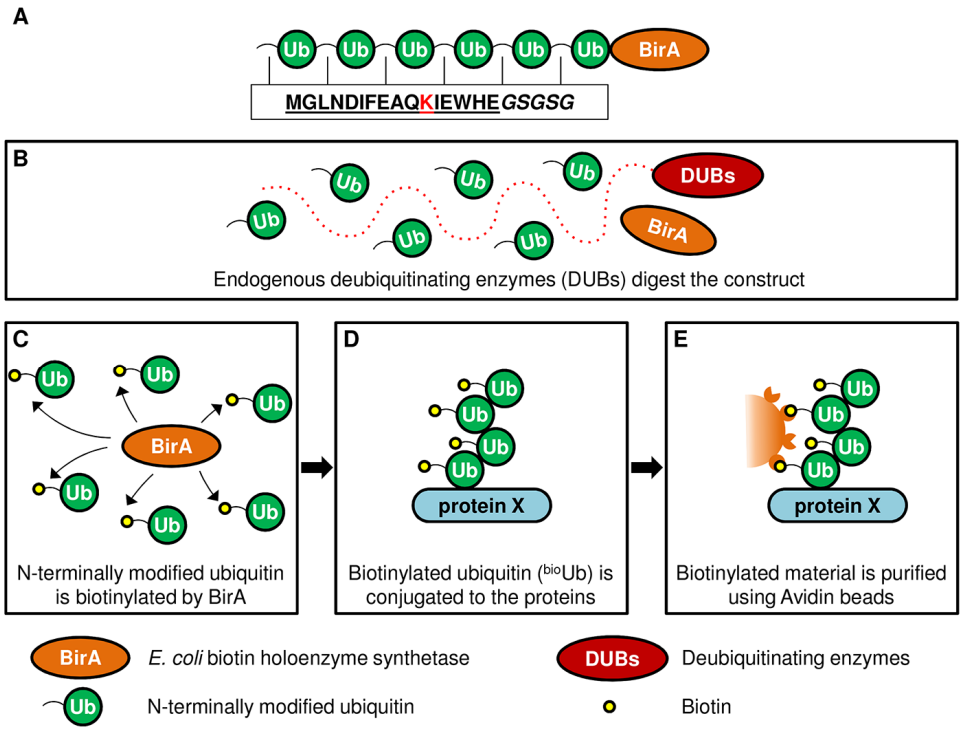

Figure 9. The *in vivo* biotinylation of ubiquitin: the ^{bio}Ub strategy.

A. The construct is expressed as a poly-ubiquitin chain fused to BirA. The sequence added at the N-terminal part of each ubiquitin molecule is shown. The target sequence for biotinylation is underlined, with the lysine where the biotin is attached highlighted in red. A five amino-acid linker (*italicised*) was additionally introduced to improve the accessibility of the ubiquitin conjugates to the avidin resin. **B**. Endogenous DUBs process the fusion ubiquitin-BirA polypeptide. The same way endogenous ubiquitin precursors are digested, DUB enzymes cut after the last glycine of each ubiquitin, generating free biotinylatable ubiquitin moieties and the BirA enzyme. **C**. BirA catalyses the conjugation of biotin to the target sequences. The BirA enzyme recognizes the short motif incorporated at the N-terminus of each ubiquitin and attaches a biotin molecule to it. Thus, a pool of biotinylated ubiquitin is generated. **D.** The biotinylated ubiquitin is then conjugated to the cellular proteins. Endogenous ubiquitin will compete with the ectopic biotinylated ubiquitin. However, the conjugation of one biotinylated ubiquitin should be enough for their isolation. **E.** Avidin beads are used to purify the ubiquitinated material. The strong interaction of avidin-biotin allows the use of very stringent washes, so interacting proteins are discarded. Modified from Franco *et al.*, 2011.

interacting proteins are removed and only ubiquitinated material and a few endogenously biotinylated carboxylases are purified. The isolated material can then be subjected to MS or Western blot analysis (Franco *et al*., 2011; Lectez *et al*., 2014; Min *et al*., 2014; Ramirez *et al*., 2015).

4. *Drosophila melanogaster*

At the beginning of the 20th century Williams E. Castle initiated studies on *Drosophila melanogaster* in his laboratory at Harvard University (Cambridge, USA) (Castle, 1906; Roberts, 2006). Since then, many studies performed with the fruit fly have helped in the understanding of basic biological processes conserved from invertebrates to humans. Probably, the most famous are those carried out by Tomas H. Morgan that led to the discovery of the sex-linked inheritance (Morgan, 1910) and to the confirmation of the chromosomal theory of inheritance (Doncaster, 1916; Roberts, 2006). He was awarded the Nobel Prize in Physiology and Medicine in 1933 for these works. Additional outstanding breakthroughs have been achieved using *Drosophila* during the past 110 years, also worthy of Nobel Prizes, such as the discovery of the mutagenic activity of the X-rays by Hermann J. Muller (Muller, 1927), the characterization of essential genes that control early embryonic development by Edward B. Lewis, Christiane Nüsslein-Volhard and Eric F. Wieschaus (Lewis, 1978; Nüsslein-Volhard and Wieschaus, 1980), or the identification of the Toll receptor as a key component required for the immune system activation by Jules Hoffmann (Lemaitre et al., 1996).

Three of the essential features for which *Drosophila* has gained such a success as a model organism are 1) its fast generation time, 2) ease of culture and 3) low maintenance cost. Besides, it contains a smaller genome distributed into one X/Y pair of sex-chromosomes and three pairs of autosomes (Adams *et al*., 2000). This greatly simplifies the genetics and the understanding of the biological functions of *Drosophila* genes, as the gene redundancy found in higher organisms is reduced. Significantly, about 75 % of human genes involved in disease have an homologue in the fly (Reiter *et al*.,

2001). Thus, *Drosophila* provides a simpler *in vivo* system in which to study the role of those genes (Pandey and Nichols, 2011). In fact, many human diseases have been modelled in flies with that purpose (Sang and Jackson, 2005; Jackson, 2008; Pandey and Nichols, 2011).

The tools and resources that have been developed over the past century for working with *Drosophila*, such as the tissue- and time-specific expression systems (see Introduction section 4.2: *GAL4/UAS binary system*), the different mutant lines or the balancer chromosomes (Bier, 2005; Matthews *et al*., 2005), have turned this small arthropod into an invaluable animal model for research that has little to envy to its mammalian colleagues.

4.1. Life cycle of *Drosophila melanogaster*

Drosophila is a holometabolous insect that undergoes complete metamorphosis. Their life cycle is divided into four main stages according to morphology: egg, larva, pupa and adult fly (**Figure 10**). The time that is required for an egg to develop into an adult fly varies with temperature, being shorter at higher temperatures. Fly embryogenesis takes place during the first 24 h following fertilization at 25 ºC. During this first day the main endodermal-, mesodermal- and ectodermal-derived larval tissues and organs are developed. Subsequently, a tiny-worm like animal hatches, known as the first instar larva (L1). L1 larva feeds for 24 h and moults into a bigger second instar larva (L2), who equally moults into the third instar larva (L3) after feeding for about another 24 h. The main external difference between L1, L2 and L3 larvae is their size, being L3 the biggest

and L1 the smallest. The L3 larval stage (about 2-3 days) is followed by the pupal stage. Shortly before pupation, larva stops feeding and finds a dry place suitable for pupation. The larva then becomes motionless and gradually acquires its pupal shape. Throughout the subsequent ~4-5 days metamorphosis occurs, and most of the larval structures are lysed or modified, leading to adult organ development. 10-11 days after the initial fertilization, the adult fly emerges from the pupa.

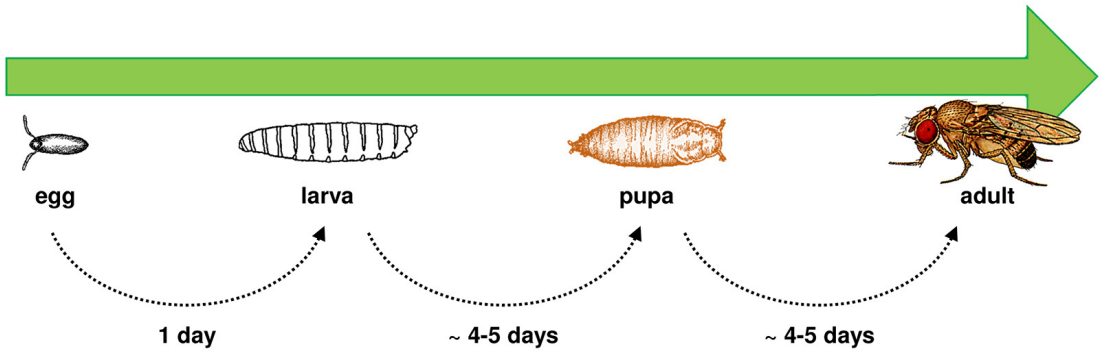

Figure 10. *Drosophila melanogaster* life cycle.

The four main stages during the *Drosophila* life cycle and the time that each stage last at 25 ºC is shown. The egg, larva, pupa and adult figures were taken from the interactive fly web page (Brody, 1999).

4.2. GAL4/UAS binary system

The GAL4 is a yeast transcription factor that promotes the expression of genes required for the catabolism of galactose (Traven *et al*., 2006). It recognizes specific DNA sites -known as upstream activating sequence (UAS)- that have the 5'-CGG-N_{11}-CCG-3' consensus sequence, where N_{11} correspond to any 11 bases (Marmorstein *et al*., 1992).

Upon galactose induction, GAL4 binds as a dimer to the UAS and activates nearby gene's transcription by recruiting co-activators and the general transcription machinery (Traven *et al*., 2006). Interestingly, the expression of GAL4 in *Drosophila* tissues was also demonstrated to induce the transcription of a reporter gene, which had been placed downstream a 17-mer sequence closely-related to UAS (Fischer *et al*., 1988).

Cahir J. O'Kane and Walter J. Gehring showed that the cell/tissue expression pattern of randomly inserted genes in the *Drosophila* genome, was affected by the transcriptional regulatory elements adjacent to their insertion sites (O'Kane and Gehring, 1987; Wilson *et al*., 1989). Based on this and on the ability of GAL4 to activate transcription in *Drosophila* (Fischer et al., 1988), Andrea H. Brand and Norbert Perrimon developed what is known as the GAL4/UAS system (Brand and Perrimon, 1993). They designed a vector (pUAST) in which genes could be inserted behind five tandemly arrayed UAS sites, so their transcription was subjected to the presence of the GAL4 protein (**Figure 11**). On the other hand, they generated two vectors that allow the expression of GAL4 either under the control of characterized *Drosophila* promoters or under endogenous genomic enhancers (**Figure 11**). In both cases, a tissue-specific GAL4 expression pattern is achieved (Brand and Perrimon, 1993). This binary system in which each vector (i.e., GAL4 and UAS vectors) is found in separated *Drosophila* lines (**Figure 11**), has been a revolutionary breakthrough as it allows for a huge number of combinations for the expression of any gene/protein of interest (including those that might cause lethality) in a tissue- and time-specific manner.

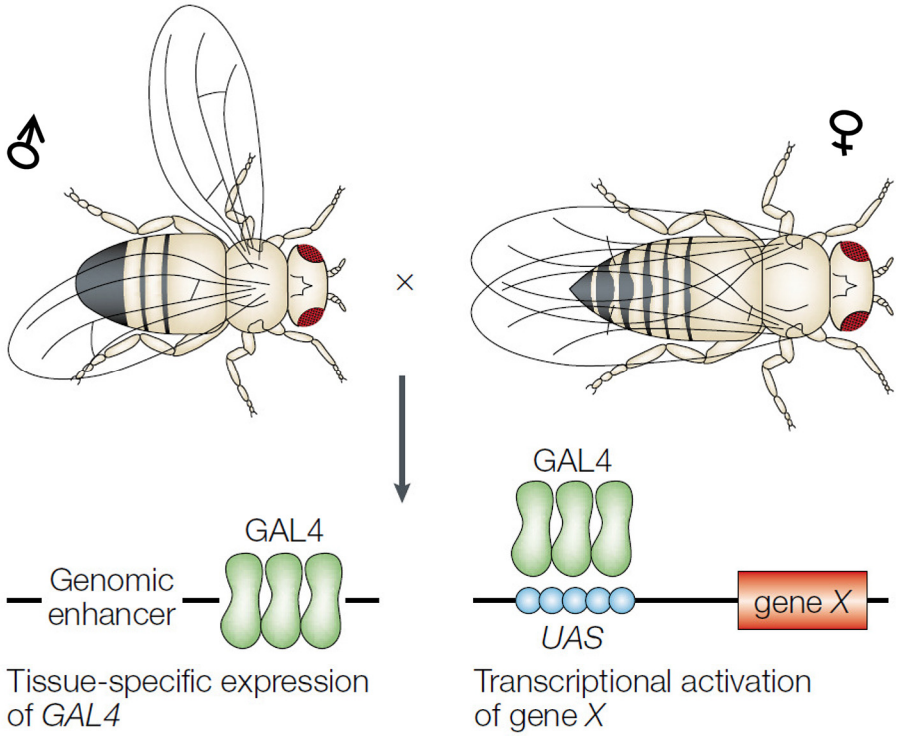

Figure 11. GAL4/UAS binary system.

The GAL4/UAS system consists of two elements: The yeast GAL4 protein and the upstream activating sequence (UAS) that can be placed before any gene of interest. GAL4 can be expressed in *Drosophila* in a tissue and time specific manner, either under the control of genomic enhancers located nearby its insertion site or under known promoters placed upstream the GAL4. On the other hand, the addition of the UAS next to a gene of interest (gene X) allows its expression to be dependent on the presence of GAL4. Thus, crossing flies that carry any UAS-gene X construct to flies with a given tissue GAL4 distribution will produce a progeny that expresses the gene X with the same pattern as the GAL4. Taken from St Johnston, 2002.

VI. Hypothesis and Objectives

The main interest of the laboratory where this Thesis project was carried out is the understanding of the role that ubiquitination plays in the nervous system. The low levels at which proteins modified with ubiquitin are found within the cells, however, make the study of this post-translational modification a difficult task to perform. Dr. Mayor's laboratory developed recently the ^{bio}Ub strategy, a novel approach based on the *in vivo* biotinylation of ubiquitin, that allows the efficient isolation and subsequent MS identification of the most abundant ubiquitin conjugates during the *Drosophila* embryo nervous system development (Franco et al., 2011). We then hypothesized that this strategy could also be expanded and applied for the identification of ubiquitin-modified proteins from other *Drosophila* tissues. Particularly, we hypothesized that this strategy could be used to monitor changes in the ubiquitination profiles caused by the blockade of the proteasomal degradation or to determine the specific substrates of an E3 ligase involved in disease.

The main objectives of this Thesis project have been the following:

1. To expand the ^{bio}Ub strategy to the *Drosophila* adult brain in order to identify those proteins that are being ubiquitinated in the context of a mature neuron.
2. To identify the *Drosophila* neuronal ubiquitin proteome that is accumulated upon inhibition of proteasomal degradation.
3. To identify the direct substrates of Ube3a, the fly homologue of the Angelman syndrome-causing UBE3A E3 ligase in *Drosophila* neurons.
4. To develop new strategies to further study and characterize the ubiquitination of the proteins isolated and identified by the ^{bio}Ub strategy.

VII. Materials and Methods

1. *Drosophila melanogaster*

1.1. Fly husbandry procedures

All *Drosophila* fly lines were grown and mated, unless otherwise indicated, at 25 ºC in 12 hours light-dark cycles in wheat flour and yeast medium, which contained 1 % of agar (Industrias Roko), 5.5 % of dextrose (VWR Chemicals), 3.5 % of wheat flour (Carrefour) and 5 % of yeast (Ynsadiet) in distilled H_2O. To prevent mould and bacterial growth 0.25 % of Nipagin (Lemmel), 0.4 % of propionic acid (Sigma) and 0.02 % of benzalkonium chloride (Sigma) were added to the food mixture when it had cooled down below 60 ºC and before aliquoting into the plastic bottles (Scientific Laboratory Supplies) and vials (Genesee Scientific).

1.2. Fly strains employed

The yeast GAL4/UAS binary system (Brand and Perrimon, 1993) was employed to drive the expression of the different transgenes used in this work. Flies expressing GAL4 under the following promoters were used: the eye-specific Glass Multimer Reporter-GAL4 (*GMR*^{GAL4}; Hay *et al*., 1994), the pan-neuronal embryonic lethal abnormal vision-GAL4 (*elav*^{GAL4}; Luo *et al*., 1994), the heat shock inducible-GAL4 (*Hs*^{GAL4}; Brand *et al*., 1994), the tubulin-GAL4 (*Tub*^{GAL4}; Lee and Luo, 1999) and the vesicular glutamate transporter-GAL4 (*OK371*^{GAL4}; Mahr and Aberle, 2006). In addition, flies expressing a temperature sensitive version of the GAL4-repressing protein, GAL80, under the control

of the tubulin promoter (*Tub*^{GAL80ts}; McGuire et al., 2003), were also used to avoid the lethality caused by Tub^{GAL4}-driven expression. Tissue expression patterns of GAL4 and GAL80 proteins with the mentioned promoters are shown in **Table 1**. *GMR*^{GAL4} (BL 1104), *elav*^{GAL4} (BL 8765), *Hs*^{GAL4} (BL 2077), *Tub*^{GAL4} (BL 5138) and *Tub*^{GAL80ts} (BL 7017) flies were supplied by the Bloomington *Drosophila* Stock Center (BDSC, Bloomington, IN, USA). The *OK371*^{GAL4} line was kindly provided by Cahir O'Kane (University of Cambridge, UK).

Table 1. *Drosophila* GAL4 and GAL80 lines used.

Genotype	GAL4- or GAL80-driver	Expression	Abbreviation
w*; GMR-GAL4	Glass Multimer Reporter-GAL4	eye	*GMR*^{GAL4}
elav-GAL4/CyO	embryonic lethal abnormal vision-GAL4	nervous system	*elav*^{GAL4}
Hsp70-GAL4	Heat shock inducible-GAL4	ubiquitous	*Hs*^{GAL4}
yw; TubP-GAL4	α-Tubulin-GAL4	ubiquitous	*Tub*^{GAL4}
VGlut^{OK371}-GAL4	Vesicular glutamate transporter-GAL4	glutamatergic neurons	*OK371*^{GAL4}
w*; TubP-GAL80ts	α-Tubulin-GAL80 temperature sensitive	ubiquitous	*Tub*^{GAL80ts}

Fly genotypes, names of the GAL4- and GAL80-drivers, tissue where GAL4 and GAL80 proteins are expressed and abbreviation with which each line is designated, are shown. All drivers are inserted on the second chromosome with the exception of *Tub*^{GAL4} and *Tub*^{GAL80ts} that are on the third one.

Drosophila transgenic lines carrying an insert preceded by an upstream activating sequence (UAS), so as to be expressed only in the presence of GAL4, are listed in **Table 2**. Flies expressing a precursor protein composed of six biotinylatable ubiquitin moieties, fused to the *E. coli* biotin ligase (BirA) enzyme were used (*^{UAS}(^{bio}Ub)$_6$-BirA*) for studying the ubiquitinated proteome in *Drosophila* tissues. As control, flies that express only the *E. coli* BirA enzyme (*^{UAS}BirA*) were used. Both flies were previously generated by Professor Ugo Mayor (Franco *et al*., 2011). Flies overexpressing the C-terminal half of the regulatory particle non-ATPase 10 protein (*^{UAS}Rpn10-ΔNTH*), kindly provided by Dr. Zoltan Lipinszki (Lipinszki *et al*., 2009), were employed for the analysis of proteins that

accumulate upon proteasome blockade. An Ube3a gain of function ($^{UAS}Ube3a^{A3}$) fly line was utilized to identify the substrates regulated by Ube3a E3 ligase. As a control, flies with the *w; If/CyO; Ube3a*^{15B}*/TM6* genotype were used, which bear a deletion on the *Ube3a* gene (designated as *Ube3a*^{15B} allele) that results in no protein production. These two fly lines were a gift from Professor Janice Fischer (Wu *et al*., 2008). Additionally, $^{UAS}GFP^{CL1}$ flies expressing Green Fluorescence Protein (GFP) fused to a degradation signal that leads to its fast degradation (Pandey *et al*., 2007), *OregonR* flies (BL 2376) as wild type strain, as well as *Sco/CyO* (BL 2555) and *w*^{1118}*; Bl/CyO; TM2/TM6B* (BL 3704) balancer flies to set up stable lines, were used. Wild type and balancer flies were obtained from the BDSC.

Table 2. *Drosophila* UAS lines used.

Genotype	Description	Abbreviation
yw; UAST-BirA	Express *E. coli* BirA enzyme	$^{UAS}BirA$
yw; UAST-(*^{bio}*Ub)*$_6$*-BirA	Express biotinylated ubiquitin and BirA	$^{UAS}(^{bio}Ub)_6$*-BirA*
yw; UAST-GFP-(*^{bio}*Ub)*$_6$*-BirA	Express GFP, biotinylated ubiquitin and BirA	$^{UAS}GFP(^{bio}Ub)_6$*-BirA*
w*^{1118}*; If/CyO; UAST-Rpn10-ΔNTH	Express C-terminal half of the Rpn10 protein	$^{UAS}Rpn10$*-ΔNTH*
w; If/CyO; UAST-Ube3a*^{A3}*/TM6B	Express Ube3a E3 ligase	$^{UAS}Ube3a^{A3}$
UAST-CL1-GFP	Express GFP protein carrying a degradation signal	$^{UAS}GFP^{CL1}$

Fly genotypes, description and abbreviation with which each line is designated are shown. $^{UAS}BirA$ and $^{UAS}(^{bio}Ub)_6$*-BirA* flies carry the insert on the second chromosome. In the case of $^{UAS}BirA$, flies carrying the insert on the third chromosome were used too. $^{UAS}GFP(^{bio}Ub)_6$*-BirA*, $^{UAS}Rpn10$*-ΔNTH*, $^{UAS}Ube3a^{A3}$ and $^{UAS}GFP^{CL1}$ have the constructs inserted on the third chromosome.

1.3. Fly crosses performed

Generation of *elav*^{GAL4},$^{UAS}(^{bio}Ub)_6$*-BirA/CyO* stable line, for the analysis of the ubiquitinated material in the *Drosophila* embryo nervous system development, has been previously described (Franco *et al*., 2011). For the analysis of the ubiquitinated material

in the fly photoreceptor cells the *GMR*^{GAL4},^{UAS}*(*^{bio}*Ub)*$_6$*-BirA/CyO* stable line was generated. *GMR*^{GAL4} homozygous flies were first mated to homozygous ^{UAS}*(*^{bio}*Ub)*$_6$*-BirA* ones. *GMR*^{GAL4}*/*^{UAS}*(*^{bio}*Ub)*$_6$*-BirA* heterozygous females obtained in the offspring were further crossed to *Sco/CyO* balancer males, so as to get flies where a recombination event has occurred. Afterwards, *GMR*^{GAL4},^{UAS}*(*^{bio}*Ub)*$_6$*-BirA/CyO* recombinants were stabilized by crossing one more time to *Sco/CyO* flies and selecting those in the offspring carrying both constructs over the *CyO* chromosome. As a control for embryonic samples the *elav*^{GAL4},^{UAS}*BirA/CyO* line was used (Franco *et al*., 2011). In the case of adult samples, the recombination of *GMR*^{GAL4}-driver with the ^{UAS}*BirA* construct could not be achieved and hence, flies carrying the ^{UAS}*BirA* transgene on the third chromosome (*GMR*^{GAL4}*/CyO;* ^{UAS}*BirA/TM6B*) were used instead.

Flies with the *elav*^{GAL4},^{UAS}*(*^{bio}*Ub)*$_6$*-BirA/CyO;* ^{UAS}*Rpn10-ΔNTH/TM6B* and *GMR*^{GAL4}*,* ^{UAS}*(*^{bio}*Ub)*$_6$*- BirA/CyO;* ^{UAS}*Rpn10-ΔNTH/TM6B* genotypes were employed for the analysis of the proteins that accumulate upon proteasome blockade in the embryo nervous system and in the adult eye, respectively. They were generated by crossing two times *elav*^{GAL4}*,* ^{UAS}*(*^{bio}*Ub)*$_6$*-BirA/CyO* and *GMR*^{GAL4},^{UAS}*(*^{bio}*Ub)*$_6$*-BirA/CyO* flies to *If/CyO; TM2/TM6B* ones, in order to obtain the *elav*^{GAL4},^{UAS}*(*^{bio}*Ub)*$_6$*-BirA/CyO; TM2/TM6B* and *GMR*^{GAL4}*,* ^{UAS}*(*^{bio}*Ub)*$_6$*-BirA/CyO; TM2/TM6B* double balanced lines, which were then crossed to *If/CyO;* ^{UAS}*Rpn10-ΔNTH/TM6B* flies.

The identification of Ube3a E3 ligase substrates was carried out with *elav*^{GAL4},^{UAS}*(*^{bio}*Ub)*$_6$*-BirA/CyO;* ^{UAS}*Ube3a*^{A3}*/TM6B* and *elav*^{GAL4},^{UAS}*(*^{bio}*Ub)*$_6$*-BirA/CyO; Ube3a*^{15B}*/TM6B* flies in embryo, and with *GMR*^{GAL4},^{UAS}*(*^{bio}*Ub)*$_6$*-BirA/CyO;* ^{UAS}*Ube3a*^{A3}*/*

TM6B and *GMR^{GAL4},^{UAS}(^{bio}Ub)$_6$-BirA/CyO; Ube3a^{15B}/TM6B* in adult. These *Drosophila* lines were generated by crossing *If/CyO; ^{UAS}Ube3a^{A3}/TM6B* and *If/CyO; Ube3a^{15B}/TM6B* animals to *elav^{GAL4},^{UAS}(^{bio}Ub)$_6$-BirA/CyO*; *TM2/TM6B* and *GMR^{GAL4}, ^{UAS}(^{bio}Ub)$_6$-BirA/CyO; TM2/TM6B* double balanced flies.

Analysis of the *in vivo* interaction between Ube3a and Rpn10 was performed with flies carrying simultaneously the *^{UAS}Ube3a^{A3}* and *^{UAS}Rpn10-ΔNTH* constructs on the same chromosome (*If/CyO; ^{UAS}Ube3a^{A3},^{UAS}Rpn10-ΔNTH/TM6B*). This line was obtained by recombining If/CyO; ^{UAS}*Ube3a^{A3}/TM6B* with *If/CyO; ^{UAS}Rpn10-ΔNTH/TM6B* following the same procedure described for *elav*^{GAL4},^{UAS}*(^{bio}Ub)$_6$-BirA/CyO* and *GMR*^{GAL4},^{UAS}*(^{bio}Ub)$_6$-BirA/CyO* lines (see above). *If/CyO; ^{UAS}Ube3a^{A3},^{UAS}Rpn10-ΔNTH/TM6B* flies were then mated to *elav^{GAL4},^{UAS}(^{bio}Ub)$_6$-BirA/CyO; TM2/TM6B* and to *GMR^{GAL4},^{UAS}(^{bio}Ub)$_6$/CyO; TM2/TM6B* lines in order to analyse their isolated ubiquitinated material. The eye phenotype was evaluated after crossing *If/CyO; ^{UAS}Ube3a^{A3},^{UAS}Rpn10-ΔNTH/TM6B* with *GMR^{GAL4}* flies. Flies carrying each construct independently were also crossed to *GMR^{GAL4}*. Flies expressing at the same time Ube3a^{A3} and GFP^{CL1}, under the control of GMR^{GAL4}, were additionally created to discard the possibility of the eye phenotype being rescued due to lower ratio of GAL4 protein for each UAS site.

1.4. Fly sample collection

Embryo sample collection was performed at 25 ºC by enclosing flies in ventilated fly cages with Petri dishes containing an apple juice-rich agar layer, made of 2.5 % of agar (Industrias Roko), 2.5 % of dextrose (VWR Chemicals), 25 % of apple juice (Carrefour),

0.25 % of Nipagin (Lemmel) and distilled H_2O, partially covered with yeast paste (Levital). Flies were then let to lay eggs over a 12 hour period, after which the Petri dishes were substituted. The 0-12 hours old embryo laid were then allowed to further age for 9 extra hours at 25 ºC, so the embryos were 9-21 hours old (stage 13 to stage 17) at the time of extract preparation. The embryos were washed with 1X Phosphate Buffered Saline (PBS) from Fisher Scientific, containing 0.1 % Triton X-100 (Sigma), dechorionated with 50 % bleach solution for 3 minutes, immediately washed with PBS-Triton (0.1%), collected into tubes and flash frozen in liquid nitrogen before been stored at -80 ºC.

Drosophila heads were collected from flies grown at 25 ºC in wheat flour and yeast medium. Two to five days old adult flies were flash frozen in liquid nitrogen. Heads were then severed by shaking the frozen flies and separated from the remaining body parts using a pair of sieves with a nominal cut-off of 710 and 425 μm. Heads were stored at -80 ºC until needed.

2. Molecular Biology

2.1. Oligonucleotides

Primers were designed to have between 18-30 nucleotides complementary to the target template and to finish with G or C bases at 3' end, in order to enhance primer annealing. New restriction sites and tags were included at their 5' ends. Primers developed for the generation of point mutations were between 25-45 bases in length, have a Tm ≥ 78 ºC and contained the desired mutation in the middle of the sequence, as suggested by the manufacturer's instructions (Stratagene). Oligonucleotides for the generation of pAc5-GFP vectors and GFP-tagged proteins were prepared jointly with Dr. So Young Lee. All primers, listed in **Table 3**, were synthesized by Invitrogen.

Table 3. List of primers used.

Primer name	Primer sequence
pAc5 GFP vectors	
N-GFP-F	GCAGGGTACCATGAGTAAAGGAGAAGAACTTTTCACTGG
N-GFP-R	GCAGTCTAGACTAGCTAGCGCGGCCGCGAATTCCTCGAGTTTGTATAGTTCATCCATGCCATGTG
C-GFP-F	GCAGGGTACCCTCGAGGAATTCGCGGCCGCGCTAGCATGAGTAAAGGAGAAGAACTTTTCACTGG
C-GFP-R	GCAGTCTAGATTATTTGTATAGTTCATCCATGCC
Flag-tagged ubiquitin	
Ub KpnI Flag-F	GCAGGTACCATGGATTACAAGGATGATGACGATAAGATGCAGATCTTCGTGAAGAC
Ub EcoRI-R	GCCGAATTCCTAACCACCACGGAGACG
HA-tagged Ube3a	
Ube3a XhoI HA-F	GCCCTCGAGATGTACCCCTACGATGTGCCCGATTACGCCATGAACGGTGGC
Ube3a XbaI-R	GCCTCTAGACTACAGCATGCCGAAGCC
Site directed mutagenesis	
Ube3a-C941S-F	TTGCCTACCTCGCACACCTCCTTCAACGTTCTCC
Ube3a-C941S-R	GGAGAACGTTGAAGGAGGTGTGCGAGGTAGGCAA
nSyb-K71R-F	CGCACGAACGTGGAGAGGGTGCTGGAGCGCGAC
nSyb-K71R-R	GTCGCGCTCCAGCACCCTCTCCACGTTCGTGCG
nSyb-K78R-F	CTGGAGCGCGACAGCAGGCTGTCGGAGCTGGACG
nSyb-K78R-R	CGTCCAGCTCCGACAGCCTGCTGTCGCGCTCCAG
GFP-tagged proteins	
CG12082 XhoI-F	GCCCTCGAGATGGAGGAACTACGCAAGC
CG12082 NheI-R	GACGCTAGCCTGTTCGCGCATATACAGATCAG

(Continued)

Table 3. *(Continued)*

Primer name	Primer sequence
Rad23 XhoI-Fw	GCCCTCGAGATGATTATTACAATTAAAAATCTTC
Rad23 NheI-Rv	GACGCTAGCATCATCGAAGCTAGACGATAGC
P47 XhoI-Fw	GCCCTCGAGATGGCCGCGCGCGGCGATTTG
P47 NheI-Rv	GACGCTAGCCTTGAGGCGCTGCATGAGTGC
TER94 XhoI-Fw	GCCCTCGAGATGGCAGATTCCAAGGGTG
TER94 NheI-Rv	GACGCTAGCACTGTAAAGATCATCGTCGC
CG8209 XhoI-Fw	GCCCTCGAGATGAGTGAAGTGCAGACATTGATGG
CG8209 NheI-Rv	GACGCTAGCTGCGGGCGTCTTGGTCATGG
Rpn13 XhoI-Fw	GCCCTCGAGATGTTTGGAAGACAAAGTGG
Rpn13 NheI-Rv	GACGCTAGCCTTTTGCTTCTCCTCCTGTT
rngo XhoI-Fw	GCCCTCGAGATGAAAATCACAGTGACGACC
rngo NheI-R	GACGCTAGCGCTGAGTTCGCTCCCCGAGG
Rpn10 XhoI-F	GCCCTCGAGATGGTTCTGGAGAGTACTATGATATGC
Rpn10 NheI-R	GACGCTAGCTTTTTTTTGCGAGTCCTTGCC
Rpn10 CH XhoI-F	GACCTCGAGATGTTCGAATTCGGTGTAGATCCC
Rpn10 NH NheI-R	GACGCTAGCGACGTTGCCGCCCAGG
Tbp-1 XhoI-F	GCCCTCGAGATGGCTCAGACTCTGGAGG
Tbp-1 NheI-R	GACGCTAGCAGCGTAGTAGTTAAGATTAGCC
Uch-L5 XhoI-F	GCCCTCGAGATGGGCGACGGTGCTGG
Uch-L5 NotI-R	GATAGCGGCCGCTGTCGGTATCCTTTTTGCGCTGC
CG15118 XhoI-F	GCCCTCGAGATGAGGAGCGTCGAGGAGATC
CG15118 NheI-R	GACGCTAGCGTGCTCTTGCAGACTAAGC
Hsp83 XhoI-F	GCCCTCGAGATGCCAGAAGAAGCAGAGACC
Hsp83 NheI-R	GACGCTAGCATCGACCTCCTCCATGTGG
Hsp26 XhoI-F	GCCCTCGAGATGTCGCTATCTACTCTGCTTTCG
Hsp26 NheI-R	GACGCTAGCCTTGTCCTTGCCGTTGGGTGC
Hsp27 XhoI-F	GCCCTCGAGATGTCAATTATACCACTGCTGC
Hsp27 NheI-R	GACGCTAGCCTTGCTAGTCTCCATTTTCTCG
HIP XhoI-F	GCCCTCGAGATGGCTTTCACAATGCAAACC
HIP NheI-R	GACGCTAGCGTCCAAACCGTCATCGACGAAG
Hsc70Cb EcoRI-F	GCCGAATTCATGTCCGTGATTGGCATCG
Hsc70Cb NotI-R	GATAGCGGCCGCTCTCCACTTCCATGGAGGGATCG
CG7033 XhoI-F	GCCCTCGAGATGGAGATGTCCTTGAATCCCGTGC
CG7033 NheI-R	GACGCTAGCGCAGTAGCCCCTGTCGGGAACG
Nrt EcoRI-F	GCCGAATTCATGGGCGAACTCGAGGAGAAGG
Nrt NheI-R	GACGCTAGCATCGACGCGCGCATACCG
Fax XhoI-F	GCCCTCGAGATGGCAAGCGAAGTGGC
Fax NheI-R	GACGCTAGCCTTTGTTTCCTCCTTCTCTTTG
Akap200 XhoI-F	GCCCTCGAGATGGGTAAAGCTCAGAGCAAGC
Akap200 NheI-R	GACGCTAGCTTCGCATGTAACGGGCAGTTG
Flo-1 XhoI-F	GCCCTCGAGATGACTTGGGGATTTGTAACCTGC
Flo-1 NheI-R	GACGCTAGCGCCAGCATGCACAGACCG
ArgK EcoRI-F	GCCGAATTCATGTTCGCTTTGTGGTATTTAACTTTTGC
ArgK NheI-R	GACGCTAGCCAGGCTCTTCTCGAGCTTGATC
Fas-2 EcoRI-F	GCCGAATTCATGGGTGAATTGCCGCCAAATTC
Fas-2 NheI-R	GACGCTAGCAGCAGTGTGCGTCGTCGG
Fas-3 NotI-F	GATAGCGGCCGCTATGTCACGGATCGTTTTTATATGTC
Fas-3 NheI-R	GACGCTAGCGTACAAGTTCAGCATAGACGAGTTG
Flo-2 XhoI-F	GCCCTCGAGATGCCTTCACACACATGCACACC
Flo-2 NheI-R	GACGCTAGCCGCCTTGGCCCCCGGTATC
Src42A XhoI-F	GCCCTCGAGATGGGTAACTGCCTCACCAC
Src42A NheI-R	GACGCTAGCGTAGGCCTGCGCCTCTTTG
β-Tub56D XhoI-F	GCCCTCGAGATGAGGGAAATCGTTCACATCC
β-Tub56D NheI-R	GACGCTAGCGTTCTCGTCGACCTCAGCC

(Continued)

Table 3. *(Continued)*

Primer name	Primer sequence
α-Tub67C EcoRI-F	GCCGAATTCATGCGCGAAGTAGTCTCCATCC
α-Tub67C NheI-R	GACGCTAGCGAACTCATCGAAGTCCTCGTCG
α-Tub84D EcoRI-F	GCCGAATTCATGCGCGAATGTATCTCTATCC
α-Tub84D NheI-R	GACGCTAGCGTACTCCTCAGCACCCTCGC
Hsc70-4 EcoRI-F	GCCGAATTCATGTCTAAAGCTCCTGCTGTTGG
Hsc70-4 NheI-R	GACGCTAGCGTCGACCTCCTCGATGGTGG
Esp15 NotI-F	GATAGCGGCCGCTATGAATGTGGACTTTGCGAGG
Esp15 XbaI-R	GCCTCTAGAGTTGTCCAGTACGCTGCG
Df31 XhoI-F	GCCCTCGAGATGGCTGATGTGGCTGAGC
Df31 NotI-R	GATAGCGGCCGCTGGCGGCCACTTCGCTAGC
CG8223 XhoI-F	GCCCTCGAGATGTCTGCTGAAGCCGAAGC
CG8223 NheI-R	GACGCTAGCGACGGCGGCACGCTTGG
RpS7 NotI-F	GATAGCGGCCGCTATGGCTATCGGCTCCAAGAT
RpS7 NheI-R	GACGCTAGCGACATTCAGGTAGTTGTCGG
Rm62 XhoI-F	GCCCTCGAGATGATGATGATGGCACCACACG
Rm62 NheI-R	GACGCTAGCGTCGAAGCGCGAGTGTCTGC
pAbp XhoI-F	GCCCTCGAGATGGCTTCTCTATACGTCGGTGATCTCC
pAbp NotI-R	GATAGCGGCCGCTGTTGGCGGGCTCGGTGACG
elF-4a XhoI-F	GCCCTCGAGATGGATGACCGAAATGAGATACC
elF-4a NheI-R	GACGCTAGCAATCAAATCGGCAATATTAGCAGG
Hrb27C XhoI-F	GCCCTCGAGATGGAGGAAGACGAGAGGG
Hrb27C NheI-R	GACGCTAGCGACAGCCTGCGAGGTTGC
Atp-α XhoI-F	GCCCTCGAGATGCCGGCCAAAGTTAATAAAAAGG
Atp-α NheI-R	GACGCTAGCGTTCTTAACTATTAACTGGGATGG
Eno XhoI-F	GCCCTCGAGATGTCTTGGACCGCTTCAG
Eno NheI-R	GACGCTAGCCTGCGGCTTCCTGAACGAC
dUTPase XhoI-F	GCCCTCGAGATGCCATCAACCGATTTCGC
dUTPase NheI-R	GACGCTAGCCGTAGCAACAGGAGCCGGAGC
CG1910 NotI-F	GATAGCGGCCGCTATGTCGGAGGCAACTGTGG
CG1910 NheI-R	GACGCTAGCGTTACACACTTTGGGCGCAGC
RpS10b XhoI-F	GCCCTCGAGATGTTTATGCCAAAGGCCCATCG
RpS10b NheI-R	GACGCTAGCGTTGCGCGATCCGCGTCC
14-3-3-ε NotI-F	GATAGCGGCCGCTATGACTGAGCGCGAGAACAATG
14-3-3-ε NheI-R	GACGCTAGCCGACACGTCCTGATCCTCAAC
Cyp1 XhoI-F	GCCCTCGAGATGGTCTCTTTTTGTGCAACTC
Cyp1 NheI-R	GACGCTAGCAAGAGAACCAGAGTTAGCCAC
14-3-3-τ XhoI-F	GCCCTCGAGATGTCGACAGTCGATAAGGAAGAGC
14-3-3-τ NheI-R	GACGCTAGCGTTGTCGCCGCCCTCCTG
hts XhoI-F	GCCCTCGAGATGACTGAAGTTGAGCAACCG
hts NheI-R	GACGCTAGCGGCCTCGGCCTTCTTCTTC
rin EcoRI-F	GCCGAATTCATGGTCATGGATGCGACC
rin NheI-R	GACGCTAGCGCGACGTCCGTAGTTGCC
nSyb XhoI-F	GCCCTCGAGATGGCGGACGCTGCACCAGCTGG
nSyb NheI-R	GCCGCTAGCCACGCCGCCGTGATCGCC
Viral ($^{bio}Ub)_6$-BirA and BirA vectors	
bioUb BamHI-F	GCCGGATCCATGGGTTTGAATGACATATTTGAAGC
BirA EcoRI-R	GCCGAATTCCTATTATTTTTCTGCACTACG
BirA BamHI-F	GCCGGATCCATGAAGGATAACACCGTGC
doubled-stranded RNA (dsRNA)	
E1-S	AATACGACTCACTATAGGGGCATTGGGGAAGTTCTTCAG
E1-R	AATACGACTCACTATAGGGTGACTCGAAATGGTTTATTGTC

Primer names and sequences are shown. Names consist on the gene name, followed by the enzyme site that this primer generates for their insertion into pAc5 or pBABE vectors. Forward or reverse orientation of the primers is indicated with an F or R letter at the end of the primer name, respectively.

2.2. DNA plasmids used

The pAc5 expression vector from Invitrogen, that contains the promoter from the *Drosophila* actin 5C gene, was used for the generation of all the constructs used in *Drosophila* BG2 cells. This plasmid was further modified by introducing between *KpnI* and *XbaI* sites the GFP protein followed by *XhoI*, *EcoRI*, *NotI* and *NheI* enzymes sites, which were introduced during the GFP amplification process using the *N-GFP-F* and *N-GFP-R* primers (**Table 3**). The modified vector (pAc5-N-GFP) allows the insertion of the protein of interest in the newly synthesized multicloning site, so as to generate N-terminally GFP-tagged proteins. Equally, using the *C-GFP-F and C-GFP-R* primers, GFP protein preceded by the same *XhoI, EcoRI, NotI* and *NheI* sites was inserted into the pAc5 vector (pAc5-C-GFP), to allow the generation of C-terminal GFP-tagged proteins, as described in Material and Methods section 2.3: *Cloning procedures*. These three vectors (i.e., pAc5, pAc5-N-GFP and pAc5-C-GFP) were used to generate the different plasmids carrying either N-terminal and C-terminal GFP-tagged proteins, as well as the Flag-tagged ubiquitin and the HA-tagged Ube3a enzyme.

Generation of viral vectors containing the *($^{bio}Ub)_6$-BirA* transgene, or the *BirA* gene alone, was performed using the hygromycin-resistant retroviral pBABE vector (Addgene; #1765), which is based on the Moloney murine leukaemia virus. This vector expresses inserted genes from the promoter within the long terminal repeat and a hygromycin drug-resistance gene from the simian vaculating virus 40 promoter (Morgenstern and Land, 1990).

2.3. Cloning procedures

PCR reactions were carried out in a GS1 Thermal Cycler (G-Storm). Generally, about 5 ng of template DNA were incubated with 200 µM of each dNTP, 1.5 mM of $MgCl_2$, 0.5 µM of each primer and 0.02 U/µL of Phusion High-Fidelity DNA polymerase enzyme in 1X Phusion HF buffer. All reagents were obtained from Thermo Scientific. A typical reaction consisted on an initial denaturation step of 30 seconds at 98 ºC, followed by 25 cycles of 10 seconds of denaturation at 98 ºC, 20 seconds of annealing at a convenient temperature and 15 second of extension per kilobase of amplicon length at 72 ºC. Afterwards, a final extension of 5 minutes at 72 ºC was applied. Annealing temperature for each primer pair was calculated with the Thermo Fisher Scientific Tm calculator tool.

All *Drosophila* genes were amplified from a Berkeley *Drosophila* Genome Project cDNA library. Flag-tagged ubiquitin was amplified using the *Ub KpnI Flag-F* and *Ub EcoRI-Rv* primers (**Table 3**) and inserted between the *KpnI* and *EcoRI* sites of the pAc5 vector (Invitrogen) to generate the Flag-Ub-pAc5 plasmid. *Ube3a XhoI HA-F* and *Ube3a XbaI-R* primers were employed to introduce an HA-tagged version of the wild type *Ube3a* gene into *XhoI* and *XbaI* sites of the pAc5 plasmid (HA-Ube3a^{WT}-pAc5). All the GFP-tagged proteins generated were amplified using the primers described in **Table 3**, and inserted in the newly generated N-terminal or C-terminal GFP pAc5 vectors. Each gene was introduced using specific combinations of enzymes sites, which are indicated in the name of each primer (**Table 3**). This work was done jointly with Dr. So Young Lee (Lee *et al*., 2014).

Generation of retroviral vectors with the *(^{bio}Ub)$_6$-BirA* transgene was performed by re-amplifying the whole construct from the initial pUAST plasmid employed to produce the ^{UAS}*(^{bio}Ub)$_6$-BirA* transgenic flies (Franco *et al*., 2011). The *bioUb BamHI-F* and *BirA EcoRI-R* primers were utilized for that purpose. *BirA* gene alone was amplified from the same vector using *BirA BamHI-R* and *BirA EcoRI-R* primers. Both transgenes were then inserted into the *BamHI* and *EcoRI* sites of pBABE-hygro vector and sent to the Viral Vector Core of the University of Tennessee Health Science Center (UTHSC, Memphis, TN, USA) for viral production.

Digestion of DNA molecules was performed at 37 ºC for a two-hour period with each of the restriction enzymes (Fermentas), followed by additional 20 minutes at the inactivation temperature recommended for each enzyme, typically 65 ºC or 80 ºC. Afterwards, ligation of the digested PCR fragments and vectors was performed overnight, at 18 ºC, in the presence of a T4 DNA ligase (England biolabs). Next day, about 1.5 µL of the ligation mixtures were used to transform 20 µL of XL-1 blue competent cells (Agilent Technologies) according to manufacturer's instruction, and let them grow overnight, at 37 ºC, in LB agar (Conda-Pronadisa) plates with appropriate antibiotic. The presence of plasmids in the grown transformants was further checked by PCR. Positive colonies were then incubated overnight with regular mixing at 37 ºC in LB broth (Conda-Pronadisa) with appropriate antibiotic (Sigma). Plasmids were purified from the overnight grown cultures using the QIAGEN miniprep kit. Correct plasmid sequence was confirmed by sequencing by STAB VIDA (Portugal).

2.4. Site directed mutagenesis

Point mutations were introduced by inverse PCR on double-stranded DNA plasmids using oligonucleotides, each complementary to opposite strand of the vectors, with the desired mutation (**Table 3**). For each reaction 50 ng of template DNA were incubated with 2 % v/v of an optimized dNTP mix solution (Stratagene), 0.25 µM of each primer and 0.05 U/µL of Pfu Turbo DNA Polymerase in 1X reaction buffer (10 mM KCl, 10 mM $(NH_4)_2$-SO_4, 20 mM Tris-HCL (pH 8.8), 2 mM $MgSO_4$, 0.1 % Triton X-100 and 0.1 mg/mL nuclease-free bovine serum albumin). Sample reactions were then subjected to the following thermal cycles: 1 minute of denaturation at 95 ºC, 18 cycles of 50 seconds of denaturation at 95 ºC, 50 seconds of annealing at 60 ºC and 10 minutes of extension at 68 ºC, and a final extension cycle of 7 minutes at 68 ºC. Parental DNA templates were then digested by DpnI enzyme and plasmids containing the desired mutations were used to transform XL1-blue super-competent cells. All mutagenesis procedure was carried out using the QuickChange Site-Directed Mutagenesis Kit (Stratagene).

The nSyb lysine to arginine mutants carrying either the lysine 71 or lysine 78 mutated to arginine (K71R and K78R) and a double mutant carrying both (DM: K71R/K78R) were generated on the pAc5-nSyb-C-terminal GFP vector with the *nSyb-K71R-F, nSyb-K71R-R, nSyb-K78R-F and nSyb-K78R-R* primers (**Table 3**). Generation of a ligase death version of the HA-tagged $Ube3a^{WT}$ protein ($HA\text{-}Ube3a^{LD}$) was performed on the $HA\text{-}Ube3a^{WT}$-pAc5 plasmid by mutating the catalytic cysteine of this E3 ligase, at position 941, to a serine using *Ube3a-C941S-F* and *Ube3a-C941S-R* primers (**Table 3**).

Plasmid purification and sequence confirmation was performed as described in Material and Methods section 2.3: *Cloning procedures*.

2.5. RNA interference experiments

A fragment of Uba1 of approximately 500 bp, containing the T7 promoter sequence on both ends, was generated using the *E1-S* and *E1-R* primers (**Table 3**). Oligonucleotides to generate this template were selected by searching the *Drosophila* RNAi Screening Center (DRSC, Boston, MA, USA) database (www.flyrnai.org). The Uba1-T7-tailed DNA was then used as template in an *in vitro* transcription reaction in order to synthesize a double-stranded RNA (dsRNA). The *in vitro* transcription was carried out using the MEGAscript kit (Ambion). The produced T7-tailed dsRNA was then purified with the RNeasy kit (QIAGEN) and the amount and quality of the produced RNA determined by spectrophotometric analysis and agarose gel electrophoresis.

3. Cell culture

3.1. BG2 cell culture procedures

BG2 cells are neuronal-like cells derived from the *Drosophila* larval central nervous system, which, despite being proliferative, contain acetylcholine neurotransmitter and positively react with antibodies against specific neuronal markers (Ui *et al*., 1994). We used them with the purpose of studying protein ubiquitination and screening for Ube3a substrates in the context of a neuron. The cells, obtained from the DRSC, were cultured at 25 ºC in Shields and Sang M3 Insect Medium (Sigma) supplemented with 10 % fetal bovine serum (FBS; Invitrogen), 100 U/mL of penicillin (Invitrogen), 100 μg/mL of streptomycin (Invitrogen), 20 μg/mL of insulin (Sigma) and 50 % conditioned medium (medium removed from cultured cells, centrifuged 5 min at 364 g, or 1250 rpm, in a Allegra X-12R centrifuge, Beckman Coulter).

3.2. Dental Pulp Stem Cell (DPSC) procedures

DPSCs are neural crest-derived cells that can be easily obtained from teeth (Graziano *et al*., 2008). They have the ability to differentiate into numerous tissues, including neurons (Kanafi *et al*., 2014). For this work teeth from three control subjects (TP023, TP024 and TP037) were obtained through the Department of Paediatric Dentistry at the UTHSC. Teeth from three AS deletion (TP055, TP059 and TP078) and three Dup15q patients (TP041, TP058 and TP044) were posted to Dr. Reiter's lab (UTHSC) by parents

of the children with these conditions. In all cases, according to UTHSC Institutional Review Board policy, an informed consent was obtained from parents or legal guardian of each participant. Exfoliated or extracted teeth were immediately placed in Dulbecco's Modified Eagle Medium: Nutrient Mixture F-12, 1:1 (DMEM/F12, 1:1) containing HEPES (Fisher Scientific) for their transportation, to which 100 U/mL of penicillin (Invitrogen) and 100 µg/mL of streptomycin (Invitrogen) were also added. Upon arrival, teeth were broken, dental pulp extracted with the help of tweezers, chopped into small pieces and further digested in a solution containing 0.9 mg/mL of Collagenase type I and 1.6 mg/mL of Dispase II for 1 hour at 37 ºC. Digested pulp was then cultured under standard condition (37 ºC, 5 % CO_2) with DMEM/F12 (1:1), supplemented with 10 % FBS (Fisher Scientific), 10 % of newborn calf serum (NCS; Fisher Scientific), 100 U/mL of penicillin (Invitrogen) and 100 µg/mL of streptomycin (Invitrogen).

3.3. Cell transfection and transduction assays

The calcium phosphate method (Kingston *et al*., 2003) was employed for BG2 cell transfection. Typically, 1 mL of BG2 cells at 1 x 10^6 cell/mL concentration was seeded per well on 12-well plates. Next day, 10 µL of 2.5 M $CaCl_2$ were mixed with 2 µg of GFP-tagged genes construct and 0.4 µg of Flag-tagged ubiquitin constructs in 100 µL of H_2O. This DNA mix solution (100 µL) was then added drop-wise to 100 µL of 2X HEPES buffer saline (50 mM HEPES, 1.5 mM NaH_2PO_4, 280 mM NaCl at pH 7.1), incubated for 40 min at room temperature and the 200 µL applied into the cell culture. After 18 hours, cells were washed twice with 1X PBS, 1 mL of supplemented M3 insect medium was added and incubated at 25 ºC for further 48 hours. Afterwards, cells were washed three times

with 1X PBS and stored at -20 ºC until required. To check the effect of HA-tagged Ube3a^{WT} and HA-tagged Ube3a^{LD}, 0.2 µg of *HA-Ube3a* plasmids were additionally added to the $CaCl_2$-DNA mixture and 1 µg of GFP-tagged protein and Flag-tagged ubiquitin used instead.

Effectene transfection reagent (QIAGEN) was used for dsRNA treatment of BG2 cells. 1 mL of cells at 5 x 10^5 cells/mL was seeded on 12 well-plates containing 800 ng of dsRNA against E1 and incubated 5 days at 25 ºC. After this period, 2 µg of GFP-tagged constructs and 0.8 µg of Flag-tagged ubiquitin plasmid were mixed with 230 µL of EC buffer and 20 µL of Enhancer. The solution was incubated for 2 min at room temperature and then 15 µL of Effectene were added and further incubated for 8 min at room temperature. The DNA mix solution was co-transfected to dsRNA pre-treated cells. Seventy-two hours later cells were washed three times with 1X PBS and store at -20 ºC until further use.

Generation of stable DPSC-lines expressing BirA protein alone or the whole $^{bio}(Ub)_6$-BirA construct was carried out on previously human telomerase reverse transcriptase (hTERT)-immortalized DPSCs (Wilson *et al*., 2015). About 1 x 10^4 of hTERT-DPSCs were seeded on 12-well plates and left to attach overnight. Next day, the medium was removed and 500 µL of DMEM/F12 medium containing 6 µL of polybrene (6 mg/mL) and virus, at a multiplicity of infection of 20, were added with no antibiotics. Two hours later the total volume of each well was increased to 1 mL with DMEM/F12. The following morning, the medium with the virus was washed away with 1X PBS, replaced with fresh supplemented DMEM/F12 media and cells were left to grow, at 37 ºC and 5 %

CO_2, for further 72 hours. After this period infected cells were selected with 15 μg/mL of hygromicin for 7-10 days.

4. Biotin pulldown of ubiquitinated material

4.1. Extract preparation

About 1 g of whole dechorionated embryos (stages 13-17) or 0.35 g of heads of 2-5 days old flies were homogenized under denaturing condition in 2.9 mL of lysis buffer using a tissue grinder (Jencons). The lysis buffer contained 8 M Urea, 1 % of Sodium Dodecyl Sulfate (SDS), 50 mM of N-ethylmaleimide (NEM) and a 1X protease inhibitor mixture (Roche Applied Science) diluted in PBS from Fisher Scientific. Urea, SDS and NEM were obtained from Sigma.

DPSCs extracts were prepared from about 1 x 10^7 cells that were pelleted at 364 g (1250 rpm) for 5 minutes using an Allegra X-12R centrifuge (Beckman Coulter) and resuspended in lysis buffer (8 M Urea, 1 % SDS, 50 mM NEM and protease inhibitor mixture). Cells were then left in a rotator (Stuart) at 4 ºC for extra 20 min. DPSC growing medium was additionally supplemented with 50 µM of biotin (Sigma) for biotin pulldown experiments.

4.2. Purification of biotinylated proteins

Fly or DPSC lysates were centrifuged for 5 minutes at 16100 g (13200 rpm), at 4 ºC, in a 5415-R centrifuge (Eppendorf). Supernatants were applied to PD10 desalting columns

(GE Healthcare), which were previously equilibrated with 25 mL of binding buffer containing 3 M Urea (Sigma), 1 M NaCl (Sigma), 0.25 % SDS (Sigma) and 50 mM NEM (Sigma) diluted in PBS. Afterwards, adult, embryo or DPSC PD10-eluates, except 50 µL that were kept for monitoring the inputs by SDS-PAGE, were incubated in a roller (Stuart) with 300 µL, 200 µL or 150 µL of NeutrAvidin agarose beads suspension (Thermo Scientific), respectively, for 1 hour at room temperature and 2 additional hours at 4 ºC. Non-bounded material (flow through) was recovered by spinning down beads at 233 g (1000 rpm) for 2 minutes in an Allegra X-12R centrifuge (Beckman Coulter). Beads were then subjected to stringent washes with six different washing buffers (WB). Number of washes and the order in which they were applied were as follows: two times with WB1 (8 M Urea, 0.25 % SDS), three times with WB2 (6 M Guanidine-HCl), 1 time with WB3 (6.4 M Urea, 1 M NaCl, 0.2 % SDS), three times with WB4 (4 M Urea, 1 M NaCl, 10 % Isopropanol, 10 % Ethanol, 0.2 % SDS), 1 time with WB1, 1 time with WB5 (8 M Urea, 1 % SDS) and three times with WB6 (2 % SDS). All buffers were prepared in PBS (Fisher Scientific). Guanidine-HCl, Isopropanol and Ethanol were provided by Sigma, Panreac and Merck, respectively. Each wash consisted on 5 minutes of incubation in a roller (Stuart) and 2 minutes of centrifugation at 233 g (1000 rpm) in an Allegra X-12R centrifuge (Beckman Coulter). Elution of beads-bounded material was performed by heating beads in a dry bath (Fisher Scientific) at 95 ºC in 4X Laemmli buffer (250 mM Tris-HCl pH 7.5, 40 % Glycerol, 4 % SDS, 0.2 % Bromophenol blue) and 100 mM Dithiothreitol (DTT). The volume of elution buffer employed was half of the NeutrAvidin agarose beads suspension used. Boiled samples were applied to 0.8 µm pore size centrifugal filters (Sartorius) and centrifuged for 2 minutes at 16160 g (14799 rpm) in a Microfuge-16 centrifuge (Beckman Coulter) to separate beads from the eluted material. Samples were then analysed by Western blot or sent to mass spectrometric analysis.

5. GFP pulldown

5.1. Extract preparation

About 1 x 10^6 transfected-BG2 cells were harvested with 300 µL of 50 mM Tris-HCl pH 7.5, 150 mM NaCl (Sigma), 1 mM EDTA (Gibco), 0.5 % Triton (Sigma), 1X Protease Inhibitor cocktail (Roche Applied Science) and 50 mM NEM (Sigma) containing lysis buffer and incubated for 20 minutes at room temperature with regular mixing in an orbital shaker (Stuart). Lysates were then centrifuged at 16100 g (13100 rpm) for 15 minutes in a cooled (4 ºC) 5415-R centrifuge (Eppendorf) and supernatants kept for the purification process.

5.2. Purification of GFP-tagged proteins

275 µL of BG2 cell lysates (25 µL were kept for monitoring the inputs by SDS-PAGE and Western blot) were mixed with 15 µL of GFP-Trap-A agarose beads suspension (Chromotek GmbH), which were previously washed twice with a dilution buffer containing 10 mM Tris-HCl pH 7.5, 150 mM NaCl (Sigma), 0.5 mM EDTA (Gibco), 1X Protease Inhibitor cocktail (Roche Applied Science) and 50 mM NEM (Sigma). The mixture was incubated for 2 hours at room temperature with gentle rolling in a rotator (Stuart) and then centrifuged for 2 minutes at 2700 g (6049 rpm) in a Microfuge-16 centrifuge (Beckman Coulter) to separated beads from the unbound material. 25 µL of the unbounded fraction were also kept to monitor the flow through fraction by Western

blot. GFP beads were subsequently washed once with dilution buffer, three times with a washing buffer composed of 8 M Urea (Sigma) and 1 % SDS (Sigma) in PBS (Fisher Scientific) and once with 1 % SDS in PBS. Beads-bound GFP proteins were eluted by heating at 95 ºC, for 10 minutes, with 4X Laemmli buffer (250 mM Tris-HCl pH 7.5, 40 % Glycerol, 4 % SDS, 0.2 % Bromophenol blue) and 100 mM DTT in a dry bath (Fisher Scientific) and then eluted suspension separated from the beads by centrifuging for 2 minutes at 16160 g (14799 rpm) in a Microfuge-16 centrifuge (Beckman Coulter).

6. Immunoblotting and silver staining

Protein samples subjected to immunoblot analysis or silver staining were first separated by SDS-PAGE using either 4-15 % gradient gels from Bio-RAD or 4-12 % gradient gels from Invitrogen. Proteins were then transferred to PVDF membrane using the iBlot system (Invitrogen) if Western blot analysis was to be performed. On the contrary, gels were fixed for 1 h at room temperature with a 40 % methanol and 10 % acetic acid containing solution in order to stain proteins with silver.

6.1. Western blotting

The amount of material loaded for Western blot analysis varied according to the tissue and the antibody employed. In the case of the material obtained from fly biotin pulldown experiments, between 0.001% and 0.2% of the input samples and 5–10% of the elution samples were loaded. When material purified from cells was used instead, either from the biotin or the GFP pulldown approach, between 10-20 % of inputs and 10-40 % of the elutions were loaded. Immunoblots with adult flies whole extracts were typically performed with six heads of 1-day-old flies, which were cut and homogenated in 60 µL of 4X Laemmli buffer (and 100 mM DTT) and boiled for 5 minutes in a dry bath (Fisher Scientific). After centrifugation of the non-soluble fraction, at 16160 g (14799 rpm) in Microfuge-16 centrifuge (Beckman Coulter), 10 µL were loaded, equating roughly to one fly head being loaded per lane. In the case of embryo whole extracts same lysis procedure was carried out with about 50 µL of embryo that were crashed in 100 µL

of 4X Laemmli buffer and 10 µL of the recovered supernatant loaded. Estimating the presence of about 50 embryos per 1 µL (Markow *et al.*, 2009), approximately 500 embryos were loaded per lane.

PVDF membranes were blocked with a blocking solution containing 5 % of fat-free milk powder and 0.1 % of Tween 20 detergent (AMRESCO) in PBS. Both primary and secondary antibodies were prepared in blocking solution containing 2.5 % of fat-free milk powder and 0.1 % of Tween 20 in PBS. In the case of biotin antibody, milk was substituted with 0.5 % of casein (Roche Applied Science) to avoid cross-reactivity between the antibody and the biotin present in the milk. Typically primary antibodies were incubated overnight at 4 ºC and secondary antibodies for 1 h at room temperature. Washes to remove excess of antibody were performed with 1X PBS containing 0.1 % Tween 20. Membranes were developed by chemiluminescence using the enhance chemiluminescence kit from Amersham (GE Healthcare). Dual-colour Western blots were prepared by assigning independent colour channels to two independent Western blots developed in the same membrane.

The following antibodies were used for immunoblot analysis: goat anti-biotin-horseradish peroxidase (HRP) conjugated antibody (Cell Signalling) at 1:200 for *Drosophila* embryo and human DPSCs samples, and at 1:1000 for *Drosophila* adult samples; chicken polyclonal anti-BirA antibody (Sigma) at 1:1000; mouse monoclonal anti-GFP antibody (Roche Applied Science) at 1:1000; rabbit polyclonal anti-GFP antibody (Santa Cruz Biotechnology) at 1:1000; mouse monoclonal anti-Flag M2-HRP conjugated antibody (Sigma) at 1:1000; mouse monoclonal anti-Syx1A antibody

(Developmental Studies of Hybridoma Bank; DSHB) at 1:50; rabbit polyclonal anti-Eps-15 antibody (Koh *et al*., 2007) at 1:150; rabbit polyclonal anti-Fax antibody, a gift from Eric Liebl (Deninson University, OH, USA) at 1:1000; mouse monoclonal anti-Atpα antibody (DSHB) at 1:50; rabbit polyclonal anti-Parkin antibody, a gift from Alex Whitworth (University of Sheffield, UK), at 1:3000; rabbit polyclonal anti-TBPH antibody (Feiguin *et al*., 2009) at 1:50; rabbit polyclonal anti-Ube3a antibody (Lu *et al*., 2009) at 1:1000; rabbit polyclonal anti-Tan antibody (Wagner *et al*., 2007) at 1:100; mouse monoclonal anti-Rpn10 antibody (Lipinszki *et al*., 2009) at 1:100; rabbit polyclonal anti-Rngo antibody (Morawe *et al*., 2011) at 1:500; rabbit polyclonal anti-Ref(2)P antibody (Pircs *et al*., 2012) at 1:500; rabbit polyclonal anti-E2-14K (to detect its *Drosophila* homologue UbcE2H) from Boston Biochem at 1:300; mouse monoclonal anti-FK1 antibody (Enzo Life Sciences) at 1:1000; mouse monoclonal anti-Nrt (DSHB) at 1:20; guinea pig polyclonal anti-Lqf (Chen *et al*., 2002) at 1:200, mouse monoclonal anti-FK2-HRP conjugated antibody (Ubiquigent) at 1:1000; mouse monoclonal anti-HA antibody (Sigma) at 1:1000; rabbit polyclonal anti-Uba1 antibody (Abcam); mouse monoclonal anti-β-Tubulin antibody (DSHB) at 1:500 and HRP-labelled secondary antibodies, typically at 1:4000, from Jackson ImmuoResearch Laboratories.

6.2. Silver staining

About 10 % of the elution samples were typically used for silver staining analysis. Stainings were performed using the SilverQuest kit from Invitrogen according to manufacturer's instructions. Briefly, gels were fixed in a 40 % Ethanol and 10 % Acetic acid solution for 1 hour at room temperature. Then, they were incubated with a

sensitizing solution to improved protein reactivity toward silver ions, and thus enhance the protein staining. After removing excessive of sensitizing solution with H_2O, gels were incubated with a staining solution, in order to bind silver ions to the proteins, and subsequently wash with H_2O to remove excess of silver from gels surfaces. Silver ions were then reduced to metallic silver until proteins were detected, which typically needs about 5-6 minutes.

7. Mass spectrometry data collection and analysis

The identification of ubiquitinated proteins isolated from embryo and adult *Drosophila* samples was performed by MS analysis. Eluted fraction from biotin pulldown experiment were trypsin digested and extracted peptides run into a mass spectrometer as described in Material and Methods section 7.2: *Mass spectrometric analysis*. Mass spectra were then analysed using the MaxQuant software (Cox and Mann, 2008), with which protein identification and quantification of protein abundance were obtained.

7.1. Analysed samples

MS analysis performed and the samples that were analysed are listed in **Table 4**. The identification of ubiquitinated material from adult heads samples was performed from three independent pulldown experiments. To identify ubiquitin-modified proteins during the embryo nervous system development four independent pulldowns were analysed by MS. Each pulldown consisted on the experimental sample expressing the $^{UAS}(^{bio}Ub)_6$-BirA construct and its corresponding control expressing only the BirA enzyme. Analysis of the proteins accumulating when C-terminal half of Rpn10 is expressed, in embryo and adult flies, was carried out from three independent biological replicas. The identification of Ube3a substrates was carried out from one MS analysis, each with embryo and adult samples, in which Ube3a loss of function or gain of function flies ($Ube3a^{15B}$ vs. $Ube3a^{A3}$) were compared.

Table 4. Mass spectrometric analysis performed.

MSC number	Tissue	BirA	^{bio}Ub	Rpn	15B	A3
MSC05753-55	eye	+	+	+		
MSC07038-42	eye	+	+	+		
MSC08962-85	eye	+	+	+	+	+
MSC03818-19	embryo NS	+	+			
MSC04306-07	embryo NS	+	+			
MSC08200-06	embryo NS	+	+	++	+	+
MSC08209-13	embryo NS	+	+	+		

Mass spectrometric analysis numbers, assigned by the mass spectrometric core facility at the Max Delbrück Center for Molecular Medicine, the tissue from which proteins were extracted and the samples that were analysed (indicated with +) are shown. (++) indicates two samples of the same genotype. **BirA:** *^{UAS}BirA*; **^{bio}Ub:** *^{UAS}(^{bio}Ub)$_6$-BirA*; **Rpn:** *^{UAS}(^{bio}Ub)$_6$-BirA; ^{UAS}Rpn10-ΔNTH*; **15B:** *^{UAS}(^{bio}Ub)$_6$-BirA; Ube3a^{15B}*; **A3:** *^{UAS}(^{bio}Ub)$_6$-BirA; ^{UAS}Ube3a^{A3}*.

7.2. Mass spectrometric analysis

All MS analyses were performed in the lab of Dr. Gunnar Dittmar, at the mass spectrometric core facility of the Max Delbrück Center for Molecular Medicine (MDC, Berlin, Germany). Eluted samples from biotin pulldowns were run on a SDS-PAGE for approximately 4 mm in the separating gel, which was afterwards cut in two slices to remove the avidin band. Proteins were converted to peptides using an in-gel digestion protocol (Shevchenko *et al.*, 2006; Kanashova *et al.*, 2015) and then separated on a 15 cm reverse phase column (packed in house, with 3 µm Reprosil beads, Dr. Maisch GmbH) using a 5 to 50% acetonitrile gradient (Proxeon nano nLC). Peptide ionization was performed on a proxeon ion source and sprayed directly into the mass spectrometer (Q-Exactive or Velos-Orbitrap, Thermo Scientific). MaxQuant software package (version 1.3.0.5), with top 10 MS/MS peaks per 100 Da and 1% FDR for both peptides and proteins (Cox and Mann, 2008), was used for the analysis of recorded spectra. Searches were performed using the Andromeda search engine against the Uniprot *Drosophila melanogaster* database. Cysteine carbamidomethylation was

selected as a fixed modification and methionine oxidation, protein N-terminal acetylation and di-glycine addition on the ε-amino group of lysines as variable modifications. Two missed trypsin (full specificity) cleavages were allowed. Mass tolerance of precursor ions was set to 6 ppm and for fragment ions to 20 ppm. The identified ubiquitination sites were checked using in house programmed software tools. Label Free Quantification was also performed with MaxQuant.

7.3. Data analysis

Label Free Quantification (LFQ) ratios were calculated for proteins identified among BirA and ^{bio}Ub samples, so as to discriminate between those purified because of being conjugated to ubiquitin and those unspecifically purified. Only proteins whose LFQ ^{bio}Ub/BirA ratio was bigger than 4 (or 2 in $\log_2$ scale) were considered to be ubiquitinated. In those situations were LFQ value was not available, raw intensities were used instead. However, as raw intensity is not a proper quantifiable measurement, proteins were only considered to be ubiquitin conjugates if their intensity was at least ten-fold bigger in ^{bio}Ub samples than in BirA. Proteins for which no intensity was recorded were discarded from further analysis. Classification of proteins found to be more ubiquitinated upon expression of C-terminal half of Rpn10 or Ube3a was only performed with LFQ ratios. Vulcano plots, generated with Prism (GraphPad Software), were used to depict the LFQ fold changes found between proteins identified in two conditions. Box plots and frequency histograms were also produced with Prism. Proportional Venn diagrams were done with eulerAPE v3 (Micallef and Rodgers, 2014).

8. Microscopy techniques

8.1. BG2 cell confocal imaging

Drosophila BG2 cells were grown over a coverslip glass and transfected with GFP-tagged genes using the calcium phosphate method (see Material and Methods section 3.3: *Cell transfection and transduction assays*). After 72 hours of growth cells were washed with 1X PBS (Fisher Scientific) and fixed with 4 % Paraformaldehyde for 30 minutes on ice. Cells were subsequently washed three times with 1X PBS-0.1 % Triton (Sigma) and the nuclei stained with DAPI (Sigma) for 10 minutes. After staining, cells were further subjected to three more washes with 1X PBS, one wash with H_2O and then the coverslips were mounted into slides with Vectashield Mounting Medium (Vector Labs). Samples were analysed in a Leica DM IRE2 confocal microscope using LCS-Leica confocal software.

8.2. *Drosophila* eye imaging

Five days old fly eye pictures were taken from CO_2 anesthetized flies in a Leica M80 microscope, incorporated with a Leica EC3 camera, and the Leica Acquire software.

9. Bioinformatic and statistical analysis

9.1. Bioinformatic analysis

Two different bioinformatic tools were employed for the gene ontology analysis: GO Term Mapper, which bins submitted gene lists into high-level and broader GO parent terms (http://go.princeton.edu/cgi-bin/GOTermMapper), also known as GO Slim (Harris *et al.*, 2004), and g:Cocoa, a tool integrated in the g:Profiler web server (http://biit.cs.ut.ee/gprofiler) that allows to perform comparative analysis of multiple gene list, providing an hierarchically sorted list of enriched GO terms. In the latter, the statistical enrichment is calculated using the Fisher's one tailed test, combined with a custom multiple correction algorithm (Reimand *et al.*, 2011).

The relative mRNA levels in the *Drosophila* eye and during the embryonic development for the MS-identified ubiquitin carrier enzymes were obtained from Flybase (www.flybase.org).

9.2. Statistical analysis

Statistical analysis between *Drosophila* nSyb mutants was performed by quantifying their ubiquitination levels, relative to the total GFP protein purified, using Image J (Schneider *et al.*, 2012). A t-test was then applied to every pair of nSyb variants.

Similarly, Rpn10 total levels in the presence of wild type or ligase dead Ube3a was assessed with Image J. Their levels were normalized to those detected in control samples and statistical differences determined using a t-test. Normal distribution was assessed by the Kolmogorov-Smirnov test and equality of variance with F test. All statistics were performed with Prism (GraphPad Software).

VIII. Results

1. Expansion of the ^{bio}Ub strategy from embryonic to adult neurons

An *in vivo* biotinylation of ubiquitin (^{bio}Ub) strategy has been successfully applied in *Drosophila melanogaster* embryos of stage 13-17 in order to identify those proteins that are ubiquitinated during the development of the nervous system (Franco *et al*., 2011). This report provided for the first time an *in vivo* empirical overview of the involvement of the ubiquitination machinery in synaptogenesis and showed that non-proteolytic roles of ubiquitination during the nervous system development are more abundant than generally believed. The post-translational modification of proteins with ubiquitin, however, is not restricted to development, but it has been shown to play important roles in synaptic plasticity in adult organisms (Hegde, 2010). We therefore decided to apply the ^{bio}Ub strategy on adult flies, aiming to discover the proteins that are ubiquitinated in mature neurons of the fruit fly, which could greatly contribute to understand the role of protein ubiquitination in brain function.

1.1. *Drosophila* eye for studying ubiquitination from mature neurons

Flies expressing the $^{UAS}(^{bio}Ub)_6$-BirA (^{bio}Ub) or the ^{UAS}BirA (BirA) constructs under the control of the pan-neuronal elav-GAL4 (elav^{GAL4}) driver (Luo *et al*., 1994) were previously used to identify proteins ubiquitinated during the development of the nervous system (Franco *et al*., 2011). When tested the expression of ^{bio}Ub in the adult heads of those elav^{GAL4} flies (**Figure 12A**), we noticed that this promoter is not suitable to perform the same approach in *Drosophila* adult brain, as the ^{bio}Ub transgene

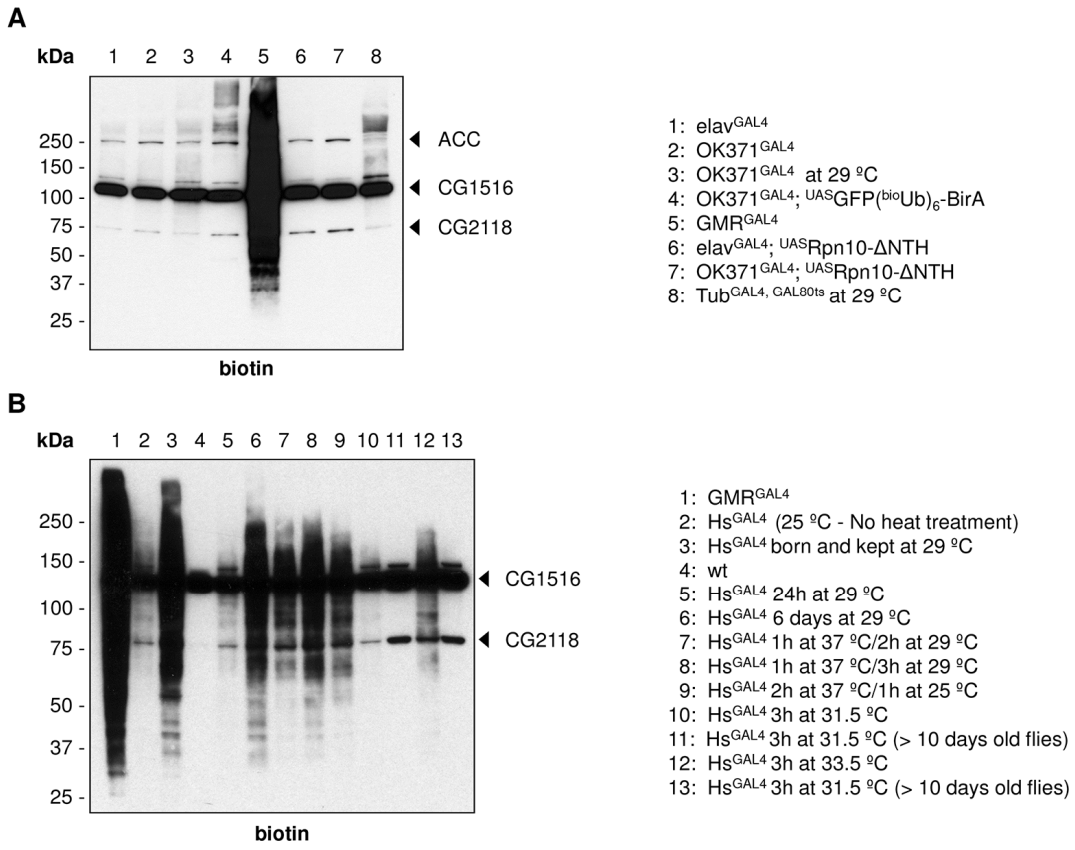

Figure 12. Expression of ^{bio}Ub under the control of distinct GAL4 drivers.

Anti-biotin immunoblots were performed to analyse the expression of the $^{UAS}(^{bio}Ub)_6$-BirA construct in *Drosophila* adult heads using various GAL4 drivers. Flies were raised at 25 ºC, unless mentioned otherwise. **A.** The pan-neuronal elav^{GAL4} (lane 1), the glutamatergic neuron-specific OK371^{GAL4} (lanes 2-4), the eye-specific GMR^{GAL4} (lane 5) and the temperature-sensitive Tub^{GAL4,GAL80ts} (lane 8) drivers were used to express ^{bio}Ub. A modified version of the construct, carrying GFP attached (^{UAS}GFP(^{bio}Ub)$_6$-BirA), was employed in the case of OK371^{GAL4} too (lane 4). Co-expression with ^{UAS}Rpn10-ΔNTH was further tested using the elav^{GAL4} (lane 6) and OK371^{GAL4} (lanes 7) drivers to accumulate more ubiquitinated material. GMR^{GAL4} provided the highest expression. **B.** Expression of ^{bio}Ub was additionally tested using the Hs^{GAL4} driver and different heat shock treatments (lanes 3, 5-13). Among the different conditions assessed, the highest expression was obtained when flies were born and kept at 29 ºC (lane 3). However, this condition did not reach the expression levels achieved with the GMR^{GAL4} driver (lane 1). Six heads (three males and three females) were collected for each condition, but only a volume equivalent to 1 head loaded per lane. Endogenously biotinylated proteins are indicated with arrowheads. Taken from Ramirez *et al*., 2015.

does not reach the expression required for MS-based proteomic studies (**Figure 12A**, lane 1). Alternatively, the expression of ^{bio}Ub was tested under the control of different GAL4 drivers, including the glutamatergic neuron-specific OK371-GAL4 (OK371^{GAL4}; Mahr and Aberle, 2006), the eye-specific glass multimer reporter-GAL4 (GMR^{GAL4}; Hay *et al*., 1994), the heat shock-GAL4 (Hs^{GAL4}; Brand *et al*., 1994) and tubulin-GAL4 (Tub^{GAL4}; Lee and Luo, 1999) (**Figure 12A and Figure 12B**). The latter was further combined with the temperature-sensitive tubulin-GAL80 (Tub^{GAL80ts}; McGuire *et al*., 2003) because expression of ^{bio}Ub with Tub^{GAL4} alone resulted in embryonic lethality (data not shown). In an attempt to enrich those proteins conjugated with the biotinylated ubiquitin, OK371^{GAL4} and elav^{GAL4} drivers were additionally combined with the expression of the C-terminal half of the proteasome regulatory particle non-ATPase 10 (Rpn10) protein (^{UAS}Rpn10-ΔNTH), whose overexpression has been reported to cause accumulation of ubiquitinated material (Lipinszki *et al*., 2009; Lee *et al*., 2014). This approach, however, did not improve the overall biotinylation yield (**Figure 12A**, lanes 6-7).

Among the panel of drivers tested GMR^{GAL4} (**Figure 12A**, lane 5; **Figure 12B**, lane 1) and Hs^{GAL4} (**Figure 12B**) provided an expression of the transgene high enough to ensure the isolation, and subsequent MS-based analysis, of the ubiquitinated proteins from the adult fly neurons. The GMR^{GAL4} driver, despite being reported to control the expression of a reporter gene on a number of different cell types (Li *et al*., 2012), drives the expression of the target genes mostly in *Drosophila* photoreceptors cells, a mature and specialized type of neurons. In addition, it has been widely used to investigate and model neurodegenerative disorders (Jackson, 2008). For these reasons, and because none of the temperature conditions tested with Hs^{GAL4} reached comparable expression

levels (**Figure 12B**), the study of the ubiquitinated proteome in *Drosophila* mature neurons was conducted with the GMR^{GAL4} driver (Ramirez *et al*., 2015).

A pre-requisite for the ^{bio}Ub strategy to work is that the ^{UAS}(^{bio}Ub)$_6$-BirA precursor has to be fully digested by endogenous DUBs. In the embryo this is successfully accomplished when the construct is expressed under the control of the elav^{GAL4} driver (Franco *et al*., 2011). Equally, this is also achieved in the *Drosophila* eye when the expression of the transgene is modulated by the GMR^{GAL4} driver. Western blot detection

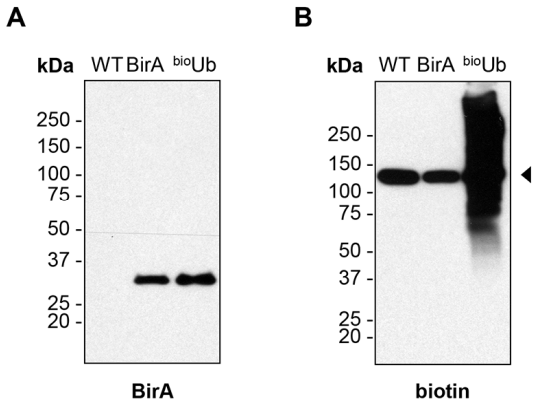

Figure 13. Biotinylated ubiquitin is conjugated to proteins in the fly eye.

A. Western blot-based detection of BirA, on *Drosophila* head whole extracts, confirmed the full digestion of the ^{bio}Ub precursor by endogenous DUBs. No undigested forms of the precursor were found above the expected molecular size of BirA (35 kDa). **B.** Anti-biotin Western blot on the same whole extracts confirmed the biotinylation and conjugation of the GMR^{GAL4}–driven expressed ubiquitin. A protein known to be endogenously biotinylated (CG1516) appeared in all the samples (arrowhead), but the expected smear corresponding to biotinylated ubiquitin conjugates was only present in the ^{bio}Ub sample. WT: *Oregon R*; BirA: *GMR^{GAL4}/CyO;^{UAS}BirA/TM6B;* ^{bio}Ub: *GMR^{GAL4},^{UAS}(^{bio}Ub)$_6$-BirA/CyO*. Taken from Ramirez *et al*., 2015.

of BirA revealed a single band of about 37 kDa corresponding to the expected size of the *E. coli* BirA enzyme in the BirA and ^{bio}Ub samples, but not in the wild type (WT), which indicates that the $^{UAS}(^{bio}Ub)_6$-BirA construct is being fully digested (**Figure 13A**). In addition, anti-biotin Western blot showed that the expression of BirA alone did not cause promiscuous biotinylation of endogenous proteins in the fly eye. A single band corresponding to the most abundant endogenously biotinylated protein (CG1516) was detected in WT and BirA extracts. By contrast, the typical smear corresponding to ubiquitin modified proteins was found in the ^{bio}Ub sample (**Figure 13B**).

1.2. Identification of the ubiquitin landscape in *Drosophila* adult eye

BirA and ^{bio}Ub extracts from 2-5 days old adult heads were prepared under denaturing conditions, incubated with NeutrAvidin agarose beads and subjected to biotin pulldown, as described in the *Material and Methods* section (see also Ramirez *et al*., 2015), in order to purify the ubiquitinated material from photoreceptors cells of *Drosophila melanogaster*. Immunoblot with anti-biotin, as well as silver staining of the purified material, suggested that the purification worked successfully (**Figure 14**). Three biologically independent pulldown experiments were therefore performed, with their corresponding BirA controls (**Figure A1 in appendix II**), and subjected to LC-MS/MS analysis. After subtraction of proteins known to be common contaminants in MS analysis (Keller *et al*., 2008), in our case mostly trypsin and keratin, and discarding detections for which no intensity was recorded, a total of 407 and 150 proteins were identified among the three ^{bio}Ub and BirA samples, respectively (**Table A1 in appendix I**). Of those, 108 were detected in both BirA and ^{bio}Ub samples. In order to discern

between true ubiquitinated proteins or background/unspecific proteins, Label Free Quantification (LFQ) ratio between ^{bio}Ub and BirA samples was calculated for each replica (^{bio}Ub/BirA LFQ ratio). Proteins displaying a ^{bio}Ub/BirA LFQ ratio higher than four (^{bio}Ub/BirA LFQ intensity > 4) in each of the replicates were considered putative

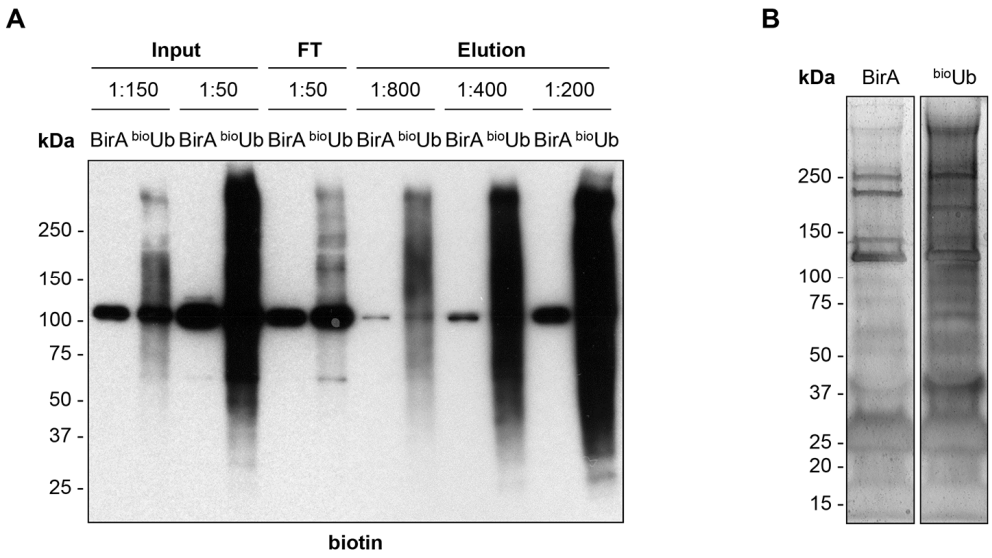

Figure 14. Biotinylated material is efficiently isolated from fly eye.

A. Representative anti-biotin Western blot performed to monitor the purification process from the *Drosophila* eye. Various dilutions of the input, flow-through (FT) and elution, as indicated, were loaded. The estimated recovery yield for all pulldowns was in the range of 20-40 %. **B.** Representative silver staining of the purified material. Equal amounts of BirA and ^{bio}Ub samples were analysed by SDS-PAGE, and stained with silver. Common bands between the two samples are expected to be composed mainly of endogenously biotinylated material, while the thick bands at around 40 kDa and below correspond to trimer, dimer and monomer forms of NeutrAvidin. The main high molecular weight smear observed in the experimental (^{bio}Ub) but not in the control (BirA) samples corresponds to the isolated ubiquitinated material. BirA: *GMR^{GAL4}/CyO;^{UAS}BirA/TM6B*; ^{bio}Ub: *GMR^{GAL4},^{UAS}(^{bio}Ub)$_6$-BirA/CyO*. Taken from Ramirez *et al.*, 2015.

ubiquitinated proteins. In the absence of LFQ values, raw intensities were used instead to separate ubiquitinated material from background. In this case the ratio threshold was increased up to ten (raw intensity ^{bio}Ub/BirA > 10), with the intention of being more conservative. With this approach a total of 369 proteins were classified as ubiquitin conjugates, while 80 (38 of which were also identified among the ^{bio}Ub samples) were assigned as experimental background (**Figure 15A, Table A1 in appendix I**).

The *Drosophila* Acetyl-CoA carboxylase (ACC), the pyruvate carboxylase (CG1516) and the biotin carboxylase (CG2118) were the only proteins classified as background that were consistently found in all the BirA replica analysed (**Figure 15A**). These three enzymes are known to be covalently modified with biotin (Chandler and Ballard, 1986), which acts as a co-factor so they can performed their function within the cells (Chapman-Smith and Cronan, 1999). The remaining background proteins were, however, mainly identified in one biological replica (MSC5753-55), and showed relatively lower MS intensities (**Figure 15B and C**). In regards to the proteins categorized as ubiquitin conjugates, 56 % of the identifications came only from one biological replica, while the remaining 44 % were detected in at least two independent experiments (**Figure 15A**). This variability positively correlates with the LFQ intensity recorded for each protein, being those with higher LFQ values the ones detected in more experiments, and vice-versa (**Figure 15B and C**).

Proteins detected in all ^{bio}Ub replicates, and hence more confidentially considered as true ubiquitinated proteins in *Drosophila* photoreceptor cells, are listed in **Table 5**. Among them, members of the ubiquitin-proteasome pathway, such as the E1 (Uba1), an

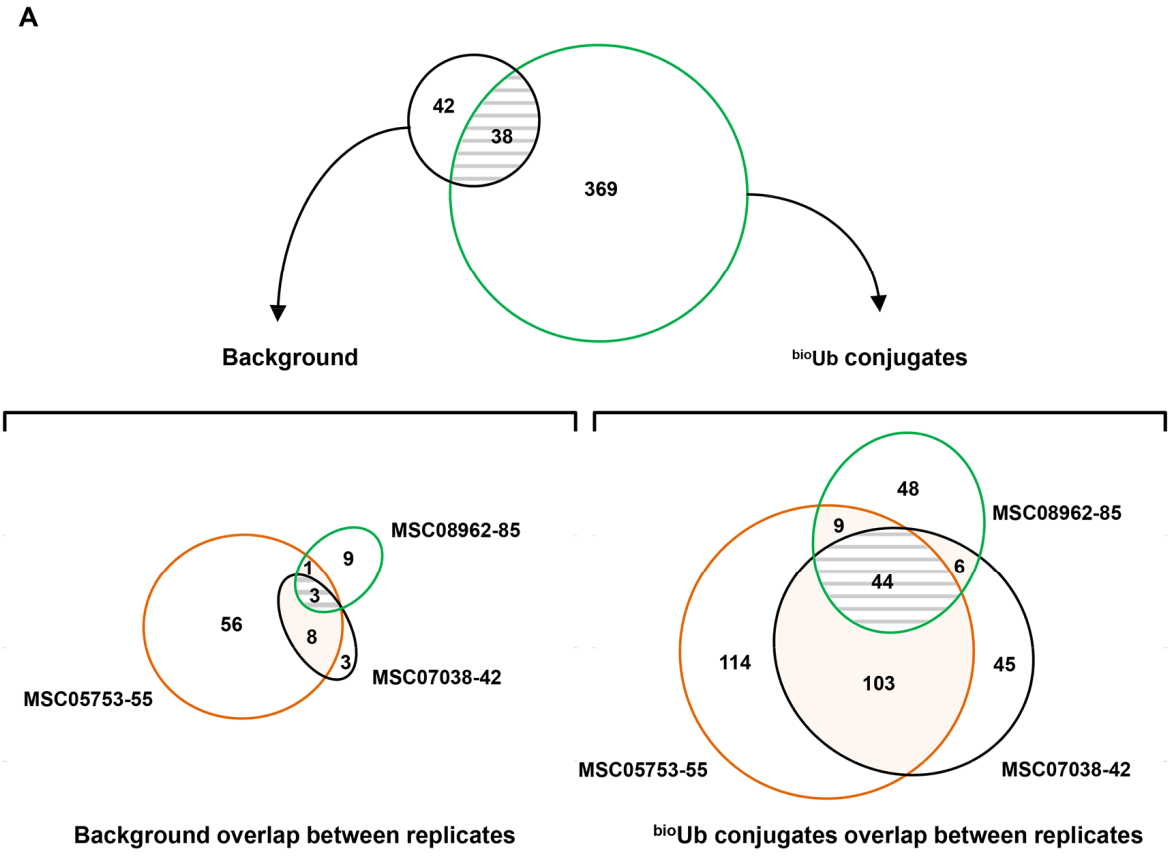
A
42
38
369
Background
bioUb conjugates
MSC08962-85
9
1
3
56
8
3
MSC07038-42
MSC05753-55
Background overlap between replicates
48
MSC08962-85
9
6
44
114
103
45
MSC05753-55
MSC07038-42
bioUb conjugates overlap between replicates

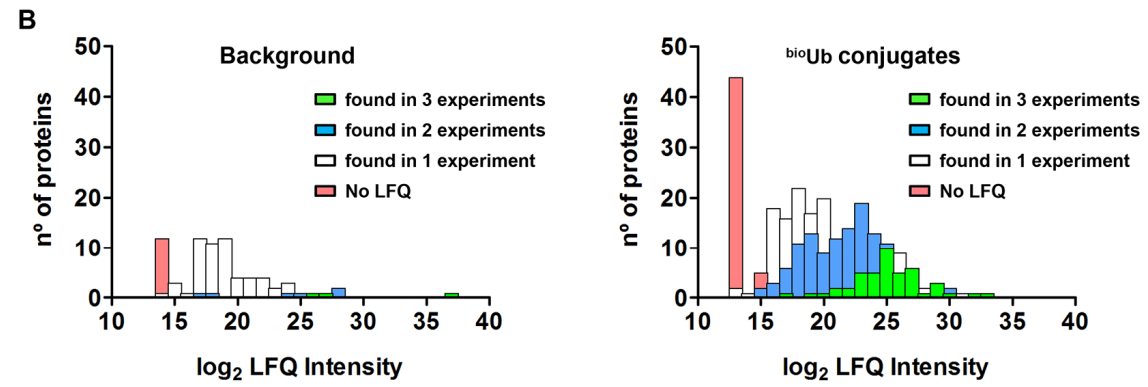
B
Background
found in 3 experiments
found in 2 experiments
found in 1 experiment
No LFQ
n° of proteins
log2 LFQ Intensity
bioUb conjugates
found in 3 experiments
found in 2 experiments
found in 1 experiment
No LFQ
n° of proteins
log2 LFQ Intensity

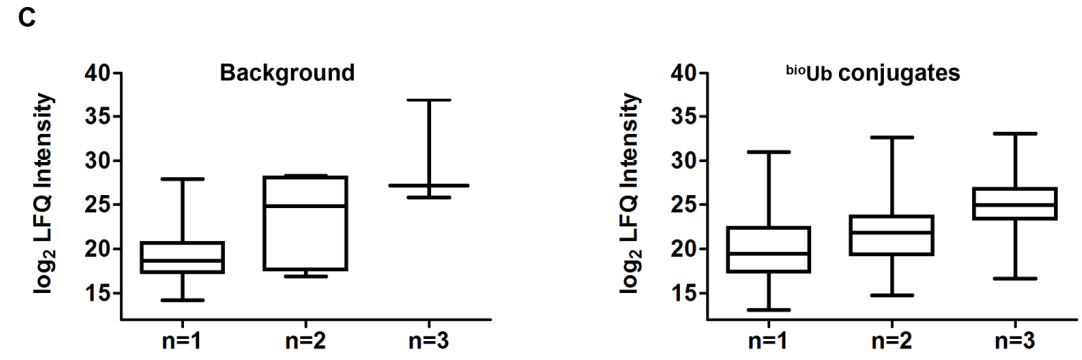
C
Background
log2 LFQ Intensity
n=1
n=2
n=3
bioUb conjugates
log2 LFQ Intensity
n=1
n=2
n=3

Figure 15. Analysis of the proteins identified by MS in the fly eye.

A. Venn diagrams showing the overlap existing between the proteins classified as background (black circle) and ^{bio}Ub conjugates (green), as well as the overlap between the identified proteins in the several pulldown experiments performed. In each independent analysis every protein displaying a ^{bio}Ub/BirA LFQ intensity ratio higher than four, or ten if using raw intensity, were considered as ubiquitin conjugates. In those situations where a protein was considered background in one biological replica but conjugate in another one was only considered a true ubiquitin conjugate if the number of times classified as so were higher than those classified as background, or if we had evidence of its ubiquitination. Each colour represents one independent pulldown experiment. For each pulldown experiment the number assigned by the MS core facility at the MDC Institute is provided. **B.** Frequency histograms indicating the number of proteins (*Y axis*) found among different range of LFQ intensity (*X axis*), represented in $\log_2$ scale, for both the protein classified as background and ubiquitin conjugates. In green, blue and white are represented those proteins found among 3, 2 or 1 independent pulldowns, respectively. In the lowest range of each group and coloured with pink are depicted the proteins for which LFQ was not available. **C.** Box plots indicating the positive correlation between the LFQ intensity recorded for the identified proteins among different replicates (*Y axis*) and the number of independent replicates (*X axis*) on which those proteins appeared.

E2 (CG7656) and an E3 (Nedd4) enzyme, as well as two proteins involved in the recruitment of proteins to the proteasome: Rad23 and TER94 (Zhang *et al*., 2013), were found. In addition, Smt3, the *Drosophila* homologue of the ubiquitin-like SUMO protein (Talamillo *et al*., 2013) was detected, suggesting the presence of mix Smt3-ubiquitin chains. Ubiquitin was found in all the ^{bio}Ub pulldowns performed too, with at least 9 peptides. More interestingly, proteins with a role in the maintenance of the neuron homeostasis and in signalling and communication between neurons, such as trans-membrane ion transport proteins or those involved in endocytic/exocytic processes were found. This suggests a role of ubiquitination in the regulation of these pathways in

Table 5. List of proteins consistently found in all three bioUb experiments.

Protein name [a]	MSC05753-55	MSC07038-42	MSC8962-85	PEP Score
Ubiquitin-proteasome pathway				
Ub/bioUb	294.98	8.42	181.64	0
Uba1	-	-	70.01	0
Rad23	-	-	-	10^{-276}
CG7656	-	-	-	10^{-274}
Nedd4	-	-	7.15	10^{-142}
TER94	82.14	-	21.87	10^{-039}
Smt3	-	-	36.38	10^{-039}
Trans-membrane ion transport				
Atpα	6.94	-	68.25	0
Calx	-	-	222.95	10^{-239}
Nrv2	57.59	-	-	10^{-157}
Vha68-2	12.29	-	-	10^{-121}
Vha55	13.49	-	-	10^{-020}
Exocytosis/Endocytosis				
AnxB10	-	-	7.53	10^{-260}
Eps-15	-	-	-	10^{-196}
Ltd	-	247.26	-	10^{-160}
Syx7	-	-	-	10^{-079}
Scamp	-	-	-	10^{-051}
Pi4KIIα	-	4.43	-	10^{-051}
Gga	-	-	-	10^{-039}
Lap	-	-	16.98	10^{-030}
Snap24	-	-	30.44	10^{-019}
Cytoskeletal/Structural proteins				
C11.1	-	-	5.82	0
Tm1	0.41	-	-	10^{-156}
CG3921	-	-	-	10^{-017}
Protein folding				
Hsc70-1	-	-	-	10^{-103}
Hop	-	-	1.03	10^{-034}
Droj2	-	-	-	10^{-014}
Metabolic enzymes				
Wat	-	-	-	0
Ald	0.96	-	-	10^{-148}
Pdh	-	-	-	10^{-128}
CG17121	-	-	10.55	10^{-088}
Sktl	-	-	-	10^{-044}
Signal transduction				
Fax	323.25	-	-	0
Uif	-	-	-	10^{-023}
Gαq	-	-	-	10^{-021}
Transcription				
Df31	-	-	-	10^{-025}
CtBP	-	-	-	10^{-018}
Wbp2	-	-	-	10^{-012}
Other function				
CG3529	-	-	-	10^{-185}
CG1648	-	0.52	-	10^{-170}
CG7675	-	-	-	10^{-101}
CG1561	-	105.16	15.05	10^{-060}
CG12025	-	-	7.97	10^{-025}
Mad1	-	-	0.81	10^{-004}

The bioUb/BirA LFQ ratios on independent MS experiments are shown. The number assigned by the MS core facility at the MDC Institute is provided. Raw intensity-based ratios are coloured in grey. Absence of ratio (-) denotes that the protein was not identified in BirA sample. The lowest Posterior Error Probabilities (PEP Score) identified among replicates are reported. All PEP Scores, peptides and intensities are shown in Table A1 in Appendix I.

[a] Protein names given following Flybase (www.flybase.org) nomenclature.

the fly eye. Some other proteins with a more common role inside the cells (structural proteins, metabolic enzymes and transcription) were also identified, as well as five proteins of a yet unknown function.

1.3. Ubiquitination sites identified in *Drosophila* photoreceptor cells

Trypsin digestion of ubiquitin conjugates produces a characteristic feature on the modified peptides known as di-gly signature (Peng *et al*., 2003). While ubiquitinated lysines remain protected from the action of trypsin, the attached ubiquitins are fully digested leaving their last two glycines still covalently attached to the target lysine (thus the name di-gly). As this fragments are identifiable by MS (Peng *et al*., 2003) they can be used in order to detect ubiquitination sites. The bioUb strategy does not particularly enrich for peptides carrying this signature, however, we did still find a total 21 di-gly remnants among the three independent replicates (**Table 6**). Some of those sites found in *Drosophila* eye seem to be conserved across mammalian homologues and had been previously identified in mouse and rat tissues, as well as in human cell lines, such as the K421 of Hsc70-1 (Kim *et al*., 2011; Wagner *et al*., 2012), the K85 of Pdh (Wagner *et al*., 2012), the K214 of Scramb2 (Wagner *et al*., 2012) and the K71 and K78 of nSyb (Danielsen *et al*., 2011; Na *et al*., 2012; Wagner *et al*., 2011, Wagner *et al.*, 2012), validating the use of *Drosophila* as a model system even for the identification of specific ubiquitination sites.

Ubiquitin has seven lysine residues along its sequence (K6, K11, K27, K29, K33, K48 and K63) that may themselves also be modified with another ubiquitin moiety, allowing

the formation of poly-ubiquitin chains. According to the position of the lysine in the receptor ubiquitin where the next ubiquitin is attached, chains of different topology may be formed, which can be homogenous if the same residue is modified along the chain (i.e., K48 linked chains) or mixed/branched if the linkages alternate (Komander and Rape, 2012). Among the ubiquitination sites identified in this analysis four of the seven lysines found in the ubiquitin molecule were detected (**Table 6**), indicating the presence of poly-ubiquitin chains of different topology in our pulldowns. Raw intensities of the ubiquitin di-gly peptides measured by MS, despite not being fully quantifiable, were further used in order to provide a view of the relative abundance of each type of ubiquitin chain linkage. As shown in **Figure 16**, the most abundant ubiquitin linkage

Table 6. Ubiquitination sites identified by MS in the fly eye.

Protein name [a]	Peptide Sequence	Position of di-glycine	PEP Score
C11.1	R ↓ GK (G-G) VM*VPGAETIYAR ↓ C	K587	10^{-003}
CG10550	R ↓ DLFESLGK (G-G) QR ↓ E	K214	10^{-003}
CG44252	R ↓ K (G-G) NLNIGDIFESNVAR ↓ R	K137	10^{-011}
Fax	K ↓ SEAPPAQK (G-G) FNVHK ↓ T	K93	10^{-006}
	K ↓ SEAPPAQK (G-G) FNVHK (G-G) ↓ T	K93(0.987) K98(0.013)	10^{-003}
Hsc70-1	R ↓ ITITNDK (G-G) GR ↓ L	K421	10^{-005}
Nrv2	M ↓ (*ac*)SK (G-G) PVPM*SPSFVDEDLHNLR ↓ K	K3	10^{-034}
nSyb	R ↓ TNVEK (G-G) VLER ↓ D	K71	10^{-006}
	R ↓ DSK (G-G) LSELDDR ↓ A	K78	10^{-007}
Pdh	K ↓ NAVVTGGAGGIGLQVSK (G-G) QLLAAGAAK(G-G) ↓ V	K40(0.993) K49(0.007)	10^{-010}
	K ↓ K (G-G) GVEATYEEIAK ↓ T	K85	10^{-009}
	R ↓ LNK (G-G) QSAADVSR ↓ C	K232	10^{-003}
Scramb2	K ↓ LELLTGFETK (G-G) NR ↓ F	K82	10^{-004}
	K ↓ VLSANNEEIGK (G-G) ISK ↓ Q	K214	10^{-009}
Spn-F	R ↓ INIIQEK (G-G) IK ↓ A	K300	10^{-003}
Syd	R ↓ ISELEDELK (G-G) K (G-G) AK ↓ E	K430 K431	10^{-003}
Ub/^{bio}Ub	K ↓ TLTGK (G-G) TITLEVEPSDTIENVK ↓ A	K11	10^{-191}
	K ↓ IQDK (G-G) EGIPPDQQR ↓ L	K33	10^{-006}
	R ↓ LIFAGK (G-G) QLEDGRTLSDYNIQK ↓ E	K48	10^{-044}
	R ↓ TLSDYNIQK (G-G) ESTLHLVLR ↓ L	K63	10^{-032}
	R ↓ TLSDYNIQK (G-G) ESTLHLVLRLR ↓ G	K63	10^{-300}

Peptides sequences, positions of di-gly (G-G) with each probability in brackets (when different from 1) and Posterior Error Probabilities (PEP Score) are reported. Oxidized methionine is indicated by an asterisk (*) and acetylation by (*ac*). Downward arrow (↓) indicates the site of trypsin digestion. All peptides and intensities are shown in table A1 in Appendix I. Modified from Ramirez *et al*., 2015.

[a] Protein names given following Flybase (www.flybase.org) nomenclature.

detected in the pulldowns was that formed along K48, followed by K63 and K11. These results are in accordance with previous reports (Peng *et al*., 2003; Danielsen *et al*., 2011; Ziv *et al*., 2011). Additionally, despite its low abundance, a di-gly site at K33, whose modification is yet poorly understood (Komander and Rape, 2012), was also detected.

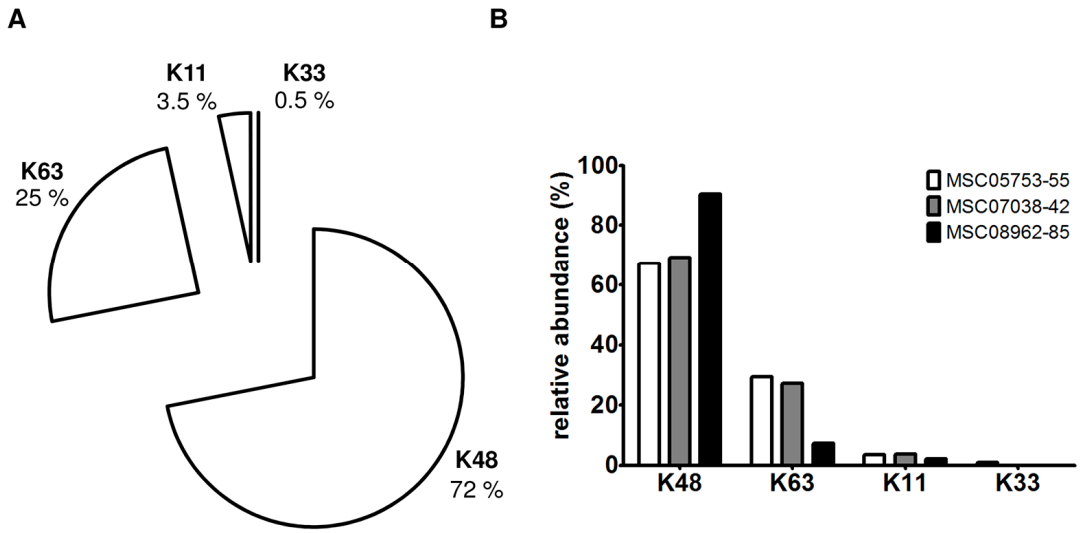

Figure 16. Relative abundance of distinct ubiquitin linkages in the fly eye.

A. Relative average abundance of the different ubiquitin linkages found among three replicates. **B.** Relative abundance of the ubiquitin linkages in each independent replicate. Each colour represents one independent MS replica. The number assigned by the MS core facility is provided. The relative abundance in (A) and (B) is given as percentage (%) of the sum of all intensities for each ubiquitin site.

1.4. *In vivo* validation of protein ubiquitination by Western blot

The bioUb strategy allows samples to be subjected to very stringent washing conditions during the pulldown process, so just those proteins that are ubiquitinated are enriched and purified. Eluted material can then be analysed by MS, or it can be subjected

to Western blot analysis in order to confirm that the purified proteins are indeed ubiquitinated *in vivo*, and further characterize whether they are mono- or poly-ubiquitinated (Franco *et al*., 2011; Lectez *et al*., 2014; Ramirez *et al*., 2015). Attachment of one ubiquitin results in an increase in the protein molecular mass of about ~10 kDa. The size of a given ubiquitinated protein detected in the eluted fraction, therefore, should be higher than the band identified in the input sample, where ubiquitin conjugates will remain undetected due to their low stoichiometry.

Some of the proteins identified in all the three independent experiments (**Table 5**) were validated by immunoblotting. The Epidermal growth factor receptor pathway substrate clone 15 (Eps-15) and Failed axon connections (Fax) proteins had been previously identified to be mono-ubiquitinated and di-ubiquitinated during the nervous system development of *Drosophila melanogaster* embryo, respectively (Franco *et al*., 2011). Equally, in the fly eye the same ubiquitination pattern for both proteins was observed (**Figure 17**). Similarly, the alpha subunit of the Na^+/K^+ ATPase (Atpα) was also detected to be di-ubiquitinated in photoreceptor cells (**Figure 17**). The di-ubiquitin band seen for both Fax and Atpα might correspond to a chain of two ubiquitins or to the attachment of two ubiquitins into two different lysines, however to discern between these two situations further experiments would be required.

Western blots to putative ubiquitinated proteins identified in two or even in a single replica were also performed. Rings lost (Rngo), the *Drosophila* homologue of the yeast Ddi1/Vsm1 and vertebrate Ddi1/Ddi2 (Morawe *et al*., 2011), is an extraproteasomal ubiquitin receptor seen in two out of three independent ^{bio}Ub replicates, but not in BirA

ones, that appeared poly-ubiquitinated in our samples (**Figure 17**). A band which *a priori* would be considered as an unmodified form of Rngo was also detected by immunoblot (marked with an asterisk in **Figure 17**). Recent studies have shown that cysteines can also be ubiquitinated through a thioester linkage (Wang *et al*., 2012; Lectez *et al*., 2014). As in the bioUb pulldown protocol DDT is used during the elution

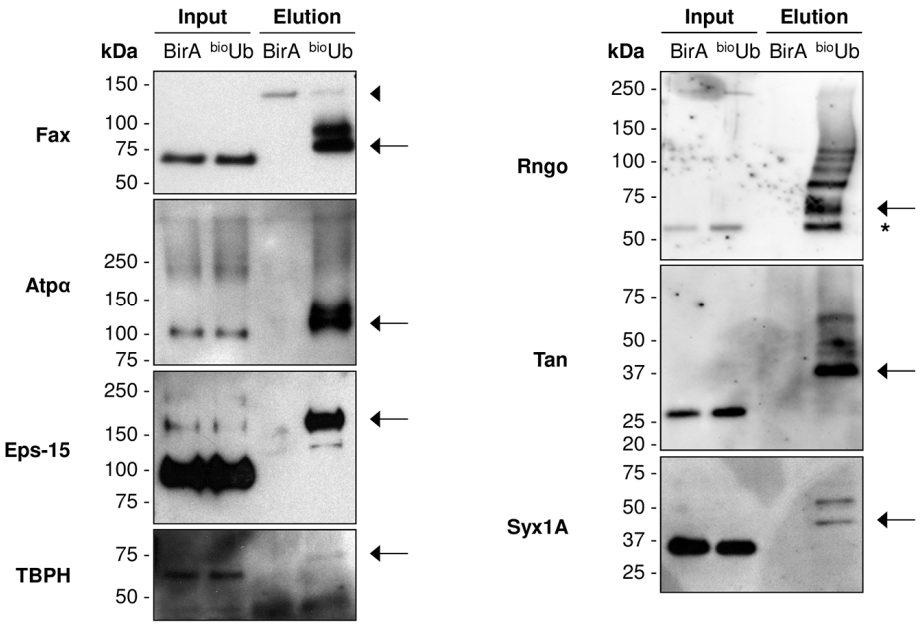

Figure 17. Western blot validation of ubiquitin conjugates identified in the fly eye.

Western blots with specific antibodies to some of the proteins identified in the adult pulldown revealed the expected increase of their molecular weight in the bioUb elution sample relative to the inputs. Covalent attachment of ubiquitin should increase the protein's molecular weight by about 10 kDa for each ubiquitin attached. Therefore, the molecular mass shift shown in the Western blots (arrows) reflects their ubiquitinated status. In the case of Rngo a band of the same size as in the input was also detected (*). Endogenously biotinylated CG1516 protein, non-specifically identified by anti-Fax antibody, is marked with an arrowhead. BirA: *GMR^{GAL4}/CyO;^{UAS}BirA/TM6B*; bioUb: *GMR^{GAL4},^{UAS}(^{bio}Ub)$_6$-BirA/CyO*. Taken from Ramirez *et al*., 2015.

step, thioester bonds are broken away (Franco *et al*., 2011; Lectez *et al*., 2014; Min *et al*., 2014), hence, this band may also correspond to a fraction of Rngo that is ubiquitinated at cysteine residues. Among proteins found only in one experiment the cysteine peptidase Tan (T), which is involved in the recycling cycle of the histamine neurotransmitter (Wagner *et al*., 2007) and the synaptic plasma membrane protein Syntaxin 1A (Syx1A), involved in the exocytosis of neurotransmitter (Ossig *et al*., 2000), were validated as ubiquitin conjugates by Western blot (**Figure 17**). Tan was found to be modified with up to four ubiquitin moieties, while Syx1A was found to be mono- and di-ubiquitinated. These results suggest that proteins identified just in one experiment are not necessarily false positives but ubiquitin conjugates of low abundance that may sometimes be below the MS detection limit. Indeed, in an ongoing collaboration with Dr. Fabian Feiguin (International Centre for Genetic Engineering and Biotechnology, Italy), the ubiquitination of the TAR DNA-binding protein-43 homologue (TBPH), a protein associated with amyotrophic lateral sclerosis (Feiguin *et al*., 2009), was also validated in *Drosophila* eye (**Figure 17**). TBPH has not yet been identified by MS in our experiments. This could be due to the amino-acid composition of this protein preventing any MS-suitable peptides being produced during the trypsin digestion process.

As mentioned above, addition of DTT in the last step of the pulldown protocol breaks thioester bonds between ubiquitin and cysteine residues (Franco *et al*., 2011; Lectez *et al*., 2014; Min *et al*., 2014). E1 activating, E2 conjugating and some E3 ligating enzymes (those classified as HECT, and also the RBR) also generate a thioester linkage in its active cysteine with ubiquitin before transferring it to substrates (Wijk and Timmers, 2010; Berndsen and Wolberger, 2014). This characteristic allows us to isolate those

enzymes that are carrying ubiquitin (i.e., enzymes with ubiquitin attached at their active cysteine) and therefore detect their carrier condition by Western blot. As it happens with ubiquitin conjugates modified at cysteine residues, E2s and E3s enzymes carrying ubiquitin via a thioester linkage will not show an increase in their molecular weight in the elution fraction, relative to the input, due to the loss of the attached ubiquitin upon DTT treatment. A total of 19 ubiquitin carriers were identified across the different samples (**Table 7**), including the ubiquitin activating enzyme E1, twelve E2 conjugating enzymes and seven E3 ligating enzymes (Ramirez *et al*., 2015). Having in the past validated the carrier status of the Uba1 and some E2 enzymes (Ubc4, UbcE2H

Table 7. List of ubiquitin carriers found by MS in the fly eye.

Protein name [a]	MSC05753-55	MSC07038-42	MSC8962-85	PEP Score
Ubiquitin activating enzyme				
Uba1	-	-	70.01	0
Ubiquitin conjugating enzymes				
CG7656	-	-	-	10^{-274}
CG40045		-	-	0
Crl		-	-	10^{-035}
CG2924	-	-		10^{-029}
Morgue	-	-		10^{-020}
Ben		-		10^{-205}
Ubc10		-		10^{-142}
TSG101	-			10^{-091}
UbcE2H		-		10^{-075}
Ubc6		-		10^{-026}
Ubc2		-		10^{-007}
Ubc4			-	10^{-003}
Ubiquitin ligase enzymes				
Nedd4	-	-	7.15	10^{-142}
Su(dx)	-	-		10^{-021}
CG5604	-		-	10^{-019}
Ube3a	-		-	10^{-016}
Park	-			10^{-013}
Ctrip			-	10^{-003}

The ^{bio}Ub/BirA LFQ ratios on independent MS experiments are shown. The number assigned by the MS core facility at the MDC Institute is provided. Absence of ratio (-) and empty cells denote that the protein was not identified in BirA and ^{bio}Ub sample, respectively. The lowest Posterior Error Probabilities (PEP Score) identified among replicates are reported. All PEP Scores, peptides and intensities are shown in Table A1 in Appendix I.

[a] Protein names given following Flybase (www.flybase.org) nomenclature.

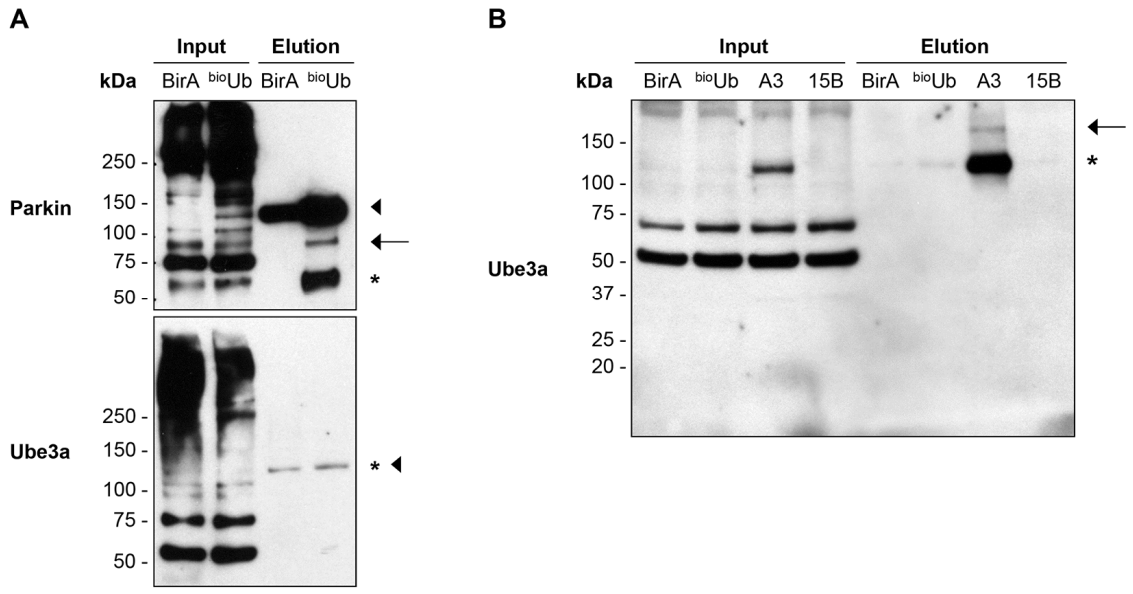

Figure 18. Confirmation of carrier activity of Parkin and Ube3a E3 ligases in the fly eye.

A. Western blots with Parkin and Ube3a antibodies on pulldowns of bioUb flies. Both Parkin and Ube3a antibodies non-specifically recognized several proteins in the inputs. The appropriate band of Parkin appears at ~55 kDa, while the one of Ube3a does at ~130 kDa. The reducing agents used in the elution step breaks the thioester linkage form between these two E3s and ubiquitin, so no increase in their molecular weight relative to the inputs is detected in the elution (*). While a fraction of Parkin appears also conjugated with ubiquitin (arrow), most of it is carrying it (*). Ube3a antibody cross-reacted with one of the endogenously biotinylated proteins (CG1516), thus, endogenous Ube3a remained hidden in the elution. Endogenously biotinylated CG1516 protein, non-specifically identified by antibodies recognizing Parkin and Ube3a, is marked with an arrowhead. BirA: *GMR^{GAL4}/CyO;^{UAS}BirA/TM6B*; bioUb: *GMR^{GAL4}, $^{UAS}(^{bio}Ub)_6$-BirA/CyO*. **B.** Western blot with Ube3a antibody on pulldowns of bioUb flies, which additionally overexpressed the Ube3a E3 ligase (A3) or carry a deletion on the *Ube3a* gene leading to no protein production (15B). Ectopically expressed Ube3a is mostly purified as a carrier protein (*), although there is also a small fraction of it ubiquitinated (arrow). BirA and bioUb genotypes as in panel A; A3 refers to flies overexpressing Ube3a: *GMR^{GAL4},$^{UAS}(^{bio}Ub)_6$-BirA/CyO;$^{UAS}Ube3a^{A3}$/TM6B*; 15B refers to flies carrying an Ube3a deletion: *GMR^{GAL4},$^{UAS}(^{bio}Ub)_6$-BirA/CyO, $Ube3a^{15B}$*/TM6B. Modified from Ramirez *et al*., 2015.

and CG40045) in the nervous system of *Drosophila* embryo (Franco *et al*., 2011), we decided to test the Western pattern for some of the E3 ligases. Based on antibody availability we were able to confirm that Parkin and Ube3a, two E3 ligases involved in Parkinson's disease and Angelman syndrome (AS), respectively (Kishino *et al*., 1997; Shimura *et al*., 2000), were carrying ubiquitin at the time the extracts were prepared (**Figure 18**) (Ramirez *et al*., 2015). A Western blot against Parkin showed a band at approximately 55 kDa in the input and elution of the ^{bio}Ub sample (indicated with an asterisk in **Figure 18A**), confirming that Parkin is being mostly pulled down because it is active and carrying ubiquitin in the *Drosophila* eye. A fraction of Parkin appeared also ubiquitinated (indicated with arrow in **Figure 18A**) probably due to self-ubiquitination at some lysine residues (Chaugule *et al*., 2011). The fraction of the endogenous Ube3a (indicated with asterisk in **Figure 18A**) was close to the limit of detection due to its low abundance and was, in addition, hindered because the antibody cross-reacted with CG1516, one of the endogenously biotinylated proteins (indicated with arrowhead in **Figure 18A**). When combining the ^{bio}Ub flies with an Ube3A overexpressing line (Wu *et al*., 2008), the preferential carrier status of the expressed Ube3a was clearly confirmed (**Figure 18B**).

2. Comparison of ubiquitinated landscapes in developing and adult neurons

Each cell type within an organism has a distinctive proteome that characterizes them according to the functions in which they are involved in. Similarly, different post-translational modifications (methylation, acetylation, phosphorylation) have also been shown to be cell-specific (Garcia *et al*., 2008; Huttlin *et al*., 2010), which further contributes to increase the complexity of the proteomes. With regards to ubiquitination, a recent work by Wagner and co-workers has uncovered differences in the ubiquitinated proteins found among a variety of mice tissues (Wagner *et al*., 2012). In order to test whether such differences are detectable not only among different type of cells but also during different stages of the development, we decided to compare the ubiquitinated landscape between a yet developing embryonic neuron and an already developed and specialized one, the eye photoreceptor cell.

2.1. Identification of the ubiquitin landscape of *Drosophila* embryo neurons

Four biologically independent pulldown experiments with elav^{GAL4}-driven BirA and ^{bio}Ub extracts from stage 13-17 *Drosophila* embryos were subjected to biotin pulldown (**Figure 19, Figure A2 in appendix II**) and LC-MS/MS analysis. Proteins identified by MS but known to be contaminants (Keller *et al*., 2008) and those with no intensity were excluded from the MS lists, leaving a total of 67 and 262 identifications in BirA and ^{bio}Ub samples, respectively (**Table A2 in appendix I**). Proteins displaying a LFQ ^{bio}Ub/BirA

intensity ratio above 4, or in absence of LFQ values a raw ^{bio}Ub/BirA intensity ratio above 10, were considered as ubiquitin conjugates. Consequently, following this criteria 37 proteins were classified as background and 234 as ubiquitin conjugates (**Figure 20A**).

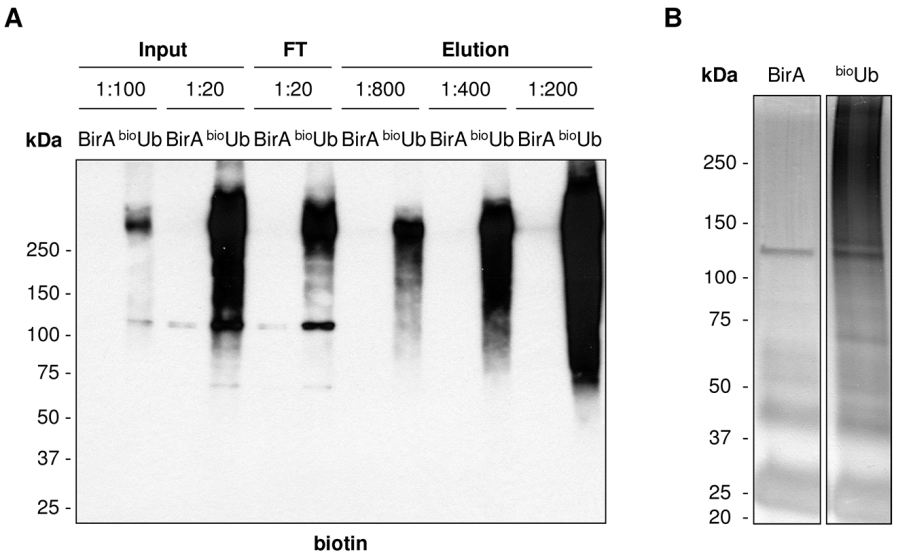

Figure 19. Biotinylated material isolated from neurons of stage 13-17 fly embryos.

A. Representative anti-biotin Western blot performed to monitor the purification process of ubiquitinated proteins from fly embryos. Dilutions of the input, flow-through (FT) and eluted samples are shown. The estimated recovery yield for all pulldowns was in the range of 20-40 %. **B.** Representative silver staining of the purified material. Equal amounts of BirA and ^{bio}Ub samples were analysed by SDS-PAGE, and stained with silver. The common band at ~130 kDa present in both samples corresponds to the endogenously biotinylated CG1516 protein. Thick bands at around 40 kDa and below correspond to trimer, dimer and monomer forms of NeutrAvidin. The smear observed at the high molecular weight range in the experimental (^{bio}Ub) but not in the control (BirA) samples corresponds to the isolated ubiquitinated material. BirA: *elav^{GAL4},^{UAS}BirA/CyO;* ^{bio}Ub: *elav^{GAL4},^{UAS}(^{bio}Ub)$_6$-BirA/CyO*. Taken from Ramirez *et al.*, 2015.

Among the identifications classified as background, the three endogenously biotinylated proteins (ACC, CG1516 and CG2118) were the only ones to be consistently detected in all the independent replicates. With regards to the proteins categorized as ubiquitin conjugates, 33 % were found in at least two ^{bio}Ub experiments (**Figure 20A**). The LFQ intensities of most of the putative ubiquitinated proteins identified in a single ^{bio}Ub replica were found to be in the lowest region of the overall LFQ intensity range detected across MS analyses (**Figure 20B**), which suggest that they are of lower abundance. In fact, while ~75 % of the proteins identified in two ^{bio}Ub experiments and the totality of proteins found in at least three experiments have a LFQ intensity above 10^6, about 80 % the identification coming from one replica showed a LFQ intensity lower than 10^6 (**Figure 20C**). The majority of the ubiquitinated proteins identified only once came from the MSC04307-06 analysis, in which a bigger depth was obtained. Among the 234 ubiquitin conjugates, 83 out of 108 proteins that were previously identified as ubiquitin conjugates in the developing nervous system of the fly embryo (Franco *et al*., 2011), were also confirmed in this new analysis.

We were confident about the MS identified proteins during the embryonic nervous system development, as Western blot to some of them provided evidence of their ubiquitination (**Figure 21**). We were able to validate that Rad23 and Rngo proteins were poly-ubiquitinated during these embryo stages, while Fax, liquid facets (Lqf) and Neurotactin (Nrt), the latter being identified in two MS analysis, were found to be mono-ubiquitinated. In addition, the carrier status of the E3 ligase Ube3a, upon its over-expression, was also confirmed. The ubiquitination of other proteins from the MS list such as Fasciclin 2 (Fas2), Eps-15, Arginine kinase (ArgK), the Heat shock protein 27

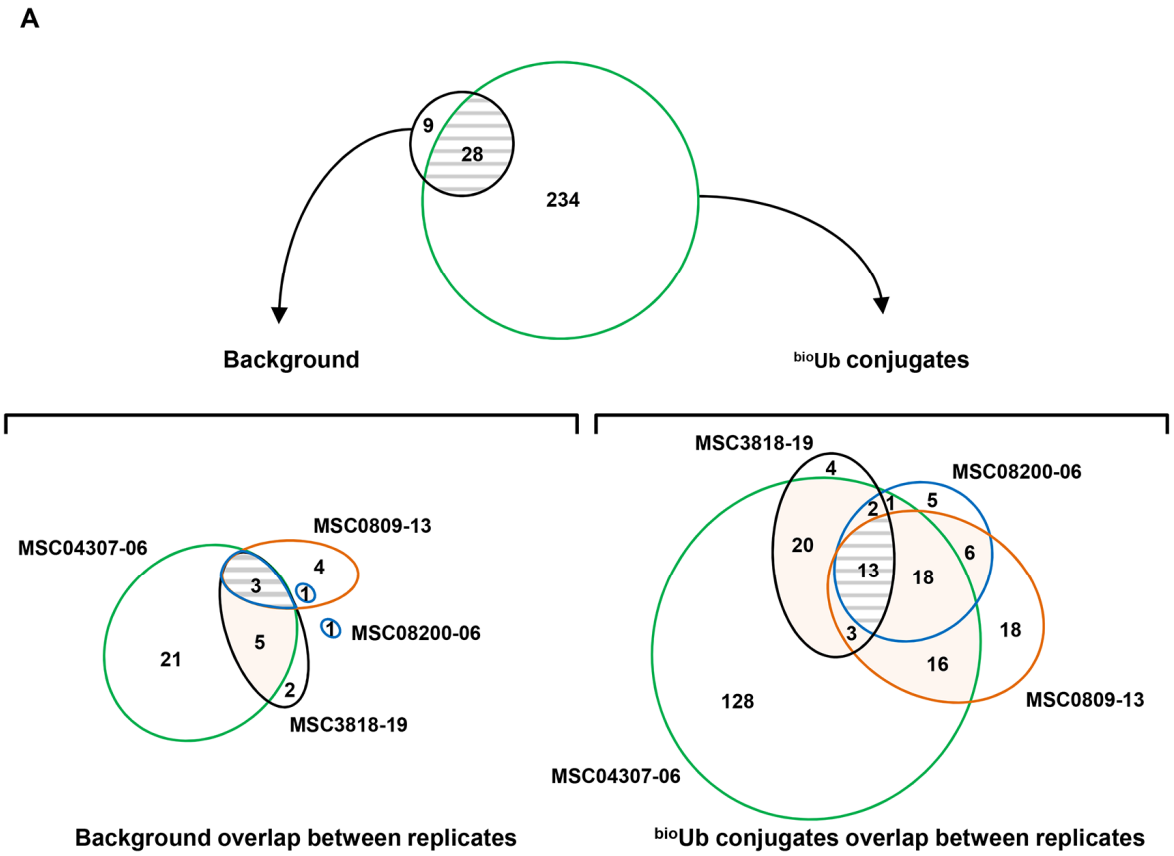
A
9
28
234
Background
bioUb conjugates
MSC04307-06
MSC0809-13
MSC08200-06
MSC3818-19
21
4
3
1
1
5
2
Background overlap between replicates
MSC3818-19
MSC08200-06
MSC04307-06
MSC0809-13
4
2
1
5
20
13
6
18
3
18
16
128
bioUb conjugates overlap between replicates

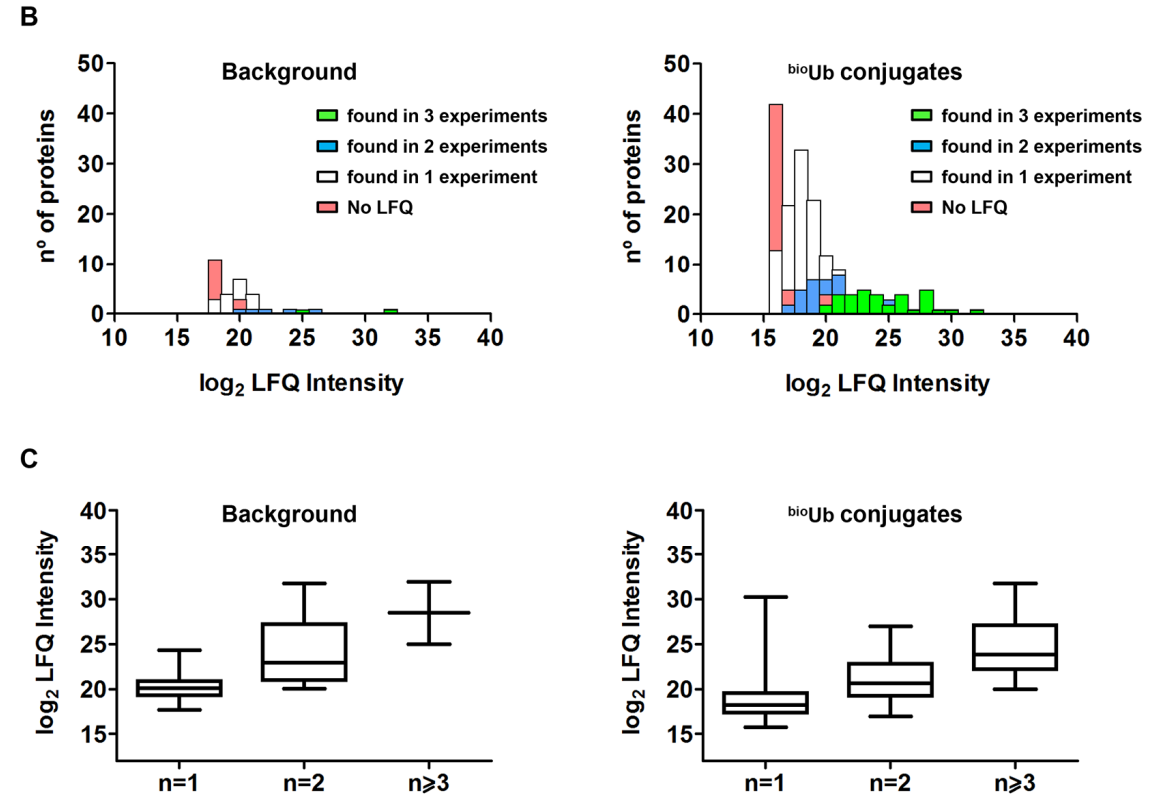
B
Background
bioUb conjugates
found in 3 experiments
found in 2 experiments
found in 1 experiment
No LFQ
n° of proteins
log2 LFQ Intensity
C
log2 LFQ Intensity
n=1
n=2
n≥3

Figure 20. Analysis of the proteins identified by MS in fly embryos.

A. Venn diagrams showing the overlap existing between the proteins classified as background (white circle) and ^{bio}Ub conjugates (green), as well as the overlap between the identified proteins in the several pulldown experiments performed. In each independent analysis every protein displaying a ^{bio}Ub/BirA LFQ intensity ratio higher than four, or ten if using raw intensity, were considered ubiquitin conjugates. In those situations where a protein was considered background in one biological replica but conjugate in another one were only considered a true ubiquitin conjugate if the number of times classified as so were higher than those classified as background, or if we had evidence of their ubiquitination. Each colour represents one independent pulldown experiment. For each pulldown experiment the number assigned by the MS core facility at the MDC Institute is provided. **B.** Frequency histograms indicating the number of proteins (*Y axis*) found among different range of LFQ intensity (*X axis*), represented in $\log_2$ scale, for both the protein classified as background and ubiquitin conjugates. In green, blue and white are represented those proteins found among 3 or more, 2 or 1 independent pulldown, respectively. In the lowest range of each group and coloured with pink are depicted the proteins for which LFQ was not available. **C.** Box plots indicating the positive correlation between the LFQ intensity recorded for the identified proteins among different replicates (*Y axis*) and the number of independent replicates (*X axis*) on which those proteins appeared.

(Hsp27) or the Regulatory particle non-ATPase 10 (Rpn10), as well as the carrier status of the E1 (Uba1) and some E2 enzymes (Ubc4, UbcE2H, Ubc2, eff and CG40045) had been previously verified using this system (Franco *et al*., 2011). It should be noted that proteins not identified by neither of the MS analysis but known to be ubiquitinated (Franco *et al*., 2011) were also validated by Western blot (**Figure 21**), such as Syx1A or the Anaplastic lymphoma kinase (ALK) protein, indicating that the pulldown process from embryonic tissues worked properly, and hence technical issues during the processing of the samples for MS analysis were likely the cause of the low number of

identification is some of the MS analyses. A list of the proteins detected in at least three out of the four different experiments (**Figure 20A**) is shown in **Table 8**.

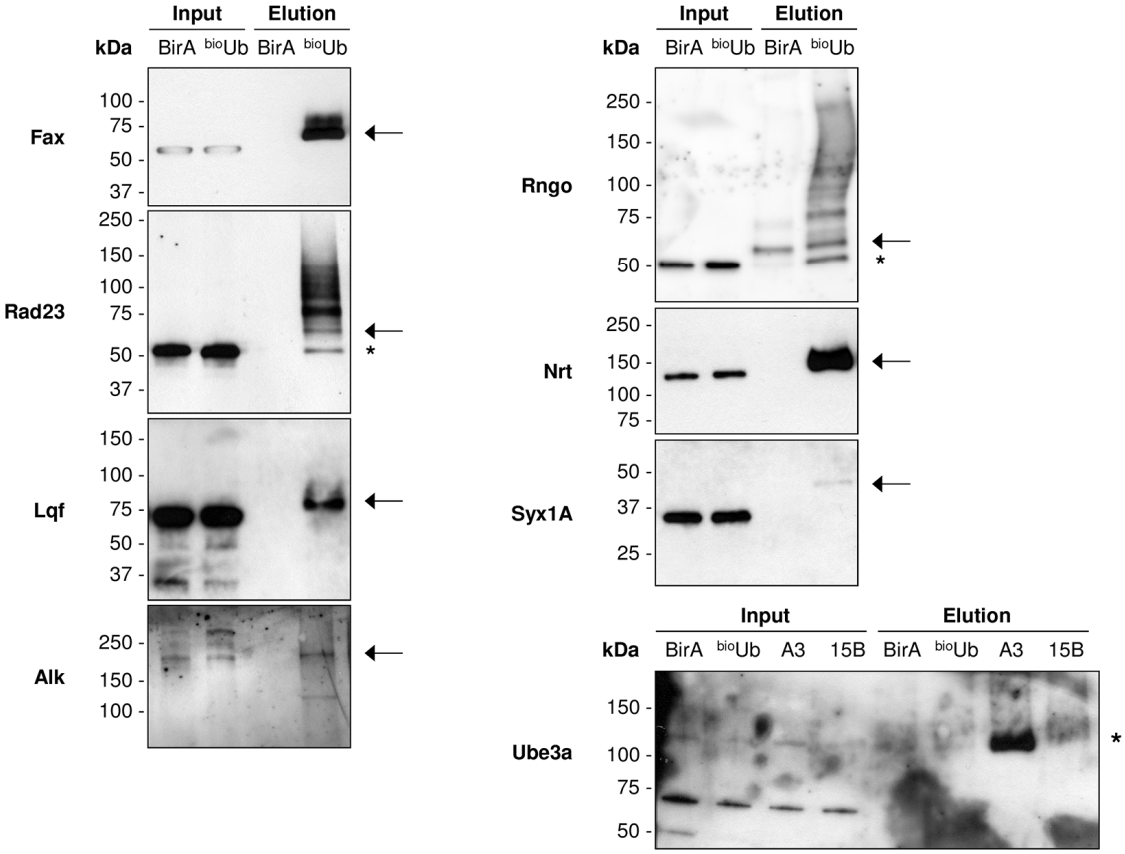

Figure 21. Western blot validation of ubiquitin conjugates and carriers identified in embryos.

Western blots with specific antibodies to some of the proteins identified in embryo pulldown revealed the expected increase of their molecular weight in the ^{bio}Ub sample relative to the inputs (arrows). Un-modified or cysteine-ubiquitinated forms of Rad23 and Rngo are indicated by an asterisk (*). In the case of Ube3a flies that overexpressed the E3 were used. The asterisk indicates the fraction of Ube3a that was carrying the ubiquitin on its active cysteine. BirA: *elav^{GAL4},^{UAS}BirA/CyO;* ^{bio}Ub: *elav^{GAL4},^{UAS}(^{bio}Ub)$_6$-BirA/CyO;* A3 (Ube3a overexpression): *elav^{GAL4},^{UAS}(^{bio}Ub)$_6$-BirA/CyO;^{UAS}Ube3a^{A3}/TM6B*; 15B (Ube3a deletion): *elav^{GAL4}, ^{UAS}(^{bio}Ub)$_6$-BirA/CyO;Ube3a^{15B}/TM6B*.

Table 8. List of proteins consistently found among embryo ^{bio}Ub experiments.

Protein name [a]	MSC3818-19	MSC04306-07	MSC08200-06	MSC08209-13	PEP Score
Ubiquitin-proteasome pathway					
Ub/^{bio}Ub		122.85	7.12	16.78	0
Uba1	-	637.32	-	-	0
CG40045	-	-	-	-	0
CG8209		-	-	-	10^{-269}
Uba2	-	17.35		-	10^{-266}
Ben	-	-	-	-	10^{-195}
Rad23	-	-	-	-	10^{-185}
UbcE2H		-	-	-	10^{-136}
CG7656		-	-	-	10^{-086}
CG2924		-	-	-	10^{-026}
CG12082		-	-	-	10^{-022}
Rngo		-	-	-	10^{-078}
Smt3	-	34.88		-	10^{-085}
Crl	-	-	-	-	10^{-032}
Ubc10	-	6.01	-	-	10^{-087}
p47		-	-	-	10^{-019}
Trans-membrane ion transport					
Atpα	-	-	-		10^{-099}
Endocytosis/Exocytosis					
Eps-15		-	-	-	0
AnxB10	-	-	-		10^{-049}
Snap24	-	-	-	-	10^{-042}
Lqf	-	-		-	10^{-015}
Metabolic enzymes					
Eno		35.62	-	-	10^{-237}
Cytoskeletal/Structural proteins					
Tm1		-	-	-	10^{-135}
CG9135		-	-	-	10^{-006}
Signal transduction					
Akap200		-	-	-	0
Fax	-	-	-	-	0
Transcription/Translation					
Df31	-	-	-	-	0
RpS7	-	-	-	-	0
Rm62	-	-	-	-	10^{-215}
His2A	115.65	1191.78	-	-	10^{-206}
Rin	-	-	-	-	10^{-089}
Other function					
Alt		-	-	-	10^{-065}
Kuk		-	-	-	10^{-022}
CG5830		-	-	-	10^{-021}
Bacc		-	-	-	10^{-227}
CG15435	-	-	-	-	10^{-064}

The ^{bio}Ub/BirA LFQ ratios on independent MS experiments are shown. The number assigned by the MS core facility at the MDC Institute is provided. Raw intensity-based ratios are coloured in grey. Absence of ratio (-) and empty cells denote that the protein was not identified in BirA and ^{bio}Ub sample, respectively. The lowest Posterior Error Probabilities (PEP Score) identified among replicates are reported. All PEP Scores, peptides and intensities are shown in Table A1 in Appendix I.

[a] Protein names given following Flybase (www.flybase.org) nomenclature.

2.2. Ubiquitination sites identified in embryo samples

A number of ubiquitination sites were detected by MS among the identified proteins in the embryonic analysis performed (**Table 9**). Some of those had been previously reported in mammalian counterparts, such as the K74 of Ben (Wagner *et al*., 2011), the

Table 9. Ubiquitination sites identified by MS in embryos.

Protein [a]	Peptide sequence	Position of di-glycine	PEP Score
Act42A	R ↓VAPEEHPVLLTEAPLNPK (G-G) ANR ↓ E	K114	10^{-003}
Ben	R ↓ FITK (G-G) IYHPNIDR ↓ L	K74	10^{-005}
CG6652	R ↓ LEEK (G-G) DNDMK (G-G) LM*AR ↓ K	K210 K215	10^{-002}
CG7768	R ↓ SDVVPK (G-G) TAENFR ↓ A	K31	10^{-002}
CG8223	K ↓ GK (G-G) ELFSQGSR ↓ N	K60	10^{-002}
CG12237	R ↓ K (G-G) GFAM*EK (G-G) HLLR ↓ N	K226(0.92) K232(0.08)	10^{-002}
CG13855	K ↓ EMGK (G-G) PIEWVGYK (G-G) DSK (G-G) ↓ I	K412(1) K420(0.975) K423(0.025)	10^{-002}
Df31	K ↓ VAAEEVDAVK (G-G) K (G-G) ↓ D	K26(0.858) K27(0.142)	10^{-002}
	K ↓ K (G-G) DAVAAEEVAAEK ↓ A	K27	10^{-006}
	R ↓ K (G-G) VDEAAAK (G-G) ADEAVATPEKK ↓ A	K142(0.03) K149(0.97)	10^{-002}
	K ↓ ADEAVATPEK (G-G) K (G-G) ↓ A	K159(0.978) K160(0.022)	10^{-002}
Eps-15	K ↓ FQSK (G-G) EPVKDK ↓ F	K1221	10^{-006}
Fax	K ↓ LDLNAHIPK (G-G) PEPETK ↓ E	K365	10^{-004}
	K ↓ SNEQEGTEGDK (G-G) IEK (G-G) ELEK (G-G) ↓ D	K392(0.008) K395(0.535) K399(0.457)	10^{-125}
His2A	K ↓ LLSGVTIAQGGVLPNIQAVLLPK (G-G) K (G-G) ↓ A	K118(0.5) K119(0.5)	10^{-015}
His2B	K ↓ AVTK (G-G) YTSSK	K118	10^{-009}
Hrb98DE	K ↓ LFVGALK (G-G) DDHDEQSIR ↓ D	K129	10^{-005}
Hsc70-4	R ↓ IINEPTAAAIAYGLDK (G-G) K (G-G) ↓ A	K187(0.5) K188(0.5)	10^{-002}
	K ↓ ITITNDK (G-G) GR ↓ L	K507	10^{-012}
Hsp26	R ↓ IIQIQQVGPAHLNVK (G-G) ANESEVK (G-G) ↓ G	K189(0.988) K196(0.012)	10^{-004}
Nlp	K ↓ QILLGAEAK (G-G) ENEFNVVEVNTPK ↓ D	K44	10^{-004}
Rin	R ↓ NNK (G-G) GDFEQR ↓ R	K475	10^{-003}
RpS10b	R ↓ RAPGGSGVDK (G-G) K (G-G) GDVGPGAGEVEFR ↓ G	K137 K138	10^{-007}
RpS20	K ↓ DIEK (G-G) PHVGDSASVHR ↓ I	K10	10^{-003}
	M ↓ (*ac*)AAAPK (G-G) DIEK (G-G) PHVGDSASVHR ↓ I	K6 K10	10^{-003}
RpS27A	K ↓ VDENGK (G-G) IHR ↓ L	K113	10^{-005}
Ub/^{bio}Ub	K ↓ TLTGK (G-G) TITLEVEPSDTIENVK ↓ A	K11	10^{-105}
	K ↓ TITLEVEPSDTIENVK (G-G) AK (G-G) ↓ I	K27(0.948) K29(0.052)	10^{-035}
	K ↓ AK (G-G) IQDKEGIPPDQQR ↓ L	K29	10^{-302}
	R ↓ LIFAGK (G-G) QLEDGR ↓ T	K48	10^{-176}
	R ↓ TLSDYNIQK (G-G) ESTLHLVLR ↓ L	K63	10^{-068}
	R ↓ TLSDYNIQK (G-G) ESTLHLVLRLR ↓ G	K63	10^{-111}

Peptides sequences, positions of di-gly (G-G) with each probability in brackets (when equal to 1) and Posterior Error Probabilities (PEP Score) are reported. Oxidized methionine is indicated by an asterisk (*) and acetylation by (*ac*). Downward arrow (↓) indicates the site of trypsin digestion. All peptides and intensities are shown in table A2 in Appendix I. Modified from Ramirez *et al*., 2015.

[a] Protein names given following Flybase (www.flybase.org) nomenclature.

K137 and K138 of RpS10b (Danielsen *et al*., 2011; Wagner *et al*., 2012), the K6 and K10 of RpS20 (Wagner *et al*., 2011, 2012) and K113 of Rps27A (Wagner *et al*., 2012). Regarding the lysines at ubiquitin, the most abundantly modified ones (i.e., K48, K63 and K11) were also detected. In addition, di-gly sites in lysines at position 27 (K27) and 29 (K29) were detected with a very low abundance (**Figure 22**).

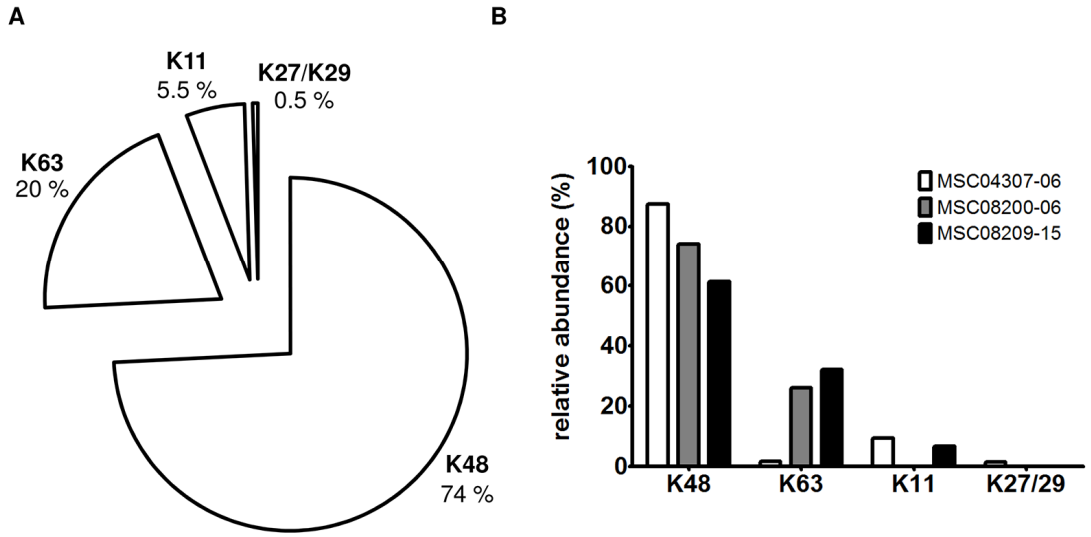

Figure 22. Relative abundance of the ubiquitin linkages in embryos.

A. Relative abundance of the different ubiquitin linkages found among three replicates **B.** Relative abundance of the ubiquitin linkages in each independent replicate. Each colour represents one independent MS replica. The number assigned by the MS core facility is provided. No ubiquitination sites on ubiquitin were detected in the MSC3818-19 analysis. The relative abundance in (A) and (B) is given as percentage (%) of the sum of all the intensities for each ubiquitin site.

2.3. Comparison of the embryo and adult neuron ubiquitin proteome

Comparison of the ubiquitin proteome between the adult (369 proteins) and the embryonic datasets (234 proteins) resulted in only 103 proteins being found to be common between them (**Figure 23**). As shown in **Table 10**, 13 of these common proteins corresponded to known ubiquitin carrier enzymes (i.e., proteins transporting ubiquitin before it is conjugated into K residues), and hence the remaining 90 were

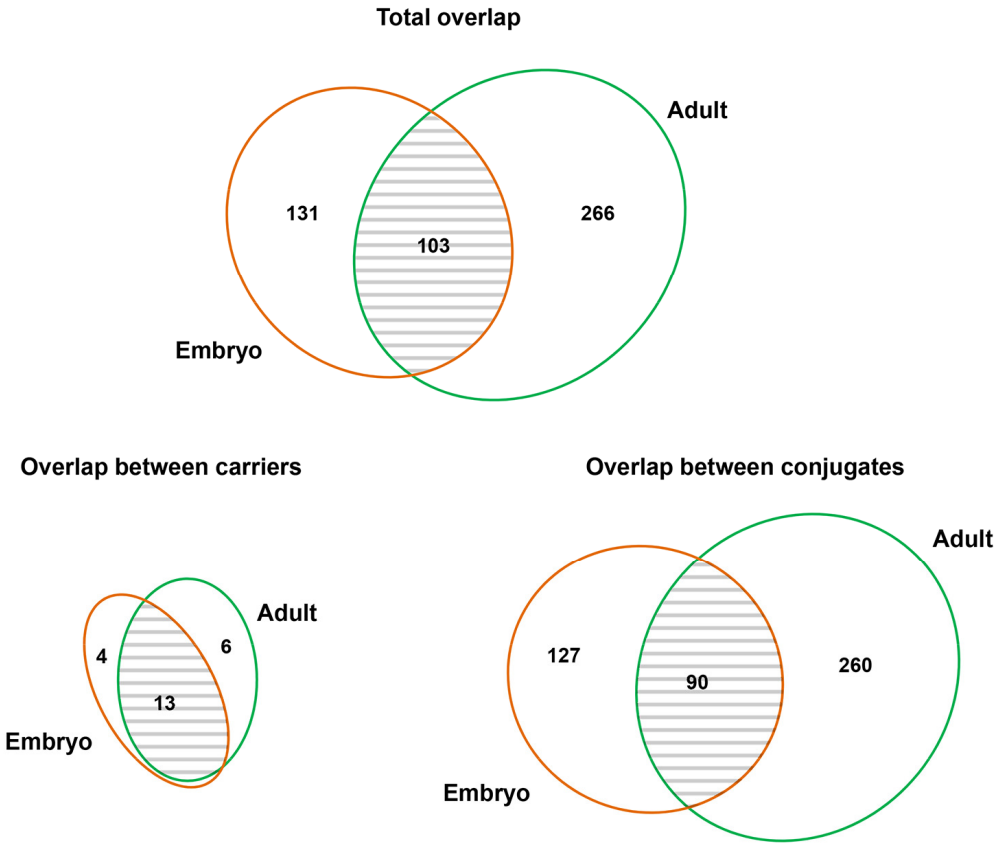

Figure 23. Overlap between the ubiquitinated proteins detected in embryo and adult samples.

Venn diagrams showing the existing overlap between the ubiquitinated proteins (^{bio}Ub/BirA ratio >4 if LFQ intensity; > 10 if raw intensity) identified from *Drosophila* embryo nervous system at stages 13-17 and the adult eye. Overlap between the complete list (Total overlap), only the ubiquitin carriers (Overlap between carriers) and only the ubiquitin conjugates (Overlap between conjugates) are shown.

proteins considered to be modified with ubiquitin at lysine residues (**Figure 23**). In a previous study, 11 active ubiquitin carriers were identified among the proteins isolated from the embryonic nervous system (Franco *et al*., 2011). Here, taking in consideration the analyses performed in both embryo and adult, a total of 23 ubiquitin carriers were identified (**Figure 23** and **Table 10**), although not all of them were found in both stages. For instance, ubiquitin activating enzyme E1 (Uba1) was detected in all the different replica of both embryo and adult samples. Out of the 16 identified ubiquitin conjugating

Table 10. Ubiquitin carrier enzymes identified in embryo and adult samples.

		elav		GMR	
Protein name [a]	**Protein description** [a]	**PEP Score**	**n**	**PEP Score**	**n**
Ubiquitin activating enzyme					
Uba1	Ubiquitin activating enzyme 1	0	4	0	3
Ubiquitin conjugating enzymes					
CG40045	-	0	4	0	2
Ubc10	Ubiquitin conjugating enzyme 10	10^{-087}	4	10^{-142}	1
Crl	Courtless	10^{-032}	4	10^{-035}	2
Ben	Bendless	10^{-195}	4	10^{-205}	1
CG7656	-	10^{-086}	3	10^{-274}	3
CG2924	-	10^{-026}	3	10^{-029}	2
UbcE2H	Ubc-E2H	10^{-136}	3	10^{-075}	1
Eff	Effete	10^{-009}	2		
Ubc4	Ubiquitin conjugating enzyme 4	10^{-142}	2	10^{-003}	1
Ubc2	Ubiquitin conjugating enzyme 2	10^{-048}	2	10^{-007}	1
CG5823	-	10^{-003}	1		
CG8188	-	10^{-006}	1		
Morgue	Modifier of rpr and grim, ubiquitously expressed	10^{-010}	1	10^{-020}	2
Vih	Vihar	10^{-040}	1		
TSG101	Tumour susceptibility gene 101			10^{-091}	1
Ubc6	Ubiquitin conjugating enzyme 6			10^{-026}	1
Ubiquitin ligase enzymes					
Ube3a	Ubiquitin protein ligase E3A	10^{-019}	2	10^{-016}	2
Ctrip	Circadian trip	10^{-004}	1	10^{-003}	1
Nedd4	Nedd4			10^{-142}	3
CG5604	-			10^{-019}	2
Su(dx)	Suppressor of deltex			10^{-021}	2
Park	Parkin			10^{-013}	1

The lowest Posterior Error Probabilities (PEP Score) identified among replicates and the number of identification in independent ^{bio}Ub experiments are reported. All PEP Scores, peptides and intensities are shown in table A1 and A2 in Appendix I.

[a] Protein name and protein description given according to Flybase nomenclature (www.flybase.org)

E2 enzymes, 10 appeared in both tissues, while the remaining 6 were detected only in embryo (CG5823, CG8188, Eff and Vih) or in adult (TSG1 and Ubc6) samples. Similarly, only two ubiquitin ligating E3 enzymes (Ctrip and Ube3a) were identified in both tissues, whereas the rest were only seen in the *Drosophila* eye. Absence of E2 and E3 enzymes in the developing embryo nervous system, is probably explained by the low expression levels of some of those genes, as suggested by reported RNA levels (**Figure A3 in appendix II**) during this stages (Graveley *et al*., 2011), as well as by the poor depth obtained in the proteomic analysis. Absence of CG5823, CG8188 and Vih E2s in the photoreceptors cells, might also be explained by the relatively low mRNA signals of these genes in the *Drosophila* eye (**Figure 24A**), as reported by the FlyAtlas webserver (www.flyatlas.org) (Chintapalli *et a*l., 2007).

According to this transcriptomic data one would expect to detect Effete (Eff) from both adult and embryo samples, since this enzyme has been classified in the group of genes presenting very high mRNA levels in the *Drosophila* eye (**Figure 24A**) as well as during the embryo development (**Figure 24B**). Moreover, in the fly eye the mRNA levels of this enzyme are supposed to be at least two fold higher than those described for Uba1, CG7656 or Nedd4 (**Figure 24A**), three proteins seen in every MS analysis performed with adult samples (**Table 10**). The fraction of Eff carrying ubiquitin, or modified with it, however, was only detected by MS and Western blot from embryonic pulldowns (**Figure 24C**). Western blot with anti-Eff antibody performed with adult samples showed a band of the appropriate size in the input fraction (**Figure 24C**), confirming that this enzyme is indeed expressed in the eye. In the eluted fraction no band was detected though, suggesting that the amount of this enzyme carrying or modified with ubiquitin is of very

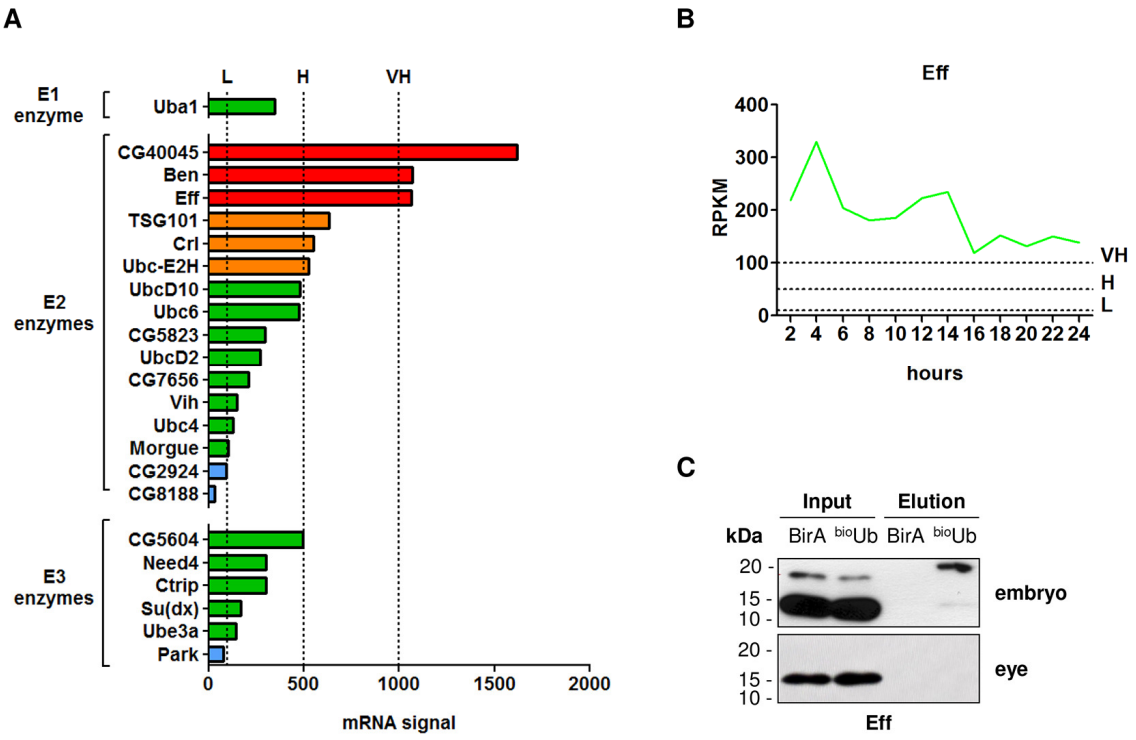

Figure 24. Reported RNA levels for the carriers detected in *Drosophila* eye.

A. mRNA signal, obtained from a GeneChip *Drosophila* Genome 2.0 array (Affymetrix) and reported on the fly atlas web server (www.flyatlas.org), for the identified E1, E2 and E3 carrier enzymes in the eye of *Drosophila melanogaster.* Dot vertical lines indicate the expression level threshold used by Flybase, where (L) is low expression level, (H) high expression and (VH) very high expression. A colour code indicating the expression level of each mRNA is also provided. Red indicates very high expression level (above VH threshold), orange high expression (between V and VH thresholds), green moderate expression (between L and V thresholds) and blue low expression (below L threshold). These publicly available data were obtained from Flybase (www.flybase.org) **B.** mRNA levels for Effete (Eff), measure as reads per kilobase of exon model per million mapped reads (RPKM), at different times of the embryo development. As for panel (A) horizontal dot lines indicate the expression level threshold used by Flybase. L: Low, H: High and VH: Very High. These publicly available data were obtained from Flybase (www.flybase.org). **C.** Western blot with Eff antibody in pulldown samples obtained from fly embryo and adult eye. BirA stands for: *elav^{GAL4},^{UAS}BirA/CyO* for embryo and *GMR^{GAL4}/CyO;^{UAS}BirA/TM6B* for adult eye; ^{bio}Ub stands for: *elav^{GAL4}, ^{UAS}(^{bio}Ub)$_6$-BirA/CyO* and *GMR^{GAL4},^{UAS}(^{bio}Ub)$_6$-BirA/CyO* for embryo and adult, respectively.

low abundance in the *Drosophila* eye, and therefore difficult to detect by MS and Western blot.

Having analysed the ubiquitin carrier enzymes separately, the remaining identifications are expected to correspond to lysine-ubiquitinated proteins, some of which were validated by Western blotting to characterize the number of ubiquitin molecules attached (**Figure 17**, **Figure 21** and Franco *et al.*, 2011). The total numbers of ubiquitin conjugates identified in embryonic and adult samples were, respectively, 217 and 350, with only 90 being common to both data sets (**Figure 23**) for each of the groups. A list of the top-20 ubiquitin conjugated proteins, based on the number of independent identification in different replicate and in PEP score, is given in **Table 11.**

Table 11. Lis of top 20 proteins found only in adult, only in embryo or in both datasets.

Identified only in adult			Common identified proteins					Identified only in embryo		
				adult		embryo				
Protein [a]	PEP Score	n	Protein [a]	PEP Score	n	PEP Score	n	Protein [a]	PEP Score	n
C11.1	0	3	Fax	0	3	0	4	Rm62	10^{-215}	4
Wat	0	3	RpS7	10^{-189}	2	0	4	Rin	10^{-089}	4
Calx	10^{-239}	3	His2A	10^{-176}	2	10^{-206}	4	Alt	10^{-065}	3
CG3529	10^{-185}	3	Rad23	10^{-276}	3	10^{-185}	4	Kuk	10^{-022}	3
Ltd	10^{-160}	3	Snap24	10^{-019}	3	10^{-042}	4	CG9135	10^{-006}	3
Nrv2	10^{-157}	3	Eps-15	10^{-196}	3	0	3	Hsp26	0	2
Pdh	10^{-128}	3	Df31	10^{-025}	3	0	3	His2B	0	2
betaTub56D	10^{-125}	3	Eno	10^{-203}	2	10^{-237}	3	CG8223	10^{-183}	2
Vha68-2	10^{-121}	3	Tm1	10^{-156}	3	10^{-135}	3	NAT1	10^{-103}	2
CG7675	10^{-101}	3	Atpα	0	3	10^{-099}	3	Lig	10^{-082}	2
CG17121	10^{-088}	3	Smt3	10^{-039}	3	10^{-085}	3	Asx	10^{-078}	2
CG1561	10^{-060}	3	AnxB10	10^{-260}	3	10^{-049}	3	Act42A	10^{-069}	2
Scamp	10^{-051}	3	CG15435	10^{-003}	2	10^{-064}	4	EIF-4a	10^{-032}	2
Pi4KIIalpha	10^{-051}	3	Akap200	10^{-011}	2	0	3	Fas2	10^{-018}	2
Sktl	10^{-044}	3	Bacc	10^{-078}	2	10^{-227}	3	His1	10^{-018}	2
Gga	10^{-039}	3	Rngo	10^{-047}	2	10^{-078}	3	HIP	10^{-017}	2
Hop	10^{-034}	3	Hsc70-1	10^{-103}	3	10^{-081}	2	dUTPase	10^{-012}	2
lap	10^{-030}	3	CtBP	10^{-018}	3	10^{-007}	2	CG1307	10^{-010}	2
CG12025	10^{-025}	3	Argk	10^{-194}	2	10^{-058}	2	CG3223	10^{-010}	2
Uif	10^{-023}	3	Hsc70Cb	10^{-125}	2	10^{-008}	2	Stai	10^{-008}	2

The lowest Posterior Error Probabilities (PEP Score) and number of identification in independent ^{bio}Ub experiments are reported. All PEP Scores, peptides and intensities are shown in table A2 in Appendix I.

[a] Protein name given according to Flybase nomenclature (www.flybase.org)

For the purpose of obtaining a functional overview of the main pathways regulated by ubiquitination at those two stages, a bioinformatic analysis was performed with GO Term mapper and g-profiler (Reimand *et al*., 2011). As illustrated with the pie charts for the gene's biological processes, localization and activities, significant differences exist between the proteins found only in embryonic and only in adult samples (**Figure 25**). Most notably, a shift was found in the "Biological processes" domain from a predominance of "Cell cycle + Reproduction" and "Cellular component organization and biogenesis" terms in the embryo to "Localization and transport" and "Cell communication" in the adult samples. Concomitantly, in regards to "Cellular compartment", a shift was detected from a predominance of proteins with "Nuclear" localization in the embryonic neurons to "Plasma membrane" in the adult ones. When analysing the "Molecular function" domain, a significant shift was observed from "Structural molecule" and "Transcription factor" activities to the "Transporter activity" and "Molecular transducer activity" categories. Similarly, the g:profiler analysis (**Figure 26**) showed the specific enrichment of terms such as "Cell cycle", "Developmental process" and "Cellular component organization or biogenesis" in the analysis performed with the proteins found only in embryo. These biological processes did not appear enriched in the analysis with the proteins found only in adult, but instead "Localization", "Synaptic transmission" and "Establishment of localization" did. Differently enriched terms in regards to the "Cellular compartment and molecular" function domains were also found. Terms as "Macromolecular complex", "Cytoskeleton", "Nucleus" and "mRNA binding" were enriched in the embryonic sample, while "Plasma membrane", "Synapse", "Transporter activity" and "SNAP receptor activity" terms were enriched in the adult sample.

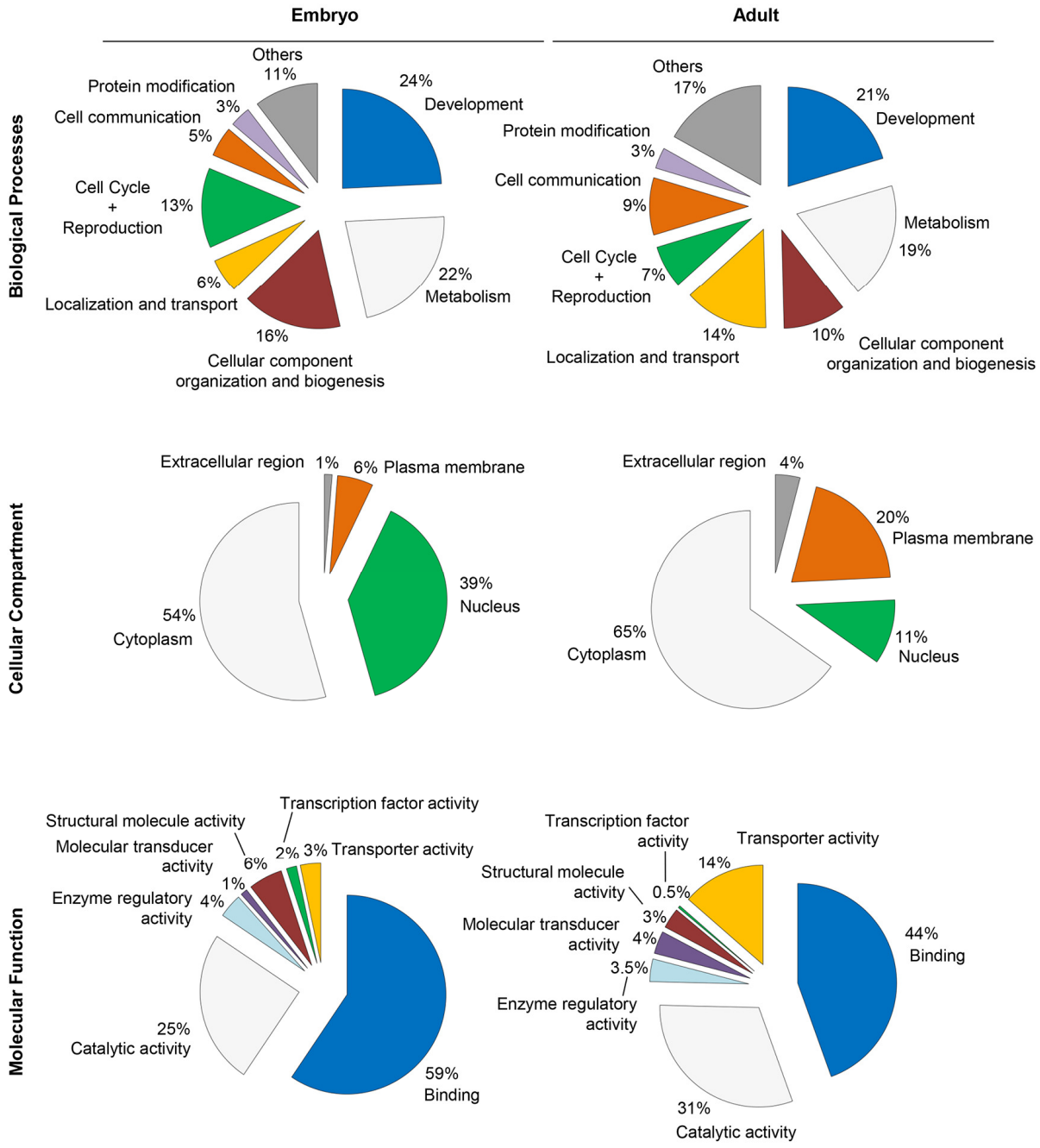

Figure 25. Functional interpretation of identified ubiquitin conjugates with GO Term mapper.

Analysis of ubiquitin conjugates identified only in the embryo or in adult provided a list of broad GO terms (GO Slim) for the biological process (72 categories), cellular compartment (30 categories) and molecular function (44 categories) domains, which were additionally grouped into fewer categories to make their representation easier to interpret. Categories representing less than 3% in the biological processes were grouped as "others". Only "extracellular matrix", "plasma membrane", "nucleus" and "cytoplasm" categories are depicted in the cellular compartment classification. Taken from Ramirez *et al.*, 2015.

Embryo p-value	Adult p-value	Go term	Go Term description	
3,84E-06	2,12E-02	GO:0009987	**cellular process**	BP
2,68E-07	1,00E+00	GO:0007049	cell cycle	BP
1,49E-03	1,00E+00	GO:0044237	cellular metabolic process	BP
5,31E-06	1,00E+00	GO:0034641	cellular nitrogen compound metabolic process	BP
4,21E-07	1,00E+00	GO:0006139	nucleobase-containing compound metabolic process	BP
9,13E-08	1,05E-01	GO:0032502	**developmental process**	BP
2,24E-10	4,17E-01	GO:0071840	**cellular component organization or biogenesis**	BP
1,00E+00	1,49E-15	GO:0051179	**localization**	BP
1,43E-06	5,10E-03	GO:0032501	**multicellular organismal process**	BP
1,98E-07	6,57E-04	GO:0044707	single-multicellular organism process	BP
1,00E+00	6,40E-09	GO:0035637	multicellular organismal signaling	BP
1,00E+00	6,40E-09	GO:0019226	transmission of nerve impulse	BP
1,00E+00	3,45E-09	GO:0007268	synaptic transmission	BP
3,65E-03	1,45E-04	GO:0065007	**biological regulation**	BP
1,00E+00	7,81E-13	GO:0065008	regulation of biological quality	BP
1,00E+00	5,18E-13	GO:0051234	**establishment of localization**	BP
1,00E+00	2,53E-12	GO:0006810	transport	BP
4,37E-12	1,76E-01	GO:0005623	**cell**	CC
7,93E-16	1,00E+00	GO:0032991	**macromolecular complex**	CC
3,06E-11	1,00E+00	GO:0043226	**organelle**	CC
3,61E-17	1,00E+00	GO:0044422	**organelle part**	CC
4,37E-12	1,76E-01	GO:0044464	**cell part**	CC
5,08E-12	1,00E+00	GO:0005622	intracellular	CC
1,90E-13	1,00E+00	GO:0044424	intracellular part	CC
6,04E-16	1,00E+00	GO:0044446	intracellular organelle part	CC
1,56E-06	1,00E+00	GO:0044428	nuclear part	CC
5,33E-16	1,00E+00	GO:0044430	cytoskeletal part	CC
1,00E+00	4,85E-16	GO:0071944	cell periphery	CC
1,00E+00	7,17E-18	GO:0005886	plasma membrane	CC
1,00E+00	6,97E-05	GO:0045202	**synapse**	CC
1,00E+00	1,03E-08	GO:0016020	**membrane**	CC
1,00E+00	6,27E-04	GO:0005215	**transporter activity**	MF
1,00E+00	3,43E-02	GO:0022857	transmembrane transporter activity	MF
1,00E+00	1,94E-03	GO:0022804	active transmembrane transporter activity	MF
1,00E+00	5,21E-04	GO:0016820	hydrolase activity, catalyzing transmembrane movement of substances	MF
6,96E-02	1,00E+00	GO:0005488	**binding**	MF
6,45E-05	7,00E-02	GO:0005515	protein binding	MF
	1,21E-04	GO:0005484	SNAP receptor activity	MF
7,62E-03	1,00E+00	GO:1901363	heterocyclic compound binding	MF
5,16E-05	1,00E+00	GO:0003676	nucleic acid binding	MF
3,16E-03	1,00E+00	GO:0003723	RNA binding	MF
8,29E-04	1,00E+00	GO:0003729	mRNA binding	MF

Figure 26. Functional interpretation of the identified ubiquitin conjugates with G:Profiler.

Proteins found only in embryo or only in adult were analysed by G:profier for GO Term enrichment analysis. Summary of the enriched GO Terms in the biological process (BP), cellular compartment (CC) and molecular function (MF) domains are shown. Statistical enrichment of each Term is provided by the p-value, which is also represented by a colour according to its value (the lower the p-value the stronger intensity of red). The software calculates p-values using Fisher´s one tailed test combined with a custom multiple testing correction algorithm (Reimand *et al*., 2011). Taken from Ramirez *et al*., 2015.

3. Changes in the ubiquitinated landscape upon different conditions

The ^{bio}Ub strategy has proven to be very efficient for the isolation and enrichment of ubiquitinated material from cells (Min *et al*., 2014) and tissue lysates (Franco *et al*., 2011; Lectez *et al*., 2014; Ramirez *et al*., 2015). The expression of biotinylated ubiquitin can be directed *in vivo* to any cell population, and at any stage during the development, with the used of specific expression systems such as the GAL4/UAS (Brand and Perrimon, 1993) or tetracycline-responsive promoters (Gossen and Bujard, 1992). Further combination of this tool with a particular treatment or a disease model could therefore be of great value in order to identify proteins whose ubiquitination is affected in response to specific perturbations. For this reason, we decided to evaluate the capacity of the ^{bio}Ub strategy to monitor changes in protein ubiquitination upon inhibition of proteasomal degradation and to identify E3-specific substrates.

3.1. ^{bio}Ub strategy upon interference with proteasomal function

Most ubiquitin proteomic studies have been performed on cell culture on which the proteasome had been inhibited using specific drugs (Kisselev and Goldberg, 2001), with the intention to lead to a significant accumulation of ubiquitinated proteins. However, while the amount of the provided drug is easily controlled in cell culture assays, in *Drosophila* a variability in the dosage might exist, due to differences in ingestion rates and even to adaptative mechanisms to prolonged exposures (Pandey and Nichols, 2011). Besides, proteasome inhibitor drugs may also affect other cellular proteases (Kisselev

and Goldberg, 2001), leading to cellular responses that are not exclusively dependent on the proteasome inhibition. Recently, flies overexpressing a truncated form of Rpn10 (^{UAS}Rpn10-ΔNTH), a proteasomal ubiquitin receptor, were reported to cause an accumulation of ubiquitinated proteins that should otherwise be degraded by the proteasome (Lipinszki *et al*., 2009). This failure on protein turnover is not a result of direct proteasomal inhibition, but caused by the inability of Rpn10 to transport the trapped proteins to the proteasome. Furthermore, Rpn10-mediated inhibition of protein degradation can be applied in a tissue specific manner, as its expression is controlled by the yeast transcription activator GAL4 protein (Lipinszki *et al*., 2009; Ramirez *et al*., 2015). Combination of those ^{UAS}Rpn10-ΔNTH flies with the ^{bio}Ub ones was therefore performed in order to analyse the *Drosophila* ubiquitination landscape upon a selective blockade of the proteasomal degradation pathway.

3.1.1. Generation of flies that accumulate ubiquitinated material

Flies with *elav^{GAL4},^{UAS}(^{bio}Ub)$_6$-BirA /CyO; TM2/TM6B* and *GMR^{GAL4},^{UAS}(^{bio}Ub)$_6$-BirA/CyO; TM2/TM6B* genotypes were crossed to those that overexpressed the C-terminal half of the proteasomal shuttling protein Rpn10 under the control of the GAL4 protein (^{UAS}Rpn10-ΔNTH; hereinafter Rpn10^{DN}). Rpn10^{DN} contains three UIMs (**Figure 27A**) that recognize and bind poly-ubiquitinated material, but lacks the von Willebrand factor A (VWFA) domain required for binding to the proteasome (Lipinszki *et al*., 2009). Overexpression of Rpn10^{DN} has been shown to act in a dominant negative manner by binding to ubiquitinated proteins and preventing their delivery to the proteasome. This results in a significant accumulation of ubiquitinated material when it is either

ubiquitously expressed in larvae, under the control of the daughterless-GAL4 (Lipinszki *et al*., 2009), or when it is expressed in the *Drosophila* eye under the control of GMR^{GAL4} (Lee *et al*., 2014).

In agreement with previous reports, combination of $Rpn10^{DN}$ with the ^{bio}Ub transgene resulted in an increase of high molecular- weight ubiquitinated material when compared to ^{bio}Ub alone, as shown by anti-biotin Western blot in embryo whole extracts (**Figure 27B**). In adults, rather than an increase, a differential distribution was observed, with a preferential attachment of the biotinylated ubiquitin to higher molecular weight proteins. Western blots performed with anti-BirA antibody revealed that the expression level of the $^{UAS}(^{bio}Ub)_6$-BirA construct was similar when expressed alone or together with $Rpn10^{DN}$ transgene in embryonic samples (**Figure 27B**). In adult a slight reduction in BirA expression was observed in $Rpn10^{DN}$ expressing flies, which might indicate a deficiency of the GAL4 protein to drive the expression of both constructs simultaneously. Similarly, when a biotin pulldown was performed with either embryo or adult fly heads of the mentioned genotype, an increased or a differential distribution of the purified material was also observed by Western blot in the eluted fraction (**Figure 27C**). Nonetheless, silver staining of the eluted proteins confirmed the presence of more material in $Rpn10^{DN}$ expressing embryo and adult flies (**Figure 27D**), as for similar level of the endogenous biotinylated protein that run at ~130 kDa (CG1516) a smear of stronger signal is observed in $Rpn10^{DN}$ samples.

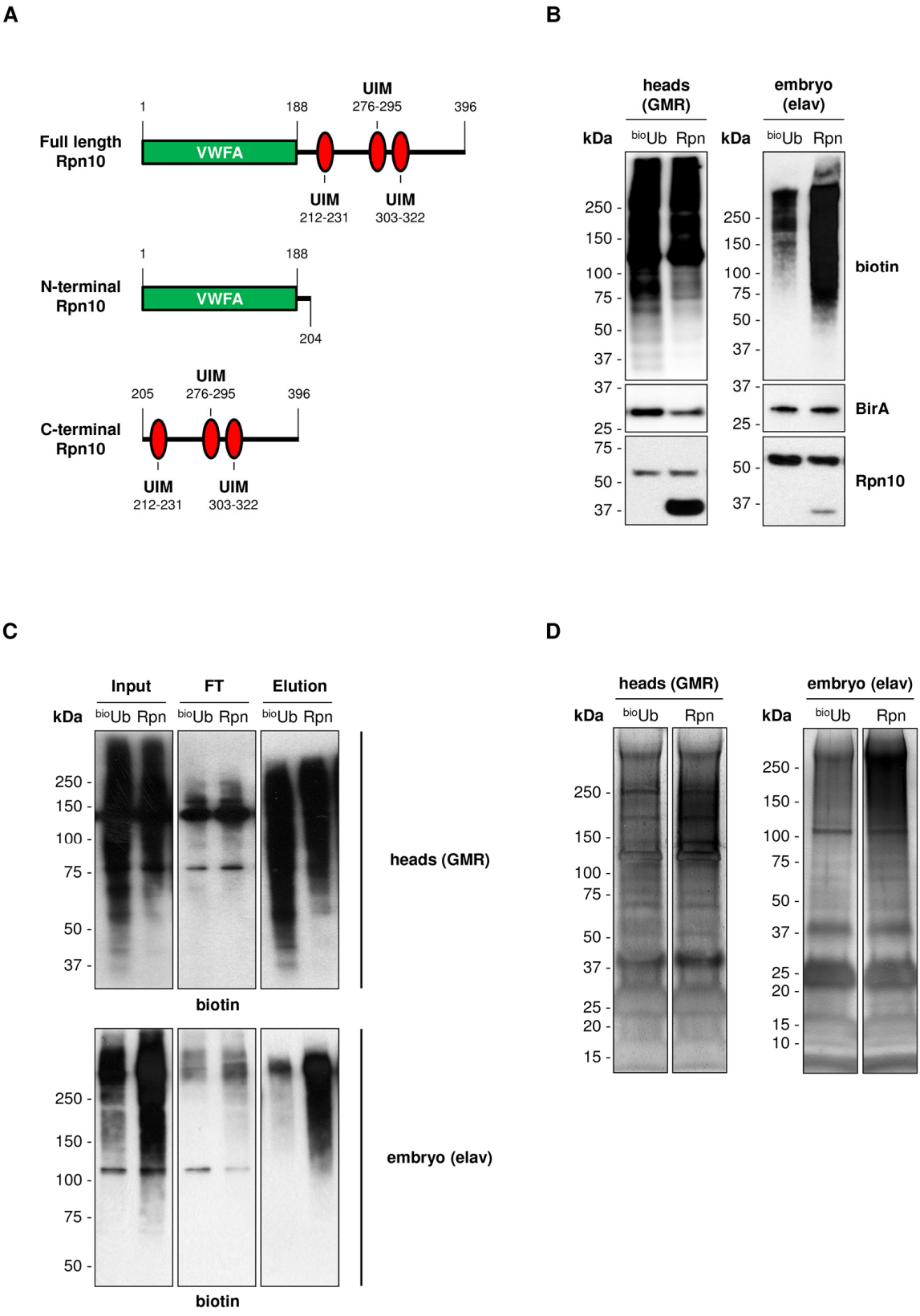
A
Full length Rpn10
VWFA
1
188
UIM 276-295
396
UIM 212-231
UIM 303-322
N-terminal Rpn10
204
C-terminal Rpn10
205
B
heads (GMR)
embryo (elav)
kDa
bioUb Rpn
biotin
BirA
Rpn10
C
Input
FT
Elution
heads (GMR)
embryo (elav)
D

Figure 27. Expression of the C-terminal half of Rpn10.

A. Schematic illustration of the main domains found in Rpn10 protein. The full length Rpn10 contains a von Willebrand factor A (VWFA) domain required for interaction with the proteasome as well as three ubiquitin-interacting motifs (UIMs) that allow Rpn10 to bind ubiquitinated proteins. The VWFA is located in the N-terminal part of the protein (residues 1-188) and the UIMs are found on the C-terminal region (residues 205-396). While the full length protein will bind and shuttle ubiquitinated proteins to the proteasome, the overexpressed C-terminal half will be able to bind the ubiquitinated material, but not the proteasome, preventing the degradation of the bound proteins **B.** Western blot analysis from adult head (GMR^{GAL4}) and embryo ($elav^{GAL4}$) whole extract expressing the $^{UAS}(^{bio}Ub)_6$-BirA construct alone (^{bio}Ub) or together with $Rpn10^{DN}$ (Rpn). The anti-biotin antibody revealed an increase in the amount of the material that is ubiquitinated with biotinylated ubiquitin when $Rpn10^{DN}$ is expressed in embryos, as compared to expression of ^{bio}Ub alone**.** In adults, a differential distribution is observed instead, with a preferential attachment of the biotinylated ubiquitin to higher molecular weight proteins. This effect is observed for similar expression levels of the $^{UAS}(^{bio}Ub)_6$-BirA construct, as detected by anti-BirA antibody, indicating that the accumulation or the differential distribution of the ^{bio}Ub conjugates is due to the overexpression of $Rpn10^{DN}$. The expression of $Rpn10^{DN}$ construct was detected using an antibody to the Rpn10 protein. **C.** Anti-biotin Western blots with adult (top) and embryo (bottom) pulldown samples confirmed that the same effect happens in the eluted fractions upon $Rpn10^{DN}$ expression (Rpn). Dilutions of the input, flow through (FT) and elution are shown. **D.** Silver staining of the material purified with the NeutrAvidin beads for $Rpn10^{DN}$ (Rpn) and ^{bio}Ub samples. Equal amounts of ^{bio}Ub and $Rpn10^{DN}$ samples were analysed for each pulldown using SDS-PAGE and stained with silver. Both for adult (left) and embryo (right) samples an accumulation of ubiquitinated material is detected on samples overexpressing the C-terminal half of Rpn10 (Rpn), as compared to the ^{bio}Ub control samples. In B, C and D panels ^{bio}Ub stands for flies expressing the $^{UAS}(^{bio}Ub)_6$-BirA construct and Rpn for flies expressing both the $^{UAS}(^{bio}Ub)_6$-BirA construct and the C-terminal half of Rpn10 ($Rpn10^{DN}$) protein. Ramirez *et al*., 2015.

3.1.2. Mass spectrometric identification of proteins accumulated upon Rpn10^{DN} expression

Three independent biological replicates, for both embryo and adult, overexpressing Rpn10^{DN} were subjected to NeutrAvidin pulldown (**Figure A4 in appendix II**) and MS analysis, with the aim of identifying the proteins that are accumulating in Rpn10^{DN} flies. Contrary to what it would have been expected, however, the MS analysis provided a reduced number of identification in all three Rpn10^{DN} experiments (**Figure 28**). These results suggest that expression of Rpn10^{DN} is interfering with the biotinylated ubiquitin pool, affecting the number of proteins that are purified under these conditions. Yet some proteins were exclusively identified in the purified material of Rpn10^{DN} expressing flies, 21 in the adult eye and 11 in the *Drosophila* embryo.

The various datasets in this work were obtained from independent biological samples, and the experiments performed independently in different days. Consequently, we were not confident enough to jointly analyse all our data sets, as MS settings might vary from experiment to experiment. Moreover, comparison of protein abundance between two conditions requires a proper quantifiable value. LFQ has proven to be a proper measurement for that purpose (Luber *et al*., 2010). In some circumstances, however, mass spectrometric software does not obtain enough data to provide a LFQ value for a given identified protein, as is the case for many of the proteins seen in Rpn10^{DN} (**Table A1 and A2 in Appendix I**). For that reason, LFQ intensity ratios between pairs of Rpn10^{DN} and ^{bio}Ub samples analysed on the same day were determined and used as selection criteria to discriminate among those proteins found more

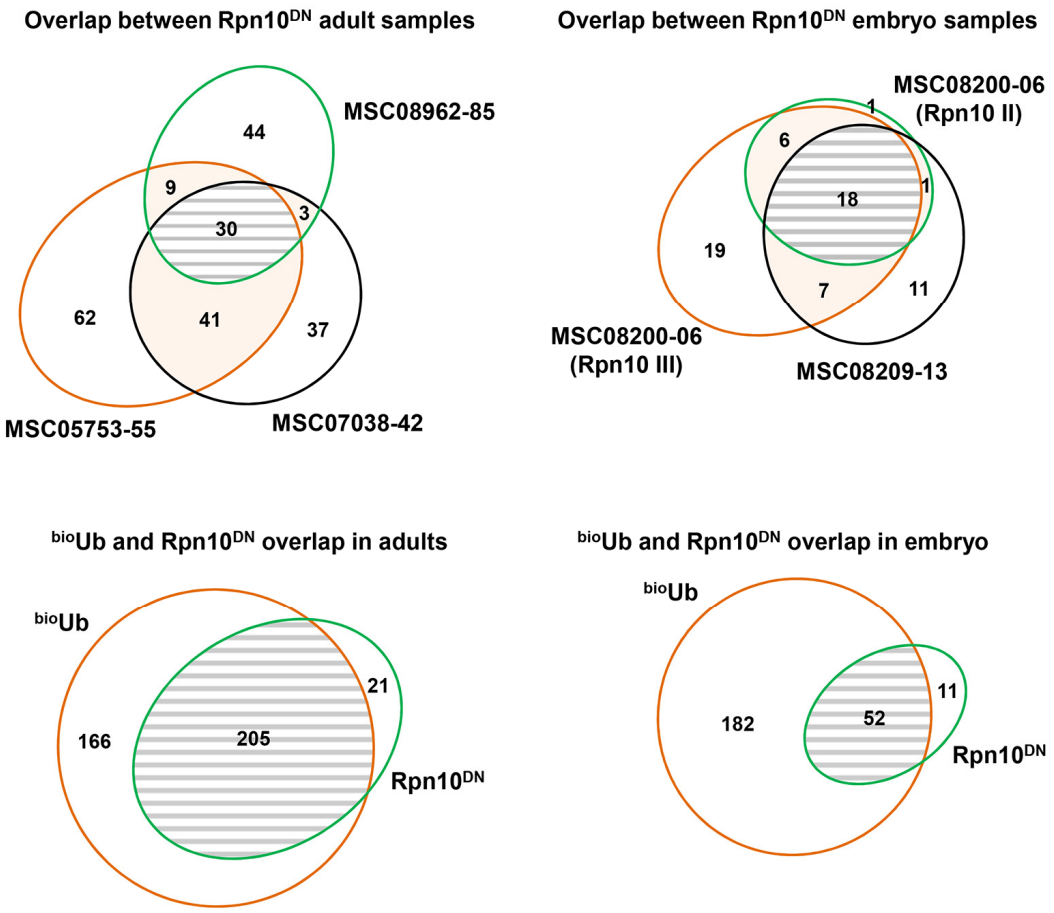

Figure 28. Number of proteins identified by MS across independent Rpn10^{DN} pulldowns.

Venn diagrams showing the overlap existing between independent biological replicates in adult and embryo samples (upper), as well as the overlap existing between the proteins identified in ^{bio}Ub and Rpn10^{DN} samples (bottom). The variability found among independent replicate is similar to that earlier found for ^{bio}Ub replicates. The total amount of proteins isolated from embryo and adult Rpn10^{DN} samples, however, was in both cases lower than the amount of proteins identified in ^{bio}Ub samples. For each pulldown experiment the number assigned by the MS core facility at the MDC Institute is provided.

ubiquitinated upon Rpn10^{DN} overexpression. Proteins identified in at least two independent Rpn10^{DN} biological replica and whose Rpn10^{DN}/^{bio}Ub LFQ intensity ratio was bigger than 4 in at least two experiments were preliminary selected as candidate Rpn10 substrates. Among Rpn10^{DN} embryo samples none of the identifications

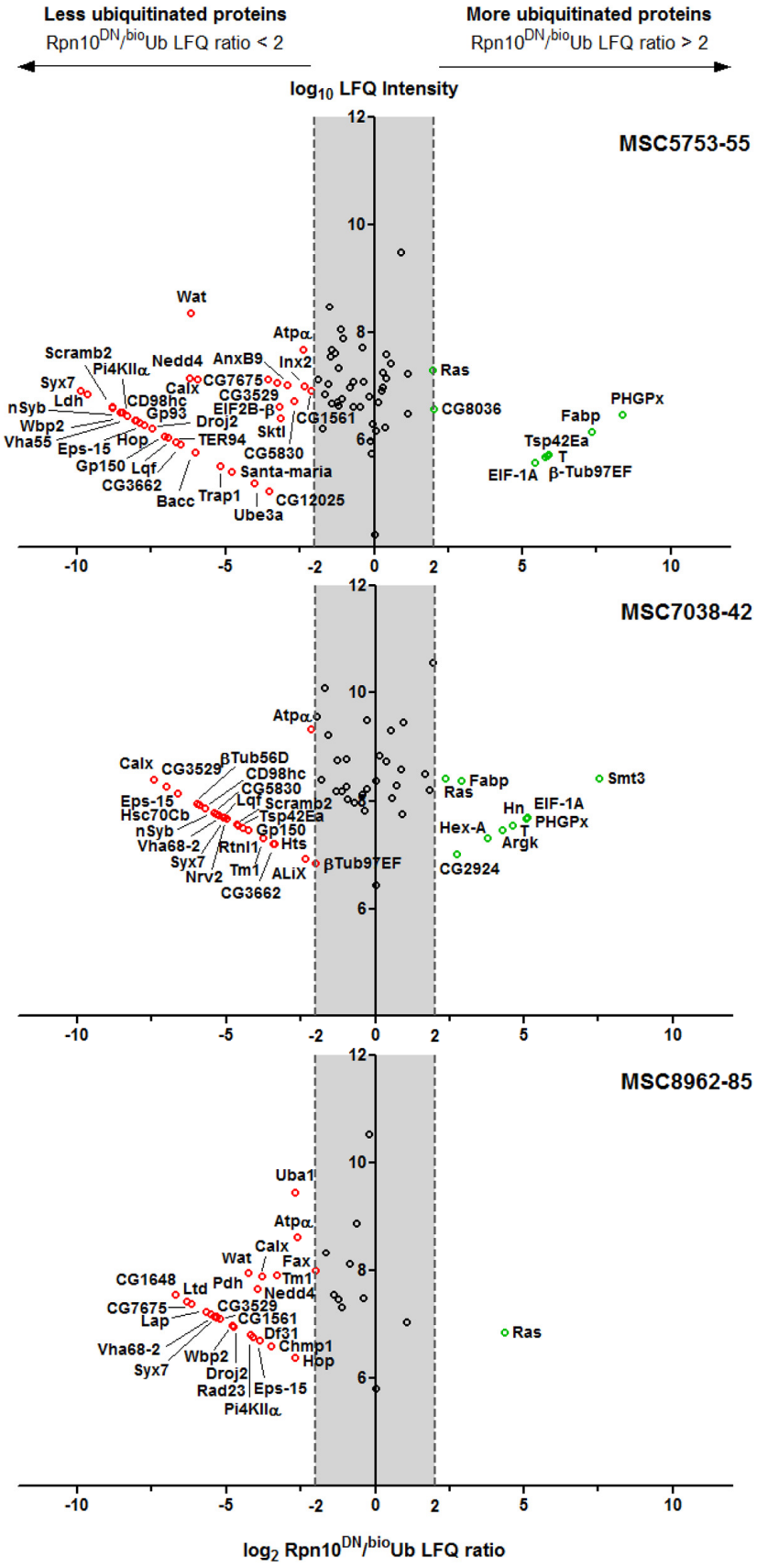
Less ubiquitinated proteins
Rpn10DN/bioUb LFQ ratio < 2
More ubiquitinated proteins
Rpn10DN/bioUb LFQ ratio > 2
log10 LFQ Intensity
MSC5753-55
MSC7038-42
MSC8962-85
log2 Rpn10DN/bioUb LFQ ratio

Figure 29. Proteins found differentially ubiquitinated in adult Rpn10^{DN} samples.

Vulcano plots showing the proteins that appeared differentially ubiquitinated upon Rpn10^{DN} overexpression. Rpn10^{DN}/^{bio}Ub LFQ ratios of those proteins identified in at least two independent Rpn10^{DN} experiments were calculated for each MS analysis. For those proteins for which LFQ values were not reported, the lowest LFQ value obtained in the analysis was assigned. Those proteins with a LFQ ratio bigger than 2 (in $\log_2$ scale) were considered to be more ubiquitinated in Rpn10^{DN} samples *vs* control samples, while those with a ratio lower than -2 were considered to be less ubiquitinated,. For each pulldown experiment the number assigned by the MS core facility at the MDC Institute is provided.

completely fulfil the applied criteria (**Figure A5 appendix II**). However, among adult Rpn10^{DN} five were found to do so (**Figure 29**): Raspberry (Ras), Fatty acid binding protein (Fabp), PHGPx, Eukaryotic initiation factor 1A (EIF-1A) and Tan (T). Besides, three ubiquitination sites (K56, K88 and K104) were also detected for EIF-1A protein in one Rpn10^{DN} pulldown (MSC7038-42) but not in ^{bio}Ub sample (**Table A1 in appendix I**).

Those proteins whose Rpn10^{DN}/^{bio}Ub LFQ ratio was lower than 0.25 (i.e., the LFQ intensity in the Rpn10^{DN} sample was 4 times lower than that detected in ^{bio}Ub sample) in at least two independent experiments, were considered to be less ubiquitinated upon Rpn10^{DN} overexpression. Those with a ratio between 0.25 and 4 were, hence, classified as having no significant variation in their ubiquitination level. For instance, ubiquitin protein levels were deemed similar between ^{bio}Ub and Rpn10^{DN} samples, as its LFQ Rpn10^{DN}/^{bio}Ub ratio was found to be between the 0.25-4 range in all the pulldown experiments performed from adult (average of 2.2 ± 1.5 SD) and embryo (average of 1.3 ± 0.05) samples. Similar results were found for Uba1 enzyme, whose LFQ ratio was between the mentioned range in two out of three adult samples (average of 0.27 ± 0.1

SD) and in all the embryo experiments (average of 1.2 ± 0.8 SD). Among the proteins found to be less ubiquitinated in at least two independent experiments Atpα, Eps-15 or Lqf were found. Those are known mono-ubiquitinated proteins (**Figure 17**, **Figure 21** and **Figure 29**). It has been proposed that upon an increase in protein poly-ubiquitination caused by the blockade of the proteasome, mono-ubiquitinated molecules, such as histones, are deubiquitinated as a mechanism to rapidly provide the cell with free ubiquitin monomers, which could not be otherwise accomplished by new ubiquitin synthesis (Dantuma *et al*., 2006; Groothuis *et al*., 2006). We can therefore conclude that exactly the same is happening here to those other mono-ubiquitinated proteins, in this case with their less modification being driven by the ectopic biotinylated ubiquitin.

3.1.3. *In vivo* validation of proteins accumulated upon Rpn10^{DN} overexpression

In order to confirm the increased ubiquitination of Ras, Fabp, PHGPx, ElF-1A and T, additional biotin pulldowns from both ^{bio}Ub and Rpn10^{DN} fly heads were performed. Unfortunately, we could not test all the proteins mentioned above as we were only able to obtained antibodies for T (Wagner *et al*., 2007) and EIF-1A. The commercially available mammalian EIF-1AX (AntibodyBcn), however, did not recognize the *Drosophila* protein despite an 80% homology between the fly and the mammalian proteins is found (data not shown). On the other side, anti-Tan Western blot did detect a band of the appropriate size in the input fractions of both ^{bio}Ub and Rpn10^{DN} pulldowns, at about 25 kDa (Wagner *et al*., 2007). Several bands in the eluted fraction corresponding to mono and poly-ubiquitinated portions of Tan were also detected,

which presented a stepwise increase of approximately 8 kDa (one ubiquitin) each. However, contrary to what would be expected from the MS data, this protein was found by Western blot to be less ubiquitinated when $Rpn10^{DN}$ was expressed (**Figure 30A**). An immunoblot with an antibody that detect poly-ubiquitin chains performed on the same membrane where anti-Tan was used, confirmed the presence of more poly-ubiquitinated material on $Rpn10^{DN}$ sample (**Figure 30B**). We therefore conclude that Tan is not enriched upon $Rpn10^{DN}$ expression, despite appearing to be so as suggested by the MS data. This result emphasizes the importance of using orthogonal approaches along with MS, as the reliance on one unique technique, no matter how advance, might lead to obtain false positives.

Western blots to the mono-ubiquitinated proteins, however, were consistent with the mass spectrometric observation of reduced ubiquitination upon $Rpn10^{DN}$ expression. For instance, Atpα protein was found to be less ubiquitinated in $Rpn10^{DN}$ expressing adult flies (**Figure 30C**). Equally, the ubiquitination of Fax was also detected by Western blot to be reduced in the $Rpn10^{DN}$ sample (**Figure 30C**). In the case of embryo samples, two antibodies, anti-Lqf and anti-Nrt, previously used to validate by Western blot the ubiquitination of these two proteins (**Figure 21**), were selected to analyse the effect of $Rpn10^{DN}$ expression on mono-ubiquitination in developing neurons. The amounts of both Lqf and Nrt, were found to be also reduced within the ubiquitin-enriched pulldown (**Figure 30D**). These results support the idea that biotinylated ubiquitin, as it has been reported for endogenous ubiquitin (Groothuis *et al*., 2006; Kaiser *et al*., 2011; Wagner *et al*., 2011), is preferentially retained by poly-ubiquitinated proteins upon $Rpn10^{DN}$

overexpression, and hence mono- ubiquitinated proteins, become absent or present on a reduced scale on the biotin purification performed on tissues expressing Rpn10^{DN}.

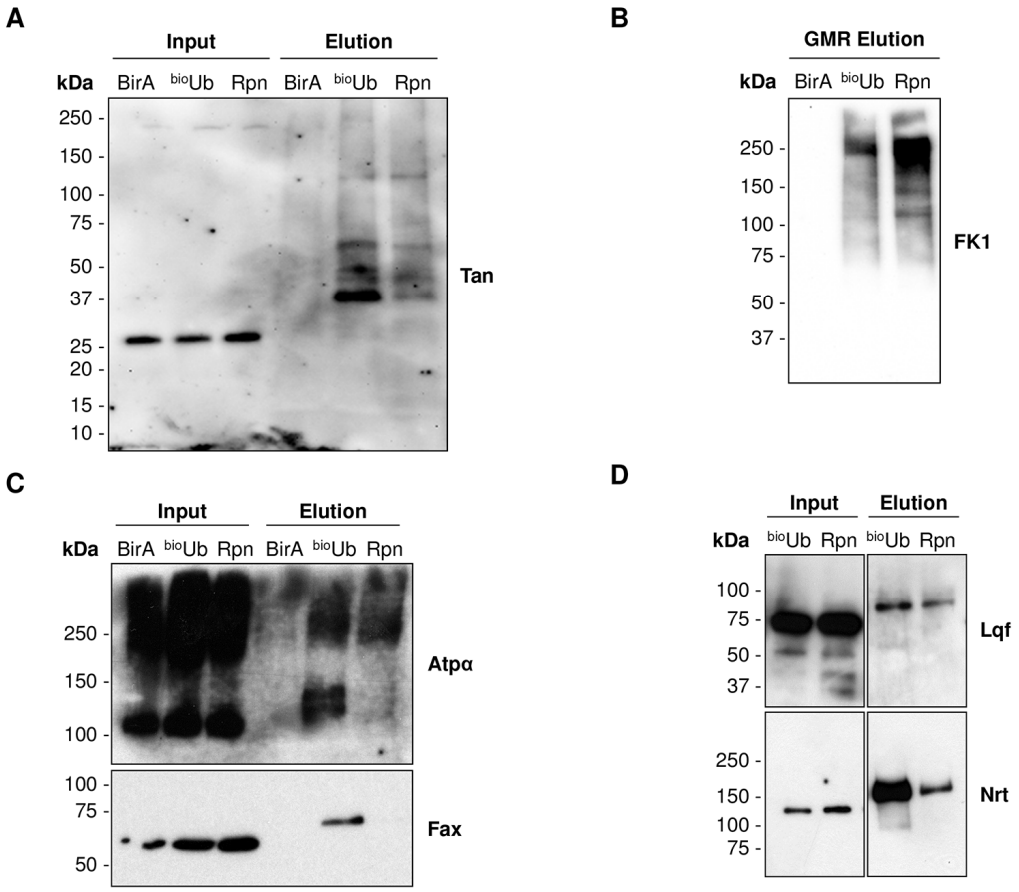

Figure 30. Western blots on ubiquitinated material isolated from Rpn10^{DN} samples.

A. Western blot to Tan protein on adult ^{bio}Ub and Rpn10^{DN} samples revealed that Tan is not found more ubiquitinated upon Rpn10^{DN} overexpression. **B.** Anti-FK1 immunoblot performed on the same membrane as in (A) showed an increase in the formation of poly-ubiquitin chains when Rpn10^{DN} is expressed. **C** and **D.** Western blot to some mono-ubiquitinated proteins confirmed that in Rpn10^{DN} samples the biotinylated ubiquitin is preferentially attached to poly-ubiquitinated proteins, in both embryos (C) and adult (D) samples. BirA: flies expressing only the BirA enzyme; ^{bio}Ub: flies expressing the $^{UAS}(^{bio}Ub)_6$-BirA construct; Rpn: flies expressing both the $^{UAS}(^{bio}Ub)_6$-BirA construct and the C-terminal half of Rpn10 (Rpn10^{DN}) protein. Taken from Ramirez *et al.*, 2015.

3.2. ^{bio}Ub strategy directed to identify substrates for specific E3 ligases

Mutations on the *UBE3A* gene that result on the loss of function of the encoded protein, a HECT type E3 ubiquitin ligase, is one of the genetic mechanism leading to Angelman syndrome (AS) development (Kishino *et al*., 1997; Matsuura *et al*., 1997). Likewise, UBE3A duplication has been related with autism spectrum disorders (ASD) (Smith *et al*., 2011; Urraca *et al*., 2013), suggesting that the pathogenesis of these two diseases could be caused by the misregulation of common ubiquitin targets. The identification of the direct substrates regulated by this E3 ligase, however, has remained elusive so far as the low level at which ubiquitinated proteins are found within the cells make them difficult to detect. In *Drosophila melanogaster* the homologue of UBE3A (Ube3a), has been identified as an active-ubiquitin carrier during the embryo nervous system development (Franco *et al*., 2011) and in the photoreceptor cells (Ramirez *et al*., 2015), suggesting that this enzyme is physiologically regulating the ubiquitination of certain proteins in the fly neurons. We hence reasoned that overexpression of Ube3a would cause an increase in its targets ubiquitination, that could be detectable using the ^{bio}Ub strategy.

3.2.1. Generation of ^{bio}Ub and Ube3a overexpressing flies

Different fly models have been generated to study AS or Ube3a duplication-based autism cases (Reiter *et al*., 2006; Wu *et al*., 2008; Lu *et al*., 2009; Valdez *et al*., 2015). Flies carrying deletions on the *Ube3a* gene, therefore leading to a loss of function of the encoded protein, have been reported to mimic characteristic of AS, such as motor

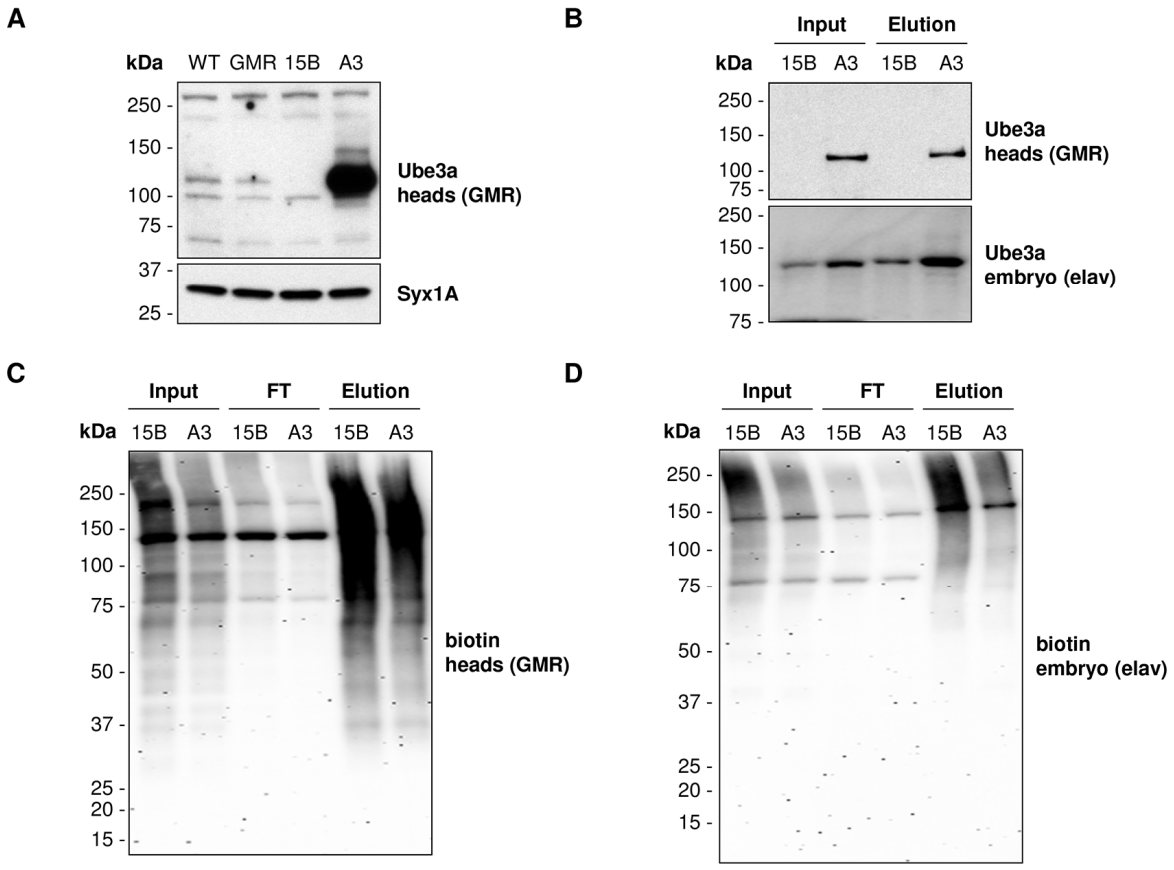

Figure 31. Ube3a mutant and Ube3a overexpressing flies.

A. Anti-Ube3a Western blot on *Drosophila* head whole extracts was used to monitor the levels of Ube3a protein when Ube3a is either overexpressed (A3) or mutated (15B). Equal protein loading was determined by anti-Syx1A immunoblot. WT**:** *OregonR*; GMR: GMR^{GAL4}*;TM2/TM6B*; 15B: *If/CyO;* $Ube3a^{15B}/Ube3a^{15B}$ (null mutant); A3: GMR^{GAL4}*/CyO;* $^{UAS}Ube3a^{A3}$*/TM6B* (Ube3a overexpression). **B.** Anti-Ube3a Western blot performed on material eluted from adult (GMR^{GAL4}) and embryo ($elav^{GAL4}$) biotin pulldowns. A significantly higher amount of the E3 ligase that was carrying ubiquitin was isolated from flies overexpressing Ube3a (A3), as compared to $Ube3a^{15B}$ heterozygous mutants (15B). **C** and **D.** Anti-biotin immunoblots on material eluted from Ube3a overexpressing (A3) and $Ube3a^{15B}$ heterozygous mutant (15B) adult heads (C) and embryo (D) samples. 15B: flies heterozygous for the Ube3a deletion and expressing the $^{UAS}(^{bio}Ub)_6$-BirA construct; A3: flies expressing both the $^{UAS}(^{bio}Ub)_6$-BirA construct and the Ube3a E3 ligase enzyme.

coordination issues or learning and memory defects (Wu *et al*., 2008). Similarly, overexpression of the *Drosophila* Ube3a has been shown to display analogous neurotransmission defects to those seen in mouse models of duplication 15q autism (Valdez *et al*., 2015). Ube3a loss of function (*Ube3a*^{15B}) and gain of function (^{UAS}Ube3a^{A3}) flies (**Figure 31A**), obtained from Dr. Janice Fischer (Wu *et al*., 2008), were crossed to flies expressing the ^{bio}Ub construct under the control of elav^{GAL4} and GMR^{GAL4}–drivers, in order to perform a comparison between the ubiquitinated proteome of flies lacking or having an extra dose of Ube3a protein. While in the absence of an E3 ligase enzyme, its substrates should not show any ubiquitination; upon E3 ligase overexpression will show a significant ubiquitination increase. Thereby, proteins identify by MS in Ube3a overexpressing flies, but absent in Ube3a null ones will be potential Ube3a substrates.

The *Drosophila* Ube3a mutants (*Ube3a*^{15B}) had been reported to be viable and fertile in homozygosis (Wu *et al*., 2008). When combined with the expression of ^{bio}Ub it was, however, required to grow them in heterozygosis, as null Ube3a flies, despite viable, were not fertile (data not shown). Nevertheless, Western blot with anti-Ube3a antibody on material eluted from flies overexpressing Ube3a showed that the amount of E3 ligase that is active in these flies is high enough, as compared to heterozygous *Ube3a*^{15B} animals (**Figure 31B**), to test our hypothesis regarding the detection by MS and Western blot of its substrates. With regards to ^{bio}Ub, a higher expression was observed in both adult (**Figure 31C**) and embryo (**Figure 31D**) *Ube3a*^{15B} flies, when compared to *Ube3a*^{A3} flies. Most probably this is due to a reduce GAL4 availability, as the amount of GAL4 protein needs to be split in *Ube3a*^{A3} flies in order to express both the ^{bio}Ub construct and the Ube3a E3 ligase. Anyhow, those proteins found to be more

ubiquitinated in Ube3a overexpressing flies should with no doubt be true Ube3a substrates.

3.2.2. Mass spectrometric identification of Ube3a ubiquitin substrates

One biotin pulldown from adult fly heads overexpressing Ube3a under the control of GMR^{GAL4} (hereinafter A3 for $Ube3a^{A3}$ allele) was compared with a pulldown from fly heads carrying a deletion on the *Ube3a* gene (hereinafter 15B for $Ube3a^{15B}$ allele), in order to identify the proteins that are regulated by this E3 ligase in the *Drosophila* photoreceptor cells. As measured by silver staining, the amount of purified material from A3 and 15B fly heads was similar (**Figure 32A**). Correspondingly, MS analysis provided a similar number of identification in both samples (**Table A1 in appendix I**). After subtraction of known contaminants and background identifications, a total of 108 and 102 proteins were classified as ubiquitin conjugates in 15B and A3 flies, respectively, of which 91 were detected in both (**Figure 32B**).

The LFQ ratio (A3/15B) for each protein was calculated in order to elucidate which of them were differentially ubiquitinated upon Ube3a overexpression. LFQ ratio threshold was set up to 4 to consider a protein to be more ubiquitinated and, in addition, only those proteins identified with at least two peptides were taken into account, to avoid the identification of false candidates due to their low abundance. As expected, Ube3a was found highly enriched in A3 flies (**Figure 33**), indicative of its high activity. Two more ubiquitin carriers were also found to be accumulated: a putative HECT type E3 ligase (CG5604) and the ubiquitin conjugating enzyme E2H (UbcE2H). The latter is the

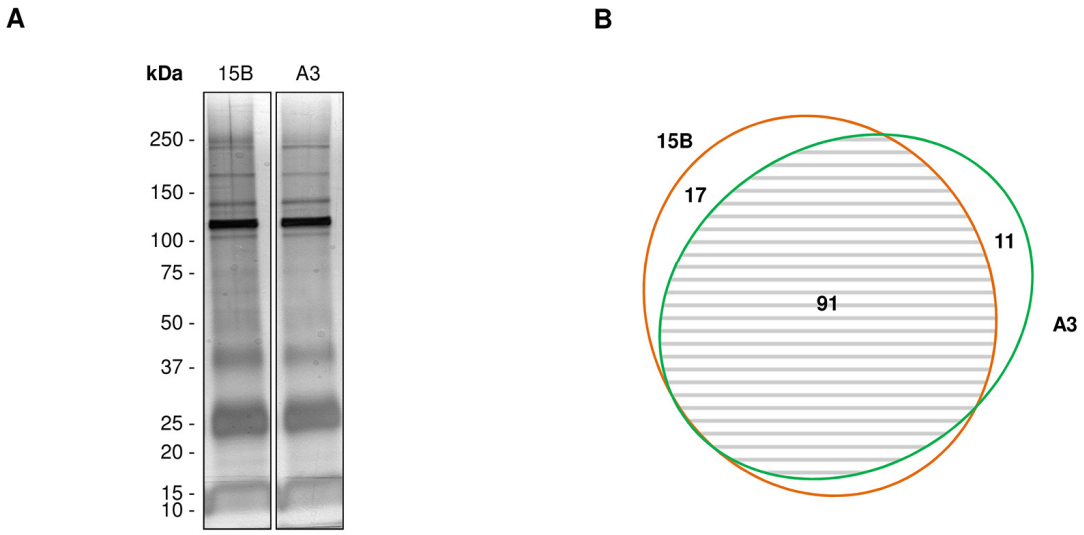

Figure 32. Purified material from Ube3a overexpressing and Ube3a-deleted fly eye.

A. Silver staining of the material purified in the biotin pulldown from Ube3a deletion (15B) and Ube3a overexpression (A3) fly eye. Equal amounts of 15B and A3 samples, as shown by the most abundant endogenously biotinylated proteins, were analysed for each sample using SDS-PAGE, and stain with silver. Thick bands at around 40 kDa and below correspond to trimer, dimer and monomer forms of NeutrAvidin. **B.** Venn diagram indicating the overlap between the proteins identified in 15B and A3 samples. About 75 % of all the proteins identified were found in both samples. 15B**:** *$GMR^{GAL4,UAS(^{bio}Ub)_6}$-BirA/CyO;$Ube3a^{15B}$/TM6B*; A3**:** *$GMR^{GAL4,UAS(^{bio}Ub)_6}$-BirA/CyO;$^{UAS}Ube3a^{A3}$/TM6B*.

homologue of the human UBE2H E2 enzyme, which has been associated with autistic disorders (Vourc'h *et al*., 2003). Five more proteins related to the ubiquitin system had an A3/15B LFQ ratio bigger than 4 (**Figure 33**): The Ubiquitin carboxy-terminal hydrolase (Uch) deubiquitinating enzyme, which is the fly homologue of the human UCH-L1 (Thao *et al*., 2012); the extraproteasomal ubiquitin receptors Ring lost (Rngo) and the Regulatory particle non-ATPase 10 (Rpn10), whose human counterpart are DDI1/DDI2 (Morawe *et al*., 2011) and PSMD4 (Haracska and Udvardy, 1997), respectively; the Refractory to sigma P (Ref(2)P) protein, homologue of the mammalian

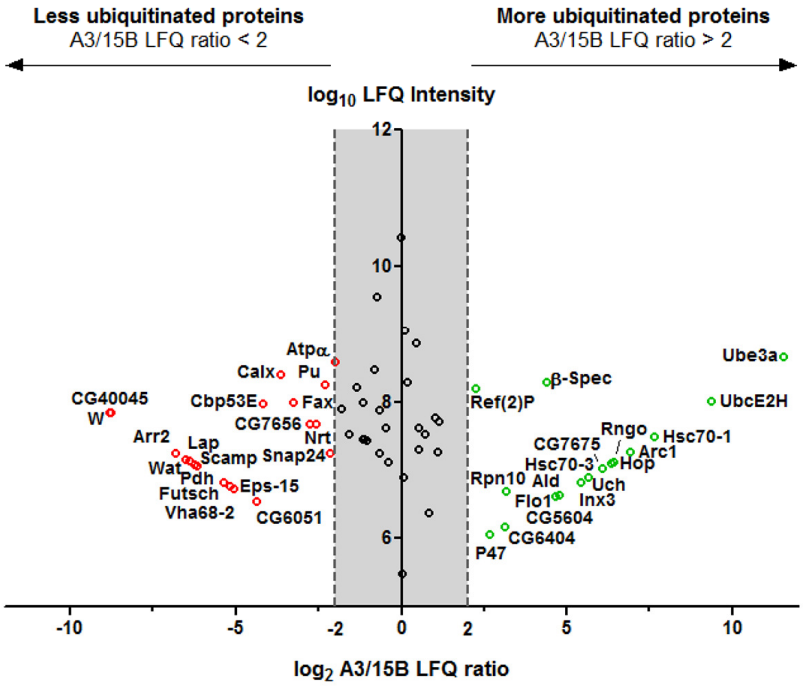

Figure 33. Proteins found differentially ubiquitinated upon Ube3a overexpression.

Vulcano plot displaying the LFQ A3/15B ratios found for each protein in $\log_2$ scale (*x* axis). In the *y* axis the sum of the LFQ intensity found in A3 and 15B pulldowns is depicted (in $\log_{10}$ scale). For those proteins that did not have LFQ intensity on one of the samples the lowest LFQ intensity recorded in the MS analysis was given, in order to provide a ratio. Proteins whose LFQ A3/15B ratio was lower than "2" and bigger than "-2" (in $\log_2$ scale) were considered to be equally ubiquitinated in both conditions (grey region). 15B: *$GMR^{GAL4,UAS(^{bio}Ub)_6}$-BirA/CyO;$Ube3a^{15B}$/TM6B*; A3: *$GMR^{GAL4,UAS(^{bio}Ub)_6}$-BirA/CyO;$^{UAS}Ube3a^{A3}$/TM6B*.

p62 (Nezis *et al.*, 2008), that also binds ubiquitinated proteins and targets them for autophagic degradation (Lippai *et al.*, 2014); and the protein p47 which acts as a co-factor of TER94/p97, an ATPase involved in protein degradation (Meyer et al., 2012) (**Figure 33**). Interestingly, Uch/UCHL-1 and Ref(2)P/p62 have been associated with a number of neurological disorders, such as Parkinson's, Alzheimer or Polyglutamine diseases (Choi *et al.*, 2004; Saitoh *et al.*, 2015). And Rpn10/PSMD4 has been shown to

regulate dendrite development in the mammalian brain (Puram *et al*., 2013), as well as to interact with Ube3a (Martínez-Noël *et al*., 2012; Tomaić and Banks, 2015).

Another three proteins enriched in the ^{bio}Ub pulldown upon Ube3a overexpression were the Heat shock protein cognate 1 (Hsc70-1), the Heat shock 70-kDa protein cognate 3 (Hsc70-3) and the Hsp70/Hsp90 organizing protein homologue (Hop). Chaperones such as the mammalian Hsp70 and Hsc70 had been previously reported to interact with Ube3a in Cos-7 cells (Mishra et al., 2009b). Finally, two metabolic enzymes: Aldolase (Ald) and CG7675; two cytoskeleton associated proteins: β-Spectrin (β-Spec) and Activity-regulated cytoskeleton associated protein 1 (Arc1); and the Innexin 3 (Inx3) protein, involved in gap junction formation, did also present a fold change bigger than 4 in Ube3a expressing flies.

On the other side, a number of proteins showed a noticeable lower LFQ intensity when Ube3a was overexpressed than when it was absent. Accordingly, they were considered to be less ubiquitinated upon Ube3a expression if their LFQ ratio (A3/15B) was lower than 0.25 (**Figure 33**). This group included two ubiquitin conjugating enzymes: CG40045 and CG7656; proteins involved in the vesicle endocytosis and exocytosis cycle (Lloyd *et al*., 2000): the synaptosomal-associated protein 24kDa (Snap24), Eps-15, Like-AP180 (Lap) and Scamp; three proteins required for axonal growth (Speicher *et al*., 1998; Hummel *et al*., 2000; Liebl *et al*., 2000): Fax, Futsch and Nrt; Three trans-membrane ion transport proteins: Atpα, the Na/Ca-exchange protein (Calx) and the Vacuolar H^+-ATPase 68 kDa subunit 2 (Vha68-2); the calcium binding protein Calbindin 53E (Cbp53E); the Photoreceptor dehydrogenase (Pdh), Waterproof

(Wat) and Punch (Pu) metabolic enzymes and the Arrestin2 (Arr2), White (W) and CG6051 proteins. The reduction in ubiquitination levels detected on these proteins suggests that they are not direct Ube3a substrates. In fact, the ubiquitination of Eps-15 and Pu had been previously reported not to be dependent on Ube3a ligase function (Ferdousy *et al*., 2011; Jensen *et al*., 2013).

A similar experiment was carried out with embryos either overexpressing Ube3a under the control of elav^{GAL4}-driver or carrying the *Ube3a^{15B}* allele. However, the MS analysis performed was of very poor quality resulting in a small number of identifications and with very low intensities (**Table A2 in appendix I**), so it was discarded for further analysis. We would also like to note that further MS analysis were carried out with both adult and embryo *Ube3a^{A3}* and *Ube3a^{15B}* flies, however, due to technical issues none of them provided good quality results (data no shown).

3.2.3. *In vivo* validation of Ube3a substrates from *Drosophila* photoreceptor cells

Biotin pulldowns from 15B and A3 *Drosophila* fly heads were performed in order to analyse by Western blot some of the proteins whose ubiquitination was seen to be affected upon Ube3a overexpression. The higher abundance of Ube3a in A3-flies-eluted material was confirmed by anti-Ube3a immunoblots (**Figure 34**). As previously shown (see **Figure 31B**), a large amount of the E3 ligase was purified from Ube3a expressing flies, while no band was detected from 15B ones. With regards to the other proteins found by MS to be more ubiquitinated, those for which antibodies were available were tested. The ubiquitination of Rngo was confirmed by Western blot to be Ube3a

dependent, since fractions of this ubiquitin receptor carrying three or more molecules of ubiquitin attached were found to be enhanced in A3 *Drosophila* line, as compared to the 15B sample (**Figure 34**). Western blot to Rpn10, Ref(2)P and UbcE2H were also performed, but no band was detected in neither of the elutions with Rpn10 antibody (data not shown) nor with Ref(2)P (**Figure 34**). It is likely that the amounts of ubiquitinated Rpn10 and Ref(2)P in the *Drosophila* eye are so low that they escape

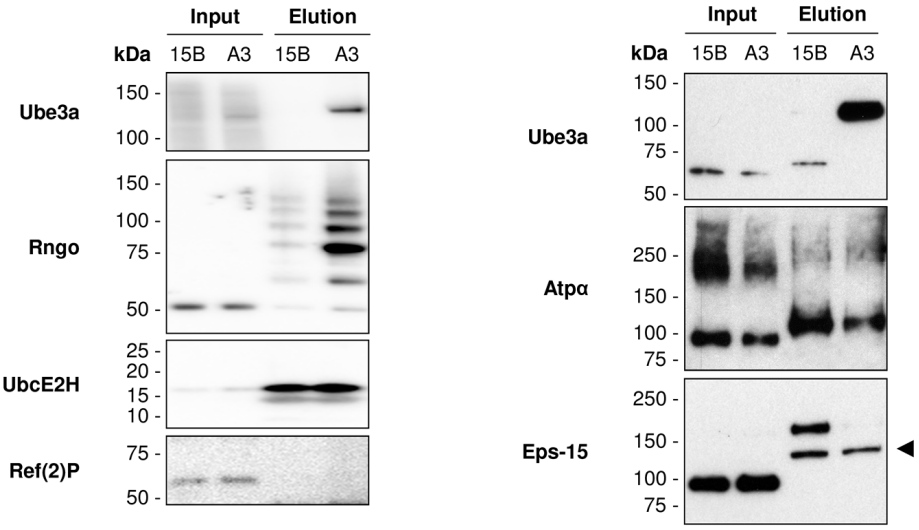

Figure 34. Validation of differentially ubiquitinated proteins upon Ube3a overexpression.

Western blotting confirmed that Ube3a is more active in the *Drosophila* eye when overexpressed, as more of it was detected in the eluted material of A3 flies. Immunoblot performed with anti-Rngo antibody confirmed the increase ubiquitination detected by MS for this protein upon Ube3a overexpression. This result places Rngo as the first substrate shown to be more ubiquitinated *in vivo* by Ube3a E3. Western blot to UbcE2H and Ref(2)P did not reveal higher ubiquitination of these two proteins in A3 flies. Western to Atpα and Eps-15 confirmed that a smaller fraction of these proteins is being conjugated with biotinylated ubiquitin upon Ube3a overexpression. Arrow heads indicate endogenously biotinylated proteins. 15B: $GMR^{GAL4,UAS(^{bio}Ub)_6}$-*BirA/CyO;Ube3a*^{15B}*/TM6B*; A3: $GMR^{GAL4,UAS(^{bio}Ub)_6}$-*BirA/CyO;*^{UAS}*Ube3a*^{A3}*/TM6B.*

Western blot detection. Indeed, these two proteins were only identified by MS in one out of three pulldown experiments earlier performed with *GMR$^{GAL4,UAS(^{bio}Ub)_6}$-BirA/CyO* flies (see **Table A1 in appendix I**). In the case of UbcE2H, no increased ubiquitination was detected (**Figure 34**).

Anti-Atpα and anti-Eps-15 immunoblots were also carried out to validate the detected reduction in their ubiquitination upon Ube3a overexpression. As shown in **Figure 34**, both proteins were found to be less ubiquitinated in A3 flies, supporting MS results. The reduce ubiquitination observed for these two proteins could be due to a cellular response produced by the overexpression of Ube3a. Likewise, it could be due to technical issues, such as a limited amount of available free biotinylated ubiquitin or the preferential attachment of the biotinylated ubiquitin to Ube3a substrates. Discerning between these situations would require further experiments. However, independently of the reason why their ubiquitination is reduced, there is no doubt to assert that Atpα and Eps-15 are not directly ubiquitinated by Ube3a in *Drosophila* photoreceptor cells, and hence that they are not direct substrates of this E3 ligase *in vivo*.

On the other hand, the observation that Rngo ubiquitination is enhanced upon Ube3a overexpression does suggest that it is a direct *in vivo* target of Ube3a in the fly eye. To our knowledge, Rngo is therefore the first Ube3a substrate to be validated *in vivo* in the context of a whole organism. In addition, despite the ubiquitination of Ube3a is thought to be a degradation signal, a decrease in the total levels of Rngo upon Ube3a expression in the input fraction of A3 flies was not detected (**Figure 34**), suggesting rather a non-degradative role.

4. GFP pulldown assay to monitor protein ubiquitination

The direct *in vivo* validation by Western blot of identified ubiquitin conjugates and carrier proteins from ^{bio}Ub-eluted material requires specific antibodies to be available. However, when this is not possible alternative approaches have to be taken. In order to allow validation of ubiquitin substrates in those cases we have developed an alternative approach based on high-affinity anti-GFP antibody-coated beads (Chromotek-GmbH). Those beads are routinely used in non-denaturing conditions to preserve interactions in co-immunoprecipitation experiments, but it has been found in our lab that they also withstand very stringent washing conditions. As the isopeptide bond of ubiquitin with its substrates is kept intact on denaturing environments, GFP-tagged proteins can be successfully isolated in order to further study their ubiquitination (Min *et al*., 2013; Lee *et al*., 2014; Ramirez *et al*., 2015). Indeed, these GFP beads had been successfully used for this purpose also on U2OS cell lysates (Min *et al*., 2013). This GFP pulldown assay can be used for the validation of protein ubiquitination and ubiquitination sites (Ramirez *et al*., 2015), as well as for the identification of direct E3 ligase targets (Lee *et al*., 2014).

4.1. Validation of ubiquitinated proteins

Previously, our lab identified 47 ubiquitin conjugates from the *Drosophila* embryonic nervous system using the ^{bio}Ub strategy (Franco *et al*., 2011). The *in vivo* ubiquitination of some of them was already validated by directly immunoblotting the eluted material

with specific antibodies (see **Figure 21** and Franco *et al*., 2011). As an alternative approach to validate their ubiquitination, N- and C-terminally GFP-tagged versions of these 47 proteins were generated by cloning them into a pAc5.1 vector carrying the GFP protein either before or after the multicloning site (Lee *et al*., 2014; see also *Material and Methods*). Confocal microscopy of transfected BG2 neuron-like cells (Ui *et al*., 1994) with the 47 fusion proteins revealed distinct localization patterns for each of them: seven localized in the nucleus, 22 in the cytoplasm and 18 were found in both compartments (**Figure 35**). In addition, 5 proteins also localized at the plasma membrane, while 3 localized at the nuclear membrane. All confocal images are shown on **Figure A6 in appendix II.**

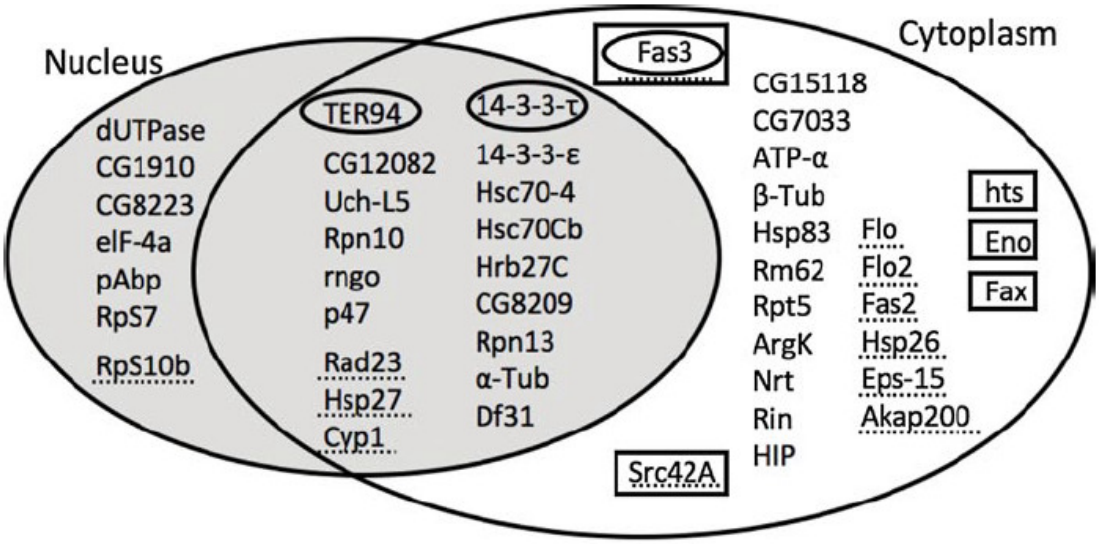

Figure 35. Localization of 47 neuronal ubiquitin substrates.

Forty-seven GFP-tagged genes were transfected into BG2 cells and protein localization analysed by confocal microscopy. Seven proteins localized in the nucleus, 22 in the cytoplasm and 18 in both compartments. Proteins also localized to the plasma membrane are inside boxes. Those localized to the nuclear membrane are surrounded with a circle. Dotted underlining indicates punctuate expression. All confocal images are found in Figure A6 in appendix II. Taken from Lee *et al*., 2014.

Analysis of the ubiquitination of these proteins was performed by transiently co-transfecting Drosophila BG2 cells with the GFP-tagged proteins together with a FLAG-tagged version of ubiquitin (Lee *et al*., 2014). The choice of those neuron-like cells for this purpose was due to our intention to perform the assay in a similar cell type where the ubiquitination of these proteins had been detected. After incubation of cell lysates with GFP-beads in a non-denaturing buffer, supplemented with protease inhibitors and NEM to prevent deubiquitination, washes with 8 M Urea and 1 % SDS were applied so all non-covalently bound interactors could be discarded. Then immunoblotting was performed on the purified material (**Figure 36A**). Anti-FLAG antibody was used to detect the ubiquitinated fraction of the proteins (red channel in **Figure 36B**), while the non-modified fraction was detected with anti-GFP (green channel in **Figure 36B**). Western blot analysis confirmed that 43 out of the 47 proteins are ubiquitinated in neuron-like cells, each of them showing a different ubiquitination pattern (**Figure 36B** and **Figure A7 in appendix II**). Three of them, however, showed no modification and a fourth one was not detectable with either of the antibodies. When GFP was expressed alone no ubiquitination was detected (**Figure 36B**), confirming that the ubiquitination seen is specific to each protein and not to the added tag. Additionally, cells were treated with RNAi to the ubiquitin activating enzyme E1, to further confirm that the ubiquitination observed was dependent on the canonical ubiquitination pathway. As shown in **Figure 36C**, RNAi treatment completely abolished the ubiquitination of the GFP-tagged proteins. These results establish that the described GFP-pulldown assay can be successfully used to characterize the ubiquitination of proteins within those neuron-like cells.

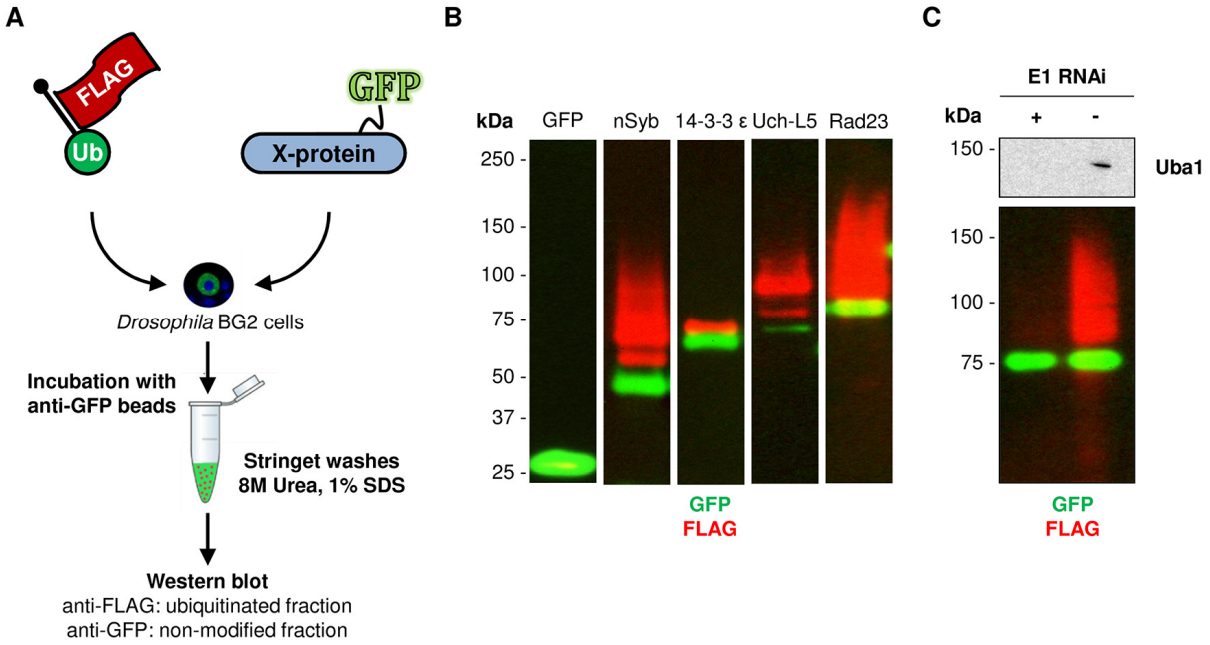

Figure 36. GFP-pulldown based strategy to validate protein ubiquitination in cells.

A. Schematic illustration of the GFP-pulldown protocol for analysing protein ubiquitination. GFP-tagged proteins are co-transfected with FLAG-tagged ubiquitin into *Drosophila* BG2 neuron-like cells. After culturing for three days cells are lysed and lysates are incubated with anti-GFP beads and subjected to washes with 8 M Urea and 1 % SDS to discard all interacting proteins. Ubiquitination of purified GFP-tagged protein can be validated by Western blot to the tagged-ubiquitin. Non-modified fraction can be detected by anti-GFP. **B.** Validation examples of the ubiquitination of some of the identified proteins using the GFP-pulldown assay, modified from Lee *et al*. (2014). Anti-GFP antibody was used to detect the non-modified forms of the proteins and anti-FLAG to monitor the ubiquitinated fraction. No ubiquitination was detected when GFP alone was expressed. Full analysis is shown in Figure A7 in appendix II. **C.** E1 RNAi treatment inhibited ubiquitination of overexpressed GFP-tagged proteins with FLAG-tagged ubiquitin, modified from Lee *et al*. (2014). Anti-GFP and anti-FLAG antibodies were used to detect the non-modified and the ubiquitinated fraction, respectively. E1 enzyme was detected using anti-Uba1 antibody. The protein shown in the example is Rad23. Modified from Lee *et al*., 2014.

4.2. Validation of ubiquitination sites

A di-gly remnant on the ubiquitin-modified lysines can be detected by MS analysis of ubiquitinated material (Peng *et al*., 2003). The GFP-pulldown approach was used to test whether identified ubiquitination sites were truly so modified. We applied the GFP-pulldown strategy to confirm two ubiquitination sites found on neuronal synaptobrevin (nSyb), a protein that belongs to the soluble N-ethylmaleimide-sensitive factor attachment protein receptor (SNARE) family (Ossig *et al*., 2000). The selection of nSyb as candidate for this purpose was based on the two ubiquitination sites identified in the *Drosophila* eye, K71 and K78 (**Table 6**), being detected twice in independent ^{bio}Ub pulldowns. Besides, those sites are found in a region of the protein (known as SNARE motif) conserved among *Drosophila* nSyb isoforms as well as in other organism (**Figure 37**), including humans (Fasshauer *et al*., 1998). They are required for the interaction and formation of a complex with Syx1A and the Synaptosomal-associated protein 25 kDa (Snap25) that triggers membrane fusion and exocytosis (Ossig *et al*., 2000). Moreover, the two lysines are surrounding an arginine that is known to be essential for the correct performance of exocytosis (Fasshauer *et al*., 1998; Ossig *et al*., 2000).

The *nSyb* gene was amplified from a *Drosophila* cDNA library and introduced into a pAc.5.1 vector carrying either an N-terminally or C-terminally GFP tag. As shown by Western blot (**Figure 38A**) the C-terminally GFP tagged version of nSyb displayed a stronger ubiquitination signal as compared with the N- terminal one when purified using GFP beads, and was therefore used for the generation of nSyb protein mutants carrying either the lysine 71 or the lysine 78 mutated to arginine (K71R or K78R) or

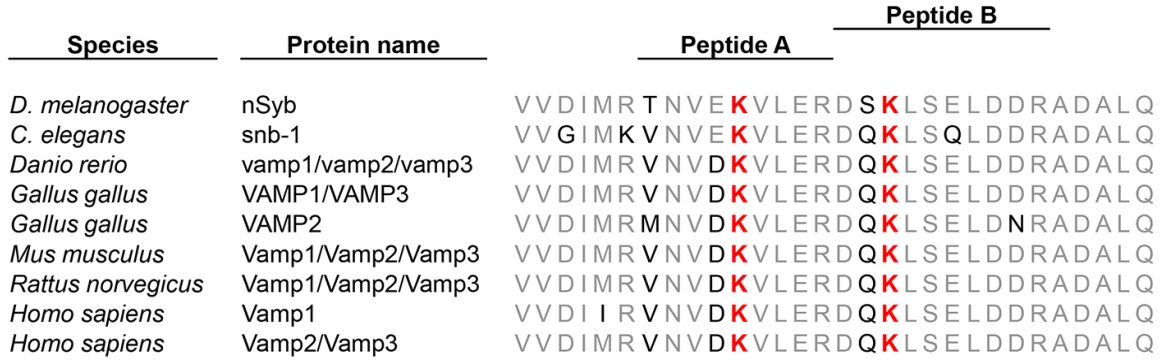

Figure 37. Homology of the nSyb region where ubiquitination sites were found.

Illustration of the peptides and the ubiquitination sites found in *Drosophila melanogaster* nSyb. The region of the protein where the modified lysines (red) were found, known as SNARE motif, is conserved among different species. The conserved amino-acids are shown in grey. Taken from Ramirez *et al*., 2015.

both (DM: K71R/K78R). Ubiquitination of nSyb mutants was monitored by Western blot on GFP-eluted nSyb from transfected BG2 cells. Both K71R and K78R single mutants showed reduced ubiquitination when compared to WT nSyb (**Figure 38B**), confirming that they are indeed true ubiquitination sites. Furthermore, there was a very significant reduction in the ubiquitinated nSyb levels ($p<0001$) if both lysines were mutated at the same time, when compared to wild type nSyb. The fact that ubiquitination was still detectable in nSyb double mutants indicates the presence of additional ubiquitination sites, which have been, indeed, previously reported for the mammalian counterpart (Na *et al*., 2012). All together, these results confirm that the GFP-pulldown assay can be successfully applied to validate ubiquitination sites.

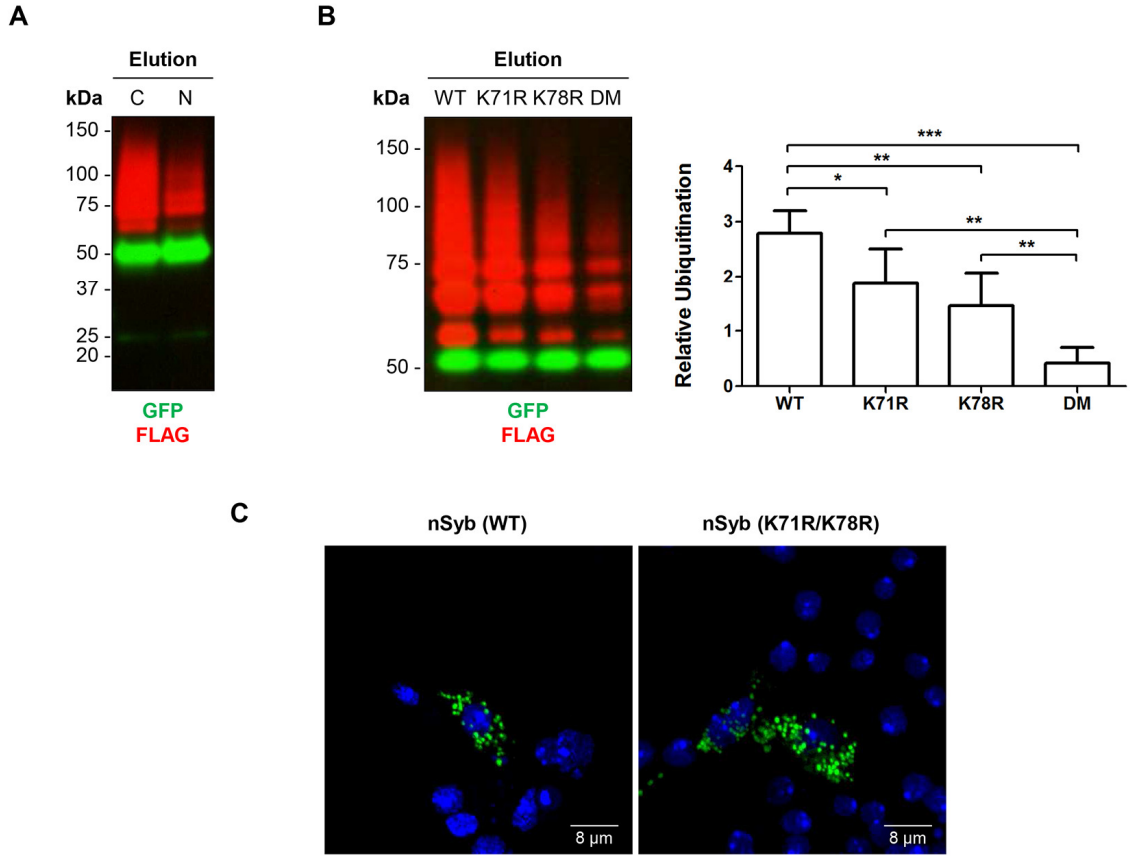

Figure 38. Ubiquitination sites on nSyb.

A. Anti-Flag (red) and anti-GFP (green) Western blots performed with C-terminally (C) or N-terminally (N) GFP-tagged WT nSyb **B.** nSyb double mutant (DM) showed a significant reduction in its ubiquitinated fraction, as shown with anti-Flag antibody western blot (red), compared to the wild type (WT) or the single lysine mutated forms (K71R or K78R). The non-modified form of nSyb was detected by GFP antibody (green). Quantification of the ubiquitination status of nSyb mutants relative to the non-modified form (Y axis: relative ubiquitination) was performed with Image-J. The plot shows relative levels of nSyb ubiquitination normalized to the GFP levels (average intensity ± SD). Statistical analysis was performed with Prism. One asterisk indicates p-value < to 0.05; two, p < to 0.01; three, p < to 0.0001. **C.** Confocal analysis of wild type (WT) and double lysine mutant (K71R/K78R) nSyb GFP-tagged protein. Scale bars indicate 8 µm. Modified from Ramirez *et al.*, 2015.

Interestingly, the absence of modification at K71 and K78 did not have a significant effect on the total protein nSyb levels, as shown by anti-GFP Western blot (**Figure 38B**), suggesting that the ubiquitination at those sites is not a signal for degradation. In addition, confocal images of BG2 cells transfected either with C-terminal GFP-tagged WT or the double lysine mutant (K71R/K78R) nSyb proteins, revealed that the localization and the expression pattern are neither affected (**Figure 38C**). Further experiments are therefore required in order to elucidate the significance of this ubiquitination.

4.3. Screening for E3 ligase-specific substrates

Among the 47 neuronal ubiquitin proteins identified from the *Drosophila* brain development (**Figure 35**) the E3 ligase Ube3a was also found, indicating that Ube3a is an active ubiquitin ligase throughout this period (Franco *et al*., 2011). We, therefore, reasoned that the ubiquitination of some of those substrates could be regulated by this enzyme. GFP-tagged proteins of the 47 candidates were hence transfected into BG2 cells in the presence of either an HA-tagged wild type Ube3a (HA-Ube3a^{WT}) or a ligase dead version (HA-Ube3a^{LD}) (**Figure 39A**). The latter was generated by mutating its active site cysteine to serine (C941S), which allows the E3 to be charged with ubiquitin but does not enable the transfer of the ubiquitin to a lysine residue on the substrate, as the oxyester link that is formed is more stable than the usual thioester bond (Levin *et al*., 2010).

Initially, whole cell extracts were analysed for changes in total protein levels with anti-GFP antibody, in order to elucidate whether any of the 47 GFP fusion proteins were

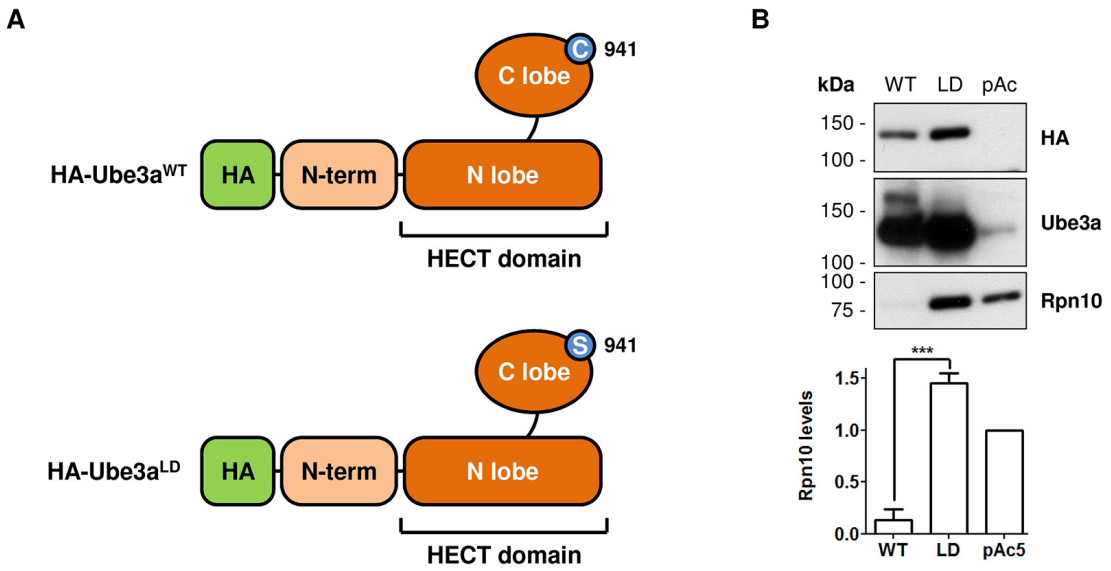

Figure 39. Rpn10 total levels are reduced upon Ube3a overexpression in BG2 cells.

A. *Drosophila Ube3a* wild type gene (*Ube3a*^{WT}) was amplified from a cDNA library and tagged with hemagglutinin (HA) at its N-terminus, to monitor by anti-HA antibody its expression. A catalytic inactive (or ligase dead) version of Ube3a was generated by the mutation of the active site cysteine residue (C941) to serine (HA-Ube3a^{LD}). **B.** Rpn10 levels were monitored in the presence of HA-Ube3a^{WT} (WT) or the ligase dead version (LD). Rpn10 was detected using anti-GFP antibody. Ube3a detection with anti-Ube3a and anti-HA antibodies is shown. Rpn10-GFP levels were quantitated using ImageJ software and intensities normalized relative to the control sample (pAc5), in which instead of Ube3a an empty pAc5 vector was co-transfected. Mean and standard deviation of three independent experiments are shown. A t-test was used for statistical analysis. Three asterisk indicates p-value < to 0.001. Modified from Lee *et al.*, 2014.

downregulated by Ube3a. Human UBE3A has been reported to generate K48 poly-ubiquitin chains *in vitro* (Wang and Pickart, 2005), a modification that targets proteins for proteasomal degradation. Direct substrates of Ube3a were hence expected to show reduced levels in the presence of HA-Ube3a^{WT}. Upon overexpression of the wild type version of this enzyme, a decreased level was only detected for one out of the 47 proteins, Rpn10 (**Figure 39B**), suggesting that Ube3a targets this protein for

proteasomal degradation. In addition, this drop on the total amount of Rpn10-GFP was found to be dependent on the Ube3a ligase activity, as the overexpression of the HA-Ube3a^{LD} did not cause the same effect, but rather seemed to protect it from degradation; total Rpn10 levels were higher in HA-Ube3a^{LD} overexpressing cells than in the control sample (**Figure 39B**). This protein was previously found by MS to be more ubiquitinated in the *Drosophila* photoreceptor cells upon Ube3a overexpression (**Figure 33**), which supports the idea that it is a direct ubiquitination substrate of Ube3a.

Changes in protein levels might be caused by different cellular processes, so in order to obtain direct evidence of the Rpn10 ubiquitination by Ube3a, BG2 cells expressing Rpn10-GFP together with HA-Ube3a^{WT} or HA-Ube3a^{LD}, as well as with FLAG-tagged ubiquitin, were subjected to the GFP-pulldown assay. As shown in **Figure 40A**, Rpn10 ubiquitination was significantly increased in the presence of wild type Ube3a (WT), as compared to cells expressing either the ligase dead E3 (LD) or to those transfected with an empty vector (pAc). Besides, a shift of the molecular weight pattern of ubiquitinated Rpn10 molecules was also detected in HA-Ube3a^{WT} expressing cells, indicating that Rpn10 is highly poly-ubiquitinated in the presence of the active E3 ligase. This effect was seen for both N and C-terminally GFP-tagged Rpn10 constructs (**Figure A8 in appendix II**).

The observed increased ubiquitination of Rpn10 by HA-Ube3a^{WT} is masked to some degree by the rapid degradation of Rpn10 and its ubiquitinated forms, which resulted in reduced total Rpn10-GFP levels (**Figure 39B**). Whole eluate of cells transfected with HA-Ube3a^{WT} was loaded in parallel with decreasing volumes of eluted material from HA-

Ube3a^{LD} overexpressing cells, in order to compare the ubiquitinated fraction of Rpn10 for similar amounts of purified Rpn10-GFP protein. For similar total GFP intensities, ubiquitinated Rpn10-GFP was very well detected in Ube3a^{WT} expressing sample, while it became completely undetectable in Ube3a^{LD} one (**Figure 40B**), indicating a very clear difference between the two samples. In addition, the molecular weight shift caused by a higher degree of poly-ubiquitination is much more evident. In the HA-Ube3a^{LD} sample the whole range of modifications to which Rpn10 is subjected (i.e., from mono-ubiquitination to high levels of poly-ubiquitination) were observed. In HA-Ube3a^{WT}, however, only a signal above 150 kDa, corresponding to highly poly-ubiquitinated Rpn10-GFP, was detected. These results confirm that Rpn10 ubiquitination is highly enhanced by Ube3a.

Four ubiquitination sites located on the VWFA of the mammalian Rpn10 homologue, S5a, and two on the C-terminal region, where the UIMs are located, have been previously reported to be modified *in vitro* by the mammalian UBE3A (Uchiki *et al*., 2009), suggesting that both regions are subjected to modification. In addition, the region containing the UIMs fused to GST has been shown to be enough for recognition and ubiquitination by two different E3 ligases, MurF1 and CHIP, *in vitro* (Uchiki *et al*., 2009). In order to elucidate whether either of the two differentiated halves of *Drosophila* Rpn10 are required or enough for Ube3a-dependent ubiquitination in BG2 cells, the N-terminal region containing the VWFA domain (ΔC, up to the residue 204) and the C-terminal region carrying three UIMs (ΔN, starting at residue 205) were cloned and C-terminally tagged with GFP (**Figure 40C**). Despite both halves showing some degree of ubiquitination, neither of them were significantly ubiquitinated by endogenous Ube3a,

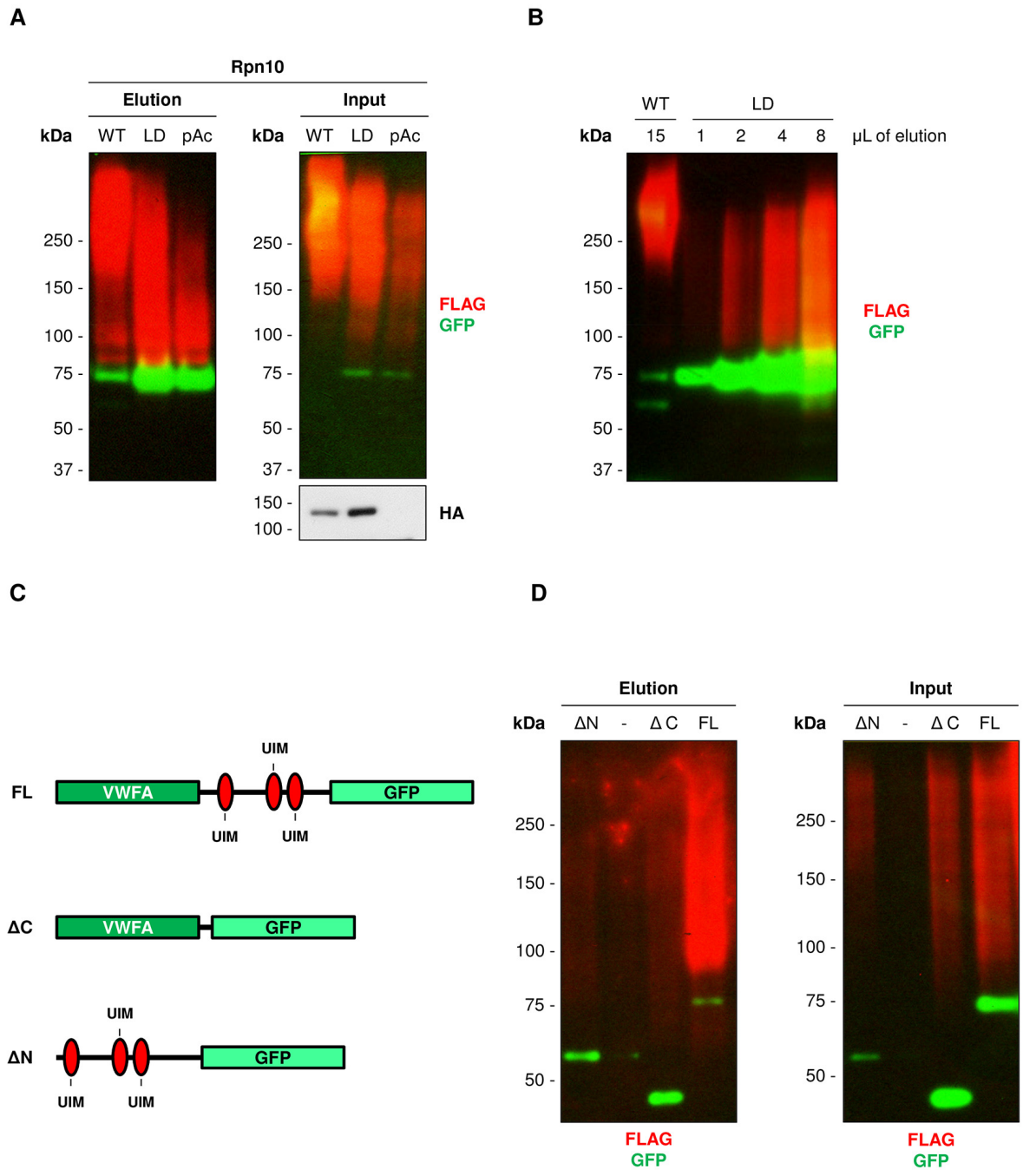

Figure 40. Ube3a directly ubiquitinates Rpn10 in BG2 cells.

A. Overexpression of Ube3a^{WT} (WT) induced a dramatic increase of Rpn10 ubiquitination, despite the low Rpn10-GFP levels detected. The apparent increased ubiquitination seen in Ube3a^{LD} (LD), relatively to pAc, is partly to due to higher levels of total Rpn10-GFP in the sample. Ube3a expression was monitored with anti-HA antibody in the input fraction. **B.** In order to compare the ubiquitinated fraction of Rpn10 upon Ube3a^{WT} and Ube3a^{LD} expression, we attempted to compare similar Rpn10-GFP levels by loading the full

eluate of WT sample and smaller volumes of the eluate for the LD one. When loading 1 μL of the purified Rpn10 protein from LD sample, where the amount of Rpn10-GFP is still higher than that purified from WT sample, the dramatic increase ubiquitination of Rpn10 in the WT sample is evident. **C.** Schematic illustration of C-terminally GFP-tagged full-length (FL), N-terminal (ΔN) and C-terminal (ΔC) truncated versions of Rpn10. **D.** Ubiquitination by endogenous Ube3a of full length Rpn10-GFP protein, as well as C- and N- terminally truncated versions, carrying the VWFA domain or the UIMs, respectively (see panel C), was tested. No significant ubiquitination was found for neither of the truncated forms. ΔN: Rpn10 C-terminal half carrying the UIMs; ΔC: Rpn10 N-terminal half carrying the von Willebrand Factor A domain (VWFA); FL: Full length Rpn10 protein; **-:** empty lane. In panel A, B and D the Rpn10 ubiquitinated fraction was detected with anti-FLAG antibody (shown in red), while the non-modified form was detected with anti-GFP (shown in green). Taken from Lee *et al*., 2014.

as compared with the full-length (**Figure 40D**). Similarly, neither of the partial constructs was targeted for degradation upon overexpression of HA-Ube3a^{WT} (**Figure A7 in appendix II**), suggesting that the full-length Rpn10 is required for Ube3a-dependent ubiquitination and degradation.

Protein modification with K48 poly-ubiquitin chains has been historically linked to proteasomal degradation. However, non-proteolytic functions for this type of chain has also been reported (Flick *et al*., 2006). For this reason, although the remaining 46 GFP-tagged proteins do not appear to be regulated by Ube3a overexpression, the GFP-based protocol was also applied to them in order to address if their ubiquitination was somehow affected by Ube3a. This way, three more proteasome-interacting proteins, the ubiquitin receptor Rngo, the Ubiquitin carboxy-terminal hydrolase L5 orthologue (Uch-L5) DUB and the product of the gene *CG8209*, as well as the ribosomal protein S10b (Rps10b), were found more ubiquitinated in HA-Ube3a^{WT} expressing cells (**Figure 41A**).

A

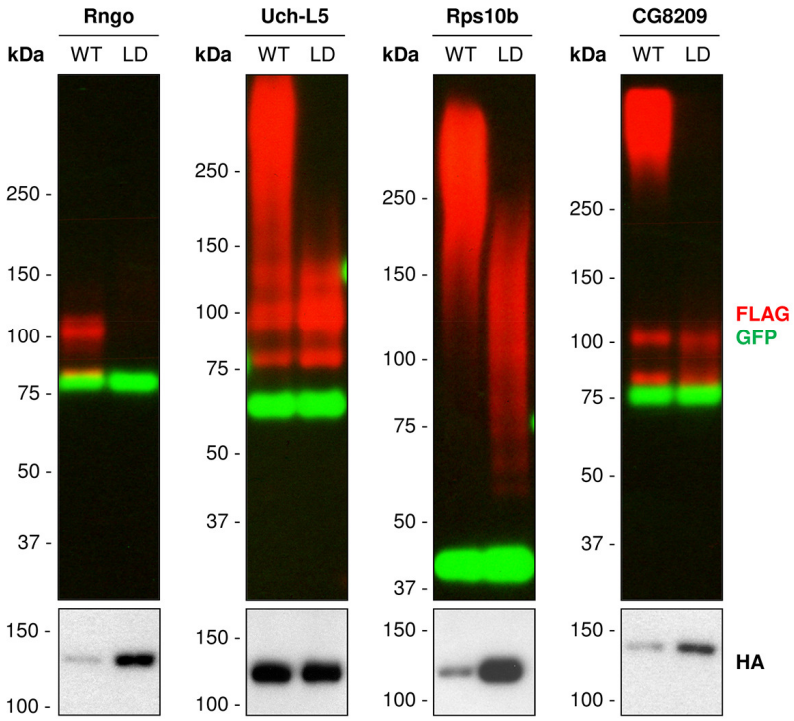
Rngo
Uch-L5
Rps10b
CG8209
kDa
WT
LD
250 -
150 -
100 -
75 -
50 -
37 -
FLAG
GFP
HA

B

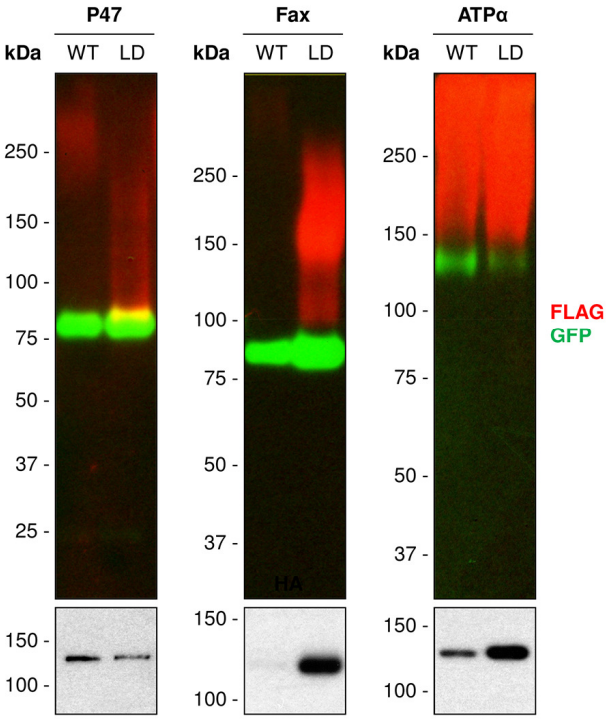
P47
Fax
ATPα
kDa
WT
LD
250 -
150 -
100 -
75 -
50 -
37 -
25 -
HA
FLAG
GFP

Figure 41. GFP-pulldown based screen for Ube3a substrates in BG2 cells.

Overexpression of HA-Ube3a^{WT} (WT) and HA-Ube3a^{LD} (LD) was used to confirm the ubiquitination of some proteins by this E3 ligase. Ubiquitination was monitored after GFP pulldown. Levels of Ube3a were detected by anti-HA antibody. Mouse anti-GFP antibody was used to detect the non-modified fraction (shown in green) of the captured proteins and anti-FLAG antibody (shown in red) to identify the ubiquitinated fraction. **A.** Rngo, Uch-L5, Rps10b and CG8209 were found to be more ubiquitinated upon Ube3a overexpression. However, none of them seemed to be targeted for degradation as suggested by the fact that total levels were similar in Ube3a WT and LD expressing cells. **B.** The ubiquitination of the remaining proteins was found not to be dependent on Ube3a, as either less or equal ubiquitination was found for all of them upon HA-Ube3a^{WT} overexpression. Western to P47, Fax and ATPα are shown as examples. Modified from Lee *et al*., 2014.

Out of those three, Rngo was also found to be more ubiquitinated *in vivo* in the photoreceptor cells of Ube3a overexpressing flies (**Figure 34**). None of those Ube3a substrates seemed to be targeted for proteasomal degradation, as suggested by the fact that total protein levels were similar in HA-Ube3a^{WT} and HA-Ube3a^{LD} samples. Therefore, their ubiquitination by Ube3a must provide some other non-proteolytic function. The fate of these proteins after their ubiquitination by Ube3a, however, is not straightforwardly interpreted with the results obtained so far, and hence, further experiments are required. Neither of the remaining 42 GFP-tagged proteins showed an increase ubiquitination upon HA-Ube3a^{WT} overexpression and even appeared reduced in some cases (see three examples in **Figure 41B**), illustrating that the enhanced poly-ubiquitination observed for Rpn10, Rngo, Uch-L5, CG8209 and Rps10b is specific to the activity of the enzyme and not an artefact caused by the overexpression of the E3 and the GFP-tagged ubiquitinated proteins.

5. Understanding the *in vivo* role of protein ubiquitination

Cell culture or *in vitro* experiments are of great value for the characterization of cellular pathways, analysis of protein interaction or, as shown in previous section, study of protein ubiquitination. Indeed, the discovery and characterization of the ubiquitin-proteasome system, as well as all the enzymes involved on it were first achieved on rabbit reticulocyte extracts (Hershko *et al*., 1980; Hough *et al*., 1987). However, the ultimate goal is to be able to understand the role that the different characterized pathways have on a living organism, particularly in humans, and in order to advance towards such knowledge, the use of *in vivo* models is required.

In the screening for Ube3a substrates performed on *Drosophila* BG2 cells five direct Ube3a substrates were identified (see Results section 4.3: *Screening for E3 ligase-specific substrates*), two of which have also been identified from neuronal tissue as being more ubiquitinated in Ube3a overexpressing flies. One of them, Rpn10, was degraded upon ubiquitination by Ube3a, as expected on what has been described so far in the literature for ubiquitin chain types formed by UBE3A (Kim and Huibregtse, 2009). We therefore decided to use *Drosophila melanogaster* flies in order to assess the biological significance of Rpn10 regulation by the ubiquitin system *in vivo*. In addition, and as a first attempt towards elucidating the role that ubiquitination plays in humans, we generated human dental pulp stem cells that constitutively express the ^{bio}Ub construct. This system should provide in the future the opportunity to study ubiquitination from human-derived cells.

5.1. Ube3a and Rpn10 interaction *in vivo* affects protein degradation

Rpn10 is an ubiquitin receptor in charge of the transport of poly-ubiquitinated proteins to the proteasome for their degradation (Lipinszki *et al*., 2009). Failure in the regulation of Rpn10 levels might therefore have a big impact on the levels of other proteins. In order to understand the biological consequences of the degradation of Rpn10 by Ube3a *in vivo*, we generated transgenic flies that overexpress both wild type $Ube3a^{A3}$ and the dominant negative C-terminal half of Rpn10 ($Rpn10^{DN}$), used earlier (see Results section 3.1: ^{bio}*Ub strategy upon interference with proteasomal function*), under the control of the GMR^{GAL4} driver.

Overexpression of Ube3a alone did not cause any significant alteration on the levels of ubiquitinated material as compared to control flies and those lacking the Ube3a protein (**Figure 42A**), but it caused a degeneration phenotype in the fly eye, which becomes more evident in flies carrying two copies of the GMR^{GAL4} driver (lane 4 and 5 in **Figure 42B**). As expected from previous experiments, overexpression of $Rpn10^{DN}$ alone significantly increased the amount of ubiquitinated proteins detected in the *Drosophila* eye (**Figure 42A**), but in contrast to what is seen with Ube3a, did not cause any phenotype in the eye (lane 3 in **Figure 42B**). Interestingly, when both proteins were co-expressed together the increase ubiquitination associated to $Rpn10^{DN}$ was significantly enhanced (**Figure 42A**), and additionally, the eye phenotype was completely suppressed (lane 6 in **Figure 42B**). Co-expression of Ube3a with GFP did somehow reduce the phenotype obtained by the overexpression of Ube3a using two copies of the GAL4-driver (lane 5 and 7 in **Figure 42B**), but no reduction was observed if the GAL4

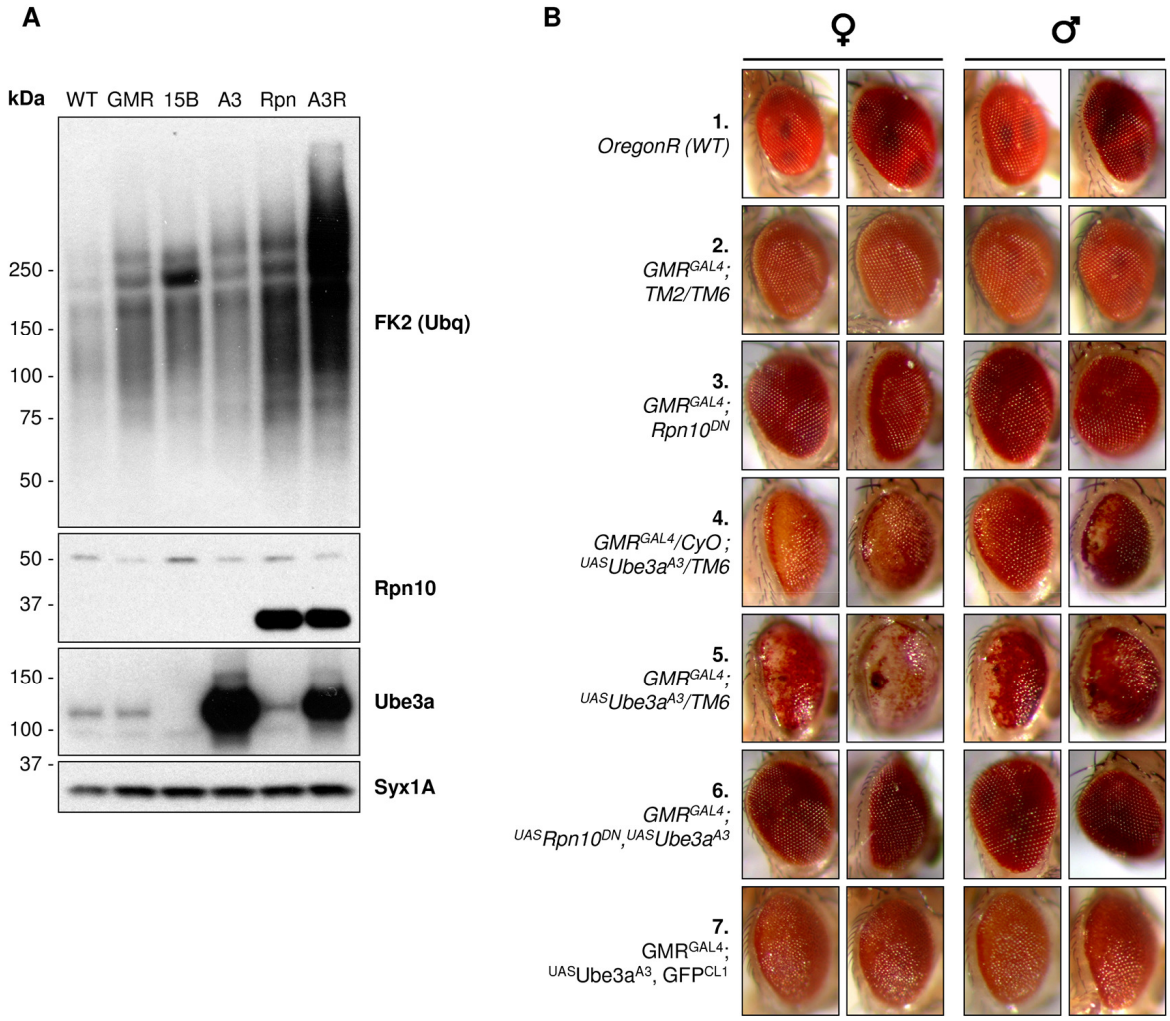

Figure 42. Ube3a and Rpn10 interaction *in vivo*.

A. Western blot analysis of ubiquitinated proteins from *Drosophila* heads whole extracts. Overexpression of Rpn10^{DN} (Rpn) causes an accumulation of ubiquitinated material. This effect is highly enhanced when Ube3a is co-expressed (A3R), despite the latter having no such effect on its own (A3), indicating an interaction between both proteins *in vivo.* Anti-Ube3a and anti-Rpn10 immunoblots illustrate the samples on which Ube3a and Rpn10^{DN} proteins were expressed, respectively. Endogenous Ube3a and Rpn10 (~50 kDa) were also detected. Ubiquitinated material was monitor with anti-FK2 antibody, which only recognizes conjugated ubiquitin. Anti-Syx1A Western is shown as loading control. WT: *OregonR*; GMR: *GMR^{GAL4};TM2/TM6B*; 15B: *If/CyO;Ube3a^{15B}/Ube3a^{15B}* null mutant; A3: *GMR^{GAL4}/CyO;^{UAS}Ube3a^{A3}/TM6B*; Rpn: *GMR^{GAL4};^{UAS}Rpn10^{DN}*; A3R: *GMR^{GAL4};^{UAS}Ube3a^{A3},^{UAS}Rpn10^{DN}/TM6B.* **B.** Overexpression of Rpn10^{DN} in the *Drosophila* eye displays an appearance similar to *OregonR* wild type flies and flies carrying only the

GMR^{GAL4} driver. Overexpression of Ube3a^{A3} results on a degenerative phenotype, which is exacerbated when two copies of *GMR^{GAL4}* are used. When both Ube3a^{A3} and Rpn10^{DN} constructs are expressed together, using two copies of *GMR^{GAL4}*, the Ube3a phenotype is rescued. This phenotype, however, is not rescue if GFP is expressed together with Ube3a, indicating that there is an interaction between Rpn10 and Ube3a *in vivo*. Modified from Lee *et al*., 2014.

dosage was accounted for (lane 4 and 7 in **Figure 42B**). However, co-expression with Rpn10^{DN} (lane 6 in **Figure 42B**) did completely abolished either phenotype, indicating clearly that this rescue effect was indeed specific to Rpn10^{DN}. The double synergistic effect seen in flies suggests that the shuttling of poly-ubiquitinated proteins by Rpn10 might be regulated by Ube3a and that the eye phenotype reported for Ube3a may be linked to the failure in the degradation by the proteasome of those poly-ubiquitinated proteins.

With the aim of further testing the increased ubiquitination seen when Ube3a and Rpn10^{DN} are co-expressed, flies carrying together both *$^{UAS}Ube3a^{A3}$* and *$^{UAS}Rpn10^{DN}$* transgenes were combined with *GMR^{GAL4}*, *^{bio}Ub* ones, so as to be able to analyse the ubiquitinated fraction obtained from each line. Overexpression of Rpn10^{DN} produced a differential distribution of the ubiquitinated material, as detected by anti-biotin Western blot (**Figure 43A**), presumably because the biotinylated ubiquitin is preferentially found attached to poly-ubiquitinated proteins (see Results section 3.1: *^{bio}Ub strategy upon interference with proteasomal function*). When the purified material was analysed by silver staining an increase in the total amount of isolated proteins was however detected, as compared to flies expressing the ^{bio}Ub construct alone (**Figure 43B**). This effect was not detected when Ube3a was overexpressed, since the signal, as well as

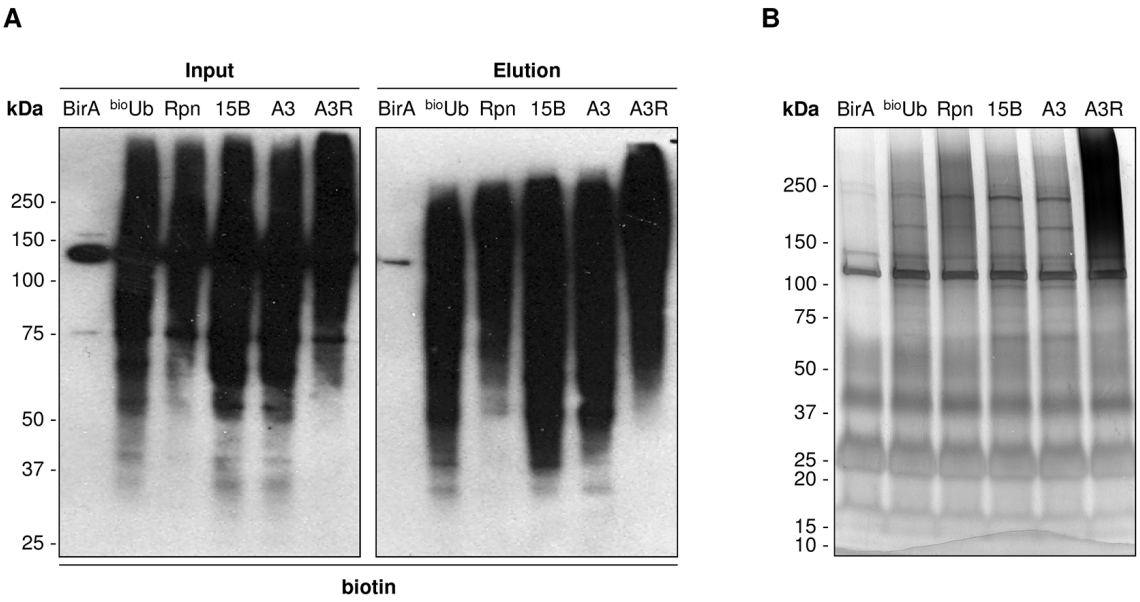

Figure 43. Ubiquitinated material purified from Ube3a and Rpn10^{DN} co-expressing flies.

A. Anti-biotin Western blot on the material purified from *Drosophila* adult samples. Similar amount of purified material is observed in the elutions of ^{bio}Ub, Ube3a mutant (15B) and Ube3a overexpressing (A3) flies. In contrast, a differential distribution is detected in the ubiquitinated proteins that are recovered in flies that overexpress Rpn10^{DN} alone (Rpn), with a preferential attachment of the biotinylated ubiquitin to higher molecular weight proteins. When Ube3a and Rpn10^{DN} are co-expressed (A3R) similar distribution as in Rpn is observed for the eluted material, but the signal appeared to be a stronger. BirA: *GMR^{GAL4}/CyO; ^{UAS}BirA/TM6B*; ^{bio}Ub: *GMR^{GAL4},^{UAS}(^{bio}Ub)$_6$-BirA/CyO*; 15B*: GMR^{GAL4},^{UAS}(^{bio}Ub)$_6$-BirA/CyO;Ube3a^{15B}/TM6B*; A3: *GMR^{GAL4},^{UAS}(^{bio}Ub)$_6$-BirA/CyO;^{UAS}Ube3a^{A3}/TM6B;* Rpn: *GMR^{GAL4},^{UAS}(^{bio}Ub)$_6$-BirA/CyO;^{UAS}Rpn10^{DN}/TM6B*; A3R: *GMR^{GAL4},^{UAS}(^{bio}Ub)$_6$-BirA/CyO; ^{UAS}Ube3a^{A3},^{UAS}Rpn10^{DN}/TM6B*. **B.** Silver staining of the proteins isolated from *Drosophila* adult samples. Equal amounts of the eluted material from each of the samples shown in panel A were separated by SDS-PAGE and stained with silver. An accumulation of proteins is detected on samples from flies overexpressing Rpn10^{DN} (Rpn), as compared to ^{bio}Ub, 15B and A3 samples. When Rpn10^{DN} and Ube3a are co-expressed (A3R) this accumulation is greatly enhanced.

distribution, of the proteins found in the elution were similar to those found in ^{bio}Ub flies, or to those carrying the Ube3a deletion (*Ube3a^{15B}*), either by Western (**Figure 43A**) or by silver staining (**Figure 43B**). When both construct were expressed together, the redistribution of the ubiquitinated material was clearly observed by Western blot (**Figure 43A**). But more importantly, the amount of ubiquitinated material isolated from these flies was significantly higher than those isolated from control (^{bio}Ub), as well as from flies expressing each construct independently (**Figure 43B**). Similar analyses were performed with *Drosophila* embryos, which yielded similar results (**Figure A9 in appendix II**).

5.2. Future directions: Dental Pulp Stem Cells (DPSCs)

The use of different animal models, such as yeast, *Drosophila* or mouse is of outstanding value. Nevertheless, it is ultimately required to confirm the obtained findings in human cells. The lack of easy access to living neuronal tissue from human patients, however, is still a major issue. Dental Pulp Stem Cells (DPSCs) are mesenchymal stem cells, which can be easily extracted from teeth, and have the ability to develop into a variety of cell types, including neurons (Kanafi *et al*., 2014). Besides, they can be obtained by non-invasive techniques, as they fall out on their own or are routinely extracted in the paediatric clinics. In collaboration with Dr. Lawrence T. Reiter (UTHSC) we, therefore, developed DPSC cell lines from which the ubiquitinated material could be easily extracted using the ^{bio}Ub strategy.

5.2.1. Establishment of ^{bio}Ub system in DPSCs

DPSC cells obtained from a control individual (TP037) were first immortalized by Dr. Sarita Goorha (UTHSC), using a virus containing the human telomerase reverse transcriptase, with the purpose of generating cell lines that have the ability to grow over long time periods. Immortalized cells were then infected with the $^{UAS}(^{bio}Ub)_6$-BirA transgene carrying six copies of ubiquitin plus BirA enzyme (^{bio}Ub), and with BirA alone as control. Both construct were cloned into a pBABE retroviral vector carrying hygromycin resistance for their stable expression in DPSCs. Cells from the TP037 control subject were successfully infected with both constructs. These cells properly expressed both the BirA standalone construct, as well as the longer poly-ubiquitin construct (^{bio}Ub), which must have been digested by endogenous DUBs as only one band corresponding to free BirA was detected by Western blot with anti-BirA antibody (**Figure 44A**). These cells were further incubated with 50 μM of biotin in order to analyse the ability of the modified ubiquitins to be biotinylated and conjugated to endogenous proteins. Anti-biotin Western blot revealed the presence of the typical smear corresponding to ubiquitinated material, proving that the ^{bio}Ub is also properly biotinylated and conjugated in DPSCs (**Figure 44B**). A confluent T150 flask expressing the ^{bio}Ub construct was subjected to biotin pulldown as described for flies, so as to provide evidence that ubiquitinated material can also be isolated from DPSCs using this system. As shown in **Figure 44C**, the isolation of ubiquitinated material was effectively accomplished from ^{bio}Ub expressing cells, while only those proteins endogenously biotinylated were exclusively purified from cells expressing the BirA.

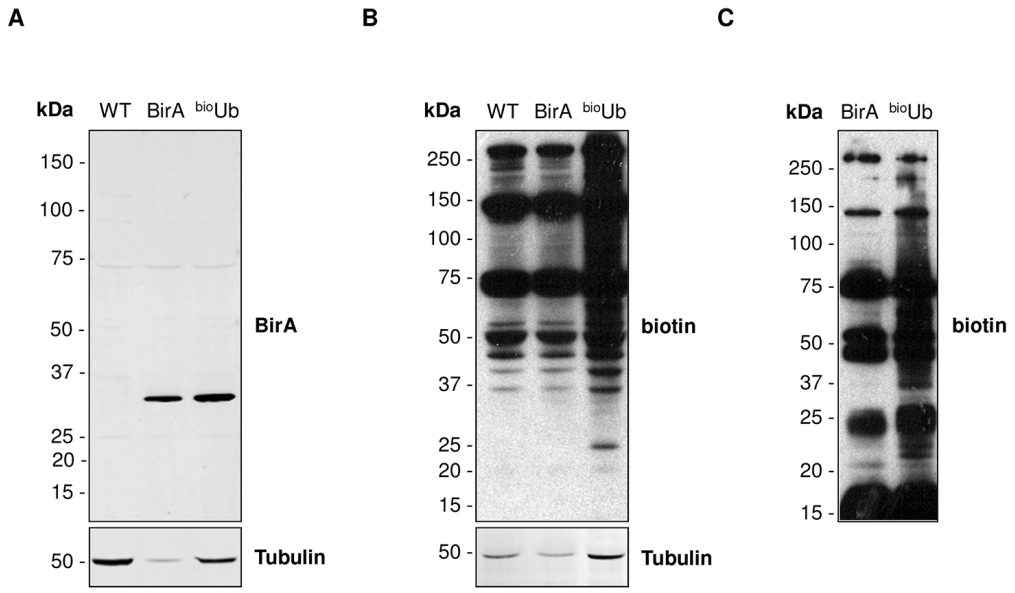

Figure 44. Western blot from transduced DPSC cells.

A. Anti-BirA Western blot showed that construct is properly expressed in DPSC cells and that it is properly digested. A band corresponding to the *E.coli* BirA enzyme is detected in both the BirA and ^{bio}Ub samples but not in the WT cells. **B.** Anti-biotin Western blot showed that the ectopically expressed ubiquitin is biotinylated and conjugated. Cells were cultured in the presence of 50 µM of biotin. **C.** A pulldown performed with DPSC-BirA and DPSC-^{bio}Ub cells showed the presence of proteins conjugated with biotinylated ubiquitin in the ^{bio}Ub sample. In the BirA sample only endogenously biotinylated proteins are found. WT: Control DPSC cells. BirA: DPSC cells expressing BirA enzyme alone. ^{bio}Ub: DPSC cells expressing the $^{UAS}(^{bio}Ub)_6$-BirA construct.

Similar approaches were carried out with DPSCs obtained from two other control individuals (TP023 and TP024). Besides, cells obtained from six different patients, three of which (TP055, TP059 and TP078) were carrying a deletion on the long arm of the maternal chromosome 15 (AS deletion) and the other three (TP041, TP044 and TP058) a maternal duplication of the same region (15q duplication syndrome) were used. The purpose of this approach was to compare the isolated ubiquitin proteome from control,

AS and 15q duplication patients. However, the six-month stay at Dr. Reiter's lab was not enough time to achieve the proper integration of the ^{bio}Ub and BirA constructs in the genome of the different cell lines and to perform the biotin pulldown experiments and MS analysis. It will be therefore necessary to follow up those experiments and ongoing collaboration with Dr. Reiter in order to fully implement and achieved the expected results.

IX. Discussion

Ubiquitination regulates a wide range of biological processes in higher eukaryotes, which go far beyond the degradation of old or misfolded proteins. *In vivo* models in which the ubiquitin proteome can be analysed under physiological, as well as under disturbed, conditions can greatly contribute to the understanding of the roles of this post-translational modification. During this Thesis project, we have expanded a strategy for the *in vivo* analysis of ubiquitinated proteins to the *Drosophila* photoreceptor cells, providing an *in vivo* system in which the proteins that are ubiquitinated in the context of a mature neuron can be studied. We have further confirmed that this strategy can be employed for the identification of changes in the ubiquitin proteome upon particular treatments. While changes due to the blockade of the proteasome were certainly expected, we were not sure about being able to detect changes in the ubiquitome upon the overexpression of a single E3 ligase. Taking into account that there are more than 600 E3s, the effect made by just one of them could have remained undetectable using available techniques. However, the combination of the ^{bio}Ub strategy with overexpression of the Ube3a E3 ligase has allowed us to identify the first *in vivo* substrate of this E3 ligase in *Drosophila*. On the other hand, we have developed a GFP-pulldown assay that allows for the isolation of just a single protein in order to further characterize its ubiquitinated fraction, both in physiological conditions and upon expression of an E3 ligase. We have applied this new protocol to cell culture but it could be exported to any transgenic living organisms.

The fly eye as an *in vivo* model to study protein ubiquitination

We tested different promoters for their ability to drive the expression of the ^{bio}Ub construct in the adult fly brain, with the aim of characterizing the ubiquitin landscape of

a mature neuron in *Drosophila melanogaster*. While elav^{GAL4} was appropriate for the study of ubiquitinated material during the embryo nervous system development (Franco *et al*., 2011), it was not strong enough to perform the same approach from the adult brain. Among the drivers tested, we found that GMR^{GAL4}, which drives expression mostly in photoreceptor cells (Li *et al*., 2012), did promote a high expression and an adequate conjugation of the biotinylated ubiquitin without the need of additional stimulus (i.e., heat shock treatment). Using this GAL4 driver, we achieved the isolation and subsequent MS identification of 369 ubiquitin conjugates and 21 ubiquitination sites from the *Drosophila* eye, also detecting several enzymes of the UPS (Ramirez *et al*., 2015).

Among the proteins identified from the fly photoreceptor cells, there was a significant enrichment by GO-Term analysis of proteins involved in synaptic transmission and transport functions, preferentially localized to the plasma membrane and synapse. In addition, many of the proteins consistently identified as ubiquitin conjugates among MS experiments were proteins with a well-known role in synaptic transmission (**Table 5**). For instance, the alpha (Atpα) and beta subunits of the Na^+/K^+ ATPase (Lebovitz et al., 1989; Sun and Salvaterra, 1995), the Na^+/C^{2+}-exchange protein (Schwarz and Benzer, 1997) or Eps-15 (Lloyd et al., 2000). These results implicate the UPS in the maintenance of neuronal homeostasis and in the communication between neurons in the fly eye. On the other hand, about 40 % of the identified proteins from *Drosophila* photoreceptor cells have orthologues that were earlier reported to be ubiquitinated in murine brain tissues *in vivo* (Na *et al*., 2012; Wagner *et al*., 2012), suggesting that the pathways

controlled by ubiquitination in mature stage neurons are conserved across different species.

The *Drosophila* eye has been widely used for the study of human neurodegenerative disorders because it provides a good system to perform unbiased screens and analyse complex neural phenotypes (Jackson, 2008). During this Thesis project, we have taken advantage of it to develop an *in vivo* neuronal system in which the ubiquitination events on a mature neuron can be successfully identified. The nature of the ^{bio}Ub strategy allows also discerning by Western blot whether such identifications correspond to proteins that are mono- or poly-ubiquitinated *in vivo*. In addition, the fly eye offers unique advantages, as particular genes or pathways can be mutated without compromising the fertility and viability of the animals. For these reasons, the use *Drosophila* photoreceptor cells as a tool for the study of ubiquitination can greatly contribute to our understanding of the mechanisms, conserved along evolution, by which this post-translational modification regulates neuronal function.

The ubiquitin proteome depends both on the tissue studied but also on the temporal context

Comparison of the ubiquitinated proteomes isolated from the *Drosophila* eye and from embryonic developing neurons revealed large differences. Only 28 % of the proteins identified from the fly photoreceptor cells were detected in embryonic developing neurons. Gene ontology analysis showed significant differences on the biological processes, cellular compartments and molecular functions targeted by the UPS between embryo and adult samples. In embryonic neurons proteins with nuclear

and cytoskeleton localization were found to be more represented. In adult neurons, synaptic and membrane proteins appeared to be highly enriched. Besides, proteins involved in transport and synaptic transmission were much more widespread in the adult eye, while cell cycle and developmental processes were more abundant in the embryo. Similarly, transporter activity and nucleic acid binding function were characteristic of the adult and embryonic neuronal tissues, respectively.

Neuronal function and activity are highly context dependent. For instance, a number of molecules involved in growth cone extension during embryonic stages, are no longer required once the axons find their final targets (Budnik, 1996; Budnik *et al*., 1996). On the other hand, remodelling of the cytoskeleton and reallocation of the membranes is required in order to modulate the synaptic plasticity of the mature neurons (Haydon and Drapeau, 1995; Chiba and Keshishian, 1996). Molecules present during the embryonic development of the brain, therefore, will be regulated differently from those necessary for synaptic transmission once the innervations have been established. Being aware that it is difficult to discern between tissue-specific protein expression and tissue-specific protein ubiquitination without further experiments, our results suggest that certain ubiquitination events are specific to each cell type. It appears that embryonic proteins more abundantly ubiquitinated are those that need to be regulated in order for the neuron to reach a mature stage. In the adult samples, proteins involved in signalling and communication between neurons, and therefore located at the cell membrane, appeared to be preferentially ubiquitinated. Since specific ubiquitination events are tissue-dependent, the choice of the correct system is therefore essential when studying the involvement of ubiquitination in a particular pathway.

An appropriate promoter and a simultaneous MS analysis of biological replicates are important factors in the biotin pulldown assay

The ^{bio}Ub approach has been successfully applied during this project for the analysis of the ubiquitin landscapes of the embryonic nervous system and the *Drosophila* photoreceptor cells, but it has the potential to be implemented to any fly tissue at any stage during the development. Using the heat shock inducible-GAL4 ubiquitous promoter we managed to identify about a hundred proteins from the fly head (data not shown), suggesting that it could also be used for the identification of the ubiquitin proteome of any other extracted organ. Similarly, the ^{bio}Ub strategy can also be applied to mammalian models, such as mice (Lectez *et al*., 2014) or human cells (Min *et al*., 2014 and **Figure 44**). One technical aspect that should be however kept in mind when setting up this approach in a new tissue/organism is the promoter that is used. The expression level of the ^{bio}Ub precursor achieved in a given tissue is very important for the success of the assay. While excessively strong expression might lead to lethality, a weak expression, such as the one obtained with elav^{GAL4}, OK371^{GAL4} or Tub^{GAL4,G80ts} drivers in adult fly heads, will limit the isolation to the endogenously biotinylated proteins (Chandler and Ballard, 1985) in detrimental of the ubiquitinated proteome, due to their different abundance. Unfortunately, no hint -other than experimental evidence- exists for the selection of a good promoter.

Another essential methodological aspect of the ^{bio}Ub approach is the careful design of the MS analysis, so the variability across MS experiments is reduced. There are many sources of variability in MS-based proteomics, ranging from the protein extraction process to the database or search engine that is used for the protein identification (Bell

et al., 2009; Piehowski *et al*., 2013). Significant variability was detected among embryo and adult MS replicates, which correlated with the abundance of the identified proteins. Ubiquitin conjugates identified in all MS experiments were those found more abundantly (higher LFQ intensity), while those with lower intensity were generally detected solely in one analysis. We noticed a bigger variability between samples that were analysed by MS in different days, despite being of the same genotype, than between samples of different genotypes analysed on the same day. However, if the MS analysis is performed in triplicate, with samples analysed on the same batch, variability is severely reduced and reproducibility significantly enhanced (Martinez *et al*., under review).

On the other hand, proteins are typically separated in a polyacrylamide gel with the in-gel digestion protocol. The gel is cut into slices and proteins are digested with trypsin to be converted into peptides (Shevchenko *et al*., 2006). For embryonic and adult samples the gels were cut into two slices in order to avoid the strong avidin bands at ~14 and ~25 kDa, as they could interfere with the detection by MS of other proteins due to its higher abundance. Similarly, there are other abundant proteins in our pulldowns, such as the endogenously biotinylated proteins (~130 and ~250 kDa), that could also interfere with the analysis. Therefore, removal of these bands prior to MS analysis by cutting the gel into more than two slices could also improve the depth of the MS analysis and reduce the variability among biological replicates. The excised bands containing specific high abundant proteins, as avidin and endogenously biotinylated carboxylases, could then be run in the mass spectrometer after all the other samples. It should be noted, however, that dividing the ubiquitinated material into too many fractions could

also reduce the number of identification, as proteins ubiquitinated with different ubiquitin chain length would then be spread across different fractions and might scape -due to lower peptide concentration- detection by MS.

Overexpression of Rpn10^{DN} results on the presence of highly ubiquitinated proteins with a concomitant reduction of mono-ubiquitinated proteins

Unravelling the roles that ubiquitination plays within cells ultimately requires physiological pathways to be perturbed, in order to detect changes that would help elucidating the function of particular ubiquitination events. The attachment of ubiquitin can among other functions trigger the targeting of proteins for degradation (Komander and Rape, 2012). We combined our ^{bio}Ub flies with a proteasomal shuttling factor dominant negative mutant (Rpn10^{DN}), in order to enrich those poly-ubiquitinated proteins that should be degraded by the proteasome in *Drosophila* neuronal tissues. Overexpression of Rpn10^{DN} caused an enrichment of high molecular-weight ubiquitinated material, in agreement with previous reports (Lipinszki *et al*., 2009; Lee *et al*., 2014; Ramirez *et al*., 2015). However, contrary to what we expected, a reduced number of proteins were identified by MS analysis in Rpn10^{DN} samples as compared to wild type flies. This occurred concomitantly to a reduction in the ubiquitination levels of a subset of other proteins, mostly mono-ubiquitinated substrates. In addition, the ubiquitination level of just a few proteins was found to be enhanced (i.e., those with a LFQ ratio >4).

It has been suggested that longer ubiquitin chains, as well as the attachment of multiple chains, might increases the affinity for the proteasome (Thrower *et al*., 2000;

Swatek and Komander, 2016). We therefore hypothesize that the strongest signal observed by silver staining and immunoblot when Rpn10^{DN} is overexpressed may be due to the generation of longer ubiquitin chains, or the attachment of multiple chains, on the same protein, rather than to an increase on the molecular fraction of a given protein that is ubiquitinated. This attempt of the cellular machinery to enhance the affinity of the ubiquitinated proteins for the proteasome is detected by Western blot and silver staining as a stronger signal. The differences in the length or number of ubiquitin chains, however, would remain undetectable by MS, as the trypsinization of a substrate molecule will display a constant intensity of its intrinsic peptides independently of the number of ubiquitin molecules attached to it.

Additionally, the presence of non-degraded highly ubiquitinated proteins (i.e., with longer or several ubiquitin chains attached to them) in Rpn10^{DN}, might affect the isolation of other ubiquitinated proteins. As poly-ubiquitinated proteins are captured by Rpn10^{DN}, they will retain a significant amount of the biotinylated ubiquitin, whose pool is limited. These Rpn10^{DN}-bound substrates will neither be processed by the proteasome nor by DUBs, as observed upon trapping by other UBDs (Hjerpe *et al*., 2009). Therefore, the available biotinylated ubiquitin will be significantly reduced. Newly synthesized ubiquitin is supposed to be transported very slowly (3 mm/day) throughout the axons (Bizzi *et al*., 1991), hence, new protein synthesis will most like not fully replenish the cells with free biotinylated ubiquitin.

Proteasome inhibition in cultured hippocampal neurons has been reported to affect dynamically ubiquitinated proteins (i.e., proteins actively subjected to ubiquitination

and deubiquitination events), due to a significant depletion of available free ubiquitin (Rinetti and Schweizer, 2010). Under this stressful circumstance, the need of free ubiquitin is compensated at the expense of mono-ubiquitinated proteins that are deubiquitinated in order to supply the cell with unconjugated ubiquitin (Dantuma *et al*., 2006; Groothuis *et al*., 2006; Kaiser *et al*., 2011; Wagner *et al*., 2011). This would explain why mono-ubiquitinated proteins, would be significantly reduced in our isolated sample of ubiquitinated proteins, and why the total amount of identified ubiquitinated proteins is also reduced.

The ^{bio}Ub system can be used to identify HECT- or RBR-type ubiquitin E3 ligases that are active on a given developmental stage or tissue

One important attribute of our ^{bio}Ub strategy is that, unlike with other approaches, the ubiquitination status of the MS-identified proteins can be directly validated from the tissue of study by Western blot (Franco *et al*., 2011; Lectez *et al*., 2014; Ramirez *et al*., 2015). With the use of specific antibodies it can be discriminated whether a protein is being covalently modified with one or additional ubiquitin molecules, as they will show a ~10 kDa increase in their molecular weight (or higher if poly-ubiquitinated) in the eluted fraction. In whole lysates, on the contrary, only unmodified forms are usually detected due to the low stoichiometry at which the ubiquitin-modified proteins are encountered. Additionally, proteins that are being modified on cysteine residues (Wang *et al*., 2012), as well as the E1, E2, HECT-type and RBR-type E3 enzymes, all of which generate a thioester linkage with ubiquitin at their active cysteine residue, can also be distinguished using the ^{bio}Ub strategy. The thioester linkage of ubiquitin with cysteine will break upon elution from the beads of the purified material due to the addition of

DTT. The purified protein will, therefore, no longer have ubiquitin attached to it, and thus, no shift in the molecular weight would be detected when comparing eluted and input samples (Franco *et al*., 2011; Lectez *et al*., 2014; Ramirez *et al*., 2015).

We have validated in the past the ubiquitin-carrier status of some E2 enzymes (Franco *et al*., 2011; Lectez *et al*., 2014), as well as the ubiquitin conjugation of proteins on cysteine residues (Lectez *et al*., 2014). For this Thesis we aimed to validate the active status of those E3 ligases for which antibodies were available. Western blot to Parkin and Ube3a, the E3 ligases involved in Parkinson's disease and Angelman syndrome, respectively (Kishino *et al*., 1997; Shimura *et al*., 2000), confirmed that these two enzymes are being isolated mainly because they were carrying ubiquitin at the moment of the purification from the *Drosophila* eye. In the case of Ube3a, this was also confirmed for embryonic samples. These results validate clearly that these two E3 ligases truly form a thioester bond with ubiquitin, which actually means that Parkin and Ube3a are active during the temporal window being studied. The identification of active E3 ligases from *in vivo* neuronal tissues suggests that some of their physiological substrates must also be present within the list of identified ubiquitin conjugates. Combination of the biotinylated ubiquitin overexpression together with Parkin or Ube3a mutant flies (see below) should help, therefore, in the identification of the proteins regulated in neurons by these two E3 ligases.

The ^{bio}Ub system can be used to identify the substrates of a given E3 ligase *in vivo*

UBE3A is an E3 ligase whose substrates have been sought since it was linked to a rare neurodevelopmental disorder, the Angelman syndrome (Kishino *et al*., 1997; Matsuura

et al., 1997). Mouse, fly and cellular models in which UBE3A has been overexpressed or removed (Reiter et al., 2006; Mishra et al., 2009a; Shimoji et al., 2009; Greer et al., 2010; Jensen et al., 2013), have led to the identification of some putative UBE3A substrates (Sell and Margolis, 2015). The design of these approaches, however, did only allow for detecting interactions or changes in total protein levels, but prevented the identification of direct substrates *in vivo*. In most cases, direct evidence of their *in vivo* ubiquitination by UBE3A remains absent or controversial (Kühnle *et al*., 2013; Mabb *et al*., 2014).

The ability of the ^{bio}Ub strategy to detect changes in the ubiquitinated proteome upon the blockade of the proteasome in *Drosophila* prompted us to generate a fly model in which changes in protein ubiquitination upon Ube3a overexpression could be tested. By combining Ube3a expressing flies with the ^{bio}Ub flies we achieved the enrichment of a number of proteins whose ubiquitination was found to be up-regulated upon Ube3a overexpression (**Figure 33**). Additionally, we further confirmed by Western blot the enhanced ubiquitination of Rngo upon overexpression of Ube3a in *Drosophila* photoreceptor cells. Rngo is found poly-ubiquitinated or multimono-ubiquitinated with up to 6 ubiquitins in the eluted fraction. Based on the yield of the biotin pulldowns (~40 %) and on the percentage of input and elution loaded for Western blot analysis, we estimated that ~1 % of Rngo is found conjugated with ubiquitin under physiological conditions. When Ube3a is overexpressed the ubiquitinated fraction of Rngo is increased up to about 3 %. This result places Rngo as the first Ube3a substrate to be validated *in vivo* in the context of a whole organism.

Rngo is the *Drosophila* homologue of the yeast Dd1/Vsm1 and vertebrate Ddi1/Ddi2 ubiquitin receptors (Morawe *et al*., 2011). Yeast Ddi1 has been shown to be involved in the transport of a few proteins to the proteasome for degradation (Kaplun *et al*., 2005; Ivantsiv *et al*., 2006). Conversely, in *Drosophila* a protective role for Rngo has been reported (Morawe *et al*., 2011), suggested to act by preventing the degradation of certain proteins in the germline cells. The Ube3a-dependent ubiquitination of Rngo could, therefore, indirectly affect the levels of many other cellular proteins. This opens a new perspective for the interpretation of previous identifications of UBE3A substrates based on changes in total protein level (further discussed below). How this ubiquitination affects Rngo/Ddi1/Ddi2, however, would require further experiments. As suggested by the fact that Rngo total levels remained unaffected upon overexpression of Ube3a in the fly eye, it would seem that its ubiquitination is not a degradation signal.

On the other hand, the ubiquitination level of a number of proteins was found to be reduced upon Ube3a overexpression. The higher activity of the ectopic Ube3a will result in the preferential attachment of the biotinylated ubiquitin toward its substrates. Therefore, the identification of proteins that are being conjugated with the tagged ubiquitin in a lower degree suggests that they are not direct substrates of Ube3a. The ubiquitination of one of those proteins, Atpα, had been earlier reported to be enhanced by Ube3a *in vitro* (Jensen *et al*., 2013). Our results, however, showed the opposite by MS, in accordance with other reports (Kaphzan *et al*., 2011). Moreover, the ubiquitination levels of Atpα were not found significantly affected by Ube3a when tested by immunoblot, confirming that Atpα is not a direct ubiquitin substrate of Ube3a *in vivo* in the *Drosophila* eye.

We have provided for the first time a list of *in vivo* ubiquitin candidate substrates of *Drosophila* Ube3a, demonstrating that the ^{bio}Ub system can be successfully used to identify proteins ubiquitinated by a given E3 ligase *in vivo*. In fact, based on these results, similar approaches have been successfully carried out *a posteriori* in the lab of Dr. Mayor to identify the *in vivo* substrates of Parkin E3 ligase (Martinez *et al*., under review). This opens the door for the generation of mammalian models in which to screen for E3 ligase substrates, so further insight can be provided into human diseases related to the UPS.

A GFP pulldown approach to confirm the ubiquitination of proteins, validate ubiquitination sites and identify/validate E3 ligase specific substrates

When using the ^{bio}Ub strategy, Western blot validation of ubiquitin conjugates eluted is subject to availability of specific antibodies. For this reason, we developed an alternative approach that takes advantage of the highly stringent washes that single chain anti-GFP beads (Chromotek) can withstand (Lee *et al*., 2014). This new methodology, relays on the overexpression of GFP-tagged proteins, which can be isolated and enriched at the same time the interacting proteins are discarded, allowing then for their ubiquitinated fraction to be easily analysed. We confirmed by this strategy that 43 fly ubiquitin-conjugates (Franco *et al*., 2011) are indeed ubiquitinated by endogenous E3 ligases in *Drosophila* BG2 cells (Lee *et al*., 2014), hence demonstrating that the GFP-pulldown is a simple and sensitive assay to study ubiquitination. Furthermore, the same approach can also be used to isolate GFP-tagged proteins from living organisms (Dr. Maribel Franco and Dr. Ugo Mayor, unpublished results), giving the possibility of characterizing the ubiquitination of a given protein *in vivo*.

The GFP-pulldown assay has also proven to be a good alternative to further characterize the ubiquitination of individual proteins as well as to identify and/or validate E3 ligase specific substrates (see below). By mutating two lysine residues on nSyb protein a significant reduction of its ubiquitination levels was detected. These two lysines are surrounding an arginine residue found in the core of the complex formed with Syx1A and Snap25 (Ossig *et al*., 2000). Interestingly, when this arginine is mutated to a glycine results in defects comparable to the deletion of the gene (Fasshauer *et al*., 1998; Ossig *et al*., 2000). The fact that the identified lysines are so close to this arginine suggests that their ubiquitination might play an important role in the exocytosis pathway, probably by interfering with the nSyb/Syx1A/Snap25 complex formation. The validation of these two ubiquitination sites, therefore, will be useful for future studies on nSyb function, both in flies and mammals.

Rngo, Rpn10, Rps10b, Uch-L5 and CG8209 are substrates of Ube3a in *Drosophila*

Co-expression of Ube3a E3 ligase allowed the identification of some of its target substrates in BG2 cells using the GFP-pulldown approach. Four of the identified proteins are interactors of the proteasome: Rpn10 and Rngo, two *Drosophila* ubiquitin receptors that shuttle ubiquitinated proteins to the proteasome for degradation (Lipinszki *et al*., 2009; Morawe *et al*., 2011); Uch-L5, a proteasome-associated DUB enzyme that cleaves K48 ubiquitin chains (Yao *et al*., 2006) and CG8209, which is the *Drosophila* homologue of UBXN1/SAKS, another ubiquitin receptor involved in the proteasome-mediated degradation of misfolded glycoproteins (McNeill *et al*., 2004; Lee *et al*., 2014). Interestingly, Rngo and Rpn10 were also found by MS to be *in vivo* substrates of Ube3a in the fly eye. On the other hand, the ribosomal protein RpS10b, a protein found

differentially expressed in patients with schizophrenia (Bowden *et al*., 2006), was also identified.

Association of UBE3A with proteasomes in several cell lines (Scanlon *et al*., 2009; Martínez-Noël *et al*., 2012), as well as in synaptosomes isolated from the rat brain (Tai *et al*., 2010), had been previously reported. However, the nature of this association was not yet clear. The identification of four proteasomal proteins that are directly ubiquitinated by Ube3a in neuron-like cells suggests that one of the roles carried out by this E3 ligase is to actually regulate proteasomal function. Ube3a-dependent changes in the levels of proteins, therefore, could be interpreted as the result of a downstream effect caused by the proteasomal regulation by Ube3a in neurons, rather than to direct ubiquitination events.

Ubiquitination by Ube3a does not necessarily lead to protein degradation

From several *Drosophila* Ube3a substrates identified in BG2 cells only Rpn10 appears to be itself targeted for degradation upon Ube3a ubiquitination. UBE3A has been reported to preferentially catalyse the formation of K48 linked-chains (Kim and Huibregtse, 2009). Therefore, it is generally believed that proteins ubiquitinated by UBE3A must be targeted for degradation. Rngo, Uch-L5, CG8209 and RpS10b total protein levels did, however, not seem to be reduced, suggesting that their ubiquitination by Ube3a is probably not a degradative signal.

According to an emerging model for proteasomal degradation, the presence of multiple short or branched chains is thought to be a better degradation signal than the

classical poly-ubiquitin chain linkage (Swatek and Komander, 2016). Based on this model, therefore, a K48-linked chain would not necessarily target proteins to the proteasome, unless additional chains are attached to the modified protein or to the previously attached chain. In fact, the formation of K48-linked chains in the yeast transcription factor Met4 has been reported to regulate its activity in a proteolysis-independent manner (Flick et al., 2004). An UBD found in Met4 has been proposed to cap the K48-ubiquitin chain inactivating the protein and protecting Met4 from degradation (Flick *et al*., 2006). Similarly, Ube3a-dependent ubiquitination of Rngo, Uch-L5, CG8209 and RpS10b could also be regulating their activity rather than their levels. These results suggest that Ube3a ubiquitination might not always be a degradation signal, and hence, the existing dogma for Ube3a function should be revised.

Ube3a and Rpn10^{DN} interact *in vivo*

Direct interaction of human UBE3A with the proteasome subunit PSMD4 (the homologue of fly Rpn10) has been described in previous reports (Martínez-Noël *et al*., 2012; Tomaić and Banks, 2015). The main role of PSMD4/Rpn10 is to shuttle poly-ubiquitinated proteins to the proteasome for their degradation (**Figure 45A**). In *Drosophila* the Ube3a-dependent degradation of Rpn10 will, therefore, prevent the transport of those proteins to the proteasome, which might remain ubiquitin-conjugated or processed by DUBs into their normal forms. When Ube3a is overexpressed in the *Drosophila* photoreceptor cells, the persisting activity of these proteins that should under normal conditions be degraded would produce the strong eye phenotype observed (**Figure 45B**).

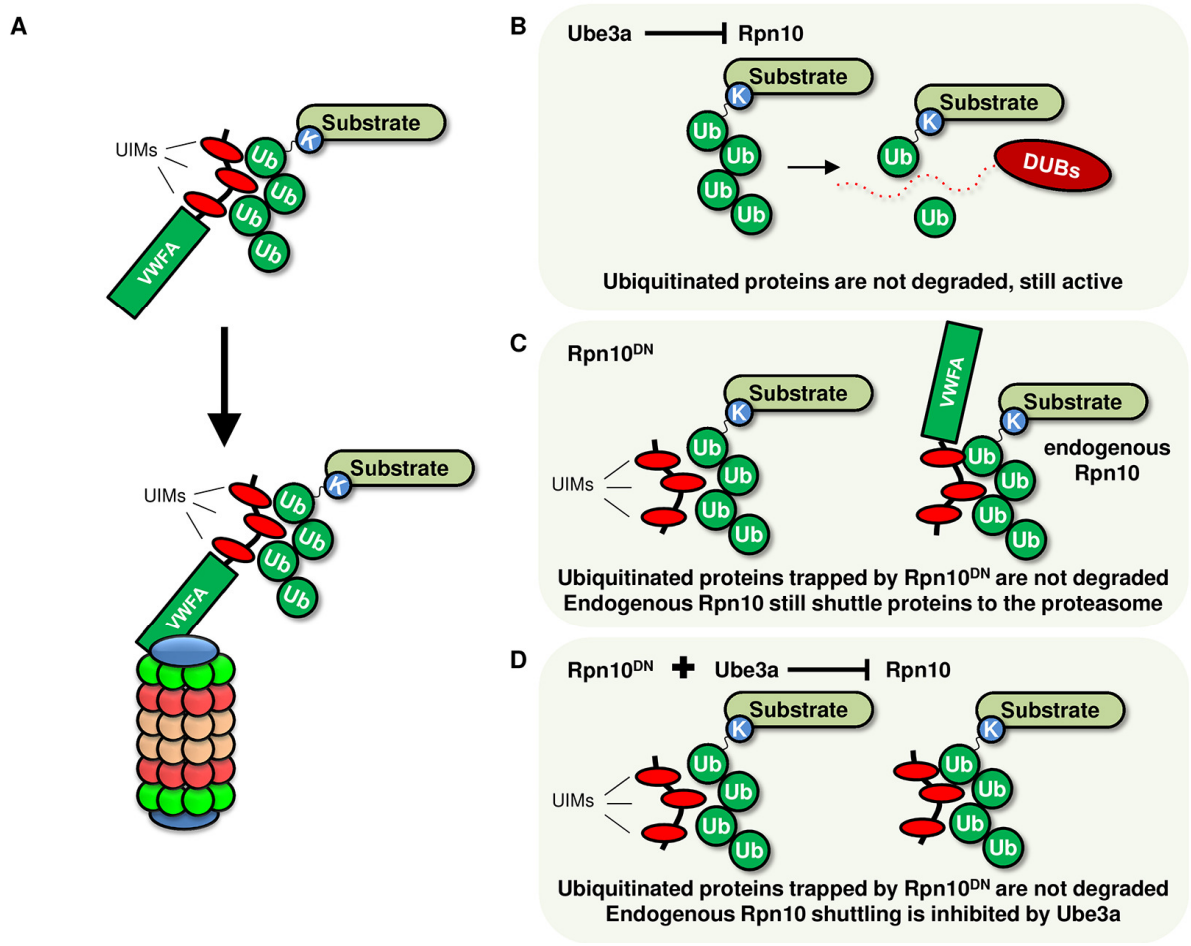

Figure 45. Model for the *in vivo* interaction between Ube3a and Rpn10.

A. The main role of Rpn10 is to shuttle poly-ubiquitinated proteins to the proteasome for degradation. Rpn10 recognizes poly-ubiquitinated proteins through its ubiquitin interacting motifs (UIMs) and interact with the proteasome through the von Willenbrand factor A (VWFA) domain. **B.** Overexpression of Ube3a will target endogenous Rpn10 for degradation. A number of proteins that should have been degraded, therefore, will stay active resulting in the degenerated eye phenotype. **C.** Overexpression of a dominant negative version of Rpn10 that lacks the VWFA domain ($Rpn10^{DN}$) results in the accumulation of poly-ubiquitinated material. This occurs because poly-ubiquitinated proteins are trapped by $Rpn10^{DN}$ and are not transported to the proteasome. In this situation endogenous Rpn10 will remain shuttling some proteins to the proteasome. **D.** If both $Rpn10^{DN}$ and Ube3a are overexpressed, the reduction of the endogenous shuttling Rpn10 is compounded by the trapping of ubiquitinated proteins by $Rpn10^{DN}$. The activity of those proteins trapped by $Rpn10^{DN}$ would be blocked, so the eye phenotype associated to their misregulation is no longer detectable.

The overexpression of a dominant negative mutant of Rpn10 ($Rpn10^{DN}$) results in some of its client proteins being trapped (**Figure 45C**), so an accumulation of poly-ubiquitinated material is observed in the fly eye. Under this circumstance, however, the endogenous Rpn10 should still shuttle poly-ubiquitinated proteins to the proteasome for their degradation. If both $Rpn10^{DN}$ and Ube3a are overexpressed an enhanced ubiquitin signal is detected. This is probably due to the inhibition of endogenous Rpn10 shuttling, due to Ube3a-dependent degradation, being aggravated by the trapping of its client ubiquitinated proteins by $Rpn10^{DN}$ (**Figure 45D**). In this situation, proteins trapped by $Rpn10^{DN}$, however, will probably be protected from DUBs (Hjerpe *et al*., 2009) and will not retain their activity, explaining why the eye phenotype associated to their misregulation is no longer detectable. This *in vivo* Ube3a-$Rpn10^{DN}$ synergy strongly supports our observation of Rpn10 as an Ube3a substrate, as well as the view of Ube3a as a key regulator of neuronal proteasomal function.

The Ube3a dependent degradation of Rpn10, and the ubiquitination of Rngo and Uch-L5 protein, place Ube3a as a master regulator of protein homeostasis.

The ^{bio}Ub- and GFP-pulldown assays have allowed for the identification and validation of five direct Ube3a substrates in *Drosophila melanogaster*, four of which are known interactors of the proteasome. Ubiquitination of proteasomal subunits, including PSMD4 and Uch37, the human homologues of the fly Rpn10 and Uch-L5, respectively, have been reported to impair the ability of the proteasome to bind, deubiquitinate and process ubiquitinated proteins (Jacobson *et al*., 2014). The fact that four of the validated fly Ube3a substrates are interactors of the proteasome places Ube3a as a master regulator of protein homeostasis in *Drosophila*.

While the ubiquitination of Rpn10 leads to its degradation, the ubiquitination of Rngo, CG8209 and Uch-L5 appears to have a non-degradative role, maybe regulating their activity (Flick *et al*., 2006). In the presence of extra activity of Ube3a, as is the case in some ASD patients (Yi et al., 2015), the transport of some ubiquitinated proteins to the proteasome, due to Rpn10, Rngo and CG8209 ubiquitination, would therefore be blocked. On the other hand, Uch37 (Uch-L5) has been suggested to trim ubiquitin chains from substrates, so they are released from the ubiquitin receptor and translocated to the proteasome (Liu and Jacobson, 2013). Therefore, the inhibition of this DUB upon ubiquitination by Ube3a would also contribute to the impairment of the proteasomal function. In AS the situation would, however, be the opposite. That is, since Ube3a ubiquitin ligase activity does not function, the absence of Rpn10, Rngo, CG8209 and Uch-L5 ubiquitination, would probably result in an increased proteasomal activity and a premature degradation of a number of proteins.

The view of Ube3a as a regulator of the proteasome opens a new perspective in which the ubiquitination of other proteins, and thus their levels or activity, can be affected as a downstream effect. This idea is further strengthened by the fact that many of the candidate substrates identified by MS in the fly eye are members of the UPS and had been linked in their own with several neurological disorders: Uch human homologue (UCHL1) is a DUB involved in Parkinson's and Alzheimer's diseases (Leroy *et al*., 1998; Choi *et al*., 2004), as well as in an early-onset neurodegeneration phenotype (Bilguvar *et al*., 2013); the human UBE2H E2 enzyme, homologue of the *Drosophila* UbcE2H, has been associated with autistic disorders (Vourc'h *et al*., 2003); mutations in Ref(2)P/p62 were found in patients with Amyotrophic Lateral Sclerosis (Fecto *et al*., 2011) and its

loss of function found to enhance the accumulation of polyQ proteins in a polyQ disease *Drosophila* model (Saitoh *et al*., 2015); and Rpn10/PSMD4 regulates dendrite development in the mammalian brain (Puram *et al*., 2013).

The application of both ^{bio}Ub and GFP-pulldown strategies has been useful for the identification of ubiquitinated proteins, validation of ubiquitination sites and identification of E3 ligase specific substrates. In the future, the application of these strategies to mammalian models, will therefore greatly contribute to our understanding of the role that ubiquitination plays in the nervous system. This molecular detail will as well help to better understand human pathologies in which ubiquitination is involved, such as those related to the UBE3A enzyme.

X. Conclusions

1. *Drosophila* photoreceptor cells can be successfully used as an *in vivo* system for the study of the proteins that are ubiquitinated in mature neurons.
2. The ubiquitin proteome is not constant and depends both on the tissue studied but also on the temporal context.
3. An appropriate promoter and a simultaneous MS analysis of biological replicates are important factors in the biotin pulldown assay.
4. Overexpression of $Rpn10^{DN}$ results on the presence of highly ubiquitinated proteins with a concomitant reduction of mono-ubiquitinated proteins.
5. The ^{bio}Ub system can be used to identify HECT- or RBR-type ubiquitin E3 ligases that are active on a given developmental stage or tissue.
6. The ^{bio}Ub system can be used to identify the substrates of a given E3 ligase *in vivo*. Ubiquitination of Rngo protein was found to be increased upon Ube3a overexpression in *Drosophila* photoreceptor cells. This places Rngo as the first Ube3a substrate to be validated *in vivo* in the context of a whole organism.
7. A GFP pulldown assay has been developed and found to be a suitable approach to confirm the ubiquitination of proteins and to validate their ubiquitination sites. This approach can also be used to identify and/or validate E3 ligase specific substrates.
8. Rngo, Rpn10, Rps10b, Uch-L5 and CG8209 are substrates of Ube3a in *Drosophila* BG2 cells. Of those, Rngo and Rpn10 have also been found to be *in vivo* substrates of Ube3a.
9. Ubiquitination by Ube3a can lead to degradation (Rpn10) or not (Rngo, Rps10b, Uch-L5, CG8209). The existing dogma for Ube3a function requires therefore to be revised.

10. Ube3a and Rpn10^{DN} interact *in vivo*. This interaction suppresses the degeneration phenotype of the eye caused by Ube3a overexpression and enhances the accumulation of ubiquitinated proteins caused by Rpn10^{DN} overexpression.
11. The Ube3a dependent degradation of Rpn10, and the ubiquitination of Rngo and Uch-L5 protein, place Ube3a as a master regulator of protein homeostasis.

XI. References

Adams, M.D., Celniker, S.E., Holt, R.A., Evans, C.A., Gocayne, J.D., Amanatides, P.G., Scherer, S.E., Li, P.W., Hoskins, R.A., Galle, R.F., *et al*. 2000. The genome sequence of *Drosophila melanogaster*. *Science*, 287, 2185–2195.

Amerik, A.Y. and Hochstrasser, M. 2004. Mechanism and function of deubiquitinating enzymes. *Biochim. Biophys. Acta.*, 1695, 189–207.

Angelman, H. 1965. "Puppet" children a report on three cases. *Dev. Med. Child Neurol.*, 7, 681–688.

Bassermann, F., Eichner, R. and Pagano, M. 2014. The ubiquitin proteasome system - implications for cell cycle control and the targeted treatment of cancer. *Biochim. Biophys. Acta*, 1843, 150–162.

Beasley, S.A., Hristova, V.A. and Shaw, G.S. 2007. Structure of the Parkin in-between-ring domain provides insights for E3-ligase dysfunction in autosomal recessive Parkinson's disease. *Proc. Natl. Acad. Sci. U. S. A.*, 104, 3095–3100.

Beckett, D., Kovaleva, E. and Schatz, P.J. 1999. A minimal peptide substrate in biotin holoenzyme synthetase-catalyzed biotinylation. *Protein Sci.*, 8, 921–929.

Bedford, L., Hay, D., Devoy, A., Paine, S., Powe, D.G., Seth, R., Gray, T., Topham, I., Fone, K., Rezvani, N., *et al*. 2008. Depletion of 26S proteasomes in mouse brain neurons causes neurodegeneration and Lewy-like inclusions resembling human pale bodies. *J. Neurosci.*, 28, 8189–8198.

Bell, A.W., Deutsch, E.W., Au, C.E., Kearney, R.E., Beavis, R., Sechi, S., Nilsson, T., Bergeron, J.J.M. and HUPO Test Sample Working Group. 2009. A HUPO test sample study reveals common problems in mass spectrometry-based proteomics. *Nat. Methods*, 6, 423–430.

Bennett, E.J. and Harper, J.W. 2008. DNA damage: ubiquitin marks the spot. *Nat. Struct. Mol. Biol.*, 15, 20–22.

Bennett, E.J., Shaler, T.A., Woodman, B., Ryu, K.-Y., Zaitseva, T.S., Becker, C.H., Bates, G.P., Schulman, H. and Kopito, R.R. 2007. Global changes to the ubiquitin system in Huntington's disease. *Nature*, 448, 704–708.

Berndsen, C.E. and Wolberger, C. 2014. New insights into ubiquitin E3 ligase mechanism. *Nat. Struct. Mol. Biol.*, 21, 301–307.

Bertolaet, B.L., Clarke, D.J., Wolff, M., Watson, M.H., Henze, M., Divita, G. and Reed, S.I. 2001. UBA domains of DNA damage-inducible proteins interact with ubiquitin. *Nat. Struct. Biol.*, 8, 417–422.

Bertram, L., Hiltunen, M., Parkinson, M., Ingelsson, M., Lange, C., Ramasamy, K., Mullin, K., Menon, R., Sampson, A.J., Hsiao, M.Y., *et al*. 2005. Family-based association between Alzheimer's disease and variants in UBQLN1. *N. Engl. J. Med.*, 352, 884–894.

Besche, H.C., Sha, Z., Kukushkin, N.V., Peth, A., Hock, E.-M., Kim, W., Gygi, S., Gutierrez, J.A., Liao, H., Dick, L., *et al*. 2014. Autoubiquitination of the 26S proteasome on Rpn13 regulates breakdown of ubiquitin conjugates. *EMBO J.*, 33, 1159–1176.

Bier, E. 2005. *Drosophila*, the golden bug, emerges as a tool for human genetics. *Nat. Rev. Genet.*, 6, 9–23.

Bilguvar, K., Tyagi, N.K., Ozkara, C., Tuysuz, B., Bakircioglu, M., Choi, M., Delil, S., Caglayan, A.O., Baranoski, J.F., Erturk, O., *et al*. 2013. Recessive loss of function of the neuronal ubiquitin

hydrolase UCHL1 leads to early-onset progressive neurodegeneration. *Proc. Natl. Acad. Sci. U. S. A.*, 110, 3489–3494.

Bird, L.M. 2014. Angelman syndrome: review of clinical and molecular aspects. *Appl. Clin. Genet.*, 7, 93–104.

Bizzi, A., Schaetzle, B., Patton, A., Gambetti, P. and Autilio-Gambetti, L. 1991. Axonal transport of two major components of the ubiquitin system: free ubiquitin and ubiquitin carboxyl-terminal hydrolase PGP 9.5. *Brain Res.*, 548, 292–299.

Bowden, N.A., Weidenhofer, J., Scott, R.J., Schall, U., Todd, J., Michie, P.T. and Tooney, P.A. 2006. Preliminary investigation of gene expression profiles in peripheral blood lymphocytes in schizophrenia. *Schizophr. Res.*, 82, 175–183.

Brand, A.H. and Perrimon, N. 1993. Targeted gene expression as a means of altering cell fates and generating dominant phenotypes. *Dev. Camb. Engl.*, 118, 401–415.

Brand, A.H., Manoukian, A.S. and Perrimon, N. 1994. Ectopic expression in *Drosophila*. *Methods Cell Biol.*, 44, 635–654.

Brody, T. 1999. The Interactive Fly: gene networks, development and the Internet. *Trends Genet.*, 15, 333–334.

Budnik, V. 1996. Synapse maturation and structural plasticity at *Drosophila* neuromuscular junctions. *Curr. Opin. Neurobiol.*, 6, 858–867.

Budnik, V., Koh, Y.H., Guan, B., Hartmann, B., Hough, C., Woods, D. and Gorczyca, M. 1996. Regulation of synapse structure and function by the *Drosophila* tumor suppressor gene dlg. *Neuron*, 17, 627–640.

Buiting, K., Saitoh, S., Gross, S., Dittrich, B., Schwartz, S., Nicholls, R.D. and Horsthemke, B. 1995. Inherited microdeletions in the Angelman and Prader-Willi syndromes define an imprinting centre on human chromosome 15. *Nat. Genet.*, 9, 395–400.

Buiting, K., Gross, S., Lich, C., Gillessen-Kaesbach, G., el-Maarri, O. and Horsthemke, B. 2003. Epimutations in Prader-Willi and Angelman syndromes: a molecular study of 136 patients with an imprinting defect. *Am. J. Hum. Genet.*, 72, 571–577.

Burroughs, A.M., Jaffee, M., Iyer, L.M. and Aravind, L. 2008. Anatomy of the E2 ligase fold: implications for enzymology and evolution of ubiquitin/Ub-like protein conjugation. *J. Struct. Biol.*, 162, 205–218.

Castle, W.E. 1906. Inbreeding, cross-breeding and sterility in *Drosophila*. *Science*, 23, 153.

Chandler, C.S. and Ballard, F.J. 1985. Distribution and degradation of biotin-containing carboxylases in human cell lines. *Biochem. J.*, 232, 385–393.

Chandler, C.S. and Ballard, F.J. 1986. Multiple biotin-containing proteins in 3T3-L1 cells. *Biochem. J.*, 237, 123–130.

Chapman-Smith, A. and Cronan, J.E. 1999. Molecular biology of biotin attachment to proteins. *J. Nutr.*, 129, 477S–484S.

Chaugule, V.K., Burchell, L., Barber, K.R., Sidhu, A., Leslie, S.J., Shaw, G.S. and Walden, H. 2011. Autoregulation of Parkin activity through its ubiquitin-like domain. *EMBO J.*, 30, 2853–2867.

Chen, Z.J. and Sun, L.J. 2009. Nonproteolytic functions of ubiquitin in cell signaling. *Mol. Cell*, 33, 275–286.

Chen, H., Polo, S., Di Fiore, P.P. and De Camilli, P.V. 2003. Rapid Ca2+-dependent decrease of protein ubiquitination at synapses. *Proc. Natl. Acad. Sci. U. S. A.*, 100, 14908–14913.

Chen, X., Zhang, B. and Fischer, J.A. 2002. A specific protein substrate for a deubiquitinating enzyme: Liquid facets is the substrate of Fat facets. *Genes Dev.*, 16, 289–294.

Chiba, A. and Keshishian, H. 1996. Neuronal pathfinding and recognition: roles of cell adhesion *Molecules. Dev. Biol.*, 180, 424–432.

Chintapalli, V.R., Wang, J. and Dow, J.A.T. 2007. Using FlyAtlas to identify better *Drosophila melanogaster* models of human disease. *Nat. Genet.*, 39, 715–720.

Choi, J., Levey, A.I., Weintraub, S.T., Rees, H.D., Gearing, M., Chin, L.-S. and Li, L. 2004. Oxidative modifications and down-regulation of ubiquitin carboxyl-terminal hydrolase L1 associated with idiopathic Parkinson's and Alzheimer's diseases. *J. Biol. Chem.*, 279, 13256–13264.

Choi, S.Y., Jang, H., Roe, J.S., Kim, S.T., Cho, E.J. and Youn, H.D. 2013. Phosphorylation and ubiquitination-dependent degradation of CABIN1 releases p53 for transactivation upon genotoxic stress. *Nucleic Acids Res.*, 41, 2180–2190.

Ciechanover, A. 2013. Intracellular protein degradation: from a vague idea through the lysosome and the ubiquitin-proteasome system and onto human diseases and drug targeting. *Bioorg. Med. Chem.*, 21, 3400–3410.

Ciechanover, A. and Ben-Saadon, R. 2004. N-terminal ubiquitination: more protein substrates join in. *Trends Cell Biol.*, 14, 103–106.

Ciechanover, A., Heller, H., Katz-Etzion, R. and Hershko, A. 1981. Activation of the heat-stable polypeptide of the ATP-dependent proteolytic system. *Proc. Natl. Acad. Sci. U. S. A.* 78, 761–765.

Clute, P. and Pines, J. 1999. Temporal and spatial control of cyclin B1 destruction in metaphase. *Nat. Cell Biol.*, 1, 82–87.

Cox, J. and Mann, M. 2008. MaxQuant enables high peptide identification rates, individualized p.p.b.-range mass accuracies and proteome-wide protein quantification. *Nat. Biotechnol.*, 26, 1367–1372.

Cox, J., Hein, M.Y., Luber, C.A., Paron, I., Nagaraj, N. and Mann, M. 2014. Accurate proteome-wide label-free quantification by delayed normalization and maximal peptide ratio extraction, termed MaxLFQ. *Mol. Cell. Proteomics*, 13, 2513–2526.

Dambacher, C.M., Worden, E.J., Herzik, M.A., Martin, A. and Lander, G.C. 2016. Atomic structure of the 26S proteasome lid reveals the mechanism of deubiquitinase inhibition. *eLife*, 5, e13027.

Danielsen, J.M.R., Sylvestersen, K.B., Bekker-Jensen, S., Szklarczyk, D., Poulsen, J.W., Horn, H., Jensen, L.J., Mailand, N. and Nielsen, M.L. 2011. Mass spectrometric analysis of lysine ubiquitylation reveals promiscuity at site level. *Mol. Cell. Proteomics*, 10, M110.003590.

Dantuma, N.P., Groothuis, T.A.M., Salomons, F.A. and Neefjes, J. 2006. A dynamic ubiquitin equilibrium couples proteasomal activity to chromatin remodeling. *J. Cell Biol.*, 173, 19–26.

De Duve, C., Pressman, B.C., Gianetto, R., Wattiaux, R. and Appelmans, F. 1955. Tissue fractionation studies. 6. Intracellular distribution patterns of enzymes in rat-liver tissue. *Biochem. J.*, 60, 604–617.

van Delft, S., Govers, R., Strous, G.J., Verkleij, A.J. and van Bergen en Henegouwen, P.M. 1997. Epidermal growth factor induces ubiquitination of Eps15. *J. Biol. Chem.*, 272, 14013–14016.

Deng, L., Wang, C., Spencer, E., Yang, L., Braun, A., You, J., Slaughter, C., Pickart, C. and Chen, Z.J. 2000. Activation of the IkappaB kinase complex by TRAF6 requires a dimeric ubiquitin-conjugating enzyme complex and a unique polyubiquitin chain. *Cell*, 103, 351–361.

Deshaies, R.J. and Joazeiro, C.A.P. 2009. RING domain E3 ubiquitin ligases. *Annu. Rev. Biochem.*, 78, 399–434.

Deveraux, Q., Ustrell, V., Pickart, C. and Rechsteiner, M. 1994. A 26 S protease subunit that binds ubiquitin conjugates. *J. Biol. Chem.*, 269, 7059–7061.

Di Fiore, P.P., Polo, S. and Hofmann, K. 2003. When ubiquitin meets ubiquitin receptors: a signalling connection. *Nat. Rev. Mol. Cell Biol.*, 4, 491–497.

DiAntonio, A., Haghighi, A.P., Portman, S.L., Lee, J.D., Amaranto, A.M. and Goodman, C.S. 2001. Ubiquitination-dependent mechanisms regulate synaptic growth and function. *Nature*, 412, 449–452.

Dikic, I., Wakatsuki, S. and Walters, K.J. 2009. Ubiquitin-binding domains - from structures to functions. *Nat. Rev. Mol. Cell Biol.*, 10, 659–671.

Dindot, S.V., Antalffy, B.A., Bhattacharjee, M.B. and Beaudet, A.L. 2008. The Angelman syndrome ubiquitin ligase localizes to the synapse and nucleus, and maternal deficiency results in abnormal dendritic spine morphology. *Hum. Mol. Genet.*, 17, 111–118.

Ding, M. and Shen, K. 2008. The role of the ubiquitin proteasome system in synapse remodeling and neurodegenerative diseases. *BioEssays*, 30, 1075–1083.

Domon, B. and Aebersold, R. 2006. Mass spectrometry and protein analysis. *Science*, 312, 212–217.

Doncaster, L. 1916. The mechanism of mendelian heredity. *Eugen. Rev.*, 8, 164–166.

Durcan, T.M., Tang, M.Y., Pérusse, J.R., Dashti, E.A., Aguileta, M.A., McLelland, G.-L., Gros, P., Shaler, T.A., Faubert, D., Coulombe, B., *et al*. 2014. USP8 regulates mitophagy by removing K6-linked ubiquitin conjugates from parkin. *EMBO J.*, 33, 2473–2491.

Eddins, M.J., Varadan, R., Fushman, D., Pickart, C.M. and Wolberger, C. 2007. Crystal structure and solution NMR studies of Lys48-linked tetraubiquitin at neutral pH. *J. Mol. Biol.*, 367, 204–211.

Ehlers, M.D. 2003. Activity level controls postsynaptic composition and signaling via the ubiquitin-proteasome system. *Nat. Neurosci.*, 6, 231–242.

Eisenhaber, B., Chumak, N., Eisenhaber, F. and Hauser, M.-T. 2007. The ring between ring fingers (RBR) protein family. *Genome Biol.*, 8, 209.

Elia, A.E.H., Boardman, A.P., Wang, D.C., Huttlin, E.L., Everley, R.A., Dephoure, N., Zhou, C., Koren, I., Gygi, S.P. and Elledge, S.J. 2015. Quantitative proteomic atlas of ubiquitination and acetylation in the DNA damage response. *Mol. Cell*, 59, 867–881.

Etlinger, J.D. and Goldberg, A.L. 1977. A soluble ATP-dependent proteolytic system responsible for the degradation of abnormal proteins in reticulocytes. *Proc. Natl. Acad. Sci. U. S. A.*, 74, 54–58.

Fasshauer, D., Sutton, R.B., Brunger, A.T. and Jahn, R. 1998. Conserved structural features of the synaptic fusion complex: SNARE proteins reclassified as Q- and R-SNAREs. *Proc. Natl. Acad. Sci. U. S. A.*, 95, 15781–15786.

Fecto, F., Yan, J., Vemula, S.P., Liu, E., Yang, Y., Chen, W., Zheng, J.G., Shi, Y., Siddique, N., Arrat, H., *et al*. 2011. SQSTM1 mutations in familial and sporadic amyotrophic lateral sclerosis. *Arch. Neurol.*, 68, 1440–1446.

Feiguin, F., Godena, V.K., Romano, G., D'Ambrogio, A., Klima, R. and Baralle, F.E. 2009. Depletion of TDP-43 affects *Drosophila* motoneurons terminal synapsis and locomotive behavior. *FEBS Lett.*, 583, 1586–1592.

Fenn, J.B., Mann, M., Meng, C.K., Wong, S.F. and Whitehouse, C.M. 1989. Electrospray ionization for mass spectrometry of large biomolecules. *Science*, 246, 64–71.

Ferdousy, F., Bodeen, W., Summers, K., Doherty, O., Wright, O., Elsisi, N., Hilliard, G., O'Donnell, J.M. and Reiter, L.T. 2011. *Drosophila* Ube3a regulates monoamine synthesis by increasing GTP cyclohydrolase I activity via a non-ubiquitin ligase mechanism. *Neurobiol. Dis.*, 41, 669–677.

Finehout, E.J. and Lee, K.H. 2004. An introduction to mass spectrometry applications in biological research. *Biochem. Mol. Biol. Educ.*, 32, 93–100.

Finley, D., Chen, X. and Walters, K.J. 2016. Gates, channels, and switches: elements of the proteasome machine. *Trends Biochem. Sci.*, 41, 77–93.

Fischer, J.A., Giniger, E., Maniatis, T. and Ptashne, M. 1988. GAL4 activates transcription in *Drosophila*. *Nature*, 332, 853–856.

Flick, K., Ouni, I., Wohlschlegel, J.A., Capati, C., McDonald, W.H., Yates, J.R. and Kaiser, P. 2004. Proteolysis-independent regulation of the transcription factor Met4 by a single Lys 48-linked ubiquitin chain. *Nat. Cell Biol.*, 6, 634–641.

Flick, K., Raasi, S., Zhang, H., Yen, J.L. and Kaiser, P. 2006. A ubiquitin-interacting motif protects polyubiquitinated Met4 from degradation by the 26S proteasome. *Nat. Cell Biol.*, 8, 509–515.

Franco, M., Seyfried, N.T., Brand, A.H., Peng, J. and Mayor, U. 2011. A novel strategy to isolate ubiquitin conjugates reveals wide role for ubiquitination during neural development. *Mol. Cell. Proteomics*, 10, M110.002188.

Garcia, B.A., Thomas, C.E., Kelleher, N.L. and Mizzen, C.A. 2008. Tissue-specific expression and posttranslational modification of histone H3 variants. *J. Proteome Res.*, 7, 4225–4236.

Gerlach, B., Cordier, S.M., Schmukle, A.C., Emmerich, C.H., Rieser, E., Haas, T.L., Webb, A.I., Rickard, J.A., Anderton, H., Wong, W.W.-L., *et al*. 2011. Linear ubiquitination prevents inflammation and regulates immune signalling. *Nature*, 471, 591–596.

Glickman, M.H. and Ciechanover, A. 2002. The ubiquitin-proteasome proteolytic pathway: destruction for the sake of construction. *Physiol. Rev.*, 82, 373–428.

Goldberg, A.L. and St John, A.C. 1976. Intracellular protein degradation in mammalian and bacterial cells: Part 2. *Annu. Rev. Biochem.*, 45, 747–803.

Goldstein, G., Scheid, M., Hammerling, U., Schlesinger, D.H., Niall, H.D. and Boyse, E.A. 1975. Isolation of a polypeptide that has lymphocyte-differentiating properties and is probably represented universally in living cells. *Proc. Natl. Acad. Sci. U. S. A.*, 72, 11–15.

Gossen, M. and Bujard, H. 1992. Tight control of gene expression in mammalian cells by tetracycline-responsive promoters. *Proc. Natl. Acad. Sci. U. S. A.*, 89, 5547–5551.

Graveley, B.R., Brooks, A.N., Carlson, J.W., Duff, M.O., Landolin, J.M., Yang, L., Artieri, C.G., van Baren, M.J., Boley, N., Booth, B.W., *et al*. 2011. The developmental transcriptome of *Drosophila melanogaster*. *Nature*, 471, 473–479.

Graziano, A., d'Aquino, R., Laino, G. and Papaccio, G. 2008. Dental pulp stem cells: a promising tool for bone regeneration. *Stem Cell Rev.*, 4, 21–26.

Greer, P.L., Hanayama, R., Bloodgood, B.L., Mardinly, A.R., Lipton, D.M., Flavell, S.W., Kim, T.-K., Griffith, E.C., Waldon, Z., Maehr, R., *et al*. 2010. The Angelman Syndrome protein Ube3A regulates synapse development by ubiquitinating arc. *Cell*, 140, 704–716.

Groll, M., Ditzel, L., Löwe, J., Stock, D., Bochtler, M., Bartunik, H.D. and Huber, R. 1997. Structure of 20S proteasome from yeast at 2.4 A resolution. *Nature*, 386, 463–471.

Groothuis, T.A., Dantuma, N.P., Neefjes, J. and Salomons, F.A. 2006. Ubiquitin crosstalk connecting cellular processes. *Cell Div.*, 1, 21–27.

Haas, A.L., Warms, J.V., Hershko, A. and Rose, I.A. 1982. Ubiquitin-activating enzyme. Mechanism and role in protein-ubiquitin conjugation. *J. Biol. Chem.*, 257, 2543–2548.

Haglund, K., Sigismund, S., Polo, S., Szymkiewicz, I., Di Fiore, P.P. and Dikic, I. 2003. Multiple monoubiquitination of RTKs is sufficient for their endocytosis and degradation. *Nat. Cell Biol.*, 5, 461–466.

Hamilton, A.M. and Zito, K. 2013. Breaking it down: the ubiquitin proteasome system in neuronal morphogenesis. *Neural Plast.*, 2013, e196848.

Haracska, L. and Udvardy, A. 1997. Mapping the ubiquitin-binding domains in the p54 regulatory complex subunit of the *Drosophila* 26S protease. *FEBS Lett.*, 412, 331–336.

Harris, M.A., Clark, J., Ireland, A., Lomax, J., Ashburner, M., Foulger, R., Eilbeck, K., Lewis, S., Marshall, B., Mungall, C., *et al*. 2004. The Gene Ontology (GO) database and informatics resource. *Nucleic Acids Res.*, 32, D258-261.

Hay, B.A., Wolff, T. and Rubin, G.M. 1994. Expression of baculovirus P35 prevents cell death in *Drosophila*. *Dev. Camb. Engl.*, 120, 2121–2129.

Haydon, P.G. and Drapeau, P. 1995. From contact to connection: early events during synaptogenesis. *Trends Neurosci.*, 18, 196–201.

Hegde, A.N. 2010. The ubiquitin-proteasome pathway and synaptic plasticity. *Learn. Mem.*, 17, 314–327.

Hershko, A., Ciechanover, A., Heller, H., Haas, A.L. and Rose, I.A. 1980. Proposed role of ATP in protein breakdown: conjugation of protein with multiple chains of the polypeptide of ATP-dependent proteolysis. *Proc. Natl. Acad. Sci. U. S. A.*, 77, 1783–1786.

Hershko, A., Heller, H., Elias, S. and Ciechanover, A. 1983. Components of ubiquitin-protein ligase system. Resolution, affinity purification, and role in protein breakdown. *J. Biol. Chem.*, 258, 8206–8214.

Hicke, L. 2001. Protein regulation by monoubiquitin. *Nat. Rev. Mol. Cell Biol.*, 2, 195–201.

Hitchcock, A.L., Auld, K., Gygi, S.P. and Silver, P.A. 2003. A subset of membrane-associated proteins is ubiquitinated in response to mutations in the endoplasmic reticulum degradation machinery. *Proc. Natl. Acad. Sci. U. S. A.*, 100, 12735–12740.

Hjerpe, R., Aillet, F., Lopitz-Otsoa, F., Lang, V., England, P. and Rodriguez, M.S. 2009. Efficient protection and isolation of ubiquitylated proteins using tandem ubiquitin-binding entities. *EMBO Rep.*, 10, 1250–1258.

Hoeck, J.D., Jandke, A., Blake, S.M., Nye, E., Spencer-Dene, B., Brandner, S. and Behrens, A. 2010. Fbw7 controls neural stem cell differentiation and progenitor apoptosis via Notch and c-Jun. *Nat. Neurosci.*, 13, 1365–1372.

Hoege, C., Pfander, B., Moldovan, G.-L., Pyrowolakis, G. and Jentsch, S. 2002. RAD6-dependent DNA repair is linked to modification of PCNA by ubiquitin and SUMO. *Nature*, 419, 135–141.

Hofmann, K. and Bucher, P. 1996. The UBA domain: a sequence motif present in multiple enzyme classes of the ubiquitination pathway. *Trends Biochem. Sci.*, 21, 172–173.

Hough, R., Pratt, G. and Rechsteiner, M. 1987. Purification of two high molecular weight proteases from rabbit reticulocyte lysate. *J. Biol. Chem.*, 262, 8303–8313.

Huang, F., Zeng, X., Kim, W., Balasubramani, M., Fortian, A., Gygi, S.P., Yates, N.A. and Sorkin, A. 2013. Lysine 63-linked polyubiquitination is required for EGF receptor degradation. *Proc. Natl. Acad. Sci. U. S. A.*, 110, 15722–15727.

Huibregtse, J.M., Scheffner, M. and Howley, P.M. 1991. A cellular protein mediates association of p53 with the E6 oncoprotein of human papillomavirus types 16 or 18. *EMBO J.*, 10, 4129–4135.

Huibregtse, J.M., Scheffner, M., Beaudenon, S. and Howley, P.M. 1995. A family of proteins structurally and functionally related to the E6-AP ubiquitin-protein ligase. *Proc. Natl. Acad. Sci. U. S. A.*, 92, 2563–2567.

Hummel, T., Krukkert, K., Roos, J., Davis, G. and Klämbt, C. 2000. *Drosophila* Futsch/22C10 is a MAP1B-like protein required for dendritic and axonal development. *Neuron*, 26, 357–370.

Husnjak, K. and Dikic, I. 2012. Ubiquitin-binding proteins: decoders of ubiquitin-mediated cellular functions. *Annu. Rev. Biochem.*, 81, 291–322.

Husnjak, K., Elsasser, S., Zhang, N., Chen, X., Randles, L., Shi, Y., Hofmann, K., Walters, K.J., Finley, D. and Dikic, I. 2008. Proteasome subunit Rpn13 is a novel ubiquitin receptor. *Nature*, 453, 481–488.

Huttlin, E.L., Jedrychowski, M.P., Elias, J.E., Goswami, T., Rad, R., Beausoleil, S.A., Villén, J., Haas, W., Sowa, M.E. and Gygi, S.P. 2010. A tissue-specific atlas of mouse protein phosphorylation and expression. *Cell*, 143, 1174–1189.

Ivantsiv, Y., Kaplun, L., Tzirkin-Goldin, R., Shabek, N. and Raveh, D. 2006. Unique role for the UbL-UbA protein Ddi1 in turnover of SCFUfo1 complexes. *Mol. Cell. Biol.*, 26, 1579–1588.

Jackson, G.R. 2008. Guide to understanding *Drosophila* models of neurodegenerative diseases. *PLoS Biol*, 6, e53.

Jacobson, A.D., MacFadden, A., Wu, Z., Peng, J. and Liu, C.W. 2014. Autoregulation of the 26S proteasome by *in situ* ubiquitination. *Mol. Biol. Cell*, 25, 1824–1835.

Jensen, L., Farook, M.F. and Reiter, L.T. 2013. Proteomic profiling in *Drosophila* reveals potential Dube3a regulation of the Actin cytoskeleton and neuronal homeostasis. *PLoS One*, 8, e61952.

Jiang, Y.H., Armstrong, D., Albrecht, U., Atkins, C.M., Noebels, J.L., Eichele, G., Sweatt, J.D. and Beaudet, A.L. 1998. Mutation of the Angelman ubiquitin ligase in mice causes increased cytoplasmic p53 and deficits of contextual learning and long-term potentiation. *Neuron*, 21, 799–811.

Kaiser, S.E., Riley, B.E., Shaler, T.A., Trevino, R.S., Becker, C.H., Schulman, H. and Kopito, R.R. 2011. Protein standard absolute quantification (PSAQ) method for the measurement of cellular ubiquitin pools. *Nat. Methods*, 8, 691–696.

Kalsner, L. and Chamberlain, S.J. 2015. Prader-Willi, Angelman, and 15q11-q13 duplication syndromes. *Pediatr. Clin. North Am.*, 62, 587–606.

Kanafi, M., Majumdar, D., Bhonde, R., Gupta, P. and Datta, I. 2014. Midbrain cues dictate differentiation of human dental pulp stem cells towards functional dopaminergic neurons. *J. Cell. Physiol.*, 229, 1369–1377.

Kanashova, T., Popp, O., Orasche, J., Karg, E., Harndorf, H., Stengel, B., Sklorz, M., Streibel, T., Zimmermann, R. and Dittmar, G. 2015. Differential proteomic analysis of mouse macrophages exposed to adsorbate-loaded heavy fuel oil derived combustion particles using an automated sample-preparation workflow. *Anal. Bioanal. Chem.*, 407, 5965–5976.

Kaphzan, H., Buffington, S.A., Jung, J.I., Rasband, M.N. and Klann, E. 2011. Alterations in intrinsic membrane properties and the axon initial segment in a mouse model of Angelman syndrome. *J. Neurosci.*, 31, 17637–17648.

Kaplun, L., Tzirkin, R., Bakhrat, A., Shabek, N., Ivantsiv, Y. and Raveh, D. 2005. The DNA damage-inducible UbL-UbA protein Ddi1 participates in Mec1-mediated degradation of Ho endonuclease. *Mol. Cell. Biol.*, 25, 5355–5362.

Karas, M. and Hillenkamp, F. 1988. Laser desorption ionization of proteins with molecular masses exceeding 10,000 daltons. *Anal. Chem.*, 60, 2299–2301.

Keller, B.O., Sui, J., Young, A.B. and Whittal, R.M. 2008. Interferences and contaminants encountered in modern mass spectrometry. *Anal. Chim. Acta*, 627, 71–81.

Kim, H.C. and Huibregtse, J.M. 2009. Polyubiquitination by HECT E3s and the determinants of chain type specificity. *Mol. Cell. Biol.*, 29, 3307–3318.

Kim, W., Bennett, E.J., Huttlin, E.L., Guo, A., Li, J., Possemato, A., Sowa, M.E., Rad, R., Rush, J., Comb, M.J., *et al*. 2011. Systematic and quantitative assessment of the ubiquitin-modified proteome. *Mol. Cell*, 44, 325–340.

Kimura, Y. and Tanaka, K. 2010. Regulatory mechanisms involved in the control of ubiquitin homeostasis. *J. Biochem.*, 147, 793–798.

Kingston, R.E., Chen, C.A. and Okayama, H. 2003. Calcium phosphate transfection. *Curr. Protoc. Cell Biol.*, 19, 20.3.1-20.3.8.

Kishino, T., Lalande, M. and Wagstaff, J. 1997. UBE3A/E6-AP mutations cause Angelman syndrome. *Nat. Genet.*, 15, 70–73.

Kisselev, A.F. and Goldberg, A.L. 2001. Proteasome inhibitors: from research tools to drug candidates. *Chem. Biol.*, 8, 739–758.

Knoll, J.H., Nicholls, R.D., Magenis, R.E., Graham, J.M., Lalande, M. and Latt, S.A. 1989. Angelman and Prader-Willi syndromes share a common chromosome 15 deletion but differ in parental origin of the deletion. *Am. J. Med. Genet.*, 32, 285–290.

Koh, T.-W., Korolchuk, V.I., Wairkar, Y.P., Jiao, W., Evergren, E., Pan, H., Zhou, Y., Venken, K.J.T., Shupliakov, O., Robinson, I.M., *et al*. 2007. Eps15 and Dap160 control synaptic vesicle membrane retrieval and synapse development. *J. Cell Biol.*, 178, 309–322.

Komander, D. and Rape, M. 2012. The ubiquitin code. *Annu. Rev. Biochem.*, 81, 203–229.

Komander, D., Clague, M.J. and Urbé, S. 2009a. Breaking the chains: structure and function of the deubiquitinases. *Nat. Rev. Mol. Cell Biol.*, 10, 550–563.

Komander, D., Reyes-Turcu, F., Licchesi, J.D.F., Odenwaelder, P., Wilkinson, K.D. and Barford, D. 2009b. Molecular discrimination of structurally equivalent Lys 63-linked and linear polyubiquitin chains. *EMBO Rep.*, 10, 466–473.

Kühne, C. and Banks, L. 1998. E3-ubiquitin ligase/E6-AP links multicopy maintenance protein 7 to the ubiquitination pathway by a novel motif, the L2G box. *J. Biol. Chem.*, 273, 34302–34309.

Kühnle, S., Mothes, B., Matentzoglu, K. and Scheffner, M. 2013. Role of the ubiquitin ligase E6AP/UBE3A in controlling levels of the synaptic protein Arc. *Proc. Natl. Acad. Sci. U. S. A.*, 110, 8888–8893.

Kumar, S., Talis, A.L. and Howley, P.M. 1999. Identification of HHR23A as a substrate for E6-associated protein-mediated ubiquitination. *J. Biol. Chem.*, 274, 18785–18792.

Kwon, K. and Beckett, D. 2000. Function of a conserved sequence motif in biotin holoenzyme synthetases. *Protein Sci.*, 9, 1530–1539.

Lander, G.C., Estrin, E., Matyskiela, M.E., Bashore, C., Nogales, E. and Martin, A. 2012. Complete subunit architecture of the proteasome regulatory particle. *Nature*, 482, 186–191.

LaSalle, J.M., Reiter, L.T. and Chamberlain, S.J. 2015. Epigenetic regulation of UBE3A and roles in human neurodevelopmental disorders. *Epigenomics*, 7, 1213–1228.

Lebovitz, R.M., Takeyasu, K. and Fambrough, D.M. 1989. Molecular characterization and expression of the (Na+ + K+)-ATPase alpha-subunit in *Drosophila melanogaster*. *EMBO J.*, 8, 193–202.

Lectez, B., Migotti, R., Lee, S.Y., Ramirez, J., Beraza, N., Mansfield, B., Sutherland, J.D., Martinez-Chantar, M.L., Dittmar, G. and Mayor, U. 2014. Ubiquitin profiling in liver using a transgenic mouse with biotinylated ubiquitin. *J. Proteome Res.*, 13, 3016–3026.

Lee, T. and Luo, L. 1999. Mosaic analysis with a repressible cell marker for studies of gene function in neuronal morphogenesis. *Neuron*, 22, 451–461.

Lee, S.Y., Ramirez, J., Franco, M., Lectez, B., Gonzalez, M., Barrio, R. and Mayor, U. 2014. Ube3a, the E3 ubiquitin ligase causing Angelman syndrome and linked to autism, regulates protein homeostasis through the proteasomal shuttle Rpn10. *Cell. Mol. Life Sci.*, 71, 2747–2758.

Leidecker, O., Matic, I., Mahata, B., Pion, E. and Xirodimas, D.P. 2012. The ubiquitin E1 enzyme Ube1 mediates NEDD8 activation under diverse stress conditions. *Cell Cycle*, 11, 1142–1150.

Lemaitre, B., Nicolas, E., Michaut, L., Reichhart, J.M. and Hoffmann, J.A. 1996. The dorsoventral regulatory gene cassette spätzle/Toll/cactus controls the potent antifungal response in *Drosophila* adults. *Cell*, 86, 973–983.

Lennox, G., Lowe, J., Morrell, K., Landon, M. and Mayer, R.J. 1988. Ubiquitin is a component of neurofibrillary tangles in a variety of neurodegenerative diseases. *Neurosci. Lett.*, 94, 211–217.

Leroy, E., Boyer, R., Auburger, G., Leube, B., Ulm, G., Mezey, E., Harta, G., Brownstein, M.J., Jonnalagada, S., Chernova, T., *et al*. 1998. The ubiquitin pathway in Parkinson's disease. *Nature*, 395, 451–452.

Levin, I., Eakin, C., Blanc, M.-P., Klevit, R.E., Miller, S.I. and Brzovic, P.S. 2010. Identification of an unconventional E3 binding surface on the UbcH5 ~ Ub conjugate recognized by a pathogenic bacterial E3 ligase. *Proc. Natl. Acad. Sci. U. S. A.*, 107, 2848–2853.

Lewis, E.B. 1978. A gene complex controlling segmentation in *Drosophila*. *Nature*, 276, 565–570.

Li, W., Bengtson, M.H., Ulbrich, A., Matsuda, A., Reddy, V.A., Orth, A., Chanda, S.K., Batalov, S. and Joazeiro, C.A.P. 2008. Genome-wide and functional annotation of human E3 ubiquitin ligases identifies MULAN, a mitochondrial E3 that regulates the organelle's dynamics and signaling. *PloS One*, 3, e1487.

Li, W.-Z., Li, S.-L., Zheng, H.Y., Zhang, S.-P. and Xue, L. 2012. A broad expression profile of the GMR-GAL4 driver in *Drosophila melanogaster*. *Genet. Mol. Res.*, 11, 1997–2002.

Liebl, E.C., Forsthoefel, D.J., Franco, L.S., Sample, S.H., Hess, J.E., Cowger, J.A., Chandler, M.P., Shupert, A.M. and Seeger, M.A. 2000. Dosage-sensitive, reciprocal genetic interactions between the Abl tyrosine kinase and the putative GEF trio reveal trio's role in axon pathfinding. *Neuron*, 26, 107–118.

Lin, A., Hou, Q., Jarzylo, L., Amato, S., Gilbert, J., Shang, F. and Man, H.Y. 2011. Nedd4-mediated AMPA receptor ubiquitination regulates receptor turnover and trafficking. *J. Neurochem.*, 119, 27–39.

Lipinszki, Z., Kiss, P., Pál, M., Deák, P., Szabó, A., Hunyadi-Gulyas, E., Klement, E., Medzihradszky, K.F. and Udvardy, A. 2009. Developmental-stage-specific regulation of the polyubiquitin receptors in *Drosophila melanogaster*. *J. Cell Sci.*, 122, 3083–3092.

Lippai, M. and Low, P. 2014. The Role of the Selective Adaptor p62 and Ubiquitin-Like Proteins in Autophagy. *BioMed Res. Int.*, 2014, e832704.

Liu, C.-W. and Jacobson, A.D. 2013. Functions of the 19S complex in proteasomal degradation. *Trends Biochem. Sci.*, 38, 103–110.

Lloyd, T.E., Verstreken, P., Ostrin, E.J., Phillippi, A., Lichtarge, O. and Bellen, H.J. 2000. A genome-wide search for synaptic vesicle cycle proteins in *Drosophila*. *Neuron*, 26, 45–50.

Lopitz-Otsoa, F., Rodriguez-Suarez, E., Aillet, F., Casado-Vela, J., Lang, V., Matthiesen, R., Elortza, F. and Rodriguez, M.S. 2012. Integrative analysis of the ubiquitin proteome isolated using Tandem Ubiquitin Binding Entities (TUBEs). *J. Proteomics*, 75, 2998–3014.

Löwe, J., Stock, D., Jap, B., Zwickl, P., Baumeister, W. and Huber, R. 1995. Crystal structure of the 20S proteasome from the archaeon *T. acidophilum* at 3.4 A resolution. *Science*, 268, 533–539.

Lu, Y., Wang, F., Li, Y., Ferris, J., Lee, J.A. and Gao, F.B. 2009. The *Drosophila* homologue of the Angelman syndrome ubiquitin ligase regulates the formation of terminal dendritic branches. *Hum. Mol. Genet.*, 18, 454–462.

Luber, C.A., Cox, J., Lauterbach, H., Fancke, B., Selbach, M., Tschopp, J., Akira, S., Wiegand, M., Hochrein, H., O'Keeffe, M., *et al*. 2010. Quantitative proteomics reveals subset-specific viral recognition in dendritic cells. *Immunity*, 32, 279–289.

Luo, L., Liao, Y.J., Jan, L.Y. and Jan, Y.N. 1994. Distinct morphogenetic functions of similar small GTPases: *Drosophila* Drac1 is involved in axonal outgrowth and myoblast fusion. *Genes Dev.*, 8, 1787–1802.

Mabb, A.M., Je, H.S., Wall, M.J., Robinson, C.G., Larsen, R.S., Qiang, Y., Corrêa, S.A.L. and Ehlers, M.D. 2014. Triad3A regulates synaptic strength by ubiquitination of arc. *Neuron*, 82, 1299–1316.

Magenis, R.E., Brown, M.G., Lacy, D.A., Budden, S. and LaFranchi, S. 1987. Is Angelman syndrome an alternate result of del(15)(q11q13)? *Am. J. Med. Genet.*, 28, 829–838.

Magenis, R.E., Toth-Fejel, S., Allen, L.J., Black, M., Brown, M.G., Budden, S., Cohen, R., Friedman, J.M., Kalousek, D. and Zonana, J. 1990. Comparison of the 15q deletions in Prader-Willi and Angelman syndromes: specific regions, extent of deletions, parental origin, and clinical consequences. *Am. J. Med. Genet.*, 35, 333–349.

Mahr, A. and Aberle, H. 2006. The expression pattern of the *Drosophila* vesicular glutamate transporter: a marker protein for motoneurons and glutamatergic centers in the brain. *Gene Expr. Patterns*, 6, 299–309.

Maiti, T.K., Permaul, M., Boudreaux, D.A., Mahanic, C., Mauney, S. and Das, C. 2011. Crystal structure of the catalytic domain of UCHL5, a proteasome-associated human deubiquitinating enzyme, reveals an unproductive form of the enzyme. *FEBS J.*, 278, 4917–4926.

Manchado, E., Eguren, M. and Malumbres, M. 2010. The anaphase-promoting complex/cyclosome (APC/C): cell-cycle-dependent and -independent functions. *Biochem. Soc. Trans.*, 38, 65–71.

Mani, A., Oh, A.S., Bowden, E.T., Lahusen, T., Lorick, K.L., Weissman, A.M., Schlegel, R., Wellstein, A. and Riegel, A.T. 2006. E6AP mediates regulated proteasomal degradation of the nuclear receptor coactivator amplified in breast cancer 1 in immortalized cells. *Cancer Res.*, 66, 8680–8686.

Margolis, S.S., Salogiannis, J., Lipton, D.M., Mandel-Brehm, C., Wills, Z.P., Mardinly, A.R., Hu, L., Greer, P.L., Bikoff, J.B., Ho, H.Y.H., *et al*. 2010. EphB-mediated degradation of the RhoA GEF Ephexin5 relieves a developmental brake on excitatory synapse formation. *Cell*, 143, 442–455.

Margolis, S.S., Sell, G.L., Zbinden, M.A. and Bird, L.M. 2015. Angelman Syndrome. *Neurotherapeutics*, 12, 641–650.

Markow, T.A., Beall, S. and Matzkin, L.M. 2009. Egg size, embryonic development time and ovoviviparity in *Drosophila* species. *J. Evol. Biol.*, 22, 430–434.

Marmorstein, R., Carey, M., Ptashne, M. and Harrison, S.C. 1992. DNA recognition by GAL4: structure of a protein-DNA complex. *Nature*, 356, 408–414.

Martinez, A., Ramirez, J., Popp, O., Sutherland, J.D., Urbé, S., Dittmar, G., Clague, M.J. and Mayor, U. 2016. Quantitative proteomic analysis of Parkin substrates in *Drosophila* neurons. *Under review*.

Martínez-Noël, G., Galligan, J.T., Sowa, M.E., Arndt, V., Overton, T.M., Harper, J.W. and Howley, P.M. 2012. Identification and proteomic analysis of distinct UBE3A/E6AP protein complexes. *Mol. Cell. Biol.*, 32, 3095–3106.

Marttila, A.T., Laitinen, O.H., Airenne, K.J., Kulik, T., Bayer, E.A., Wilchek, M. and Kulomaa, M.S. 2000. Recombinant NeutraLite Avidin: a non-glycosylated, acidic mutant of chicken avidin that exhibits high affinity for biotin and low non-specific binding properties. *FEBS Lett.*, 467, 31–36.

Matsumoto, M., Hatakeyama, S., Oyamada, K., Oda, Y., Nishimura, T. and Nakayama, K.I. 2005. Large-scale analysis of the human ubiquitin-related proteome. *Proteomics*, 5, 4145–4151.

Matsuura, T., Sutcliffe, J.S., Fang, P., Galjaard, R.J., Jiang, Y., Benton, C.S., Rommens, J.M. and Beaudet, A.L. 1997. *De novo* truncating mutations in E6-AP ubiquitin-protein ligase gene (UBE3A) in Angelman syndrome. *Nat. Genet.*, 15, 74–77.

Matthews, K.A., Kaufman, T.C. and Gelbart, W.M. 2005. Research resources for *Drosophila*: the expanding universe. *Nat. Rev. Genet.*, 6, 179–193.

Matthews, W., Driscoll, J., Tanaka, K., Ichihara, A. and Goldberg, A.L. 1989. Involvement of the proteasome in various degradative processes in mammalian cells. *Proc. Natl. Acad. Sci. U. S. A.*, 86, 2597–2601.

Mayor, U. and Peng, J. 2012. Deciphering tissue-specific ubiquitylation by mass spectrometry. *Methods Mol. Biol.*, 832, 65–80.

Mayor, T., Graumann, J., Bryan, J., MacCoss, M.J. and Deshaies, R.J. 2007. Quantitative profiling of ubiquitylated proteins reveals proteasome substrates and the substrate repertoire influenced by the Rpn10 receptor pathway. *Mol. Cell. Proteomics*, 6, 1885–1895.

McGrath, J.P., Jentsch, S. and Varshavsky, A. 1991. UBA1: an essential yeast gene encoding ubiquitin-activating enzyme. *EMBO J.*, 10, 227–236.

McGuire, S.E., Le, P.T., Osborn, A.J., Matsumoto, K. and Davis, R.L. 2003. Spatiotemporal rescue of memory dysfunction in *Drosophila*. *Science*, 302, 1765–1768.

McNeill, H., Knebel, A., Arthur, J.S.C., Cuenda, A. and Cohen, P. 2004. A novel UBA and UBX domain protein that binds polyubiquitin and VCP and is a substrate for SAPKs. *Biochem. J.*, 384, 391–400.

Metzger, M.B., Pruneda, J.N., Klevit, R.E. and Weissman, A.M. 2014. RING-type E3 ligases: master manipulators of E2 ubiquitin-conjugating enzymes and ubiquitination. *Biochim. Biophys. Acta*, 1843, 47–60.

Meyer, H., Bug, M. and Bremer, S. 2012. Emerging functions of the VCP/p97 AAA-ATPase in the ubiquitin system. *Nat. Cell Biol.*, 14, 117–123.

Miao, S., Chen, R., Ye, J., Tan, G.H., Li, S., Zhang, J., Jiang, Y., and Xiong, Z.Q. 2013. The Angelman syndrome protein Ube3a is required for polarized dendrite morphogenesis in pyramidal neurons. *J. Neurosci.*, 33, 327–333.

Micallef, L. and Rodgers, P. 2014. eulerAPE: drawing area-proportional 3-Venn diagrams using ellipses. *PloS One*, 9, e101717.

Michelle, C., Vourc'h, P., Mignon, L. and Andres, C.R. 2009. What was the set of ubiquitin and ubiquitin-like conjugating enzymes in the eukaryote common ancestor? *J. Mol. Evol.*, 68, 616–628.

Min, M., Mayor, U. and Lindon, C. (2013). Ubiquitination site preferences in anaphase promoting complex/cyclosome (APC/C) substrates. *Open Biol.*, 3, 130097.

Min, M., Mayor, U., Dittmar, G. and Lindon, C. 2014. Using *in vivo* biotinylated ubiquitin to describe a mitotic exit ubiquitome from human cells. *Mol. Cell. Proteomics*, 13, 2411–2425.

Mishra, A., Godavarthi, S.K. and Jana, N.R. 2009a. UBE3A/E6-AP regulates cell proliferation by promoting proteasomal degradation of p27. *Neurobiol. Dis.*, 36, 26–34.

Mishra, A., Godavarthi, S.K., Maheshwari, M., Goswami, A. and Jana, N.R. 2009b. The ubiquitin ligase E6-AP is induced and recruited to aggresomes in response to proteasome inhibition and may be involved in the ubiquitination of Hsp70-bound misfolded proteins. *J. Biol. Chem.*, 284, 10537–10545.

Morawe, T., Honemann-Capito, M., von Stein, W. and Wodarz, A. 2011. Loss of the extraproteasomal ubiquitin receptor Rings lost impairs ring canal growth in *Drosophila* oogenesis. *J. Cell Biol.*, 193, 71–80.

Morgan, T.H. 1910. Sex limited inheritance in *Drosophila*. *Science*, 32, 120–122.

Morgenstern, J.P. and Land, H. 1990. Advanced mammalian gene transfer: high titre retroviral vectors with multiple drug selection markers and a complementary helper-free packaging cell line. *Nucleic Acids Res.*, 18, 3587–3596.

Mori, H., Kondo, J. and Ihara, Y. 1987. Ubiquitin is a component of paired helical filaments in Alzheimer's disease. *Science*, 235, 1641–1644.

Morreale, F.E. and Walden, H. 2016. Types of ubiquitin ligases. *Cell*, 165, 248–248.e1.

Mueller, R.D., Yasuda, H., Hatch, C.L., Bonner, W.M. and Bradbury, E.M. 1985. Identification of ubiquitinated histones 2A and 2B in *Physarum polycephalum*. Disappearance of these proteins at metaphase and reappearance at anaphase. *J. Biol. Chem.*, 260, 5147–5153.

Muller, H.J. 1927. Artificial transmutation of the gene. *Science*, 66, 84–87.

Na, C.H., Jones, D.R., Yang, Y., Wang, X., Xu, Y. and Peng, J. 2012. Synaptic protein ubiquitination in rat brain revealed by antibody-based ubiquitome analysis. *J. Proteome Res.*, 11, 4722–4732.

Nawaz, Z., Lonard, D.M., Smith, C.L., Lev-Lehman, E., Tsai, S.Y., Tsai, M.J. and O'Malley, B.W. 1999. The Angelman syndrome-associated protein, E6-AP, is a coactivator for the nuclear hormone receptor superfamily. *Mol. Cell. Biol.*, 19, 1182–1189.

Newton, K., Matsumoto, M.L., Wertz, I.E., Kirkpatrick, D.S., Lill, J.R., Tan, J., Dugger, D., Gordon, N., Sidhu, S.S., Fellouse, F.A., *et al*. 2008. Ubiquitin chain editing revealed by polyubiquitin linkage-specific antibodies. *Cell*, 134, 668–678.

Nezis, I.P., Simonsen, A., Sagona, A.P., Finley, K., Gaumer, S., Contamine, D., Rusten, T.E., Stenmark, H. and Brech, A. 2008. Ref(2)P, the *Drosophila melanogaster* homologue of mammalian p62, is required for the formation of protein aggregates in adult brain. *J. Cell Biol.*, 180, 1065–1071.

Nicholls, R.D., Pai, G.S., Gottlieb, W. and Cantú, E.S. 1992. Paternal uniparental disomy of chromosome 15 in a child with Angelman syndrome. *Ann. Neurol.*, 32, 512–518.

Nijman, S.M.B., Luna-Vargas, M.P.A., Velds, A., Brummelkamp, T.R., Dirac, A.M.G., Sixma, T.K. and Bernards, R. 2005. A genomic and functional inventory of deubiquitinating enzymes. *Cell*, 123, 773–786.

Noor, A., Dupuis, L., Mittal, K., Lionel, A.C., Marshall, C.R., Scherer, S.W., Stockley, T., Vincent, J.B., Mendoza-Londono, R. and Stavropoulos, D.J. 2015. 15q11.2 Duplication encompassing only the UBE3A gene is associated with developmental delay and neuropsychiatric phenotypes. *Hum. Mutat.*, 36, 689–693.

Nuber, U., Schwarz, S.E. and Scheffner, M. 1998. The ubiquitin-protein ligase E6-associated protein (E6-AP) serves as its own substrate. *Eur. J. Biochem.*, 254, 643–649.

Nüsslein-Volhard, C. and Wieschaus, E. 1980. Mutations affecting segment number and polarity in *Drosophila*. *Nature*, 287, 795–801.

Oda, H., Kumar, S. and Howley, P.M. 1999. Regulation of the Src family tyrosine kinase Blk through E6AP-mediated ubiquitination. *Proc. Natl. Acad. Sci. U. S. A.*, 96, 9557–9562.

O'Kane, C.J. and Gehring, W.J. 1987. Detection *in situ* of genomic regulatory elements in *Drosophila*. *Proc. Natl. Acad. Sci. U. S. A.*, 84, 9123–9127.

Olsen, J.V., Ong, S.E. and Mann, M. 2004. Trypsin cleaves exclusively C-terminal to arginine and lysine residues. *Mol. Cell. Proteomics*, 3, 608–614.

Ossig, R., Schmitt, H.D., de Groot, B., Riedel, D., Keränen, S., Ronne, H., Grubmüller, H. and Jahn, R. 2000. Exocytosis requires asymmetry in the central layer of the SNARE complex. *EMBO J.*, 19, 6000–6010.

Pandey, U.B. and Nichols, C.D. 2011. Human disease models in *Drosophila melanogaster* and the role of the fly in therapeutic drug discovery. *Pharmacol. Rev.*, 63, 411–436.

Pandey, U.B., Nie, Z., Batlevi, Y., McCray, B.A., Ritson, G.P., Nedelsky, N.B., Schwartz, S.L., DiProspero, N.A., Knight, M.A., Schuldiner, O., *et al*. 2007. HDAC6 rescues neurodegeneration and provides an essential link between autophagy and the UPS. *Nature*, 447, 859–863.

Pang, Z.P. and Südhof, T.C. 2010. Cell biology of Ca2+-triggered exocytosis. *Curr. Opin. Cell Biol.*, 22, 496–505.

Pelzer, C., Kassner, I., Matentzoglu, K., Singh, R.K., Wollscheid, H.-P., Scheffner, M., Schmidtke, G. and Groettrup, M. 2007. UBE1L2, a novel E1 enzyme specific for ubiquitin. *J. Biol. Chem.*, 282, 23010–23014.

Peng, J., Schwartz, D., Elias, J.E., Thoreen, C.C., Cheng, D., Marsischky, G., Roelofs, J., Finley, D. and Gygi, S.P. 2003. A proteomics approach to understanding protein ubiquitination. *Nat. Biotechnol.*, 21, 921–926.

Peters, J.M., Franke, W.W. and Kleinschmidt, J.A. 1994. Distinct 19 S and 20 S subcomplexes of the 26 S proteasome and their distribution in the nucleus and the cytoplasm. *J. Biol. Chem.*, 269, 7709–7718.

Pham, A.D. and Sauer, F. 2000. Ubiquitin-activating/conjugating activity of TAFII250, a mediator of activation of gene expression in *Drosophila*. *Science*, 289, 2357–2360.

Piehowski, P.D., Petyuk, V.A., Orton, D.J., Xie, F., Ramirez-Restrepo, M., Engel, A., Lieberman, A.P., Albin, R.L., Camp, D.G., Smith, R.D., *et al*. 2013. Sources of technical variability in quantitative LC-MS proteomics: human brain tissue sample analysis. *J. Proteome Res.*, 12, 2128–2137.

Pircs, K., Nagy, P., Varga, A., Venkei, Z., Erdi, B., Hegedus, K. and Juhasz, G. 2012. Advantages and limitations of different p62-based assays for estimating autophagic activity in *Drosophila*. *PloS One*, 7, e44214.

Popovic, D., Vucic, D. and Dikic, I. 2014. Ubiquitination in disease pathogenesis and treatment. *Nat. Med.*, 20, 1242–1253.

Puram, S.V., Kim, A.H., Park, H.-Y., Anckar, J. and Bonni, A. 2013. The ubiquitin receptor S5a/Rpn10 links centrosomal proteasomes with dendrite development in the mammalian brain. *Cell Rep.*, 4, 19–30.

Raasi, S., Varadan, R., Fushman, D. and Pickart, C.M. 2005. Diverse polyubiquitin interaction properties of ubiquitin-associated domains. *Nat. Struct. Mol. Biol.*, 12, 708–714.

Ramirez, J., Martinez, A., Lectez, B., Lee, S.Y., Franco, M., Barrio, R., Dittmar, G. and Mayor, U. 2015. Proteomic analysis of the ubiquitin landscape in the *Drosophila* embryonic nervous system and the adult photoreceptor cells. *PLoS One*, 10, e0139083.

Ramser, J., Ahearn, M.E., Lenski, C., Yariz, K.O., Hellebrand, H., von Rhein, M., Clark, R.D., Schmutzler, R.K., Lichtner, P., Hoffman, E.P., *et al*. 2008. Rare missense and synonymous variants in UBE1 are associated with X-linked infantile spinal muscular atrophy. *Am. J. Hum. Genet.*, 82, 188–193.

Reimand, J., Arak, T. and Vilo, J. 2011. g:Profiler—a web server for functional interpretation of gene lists (2011 update). *Nucleic Acids Res.*, 39, W307–W315.

Reiter, L.T., Potocki, L., Chien, S., Gribskov, M. and Bier, E. 2001. A systematic analysis of human disease-associated gene sequences in *Drosophila melanogaster*. *Genome Res.*, 11, 1114–1125.

Reiter, L.T., Seagroves, T.N., Bowers, M. and Bier, E. 2006. Expression of the Rho-GEF Pbl/ECT2 is regulated by the UBE3A E3 ubiquitin ligase. *Hum. Mol. Genet.*, 15, 2825–2835.

Rinetti, G.V. and Schweizer, F.E. 2010. Ubiquitination acutely regulates presynaptic neurotransmitter release in mammalian neurons. *J. Neurosci.*, 30, 3157–3166.

Roberts, D.B. (2006). *Drosophila melanogaster*: the model organism. *Entomol. Exp. Appl.*, 121, 93–103.

Rosenzweig, R., Bronner, V., Zhang, D., Fushman, D. and Glickman, M.H. 2012. Rpn1 and Rpn2 coordinate ubiquitin processing factors at the proteasome. *J. Biol. Chem.*, 287, 14659–14671.

Rougeulle, C., Glatt, H. and Lalande, M. 1997. The Angelman syndrome candidate gene, UBE3A/E6-AP, is imprinted in brain. *Nat. Genet.*, 17, 14–15.

Sadikovic, B., Fernandes, P., Zhang, V.W., Ward, P.A., Miloslavskaya, I., Rhead, W., Rosenbaum, R., Gin, R., Roa, B. and Fang, P. 2014. Mutation update for UBE3A variants in Angelman syndrome. *Hum. Mutat.*, 35, 1407–1417.

Sahoo, T., Bacino, C.A., German, J.R., Shaw, C.A., Bird, L.M., Kimonis, V., Anselm, I., Waisbren, S., Beaudet, A.L. and Peters, S.U. 2007. Identification of novel deletions of 15q11q13 in Angelman syndrome by array-CGH: molecular characterization and genotype-phenotype correlations. *Eur. J. Hum. Genet.*, 15, 943–949.

Saitoh, Y., Fujikake, N., Okamoto, Y., Popiel, H.A., Hatanaka, Y., Ueyama, M., Suzuki, M., Gaumer, S., Murata, M., Wada, K., *et al*. 2015. p62 plays a protective role in the autophagic degradation of polyglutamine protein oligomers in polyglutamine disease model flies. *J. Biol. Chem.*, 290, 1442–1453.

Sang, T.K. and Jackson, G.R. 2005. *Drosophila* Models of Neurodegenerative Disease. *NeuroRx*, 2, 438–446.

Sarraf, S.A., Raman, M., Guarani-Pereira, V., Sowa, M.E., Huttlin, E.L., Gygi, S.P. and Harper, J.W. 2013. Landscape of the PARKIN-dependent ubiquitylome in response to mitochondrial depolarization. *Nature*, 496, 372–376.

Scanlon, T.C., Gottlieb, B., Durcan, T.M., Fon, E.A., Beitel, L.K. and Trifiro, M.A. 2009. Isolation of human proteasomes and putative proteasome-interacting proteins using a novel affinity chromatography method. *Exp. Cell Res.*, 315, 176–189.

Scheffner, M. and Kumar, S. 2014. Mammalian HECT ubiquitin-protein ligases: biological and pathophysiological aspects. *Biochim. Biophys. Acta*, 1843, 61–74.

Scheffner, M., Huibregtse, J.M., Vierstra, R.D. and Howley, P.M. 1993. The HPV-16 E6 and E6-AP complex functions as a ubiquitin-protein ligase in the ubiquitination of p53. *Cell*, 75, 495–505.

Scheffner, M., Nuber, U. and Huibregtse, J.M. 1995. Protein ubiquitination involving an E1–E2–E3 enzyme ubiquitin thioester cascade. *Nature*, 373, 81–83.

Schneider, C.A., Rasband, W.S. and Eliceiri, K.W. 2012. NIH Image to ImageJ: 25 years of image analysis. *Nat. Methods*, 9, 671–675.

Schoenheimer, R., Ratner, S. and Rittenberg, D. 1939. Studies in protein metabolism X. The metabolic activity of body proteins investigated with l (-)-leucine containing two isotopes. *J. Biol. Chem.*, 130, 703–732.

Schulman, B.A. and Wade Harper, J. 2009. Ubiquitin-like protein activation by E1 enzymes: the apex for downstream signalling pathways. *Nat. Rev. Mol. Cell Biol.*, 10, 319–331.

Schwarz, E.M. and Benzer, S. 1997. Calx, a Na-Ca exchanger gene of *Drosophila melanogaster*. *Proc. Natl. Acad. Sci. U. S. A.*, 94, 10249–10254.

Sell, G.L. and Margolis, S.S. 2015. From UBE3A to Angelman syndrome: a substrate perspective. *Front. Neurosci.*, 9, 322.

Shevchenko, A., Tomas, H., Havlis, J., Olsen, J.V. and Mann, M. 2006. In-gel digestion for mass spectrometric characterization of proteins and proteomes. *Nat. Protoc.*, 1, 2856–2860.

Shimoji, T., Murakami, K., Sugiyama, Y., Matsuda, M., Inubushi, S., Nasu, J., Shirakura, M., Suzuki, T., Wakita, T., Kishino, T., *et al*. 2009. Identification of annexin A1 as a novel substrate for E6AP-mediated ubiquitylation. *J. Cell. Biochem.*, 106, 1123–1135.

Shimura, H., Hattori, N., Kubo, S. i, Mizuno, Y., Asakawa, S., Minoshima, S., Shimizu, N., Iwai, K., Chiba, T., Tanaka, K., *et al*. 2000. Familial Parkinson disease gene product, parkin, is a ubiquitin-protein ligase. *Nat. Genet.*, 25, 302–305.

Shin, J.E. and DiAntonio, A. 2011. Highwire regulates guidance of sister axons in the *Drosophila* mushroom body. *J. Neurosci.*, 31, 17689–17700.

Sims, J.J. and Cohen, R.E. 2009. Linkage-specific avidity defines the lysine 63-linked polyubiquitin-binding preference of rap80. *Mol. Cell*, 33, 775–783.

Smith, S.E.P., Zhou, Y.-D., Zhang, G., Jin, Z., Stoppel, D.C. and Anderson, M.P. 2011. Increased gene dosage of Ube3a results in autism traits and decreased glutamate synaptic transmission in mice. *Sci. Transl. Med.*, *3*, 103ra97.

Song, S. and Jung, Y.K. 2004. Alzheimer's disease meets the ubiquitin-proteasome system. *Trends Mol. Med.*, 10, 565–570.

Speese, S.D., Trotta, N., Rodesch, C.K., Aravamudan, B. and Broadie, K. 2003. The ubiquitin proteasome system acutely regulates presynaptic protein turnover and synaptic efficacy. *Curr. Biol.*, 13, 899–910.

Speicher, S., García-Alonso, L., Carmena, A., Martín-Bermudo, M.D., de la Escalera, S. and Jiménez, F. 1998. Neurotactin functions in concert with other identified CAMs in growth cone guidance in *Drosophila*. *Neuron*, 20, 221–233.

St Johnston, D. 2002. The art and design of genetic screens: *Drosophila melanogaster*. *Nat. Rev. Genet.*, 3, 176–188.

Steen, H. and Mann, M. 2004. The abc's (and xyz's) of peptide sequencing. *Nat. Rev. Mol. Cell Biol.*, 5, 699–711.

Stegmeier, F., Rape, M., Draviam, V.M., Nalepa, G., Sowa, M.E., Ang, X.L., McDonald Iii, E.R., Li, M.Z., Hannon, G.J., Sorger, P.K., *et al*. 2007. Anaphase initiation is regulated by antagonistic ubiquitination and deubiquitination activities. *Nature*, 446, 876–881.

Sun, B. and Salvaterra, P.M. 1995. Two *Drosophila* nervous system antigens, Nervana 1 and 2, are homologous to the beta subunit of Na+,K(+)-ATPase. *Proc. Natl. Acad. Sci. U. S. A.*, 92, 5396–5400.

Swatek, K.N. and Komander, D. 2016. Ubiquitin modifications. *Cell Res.*, 26, 399–422.

Tai, H.C., Besche, H., Goldberg, A.L. and Schuman, E.M. 2010. Characterization of the brain 26S proteasome and its interacting proteins. *Front. Mol. Neurosci.*, 3.

Talamillo, A., Herboso, L., Pirone, L., Pérez, C., González, M., Sánchez, J., Mayor, U., Lopitz-Otsoa, F., Rodriguez, M.S., Sutherland, J.D., *et al*. 2013. Scavenger receptors mediate the role of SUMO and Ftz-f1 in *Drosophila* steroidogenesis. *PLoS Genet.*, 9, e1003473.

Terrell, J., Shih, S., Dunn, R. and Hicke, L. 1998. A function for monoubiquitination in the internalization of a G protein-coupled receptor. *Mol. Cell*, 1, 193–202.

Thao, D.T.P., An, P.N.T., Yamaguchi, M. and LinhThuoc, T. 2012. Overexpression of ubiquitin carboxyl terminal hydrolase impairs multiple pathways during eye development in *Drosophila melanogaster*. *Cell Tissue Res.*, 348, 453–463.

Thomas, M. and Banks, L. 1998. Inhibition of Bak-induced apoptosis by HPV-18 E6. *Oncogene*, 17, 2943–2954.

Thrower, J.S., Hoffman, L., Rechsteiner, M. and Pickart, C.M. 2000. Recognition of the polyubiquitin proteolytic signal. *EMBO J.*, 19, 94–102.

Tirard, M., Hsiao, H.-H., Nikolov, M., Urlaub, H., Melchior, F. and Brose, N. 2012. *In vivo* localization and identification of SUMOylated proteins in the brain of His6-HA-SUMO1 knock-in mice. *Proc. Natl. Acad. Sci. U. S. A.*, 109, 21122–21127.

Tomaić, V. and Banks, L. 2015. Angelman syndrome-associated ubiquitin ligase UBE3A/E6AP mutants interfere with the proteolytic activity of the proteasome. *Cell Death Dis.*, 6, e1625.

Tomko, R.J., Funakoshi, M., Schneider, K., Wang, J. and Hochstrasser, M. 2010. Heterohexameric ring arrangement of the eukaryotic proteasomal ATPases: implications for proteasome structure and assembly. *Mol. Cell*, 38, 393–403.

Tong, L. 2013. Structure and function of biotin-dependent carboxylases. *Cell. Mol. Life Sci.*, 70, 863–891.

Traven, A., Jelicic, B. and Sopta, M. 2006. Yeast Gal4: a transcriptional paradigm revisited. *EMBO Rep.*, 7, 496–499.

Trempe, J.-F., Brown, N.R., Lowe, E.D., Gordon, C., Campbell, I.D., Noble, M.E.M. and Endicott, J.A. 2005. Mechanism of Lys48-linked polyubiquitin chain recognition by the Mud1 UBA domain. *EMBO J.*, 24, 3178–3189.

Uchiki, T., Kim, H.T., Zhai, B., Gygi, S.P., Johnston, J.A., O'Bryan, J.P. and Goldberg, A.L. 2009. The ubiquitin-interacting motif protein, S5a, is ubiquitinated by all types of ubiquitin ligases by a mechanism different from typical substrate recognition. *J. Biol. Chem.*, 284, 12622–12632.

Ui, K., Nishihara, S., Sakuma, M., Togashi, S., Ueda, R., Miyata, Y. and Miyake, T. 1994. Newly established cell lines from *Drosophila* larval CNS express neural specific characteristics. *In Vitro Cell. Dev. Biol. Anim.*, 30A, 209–216.

Urraca, N., Cleary, J., Brewer, V., Pivnick, E.K., McVicar, K., Thibert, R.L., Schanen, N.C., Esmer, C., Lamport, D. and Reiter, L.T. 2013. The interstitial duplication 15q11.2-q13 syndrome includes autism, mild facial anomalies and a characteristic EEG signature. *Autism Res.*, 6, 268–279.

Valdez, C., Scroggs, R., Chassen, R. and Reiter, L.T. 2015. Variation in Dube3a expression affects neurotransmission at the *Drosophila* neuromuscular junction. *Biol. Open*, 4, 776–782.

Vasilescu, J., Smith, J.C., Ethier, M. and Figeys, D. 2005. Proteomic analysis of ubiquitinated proteins from human MCF-7 breast cancer cells by immunoaffinity purification and mass spectrometry. *J. Proteome Res.*, 4, 2192–2200.

Verma, R., Aravind, L., Oania, R., McDonald, W.H., Yates, J.R., Koonin, E.V. and Deshaies, R.J. 2002. Role of Rpn11 metalloprotease in deubiquitination and degradation by the 26S proteasome. *Science*, 298, 611–615.

Vourc'h, P., Martin, I., Bonnet-Brilhault, F., Marouillat, S., Barthélémy, C., Pierre Müh, J. and Andres, C. 2003. Mutation screening and association study of the UBE2H gene on chromosome 7q32 in autistic disorder. *Psychiatr. Genet.*, 13, 221–225.

Vu, T.H. and Hoffman, A.R. 1997. Imprinting of the Angelman syndrome gene, UBE3A, is restricted to brain. *Nat. Genet.*, 17, 12–13.

Wagner, S., Heseding, C., Szlachta, K., True, J.R., Prinz, H. and Hovemann, B.T. 2007. *Drosophila* photoreceptors express cysteine peptidase tan. *J. Comp. Neurol.*, 500, 601–611.

Wagner, S.A., Beli, P., Weinert, B.T., Nielsen, M.L., Cox, J., Mann, M. and Choudhary, C. 2011. A proteome-wide, quantitative survey of *in vivo* ubiquitylation sites reveals widespread regulatory roles. *Mol. Cell. Proteomics*, 10, M111.013284.

Wagner, S.A., Beli, P., Weinert, B.T., Schölz, C., Kelstrup, C.D., Young, C., Nielsen, M.L., Olsen, J.V., Brakebusch, C. and Choudhary, C. 2012. Proteomic analyses reveal divergent ubiquitylation site patterns in murine tissues. *Mol. Cell. Proteomics*, 11, 1578–1585.

Wang, M. and Pickart, C.M. 2005. Different HECT domain ubiquitin ligases employ distinct mechanisms of polyubiquitin chain synthesis. *EMBO J.*, 24, 4324–4333.

Wang, X., Herr, R.A. and Hansen, T.H. 2012. Ubiquitination of substrates by esterification. *Traffic Cph. Den.*, 13, 19–24.

Wenzel, D.M., Stoll, K.E. and Klevit, R.E. 2010. E2s: structurally economical and functionally replete. *Biochem. J.*, 433, 31–42.

Wickliffe, K.E., Williamson, A., Meyer, H.J., Kelly, A. and Rape, M. 2011. K11-linked ubiquitin chains as novel regulators of cell division. *Trends Cell Biol.*, 21, 656–663.

van Wijk, S.J. and Timmers, H.T. 2010. The family of ubiquitin-conjugating enzymes (E2s): deciding between life and death of proteins. *FASEB J.*, 24, 981–993.

Wilkinson, K.D., Urban, M.K. and Haas, A.L. 1980. Ubiquitin is the ATP-dependent proteolysis factor I of rabbit reticulocytes. *J. Biol. Chem.*, 255, 7529–7532.

Williams, C.A., Driscoll, D.J. and Dagli, A.I. 2010. Clinical and genetic aspects of Angelman syndrome. *Genet. Med.*, 12, 385–395.

Wilson, C., Pearson, R.K., Bellen, H.J., O'Kane, C.J., Grossniklaus, U. and Gehring, W.J. 1989. P-element-mediated enhancer detection: an efficient method for isolating and characterizing developmentally regulated genes in *Drosophila*. *Genes Dev.*, 3, 1301–1313.

Wilson, R., Urraca, N., Skobowiat, C., Hope, K.A., Miravalle, L., Chamberlin, R., Donaldson, M., Seagroves, T.N. and Reiter, L.T. 2015. Assessment of the tumorigenic potential of spontaneously immortalized and hTERT-immortalized cultured dental pulp stem cells. *Stem Cells Transl. Med.*, 4, 905–912.

Wilson, R.C., Hughes, R.C., Flatt, J.W., Meehan, E.J., Ng, J.D. and Twigg, P.D. 2009. Structure of full-length ubiquitin-conjugating enzyme E2-25K (huntingtin-interacting protein 2). *Acta Crystallograph. Sect. F Struct. Biol. Cryst. Commun.*, 65, 440–444.

Wójcik, C. and DeMartino, G.N. 2003. Intracellular localization of proteasomes. *Int. J. Biochem. Cell Biol.*, 35, 579–589.

Wu, Y., Bolduc, F.V., Bell, K., Tully, T., Fang, Y., Sehgal, A. and Fischer, J.A. 2008. A *Drosophila* model for Angelman syndrome. *Proc. Natl. Acad. Sci. U. S. A.*, 105, 12399–12404.

Xu, G., Paige, J.S. and Jaffrey, S.R. 2010. Global analysis of lysine ubiquitination by ubiquitin remnant immunoaffinity profiling. *Nat. Biotechnol.*, 28, 868–873.

Xu, P., Duong, D.M., Seyfried, N.T., Cheng, D., Xie, Y., Robert, J., Rush, J., Hochstrasser, M., Finley, D. and Peng, J. 2009. Quantitative proteomics reveals the function of unconventional ubiquitin chains in proteasomal degradation. *Cell*, 137, 133–145.

Yamamoto, Y., Huibregtse, J.M. and Howley, P.M. 1997. The human E6-AP gene (UBE3A) encodes three potential protein isoforms generated by differential splicing. *Genomics*, 41, 263–266.

Yao, T. and Cohen, R.E. 2002. A cryptic protease couples deubiquitination and degradation by the proteasome. *Nature*, 419, 403–407.

Yao, I., Takagi, H., Ageta, H., Kahyo, T., Sato, S., Hatanaka, K., Fukuda, Y., Chiba, T., Morone, N., Yuasa, S., et al. 2007. SCRAPPER-dependent ubiquitination of active zone protein RIM1 regulates synaptic vesicle release. *Cell*, 130, 943–957.

Yao, T., Song, L., Xu, W., DeMartino, G.N., Florens, L., Swanson, S.K., Washburn, M.P., Conaway, R.C., Conaway, J.W. and Cohen, R.E. 2006. Proteasome recruitment and activation of the Uch37 deubiquitinating enzyme by Adrm1. *Nat. Cell Biol.*, 8, 994–1002.

Yates, J.R., Ruse, C.I. and Nakorchevsky, A. 2009. Proteomics by mass spectrometry: approaches, advances, and applications. *Annu. Rev. Biomed. Eng.*, 11, 49–79.

Ye, Y. and Rape, M. 2009. Building ubiquitin chains: E2 enzymes at work. *Nat. Rev. Mol. Cell Biol.*, 10, 755–764.

Yi, J.J. and Ehlers, M.D. 2007. Emerging roles for ubiquitin and protein degradation in neuronal function. *Pharmacol. Rev.*, 59, 14–39.

Yi, J.J., Berrios, J., Newbern, J.M., Snider, W.D., Philpot, B.D., Hahn, K.M. and Zylka, M.J. 2015. An autism-linked mutation disables phosphorylation control of UBE3A. *Cell*, 162, 795–807.

Young, P., Deveraux, Q., Beal, R.E., Pickart, C.M. and Rechsteiner, M. 1998. Characterization of two polyubiquitin binding sites in the 26 S protease subunit 5a. *J. Biol. Chem.*, 273, 5461–5467.

Yuan, W.C., Lee, Y.R., Lin, S.Y., Chang, L.Y., Tan, Y.P., Hung, C.C., Kuo, J.C., Liu, C.H., Lin, M.Y., Xu, M., *et al*. 2014. K33-linked polyubiquitination of Coronin 7 by Cul3-KLHL20 ubiquitin E3 ligase regulates protein trafficking. *Mol. Cell*, 54, 586–600.

Zaaroor-Regev, D., de Bie, P., Scheffner, M., Noy, T., Shemer, R., Heled, M., Stein, I., Pikarsky, E. and Ciechanover, A. 2010. Regulation of the polycomb protein Ring1B by self-ubiquitination or by E6-AP may have implications to the pathogenesis of Angelman syndrome. *Proc. Natl. Acad. Sci. U. S. A.*, 107, 6788–6793.

Zhang, D., Raasi, S. and Fushman, D. 2008. Affinity makes the difference: nonselective interaction of the UBA domain of Ubiquilin-1 with monomeric ubiquitin and polyubiquitin chains. *J. Mol. Biol.*, 377, 162–180.

Zhang, Z., Lv, X., Yin, W., Zhang, X., Feng, J., Wu, W., Hui, C., Zhang, L. and Zhao, Y. 2013. Ter94 ATPase complex targets K11-linked ubiquitinated Ci to proteasomes for partial degradation. *Dev. Cell*, 25, 636–644.

Zhao, G.Y., Sonoda, E., Barber, L.J., Oka, H., Murakawa, Y., Yamada, K., Ikura, T., Wang, X., Kobayashi, M., Yamamoto, K., *et al*. 2007. A critical role for the ubiquitin-conjugating enzyme Ubc13 in initiating homologous recombination. *Mol. Cell*, 25, 663–675.

Ziv, I., Matiuhin, Y., Kirkpatrick, D.S., Erpapazoglou, Z., Leon, S., Pantazopoulou, M., Kim, W., Gygi, S.P., Haguenauer-Tsapis, R., Reis, N., *et al*. 2011. A perturbed ubiquitin landscape distinguishes between ubiquitin in trafficking and in proteolysis. *Mol. Cell. Proteomics*, 10, M111.009753.

XII. Appendixes

Mass spectrometry Tables

Mass spectrometric data tables can be found on the enclosed CD.

Table A1. Proteins purified from *Drosophila* adult eye.

Table A2. Proteins purified from *Drosophila* embryonic nervous system.

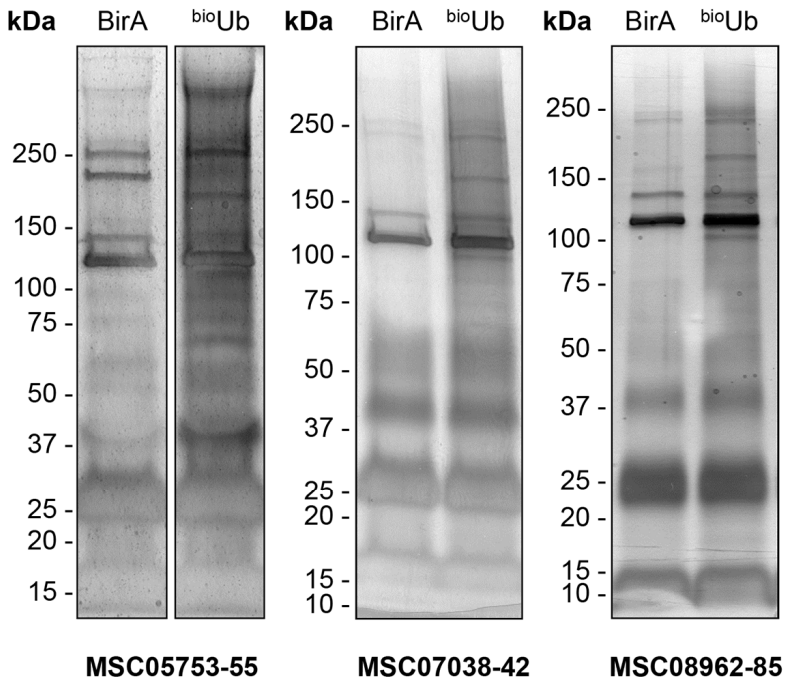

Figure A1. Silver staining of the material purified from adult samples.

Equal amounts of eluted BirA and ^{bio}Ub samples were analysed for each pulldown using SDS-PAGE, and stained with silver. Common bands between BirA and ^{bio}Ub are expected to be composed mainly of endogenously biotinylated material. Thick bands at around 40 kDa and below correspond to trimer, dimer and monomer forms on NeutrAvidin. The main high molecular weight smear observed in the experimental (^{bio}Ub) but not in the control (BirA) samples correspond to the isolated ubiquitinated material. For each pulldown experiment the number assigned by the MS core facility at the MDC Institute is provided. Taken from Ramirez *et al.*, 2015.

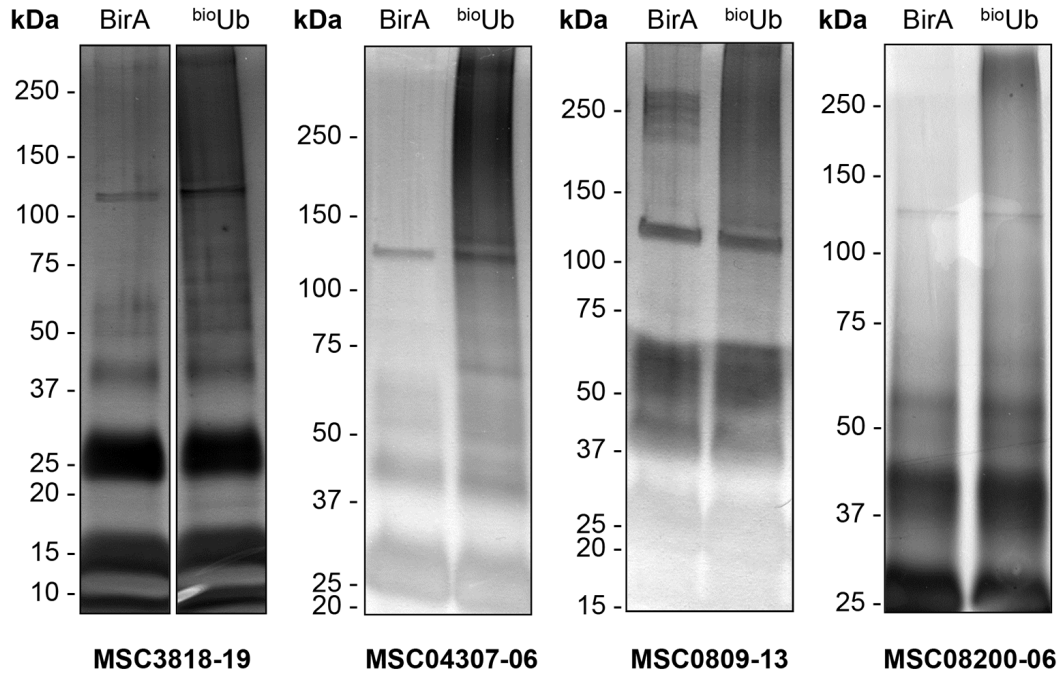

Figure A2. Silver staining of the material purified from embryo samples.

Equal amounts of eluted BirA and ^{bio}Ub samples were analysed for each pulldown using SDS-PAGE, and stained with silver. Common bands between BirA and ^{bio}Ub are expected to be composed mainly of endogenously biotinylated material. Thick bands at around 40 kDa and below correspond to trimer, dimer and monomer forms on NeutrAvidin. The main high molecular weight smear observed in the experimental (^{bio}Ub) but not in the control (BirA) samples correspond to the isolated ubiquitinated material. For each pulldown experiment the number assigned by the MS core facility at the MDC Institute is provided. Taken from Ramirez *et al.*, 2015.

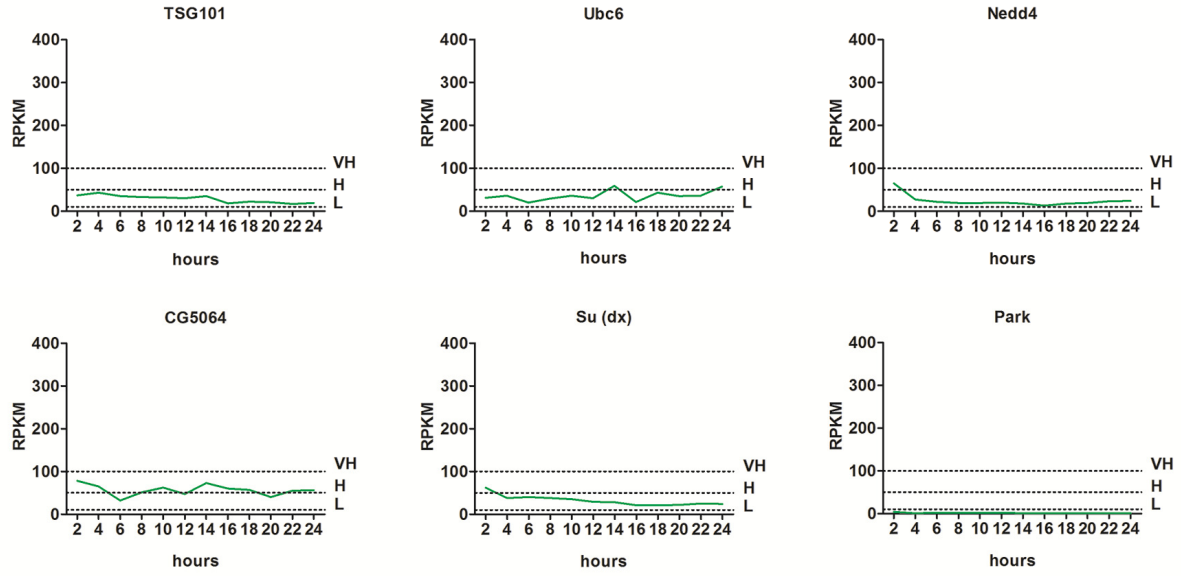

Figure A3. RNA levels of ubiquitin carriers not detected in embryonic samples.

mRNA levels during the embryo development, measure as reads per kilobase of exon model per million mapped reads (RPKM), of the E2 and E3 enzymes not detected in neither of the embryonic pulldowns. Horizontal dot lines indicate the expression level threshold used by Flybase where (L) is low, (H) high and (VH) very high expression. These data were obtained from Flybase (www.flybase.org).

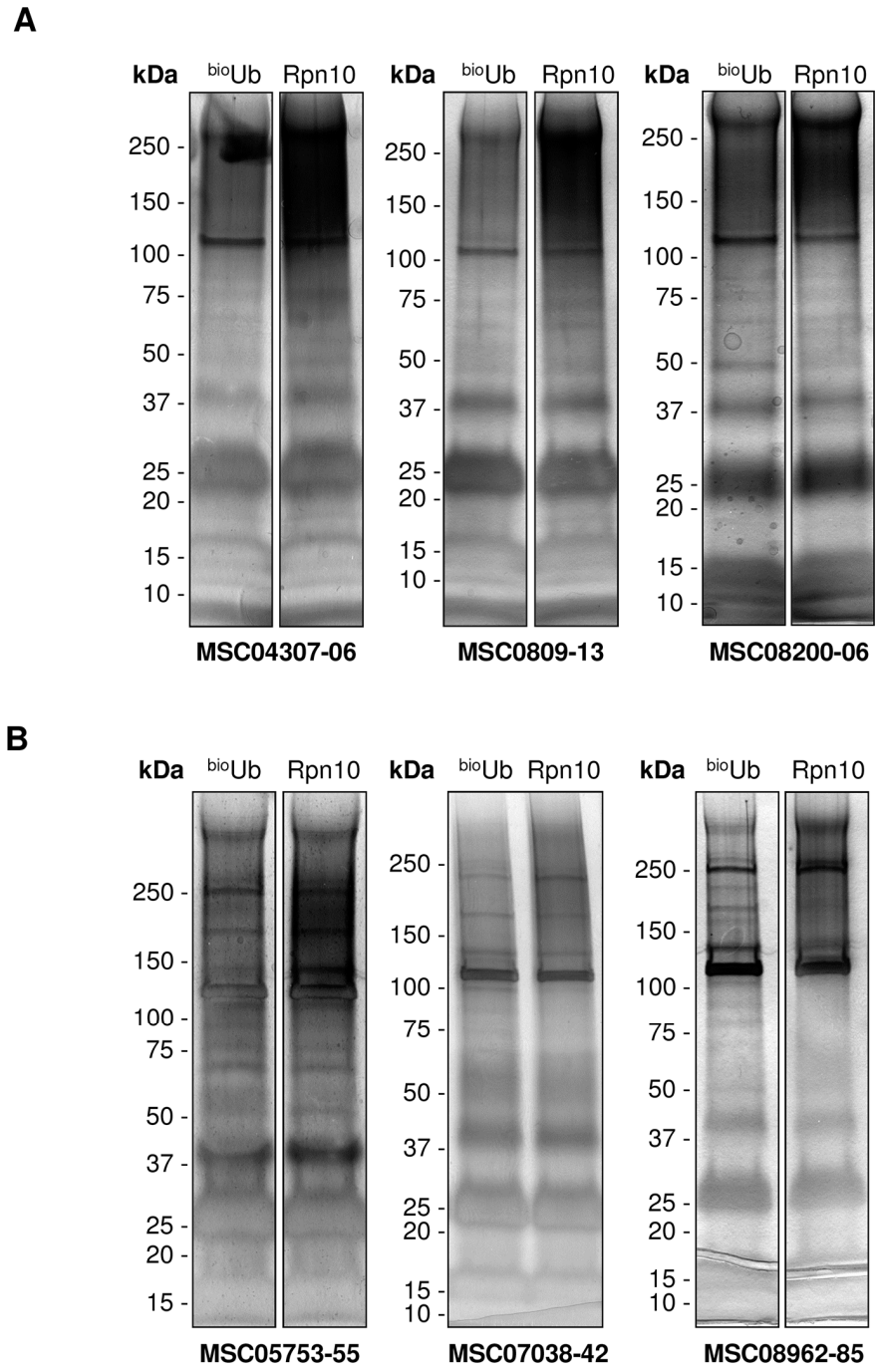

Figure A4. Silver staining of the material purified from Rpn10^{DN} and ^{bio}Ub samples.

Equal amounts of ^{bio}Ub and ^{bio}Ub+Rpn10^{DN} samples were analysed for each pulldown using SDS-PAGE and stained with silver. Both for embryo (**A**) and for adult (**B**) samples an accumulation of proteins is detected on samples from flies overexpressing Rpn10^{DN} compared to ^{bio}Ub flies. For each pulldown experiment the number assigned by the MS core facility at the MDC Institute is provided. Taken from Ramirez *et al.*, 2015.

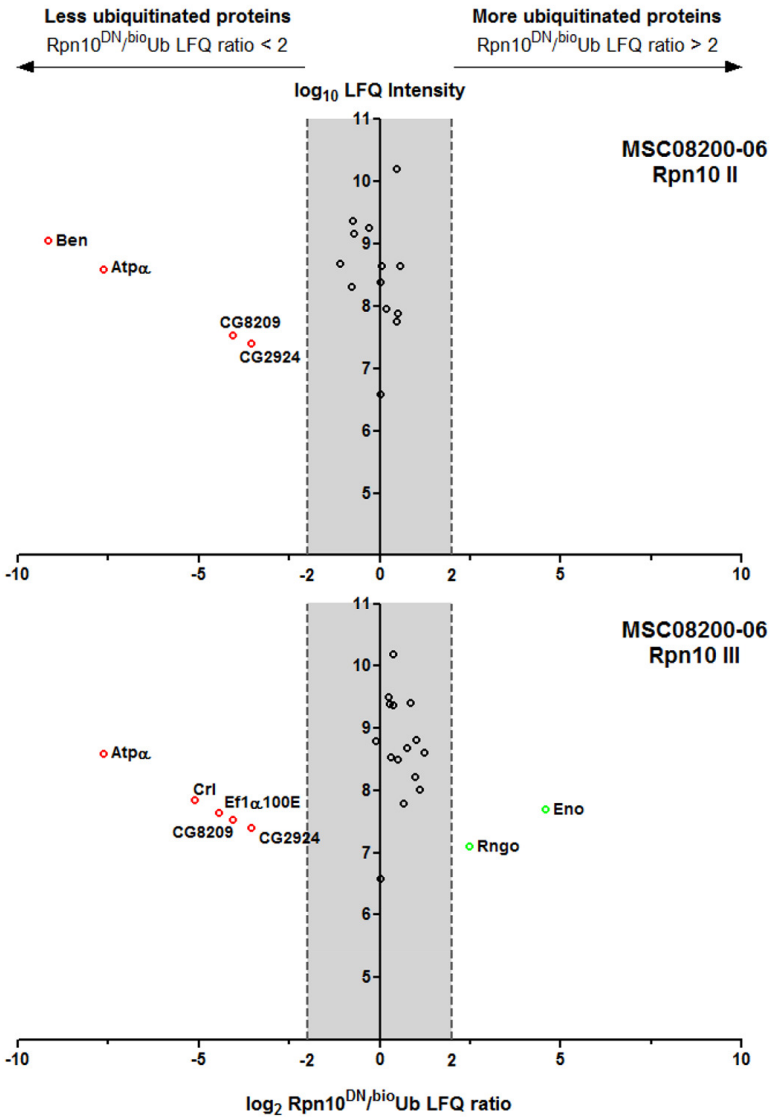
Less ubiquitinated proteins
Rpn10DN/bioUb LFQ ratio < 2
More ubiquitinated proteins
Rpn10DN/bioUb LFQ ratio > 2
log10 LFQ Intensity
MSC08200-06
Rpn10 II
Ben
Atpα
CG8209
CG2924
MSC08200-06
Rpn10 III
Atpα
Crl
Ef1α100E
CG8209
CG2924
Eno
Rngo
log2 Rpn10DN/bioUb LFQ ratio

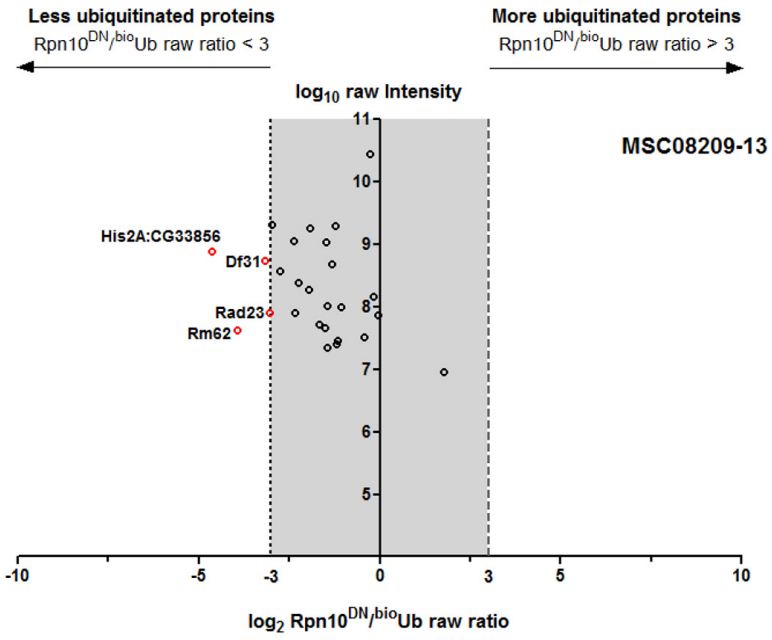
Less ubiquitinated proteins
Rpn10DN/bioUb raw ratio < 3
More ubiquitinated proteins
Rpn10DN/bioUb raw ratio > 3
log10 raw Intensity
MSC08209-13
His2A:CG33856
Df31
Rad23
Rm62
log2 Rpn10DN/bioUb raw ratio

Figure A5. Proteins found differentially ubiquitinated in embryo Rpn10^{DN} samples.

Vulcano plots showing the proteins that appear differentially ubiquitinated upon Rpn10^{DN} overexpression. LFQ Rpn10^{DN}/^{bio}Ub ratio of those proteins identified in at least two independent Rpn10^{DN} experiments were calculated for each MS analysis. In order to be able to plot all the ratios, in those proteins were LFQ value was not reported, the lowest LFQ value obtained in the analysis was given to these proteins. Those proteins with a LFQ ratio bigger than 2 (in $\log_2$ scale) were considered to be more ubiquitinated, while those with a ratio lower than -2 were considered to be less ubiquitinated. For each pulldown experiment the number assigned by the MS core facility at the MDC Institute is provided.

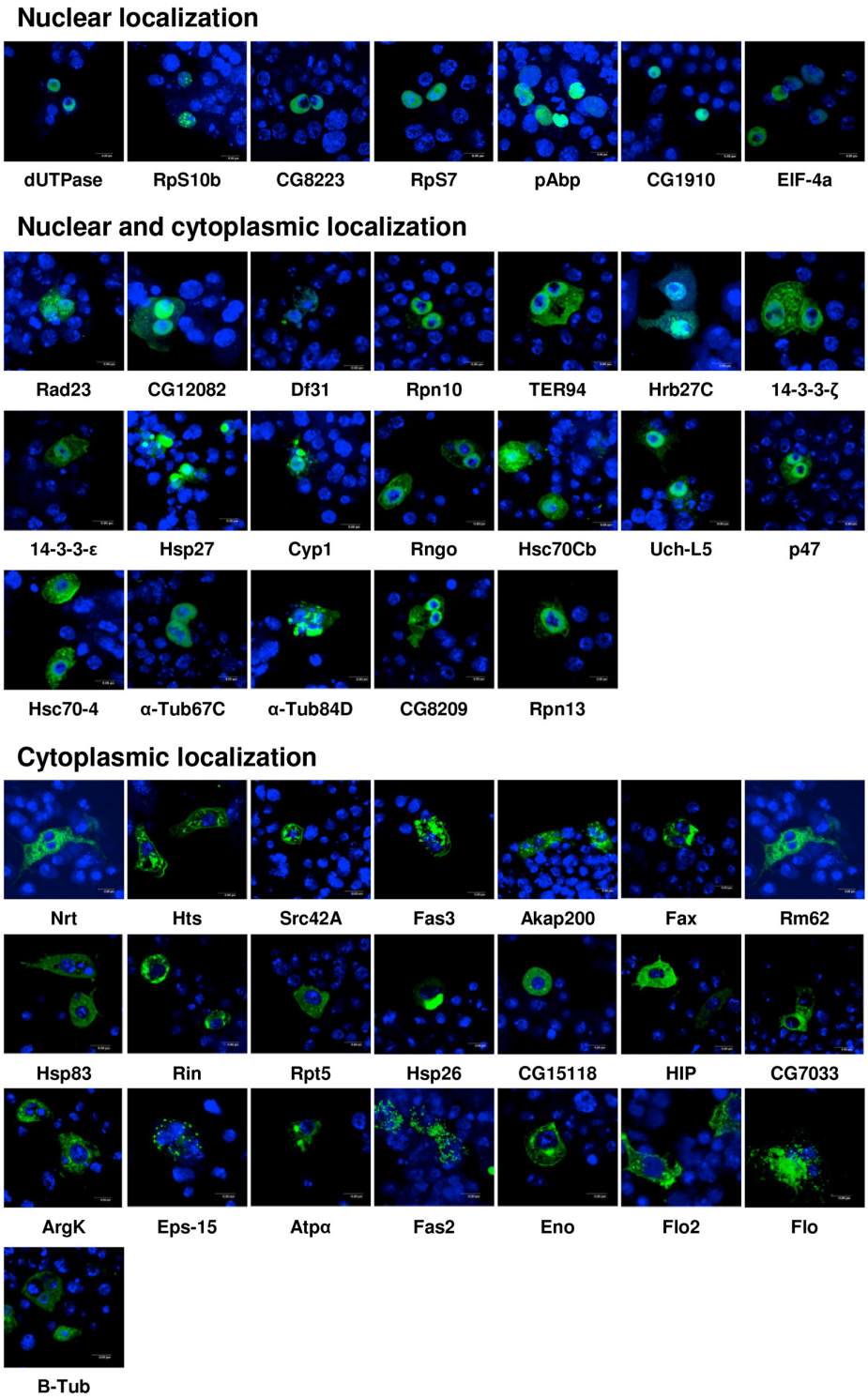

Figure A6. Localization of 47 neuronal ubiquitination substrates in *Drosophila* BG2 cells.

Taken from Lee *et al.*, 2014.

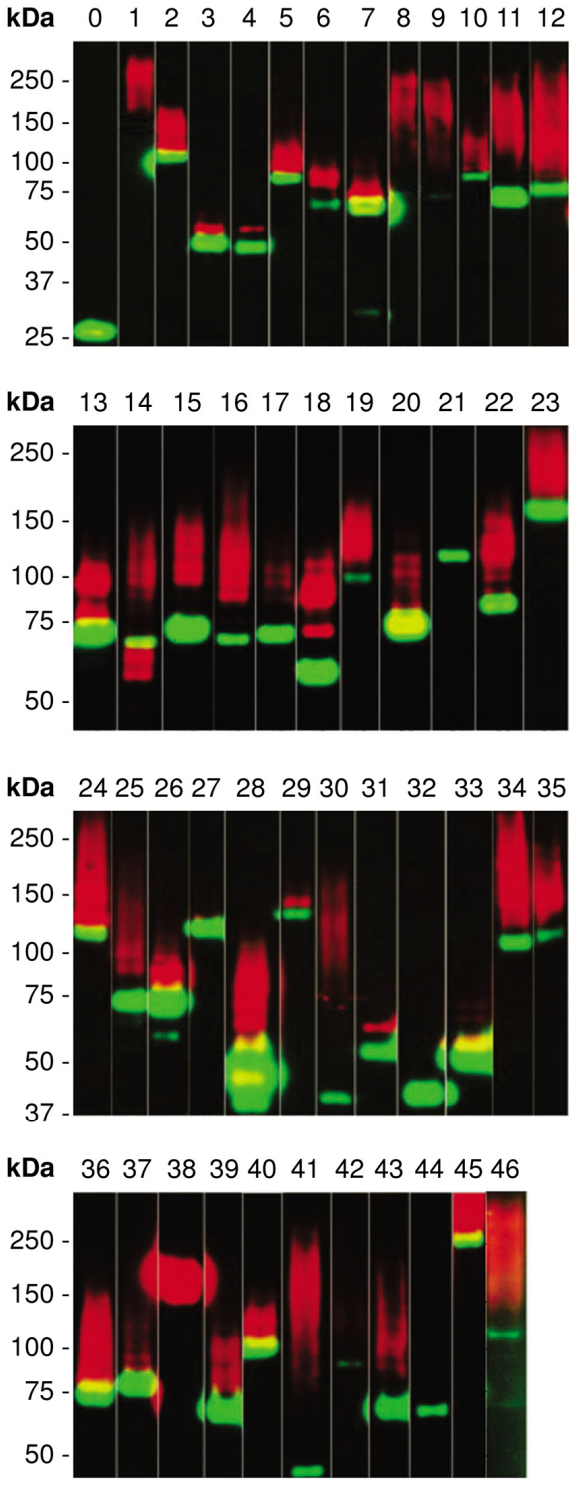

Figure A7. Ubiquitination of the 47 candidate substrate in neuronal-like cell culture.

GFP pulldown assay was applied to all of them. No signal could be detected for Rm62. From the remaining 46 proteins, 43 were confirmed to be ubiquitinated by endogenous E3 ligases in BG2 cells (all except Hsc70Cb, Cyp1 and Hrb27C). Taken from Lee *et al.*, 2014.

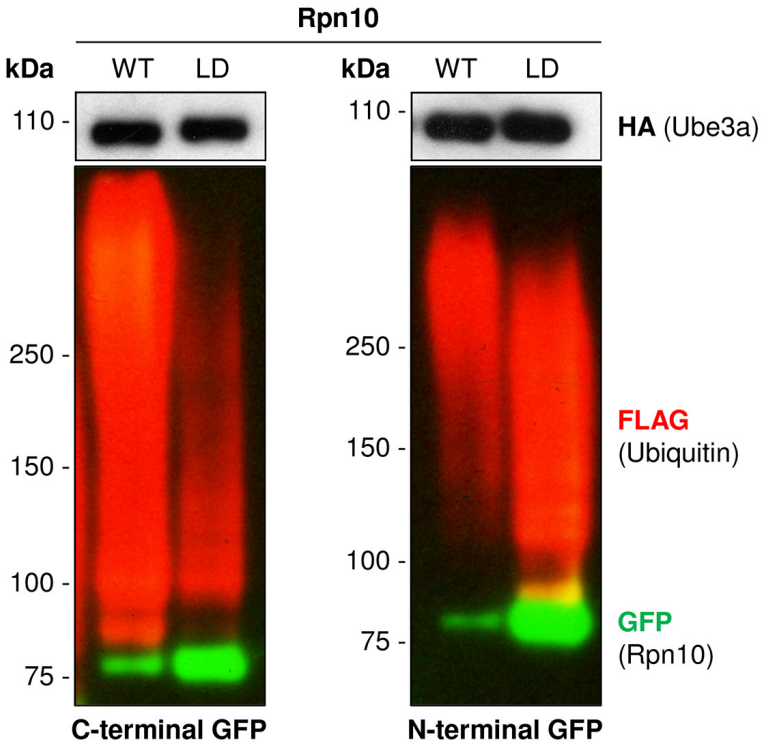

Figure A8. Rpn10 ubiquitination by Ube3a

Both N- and C-terminally GFP-tagged Rpn10 are ubiquitinated and targeted for degradation by Ube3a-WT. Taken from Lee *et al.*, 2014.

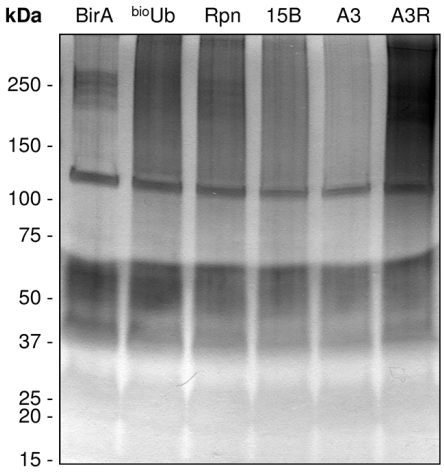

Figure A9. Silver staining of material purified from *Drosophila* embryonic samples.

Equal amounts of the eluted material from each of the samples were separated by SDS-PAGE and stained with silver. An accumulation of proteins is detected on samples from flies overexpressing Rpn10^{DN} (Rpn), as compared to control (^{bio}Ub), Ube3a mutant (15B) and Ube3a overexpression (A3) samples. When Rpn10^{DN} and Ube3a are co-expressed (A3R) this accumulation is greatly enhanced. BirA: *elav^{GAL4},^{UAS}BirA/CyO*; ^{bio}Ub: *elav^{GAL4},^{UAS}(^{bio}Ub)$_6$-BirA/CyO*; Rpn: *elav^{GAL4},^{UAS}(^{bio}Ub)$_6$-BirA/CyO;^{UAS}Rpn10^{DN}/TM6B*; 15B: *elav^{GAL4},^{UAS}(^{bio}Ub)$_6$-BirA/CyO;Ube3a^{15B}/TM6B*; A3: *elav^{GAL4},^{UAS}(^{bio}Ub)$_6$-BirA/CyO;^{UAS}Ube3a^{A3}/TM6B*; A3R: *elav^{GAL4},^{UAS}(^{bio}Ub)$_6$-BirA/CyO;^{UAS}Ube3a^{A3},^{UAS}Rpn10^{DN}/TM6B.*

Cell. Mol. Life Sci.
DOI 10.1007/s00018-013-1526-7

Cellular and Molecular Life Sciences

RESEARCH ARTICLE

Ube3a, the E3 ubiquitin ligase causing Angelman syndrome and linked to autism, regulates protein homeostasis through the proteasomal shuttle Rpn10

So Young Lee · Juanma Ramirez · Maribel Franco · Benoît Lectez · Monika Gonzalez · Rosa Barrio · Ugo Mayor

Received: 17 September 2013 / Accepted: 15 November 2013

Abstract Ubiquitination, the covalent attachment of ubiquitin to a target protein, regulates most cellular processes and is involved in several neurological disorders. In particular, Angelman syndrome and one of the most common genomic forms of autism, dup15q, are caused respectively by lack of or excess of UBE3A, a ubiquitin E3 ligase. Its *Drosophila* orthologue, Ube3a, is also active during brain development. We have now devised a protocol to screen for substrates of this particular ubiquitin ligase. In a neuronal cell system, we find direct ubiquitination by Ube3a of three proteasome-related proteins Rpn10, Uch-L5, and CG8209, as well as of the ribosomal protein Rps10b. Only one of these, Rpn10, is targeted for degradation upon ubiquitination by Ube3a, indicating that degradation might not be the only effect of Ube3a on its substrates. Furthermore, we report the genetic interaction in vivo between Ube3a and the C-terminal part of Rpn10. Overexpression of these proteins leads to an enhanced accumulation of ubiquitinated proteins, further supporting the biochemical evidence of interaction obtained in neuronal cells.

Keywords Ube3a · Ubiquitin · Angelman syndrome · Autism · Proteasome · Rpn10

Introduction

Angelman syndrome (AS) is a severe neurodevelopmental disorder related to autism, which presents also with intellectual disability [1]. The cause of AS is the loss of function in the brain of the ubiquitin E3 ligase coded by the *UBE3A* gene, which is located on chromosome 15q [2, 3]. Autism is a neurodevelopmental disorder characterized by social deficits, communication difficulties, stereotyped or repetitive behaviors and interests, and in some cases, cognitive delays. The prevalence for autism spectrum disorders (ASD) as a whole is six per 1,000 but in only 10 % of the cases is there a recognized genetic cause. Duplication of the 15q locus including the *UBE3A* gene is one of the most common genomic causes for autism, the preference for maternal duplications lending further support to the involvement of the maternally expressed *UBE3A* gene [4–7]. The pathogenic mechanisms that underlie autism and AS, due to the excess or lack of UBE3A activity, are still unknown. Importantly, these phenotypes could be caused by the misregulation of common ubiquitination targets of UBE3A. Interestingly, while in the cortex of ASD subjects the spine densities on pyramidal cells are greater than in controls [8], the opposite is true for *UBE3A* null AS animal models. There, reduced spine density is observed on cerebellar Purkinje cells and on pyramidal neurons in hippocampus and cortex [9, 10]. Other reports, however, have

Authors S. Y. Lee and J. Ramirez contributed equally to this work.

Electronic supplementary material The online version of this article (doi:10.1007/s00018-013-1526-7) contains supplementary material, which is available to authorized users.

S. Y. Lee · J. Ramirez · M. Franco · B. Lectez · M. Gonzalez · R. Barrio · U. Mayor (✉)
CIC bioGUNE, Bizkaia Teknologia Parkea, Building 801-A, Derio, 48160 Derio, Basque Country, Spain
e-mail: umayor@cicbiogune.com

Present Address:
M. Franco
Instituto de Neurociencias CSIC/UMH, 03550 Sant Joan d'Alacant, Spain

U. Mayor
Ikerbasque, Basque Foundation for Science, 48011 Bilbao, Spain

Published online: 01 December 2013

PLOS | ONE

RESEARCH ARTICLE

Proteomic Analysis of the Ubiquitin Landscape in the *Drosophila* Embryonic Nervous System and the Adult Photoreceptor Cells

Juanma Ramirez[1,2], Aitor Martinez[1,2,3], Benoit Lectez[2,4], So Young Lee[2], Maribel Franco[2,5], Rosa Barrio[2], Gunnar Dittmar[6], Ugo Mayor[1,2,7]*

1 Department of Biochemistry and Molecular Biology, University of the Basque Country (UPV/EHU), Leioa, Bizkaia, Spain, **2** Functional Genomics Unit, CIC bioGUNE, Derio, Spain, **3** Department of Cellular and Molecular Physiology, Institute of Translational Medicine, University of Liverpool, Liverpool, United Kingdom, **4** Mollecular Cell Biology, Turku Centre for Biotechnology, Turku, Finland, **5** Developmental Neurobiology, Institute of Neurosciences, CSIC/UMH, Sant Joan d'Alacant, Alicante, Spain, **6** Max Delbrück Center for Molecular Medicine, Berlin, Germany, **7** Ikerbasque, Basque Foundation for Science, Bilbao, Bizkaia, Spain

* ugo.mayor@ehu.eus

OPEN ACCESS

Citation: Ramirez J, Martinez A, Lectez B, Lee SY, Franco M, Barrio R, et al. (2015) Proteomic Analysis of the Ubiquitin Landscape in the *Drosophila* Embryonic Nervous System and the Adult Photoreceptor Cells. PLoS ONE 10(10): e0139083. doi:10.1371/journal.pone.0139083

Editor: Brian D. McCabe, Columbia University, UNITED STATES

Received: July 15, 2015

Accepted: September 9, 2015

Published: October 13, 2015

Data Availability Statement: All relevant data are within the paper and its Supporting Information files.

Funding: UM was supported by the Basque Government research grant (PI2011-24), the Asociación Síndrome de Angelman, and the March of Dimes Basil O´Connor Award (5-FY12-16). JR was supported by the CIC bioGUNE PhD fellowship. The funders had no role in study design, data collection and analysis, decision to publish, or preparation of the manuscript.

Abstract

Background

Ubiquitination is known to regulate physiological neuronal functions as well as to be involved in a number of neuronal diseases. Several ubiquitin proteomic approaches have been developed during the last decade but, as they have been mostly applied to non-neuronal cell culture, very little is yet known about neuronal ubiquitination pathways *in vivo*.

Methodology/Principal Findings

Using an *in vivo* biotinylation strategy we have isolated and identified the ubiquitinated proteome in neurons both for the developing embryonic brain and for the adult eye of *Drosophila melanogaster*. Bioinformatic comparison of both datasets indicates a significant difference on the ubiquitin substrates, which logically correlates with the processes that are most active at each of the developmental stages. Detection within the isolated material of two ubiquitin E3 ligases, Parkin and Ube3a, indicates their ubiquitinating activity on the studied tissues. Further identification of the proteins that do accumulate upon interference with the proteasomal degradative pathway provides an indication of the proteins that are targeted for clearance in neurons. Last, we report the proof-of-principle validation of two lysine residues required for nSyb ubiquitination.

Conclusions/Significance

These data cast light on the differential and common ubiquitination pathways between the embryonic and adult neurons, and hence will contribute to the understanding of the mechanisms by which neuronal function is regulated. The *in vivo* biotinylation methodology

Chapter 10

Isolation of Ubiquitinated Proteins to High Purity from In Vivo Samples

Juanma Ramirez, Mingwei Min, Rosa Barrio, Catherine Lindon, and Ugo Mayor

Abstract

Ubiquitination pathways are widely used within eukaryotic cells. The complexity of ubiquitin signaling gives rise to a number of problems in the study of specific pathways. One problem is that not all processes regulated by ubiquitin are shared among the different cells of an organism (e.g., neurotransmitter release is only carried out in neuronal cells). Moreover, these processes are often highly temporally dynamic. It is essential therefore to use the right system for each biological question, so that we can characterize pathways specifically in the tissue or cells of interest. However, low stoichiometry, and the unstable nature of many ubiquitin conjugates, presents a technical barrier to studying this modification in vivo. Here, we describe two approaches to isolate ubiquitinated proteins to high purity. The first one favors isolation of the whole mixture of ubiquitinated material from a given tissue or cell type, generating a survey of the ubiquitome landscape for a specific condition. The second one favors the isolation of just one specific protein, in order to facilitate the characterization of its ubiquitinated fraction. In both cases, highly stringent denaturing buffers are used to minimize the presence of contaminating material in the sample.

Key words Ubiquitination, Substrates, Isolation, Denaturing conditions

1 Introduction

Ubiquitination of proteins is facilitated by the coordinated action of ubiquitin-activating E1, -conjugating E2, and -ligating E3 enzymes, and can be reversed by the so-called deubiquitinating enzymes (DUBs) [1]. Along with these ubiquitinating enzymes, proteasomal subunits, shuttling factors and other ubiquitin binding proteins regulate the fate of the ubiquitinated substrates. Altogether, nearly 1000 proteins integrate the ubiquitin proteasome system (UPS), which in addition to being the main intracellular protein degradation pathway, dynamically regulates the proteome by various other means too. Despite great advances in the mass spectrometry (MS) field, the identification of proteins regulated by the UPS is still a challenge, mostly because of the low

Rune Matthiesen (ed.), *Proteostasis: Methods and Protocols*, Methods in Molecular Biology, vol. 1449,
DOI 10.1007/978-1-4939-3756-1_10,